Enhancing Bioavailability Of Drugs

A THESIS

SUBMITTED TO THE

UNIVERSITY OF PUNE

FOR THE DEGREE OF

DOCTOR OF PHILOSOPHY

(IN PHARMACEUTICAL CHEMISTRY)

(FACULTY: PHARMACEUTICAL SCIENCES)

By

ANUPA R. MENJOGE

POLYMER SCIENCE & ENGINEERING DIVISION

NATIONAL CHEMICAL LABORATORY (NCL)

PUNE - 411008, INDIA

25 AUGUST 2006

CERTIFICATE

This is to certify that the work incorporated in the thesis entitled "Enhancing Bioavailability of Drugs" submitted by Ms. Anupa R. Menjoge, was carried out under my supervision. Such material as has been obtained from other sources has been duly acknowledged in the thesis.

Date: 25 Aug 2006
National Chemical Laboratory
Pune, 411008

Dr. M.G. Kulkarni
(Research Guide)

DECLARATION

I hereby declare that the work embodied in the thesis entitled "**Enhancing Bioavailability of Drugs**" submitted for Ph. D. degree to the University of Pune, has been carried out by me at the National Chemical Laboratory, Pune, under the supervision of Dr. M.G. Kulkarni. The work is original and has not been submitted in part or full by me for any degree or diploma to this or any other University. Whenever references have been made to previous works of other, it has been clearly indicated as such and included in the Bibliography.

Date: 25 Aug 2006 **Ms. Anupa R. Menjoge**

National Chemical Laboratory

Pune, 411008

Acknowledgements

At the onset, my heartfelt indebtedness to Dr. M. G. Kulkarni (Head, PSE), my supervisor, for his cogent and stimulating suggestions, probing questions, constructive critiques, constant encouragement. This helped me throughout the research and writing of this thesis. During the last phase of work, his steady support and accommodative nature made this daunting task easy. He infused the importance of patent law and was the source of inspiration to undertake the diploma in patent law. I adore his remarkable patience, enthusiasm; commitment, quest to explore new research areas and above all the penchant for perfection.

It is my pleasure to acknowledge Dr. Sivaram, Director, NCL, for permitting me to present this work in form of thesis.

I would like to acknowledge the financial support received from CSIR in the form of Senior Research and Research Associate Fellowships respectively.

My sincere thanks go to Dr. B.D. Kulkarni, Head of CE Division, Dr. Badiger, Mr. Thakar and Mr. P.R. Suresha for the support given to me during this work.

I'm highly obliged to Dr. Ponrathnam, Dr. Rajmohanan, Dr. Ramesh, Dr. Jog, Mr. Pandare, Dr. Neelima, Ms. Poorvi and Mr. Gaikwad for the support extended during the course of work.

I am grateful to all my friends Sunita, Prerana, Smitha, Dr. Shubhangi, Dr. Karmarkar, Rupali KS, Rupali, Aarti, Nivika, Ujwal, Hemant, Ramesh, Santosh, Gaihninath, Mahesh, Sachin, Satish, Swapnil, Jiten, Kiran and Vijay for timely help, co-operation and making my stay at NCL pleasant.

I would like to thank Mr. Dhavale, Mr. Grime, Mr. Kokane, Mr. Mahajan and Mr. Bharati for all the help rendered by them.

The light conversations with Dr. Rathna always helped me fight my blues.

Completion of this thesis would not have been possible without the unconditional support, faith and liberty to pursue career, bestowed by Harshal, my husband and my in-laws.

Amrish and Shweta have always brought the desired respite at difficult times. Your encouragement and support has made the sailing easy.

Mom and Dad, am too overwhelmed to express in words, you have always been there for me. Your principles and faith in education have inspired and gave me the strength to pursue for PhD…..

Anupa Menjoge

Dedicated to my Parents

CONTENTS

CONTENTS

CONTENTS

Page No.

CONTENTS

Page No.

CONTENTS

CHAPTER 4

Taste masked Compositions Comprising NREP & Bitter Drugs: Enhancing Bioavailability with Rapid Gastric Release

CONTENTS

Page No.

CHAPTER 5

Drug-Polymer Compatibility Studies: Implications on Bioavailability of Drugs

CONTENTS

CHAPTER 6

Miscible Blends Of New Reverse Enteric Polymer With Enteric And pH Independent Polymers For Sustained Gastric Release

CONTENTS

Page No.

CONTENTS

CONTENTS

CONTENTS

Page No.

CHAPTER 9

Enhancement Of Bioavailability By Polymorphism Inhibition

CONTENTS

Page No.

CHAPTER 10

Conclusions & Suggestions For Future Work

Fig. No. **List of Figures** **Page No.**

CHAPTER 1

CHAPTER 3

CHAPTER 4

CHAPTER 5

List of Figures

List of Figures

Page No.

CHAPTER 6

List of Figures

CHAPTER 7

CHAPTER 9

List of Figures

Page No.

Table No. **List of Tables** **Page No.**

List of Tables

Page No.

CHAPTER 6

CHAPTER 7

CHAPTER 8

List of Tables

Page No.

CHAPTER 9

Abbreviations

BA	Bioavailability
BCS	Biopharmaceutical classification system
BuMA	Butyl methacrylate
CP	Cefpodoxime proxetil
Δ *Cp*	Specific heat
CA	Cefuroxime axetil
COX-2	Cyclooxygenase-2
CAT	Cellulose acetate trimellitate
CAP	Cellulose acetate phthalate
CMC	Carboxymethylcellulose
$CDCl_3$	Dueterated chloroform
DSC	Differential scanning calorimetry
DMAMEA	Dimethylamino ethylmethacrylate
DCM	Dichloromethane
ESEM	Environmental scanning electron microscopy
EC	Ethylcellulose
EE	Eudragit E
EL	Eudragit L
ES	Eudragit S
FTIR	Fourier transform infrared spectroscopy
GRAS	Generally recognized as safe
GPC	Gel permeation chromatography
HPMCP	Hydroxypropyl methylcellulose phthalate
HPMC	Hydroxypropyl methylcellulose
HPC	Hydroxypropyl cellulose
H. pylori	Helicobacter pylori
HEMA	2-hydroxy ethyl methacrylate
HEEMA	2-hydroxyethoxy ethyl methacrylate
IPEC	International Pharmaceutical Excipients Council
K_1 & K_2	Values of fitting parameters by Schneider equation
MC	Methylcellulose
MMA	Methyl methacrylate
MDSC	Modulated differential scanning calorimetry

MeOH	Methanol
n	Diffusional exponent
NREP	New reverse enteric polymer
NDA	New drug application
NMR	Nuclear magnetic resonance spectroscopy
ODT's	Orally disintergrating tablets
PITs	Processing induced transformations
pKa	Dissociation constant
PVP	Polyvinylpyrrolidone
PAA	Polyacrylic acid
PVA	Polyvinyl acetate
PEMA	Piperidine ethyl methacrylate
RH	Relative humidity
ρ_D	Density of drug
ρ_C	Density of matrix
T_g	Glass transition temperature
$T_{g,MIX}$	Glass transition of the solid dispersion
$T_{g,D}$	Glass transition of drug
$T_{g,C}$	Glass transition of matrix
T_{g1} & T_{g2}	T_gs of polymer 1 and polymer 2
T_{g1b} & T_{g2b}	T_g of the first and second T_g phase observed in blends respectively
4-VP	4- Vinylpyridine
W_s	Weight of the swollen polymer film
W_d	Weight of dry polymer film
w_{2c}	Corrected weight fraction
w'_1 & w''_1	Apparent weight fractions of polymers
W' & W''	Overall weight fraction of phase rich in polymer component with higher T_g and lower T_g respectively
W_{1T} & W_{2T}	Overall weight fractions of polymer 1 and polymer 2
XRD	x-ray diffraction
X_1 & X_2	Weight fractions of polymers in blend

ABSTRACT

"Bioavailability" is defined as the rate and extent of drug absorption. Any alteration in drug bioavailability is reflected in its pharmacologic effects. To attain the desired therapeutic objective, the drug has to be delivered at an optimal rate and amount. Three major approaches to enhance bioavailability are the *Pharmaceutic* approach, the *Pharmacokinetic* approach and the *Biological* approach [1]. The *Pharmacokinetic and Biologic* approaches involve alteration in chemical structure and route of administration respectively. Both these approaches have drawbacks such as repetition of clinical trials, regulatory approvals and lower patient compliance respectively. Hence the *Pharmaceutic* approach which involves modification of the formulation, manufacturing process or physicochemical properties of drug without changing the chemical structure, is the most preferred approach to enhance bioavailability. The attempts are mainly aimed at enhancing rate of dissolution of drug as it is the rate limiting step in absorption of most drugs.

The therapeutic effectiveness of the drug depends on the ability of the dosage form to deliver the drug to its site of action at a rate and amount sufficient to elicit desired therapeutic response. An oral drug delivery system providing a uniform drug release can only partly satisfy the therapeutic and biopharmaceutical needs, as it does not take in to account site specific absorption rates within the gastrointestinal tract. For oral therapeutic use this means the creation of dosage form delivering the drug during its gastrointestinal transit at the right time and at right site at therapeutically optimal rate [2]. This implies 1) delivering locally effective drugs like antibiotics, anti inflammatory or cytostatic agents only at their target site and 2) releasing drugs such as Digoxin, Ampicillin, Ciprofloxacin and Cefuroxime axetil which have a limited absorption window at the preferred absorption site. To attain the desired therapeutic effectiveness without altering drug bioavailability, the design and evaluation of delivery systems for gastrointestinal tract requires the knowledge of three inter-related topics, *the drug*, *the delivery system* and the *destination intended* [3].

The primary concern for drugs exhibiting lower bioavailability and restricted absorption window is designing the delivery systems which release the drug at the desired site thus enhancing their absorption and in turn the bioavailability. To achieve

this goal, spatial and temporal release formulations have been developed in the past [4, 5]. Polymers play an important role in the design of these advanced drug products. A major consideration in use of polymers for drug delivery is drug-polymer interaction, drug transformation and its degradation [6]. The drug-excipient interactions often modify the physicochemical characteristics of the drug [7] and sometimes these result in complete loss of activity of drug or delayed release.

In the present work we have identified drugs which have limited absorption window, which in turn affects their absorption and consequently bioavailability. Also we identified drugs which were inactivated due to the drug-polymer interaction adversely affecting their bioavailability. In particular, drugs such as Cefuroxime axetil, Ciprofloxacin HCl and Clarithromycin which are absorbed in upper gastric region and those required for local and immediate action were selected.

The complexity of the molecule Cefuroxime axetil poses a great challenge to formulation scientist to administer it without alteration of bioavailability. Cefuroxime axetil has a limited absorption window restricted to upper gastric region as it is hydrolyzed by esterase enzyme in intestine to Cefuroxime, a form, which cannot be absorbed orally [8, 9]. Bioavailability of orally administered CA is low (37-52 %) [10]. It is therefore essential that the drug be released in gastric region under acidic pH conditions so that its bioavailability is not further affected. Extensive efforts have been made in the past to taste mask it using Cellulose acetate trimellitate (CAT), Hydroxypropyl methylcellulose phthalate (HPMCP) and Eudragit E (EE). Cefuroxime axetil was completely degraded in the presence of the Eudragit E and led to unacceptably high proportions of impurities in presence of CAT [11,12]. Ciprofloxacin HCL is a bitter drug better absorbed from gastric region, but is associated with extremely bitter taste. It is highly water soluble and hence requires a coating which is completely impermeable to water. Eudragit E is soluble below pH 5 and permeable above it so it cannot be used. To overcome this it has been coated with enteric polymers to mask the bitter taste. However this affects its absorption in the gastric region.

The limitations of the existing polymers described above, have restricted the formulation development of taste masked products of these drugs. This has educed the need to develop a polymer which is capable of catering to these formulation needs.

To overcome the above limitations we undertook the development of a new reverse enteric polymer (NREP) which dissolves at gastric pH and can be used for the development of drug delivery systems for taste masking, immediate and sustained gastric release. We undertook detailed investigation of the polymers for physicochemical characteristics and their adaptability to pharmaceutical process. We also undertook evaluation of biological reactivity (*in-vitro* and *in-vivo*) to ensure biocompatibility. A detailed investigation of drug-polymer compatibility to ensure availability of the drug in active form was undertaken. We evaluated the blends of NREP with other polymers to bring about sustained release of these drugs at gastric and intestinal pH. The extent of interaction between polymer blends was quantified in terms of Schneider equation. The *in-vitro* drug release experiments were carried out to ensure the complete release of drugs. For all the drugs investigated the *in-vitro* and *in-vivo* correlation is well established. The *in-vitro* release of drugs therefore provides a good measure for ensuring the absorption of drugs.

NREP was found to effectively taste mask the drugs with immediate release in gastric pH. Also sustained release formulation for gastric release of drugs can be formulated using NREP. This ensured the release of drugs better absorbed from gastric region at the right site and at the rate desired.

The work is presented in ten chapters and a brief outline of each is given below.

Chapter 1: Introduction and motivation

This is an introductory chapter where the problems arising in formulating drugs with complex pharmacokinetic and physicochemical properties resulting in compromising with bioavailability are discussed. Various pharmaceutical compositions aimed at achieving one formulation attribute (eg taste masking) compromising on the release and bioavailability were analyzed. The restrictions faced by formulation scientists due to non availability of polymer with specific functionality leading to constraints imposed on formulation development are described. One of the areas where the polymers are most extensively used is the taste masking of the drugs. The gastric soluble polymer Eudragit E is most commonly used for the taste masking of the drugs. However certain drugs like cefuroxime axetil, indomethacin and warfarin are reported

to interact with Eudragit E resulting in either complete deactivation or delayed release of drug. In addition, there may also be issues that must be addressed relative to region-specific absorption.

The polymers widely used for taste masking include the enteric polymers like cellulose acetate phthalate, hydroxymethyl cellulose phthalate, cellulose trimellitate, hydroxymethyl cellulose acetate succinate, shellac and polymethacrylates like Eudragit L and S. However the use of these polymers delays the release of the drug till they reach the intestine where the polymers are soluble. This causes a delay in the release of the drugs due to the design of the delivery system based on such enteric polymers which cannot release drugs having limited absorption window restricted to the upper GI tract. This adversely affects the bioavailability of the drugs. This literature survey reveals that a clear understanding and consideration of these issues in the design and execution of a successful development program for bioavailability enhancement in taste masked products is lacking. It also highlights the need to identify and synthesize new polymers that can overcome the above mentioned limitations. Based on the summary of the literature we identified new polymer compositions, which could be explored for these applications. We further validated their utility by investigating the drug-polymer interactions by various tools such as FTIR, NMR, HPLC and DSC and drug release studies.

Chapter 2: Objective and scope of work

The major focus of this work is to design and evaluate new reverse enteric polymer for the development of taste masked, immediate and sustained gastric release product. The polymer and formulation development is aimed to provide the site specific delivery of drugs with restricted absorption window to gastric region to enable better absorption and ensure bioavailability without deactivation of the drug. This chapter highlights the major objectives and also the scope of entire work and these are;

1. To identify the reverse enteric polymer capable of taste masking drugs like Cefuroxime axetil without its inactivation.

2. To develop reverse enteric polymer which is insoluble and exhibits negligible swelling at higher pH to enable development of taste masked products of highly water soluble drugs like Ciprofloxacin HCl.
3. To undertake synthesis and physicochemical characterization of polymer to meet the above requirements. Characterize polymers for solubility / swelling at different pH. Optimize polymer composition to yield stringent pH dependent behavior (solubility < pH 4 and insoluble above it). Evaluate the effect of polymer structure on T_g and biocompatibility.
4. To encapsulate the drugs and evaluate rapid release of drugs at gastric pH where they are better absorbed thereby ensuring the bioavailability. Encapsulate Cefuroxime axetil, Ciprofloxacin HCL and Clarithromycin by various techniques and undertake drug release studies at both gastric and near neutral pH.
5. To investigate drug polymer interaction to establish that the drug is being retained in biologically active form, by techniques such as DSC, FTIR, NMR and HPLC analysis.
6. To evaluate blends of new reverse enteric polymer with enteric and pH dependent polymers for miscibility for attaining sustained gastric release useful for drugs better absorbed from upper gastric region. Evaluate polymer blend miscibility by FTIR and Thermal analysis and quantify the extent of interaction in terms of Schneider equation. Investigate the utility of the blends in the sustained release of Cefuroxime axetil at gastric pH.
7. To evaluate hydrophobic blends of new reverse enteric polymer with fatty acids to attain rapid release at gastric pH with taste masking ability. Investigate the effect of encapsulation of drugs by these blends using emulsification solvent evaporation technique, hot melt granulation and spray drying on drug release at gastric pH.
8. To evaluate the effect of polymer molecular weight on polymorphism inhibition of Cefuroxime axetil and Celecoxib thereby ensuring their bioavailability. Evaluate drug-polymer co-precipitates by XRD.

Chapter 3: A new reverse enteric polymer for immediate gastric release: design and evaluation

The major focus of this work was to design and evaluate a new reverse enteric polymer which dissolves at pH $\leq$ 4 and does not swell or dissolve in water and at higher pH and pH of saliva so that it can be used to formulate drugs like Cefuroxime axetil and Ciprofloxacin HCl. The polymer would be evaluated for its ability to taste mask these drugs without their inactivation and release rapidly in stomach where they are better absorbed. Various copolymers based on the hydrophobic and basic monomer and ter-polymers containing a hydrophilic monomer in addition to hydrophobic and basic monomer were synthesized. The influence of monomer choice and composition on dissolution behavior of the films at pH 1.2, 4.5 and 5.8 was investigated. The monomer composition was optimized to yield the stringent requirements of pH dependent dissolution behavior of polymer. The polymer compositions yielding solubility at pH $\leq$ 4 were obtained by polymerizing methyl methacrylate (MMA), 2-hydroxy ethyl methyl methacrylate (HEMA) and 4-vinyl pyridine (4-VP). The influence of monomer choice and composition on T_g and biocompatibility is discussed. The physicochemical characteristics of the polymer were determined by NMR, FTIR, GPC and DSC. The details of polymer synthesis are discussed in patent application (M.G. Kulkarni and A.R. Menjoge, US 20050137372, 23 June 2005).

NREP was found to be suitable for the pharmaceutical applications and evaluation of *in-vitro* and *in-vivo* biological reactivity as per USP 26 NF XXI (2003) indicated that the polymer was non-toxic and can be used for further investigation.

Chapter 4: Taste masked compositions comprising NREP & bitter drugs: enhancing bioavailability with rapid gastric release

This chapter discloses the use of NREP for coating the drugs to attain taste masking and with rapid dissolution at gastric pH to enable rapid absorption of drugs. Bitter drugs Cefuroxime axetil (CA), Ciprofloxacin HCl and Clarithromycin were coated using NREP. The coating was done using emulsification solvent evaporation and spray drying technique. CA was released rapidly at gastric pH. The release was inhibited at salivary pH. NREP prevented CA leaching in aqueous media. The

palatability of the reconstituted CA suspensions was evaluated on the basis of numerical grading by the volunteers. The mean grading for the reconstituted taste masked CA microspheres was compared with market product Ceftum. The CA compositions based on NREP showed a lower release at pH 4.4 and retained the palatability over seven days. The volunteers graded the formulations between 0-2 and rated the formulations as palatable. The taste of the reconstituted microspheres was better than the market formulation Ceftum initially for a period of 3 days and was comparable thereafter.

Taste masked Ciprofloxacin and Clarithromycin microparticles were evaluated for the drug release at acidic pH. These drugs were released rapidly under gastric conditions. The polymer can be used for taste masking of variety of drugs in different dosage forms. The details of taste masked compositions are discussed in patent application (M.G. Kulkarni and A.R. Menjoge, US 20050136114, 23 June 2005).

Chapter 5: Drug polymer compatibility studies: implications for bioavailability of drugs

This chapter provides a detailed investigation on drug-polymer interactions. Inactivation of Cefuroxime axetil by Eudragit E is reported in the past. The inactivation of Cefuroxime axetil in the presence of Eudragit E was investigated as a reference. The influence of polymer composition on drug inactivation was investigated. The dimethylamino group of Eudragit E interacts with Cefuroxime axetil resulting in carboxylate salt formation. This causes its inactivation. These studies provided useful insights in evaluating the interactions between NREP synthesized by us and Cefuroxime axetil. A detailed investigation of physicochemical interactions between Cefuroxime axetil and NREP by DSC, FTIR, NMR and HPLC analysis is presented. The self associations between NREP and its lower basicity prevent the interaction between NREP and Cefuroxime axetil. The acetoxy ethyl group in cefuroxime axetil is not cleaved by NREP. These investigations were of paramount importance as they establish the usefulness of NREP in development of taste masked formulation of CA without causing its inactivation or degradation.

Chapter 6: Miscible blends of new reverse enteric polymer with enteric and pH independent polymers for sustained gastric release

This chapter describes the evaluation of miscible blends of NREP with enteric and pH independent polymers to attain sustained gastric release of Cefuroxime axetil. Cefuroxime axetil has a short half life (2 hr), so sustained release formulations are desirable [13]. However its gelling tendency in presence of moisture and the limited absorption window make it difficult to attain sustained release. Further, blends of reverse enteric polymer with enteric polymers result in insoluble polyelectrolyte complexes and hence cannot be used in film coatings. The novelty of our work is that it provides a new set of polymer blends containing reverse enteric and enteric polymers capable of film forming which can be investigated for tailoring varied drug release patterns. The nature of interactions between blend constituents was established by analyzing FTIR spectra of blends. The extent of interaction has been investigated by thermal analysis and quantified in terms parameters K_1 and K_2 derived from the third power Schneider equation. Based on these values, the interactions between NREP and these polymers have been ranked in the order Zein < Ethylcellulose < Eudragit S < Eudragit L < Hydroxypropyl methylcellulose phthalate < Cellulose acetate phthalate. These investigations help interpret the drug release pattern from the blends based on the extent of interactions. The results of the mechanistic investigations provided a more rational approach to tailor polymer blends for drug release. The utility of the blends in sustained release of Cefuroxime axetil under gastric conditions over 3 hrs has been established. The details of polymer blends for drug delivery are discussed in patent application (A.R. Menjoge and M.G. Kulkarni, US 20050281874, Dec 2005).

Chapter 7: Mechanistic investigations contributing to the miscibility of NREP with enteric polymers

This chapter provides insights to achieve controlled hydrogen bonding in polymer-polymer blends to attain the desired extent of interactions needed to ensure miscibility without complexation. These investigations provided a rational basis to understand the miscibility in NREP-polymer blends and also led to a new set of polymer blends, which were subsequently investigated to achieve the desired release

rate. The structural attributes of NREP, which contribute to miscibility without complexation as seen in Eudragit E have been explained. A detailed investigation of the interactions between Eudragit E with enteric and pH independent polymers was undertaken. The effect of basicity, spacer length and structural defects provided an in depth knowledge on polymer structure affecting the extent of miscibility. The investigations reveal that miscible blends result as the extent of interaction between immiscible polymer blend increases. Further increase in interaction leads to complexation.

Chapter 8: Blends of NREP with fatty acids for enhancing drug release at gastric pH

This chapter describes the use of blends of fatty acids with NREP to enhance the release from the fatty acid based compositions. Fatty acids are largely investigated for taste masking applications. Fatty acids like stearic acid release the drug upon formation of soluble sodium salt in intestinal region. This restricts their application for drugs absorbed from gastric region. The blends of NREP with fatty acids provide gastric release of drugs. These formulations are highly hydrophobic and hence are very effective for taste masking. Pharmaceutical compositions containing Cefuroxime axetil and Ciprofloxacin using NREP-fatty acid blends were investigated for drug release at gastric pH. The formulations were made by emulsification solvent evaporation technique, spray drying and holt melt granulations. The advantage of using these formulations is that gastric release for both Cefuroxime axetil and Ciprofloxacin HCL is attained due to dissolution of NREP. The details of these blends for drug delivery are discussed in patent application (A.R. Menjoge and M.G. Kulkarni, PCT/IN04/ 00379).

Chapter 9: Enhancement of bioavailability by polymorphism inhibition

This chapter describes the polymer (NREP) attributes which inhibit conversion of amorphous Cefuroxime axetil to crystalline form. Certain drugs exist as polymorphs or are more bioavailable in an anhydrous or amorphous form and which pose the stability problems fall under this category. Therefore, stability of the drug from moisture and conversion from an unstable form to a stable form and moisture

permeability assessment and release enhancement efforts for the drug as an initial step in development of dosage form is often warranted. Cefuroxime axetil is more bioavailable in the amorphous form. The co-precipitation of Cefuroxime axetil and Celecoxib with low molecular weight polymer results in its crystallization at lower polymer loading. The high molecular weight NREP polymers were found to retain Cefuroxime axetil and Celecoxib in amorphous form thereby ensuring the bioavailability of these drugs. Further NREP is hydrophobic so it warrants the moisture protection of these drugs. The details of polymorphism inhibition are discussed in patent application (M.G. Kulkarni and A.R. Menjoge, US 20050136115, 23 June 2005).

Chapter 10: Conclusions and suggestions for future work

The important conclusions arrived at from the work are discussed in this chapter. Briefly these can be summarized as follows;

1. The polymer architecture affects the physiochemical properties like pH dependent behavior, glass transition temperature and the nature of its interactions. The choice of 4-vinyl pyridine as basic monomer contributes to acid solubility.
2. The charge density on the NREP, basicity of the 4-vinyl pyridine and self associations reduce the drug-polymer interactions between NREP and Cefuroxime axetil avoiding its degradation and inactivation thus ensuring drug release in biologically active form.
3. The encapsulation of Cefuroxime axetil by NREP thus provides site specific delivery for enhanced absorption with taste masking. Similarly other drugs like Ciprofloxacin HCl and Clarithromycin can be taste masked and released at the desired site.
4. It was demonstrated that blends of NREP with enteric polymers are capable of film coating. This provided a new set of polymer blends which can be further tailored to attain sustained gastric and intestinal release. These blends were found to be useful to attain sustained gastric release of Cefuroxime axetil.
5. High molecular weight NREP was found to be effective in polymorphism inhibition. NREP prevented the conversion of highly bioavailable amorphous form of Cefuroxime axetil into crystalline thereby retaining its bioavailability.
6. The self associations in NREP enhance the glass transition temperature making the polymer adaptable to pharmaceutical processes involving heat and enable ease of

storage. The self associations and charge density on the polymer suppress its biological reactivity, eliminating any adverse biological response rendering the polymer biocompatible.

This chapter also gives insights for the future scope of the work. Certain drugs exhibit interactions with anionic polymers resulting in delayed release. This is not desired as these drugs are expected to be released in the intestine. Since NREP is polybase its blending with enteric polymers can prevent the interactions between enteric polymers and cationic drugs. These assumptions need to be validated.

The use of NREP as a barrier coating material to protect the moisture sensitive drug needs to be evaluated. Normally seal coat with polymers such as shellac and ethyl cellulose is used to protect many of the moisture sensitive drugs. Apart from this, special packaging materials are used to restrict the moisture permeation. However the use enteric polymers or water resistant polymers, retards the release of the drug. NREP is hydrophobic in nature and its utility for such applications can be investigated.

References:

(1) S.B. Jaiswal and D.M. Bramhankar in Biopharmaceutics and Pharmacokinetics a Treatise, 1st Ed., Vallabh Prakashan, Delhi, India, 1995

(2) K. Klokkers-Bethke and W. J. Fischer. J. Control. Rel. 1991, 15, 105-112.

(3) S.S. Davis. J. Control. Rel. 1985, 2; 27-38.

(4) M.V. Risbud, A.A. Hardikar, S.V. Bhat, R.R. Bhonde. J. Control. Rel. 2000, 68, 23–30.

(5) N.J. Joseph, S. Lakshmi, A. Jayakrishnan. J. Control. Rel. 2002, 79, 71–79.

(6) R. Langer, L. G. Cima, J. A. Tamada, E. Wintermantel. *Biomaterials* 1990, 11, 738-745

(7) A.M Serajuddin, A.B. Thakur, R.N. Ghoshal, M.G.Fakes, S.A. Ranadive, K.R. Morris, S.A. Varia. J. Pharm. Sci. 1999, 88, 696-704.

(8) A.Finn, A. Straughn, M. Meyer, J.Chubb. Biopharm. Drug Disposit. 1987, 8, 519-526.

(9) C. J. Campbell, L. J. Chantrell, R. Eastmond. Biochem. Pharmacol. 1987, 36, 2317–2324.

(10) Ceftin Prescription Information, Physicians' Desk Reference 2003

(11) M.LL. Lorenzo-Lamosa, M. Cuna, J.L. Vila-Jato, D.Torres, M. J Alonso. J. Microencap. 1997,14, 607-616.

(12) M. Cuna, M. L. Lorenzo-Lamosa, J. L.Vila- Jato, D.Torres, M. J. Alonso. Drug Dev. Ind. Pharm. 1997, 23, 259-265.

(13) H. Sen, R. S. Kshirsagar and A. R. Menjoge, US Patent 6,932,981 B2, Aug 23 2005

CHAPTER 1

Introduction & Motivation

1.1. INTRODUCTION

The most convenient route of drug administration is peroral. To reach their target, drug molecules have to be absorbed from the gastrointestinal tract and enter the systemic circulation in sufficient quantities [1]. To exert an optimal therapeutic action the drug should be delivered to its site of action at an effective concentration for the desired period. To allow reliable prediction of the therapeutic effect, the performance of the dosage form containing the active substance should be well characterized. The concept of bioavailability was introduced by Oser *et al* in 1945 [2], however its importance was recognized and discussed, as a result of several therapeutic misadventures related to differences in bioavailability (e.g. digoxin, phenytoin, primidone [1,2]. A change in formulation resulted in decreased bioavailability of digoxin in Britain [3] and phenytoin intoxication in Australia [2]. In 1966, FDA found that of 4000 formulations available in USA, more than 300 were ineffective [2]. These events testified the necessity of testing the performance of dosage forms in delivering the drug to the systemic circulation and thereby to the site of action. Thus the bioavailability of an active substance from a pharmaceutical product should be known and reproducible.

"Bioavailability" is defined as the rate and extent of drug absorption [1, 4, 5]. Any alteration in drug bioavailability is reflected in its pharmacologic effects. To attain the desired therapeutic objective, the drug has to be delivered at an optimal rate and amount. By proper biopharmaceutic design, the rate and extent of drug absorption or systemic delivery of drug to the body can be varied from rapid and complete absorption to slow and sustained absorption depending upon the desired therapeutic objective [5,6].

Three major approaches to enhance bioavailability are the *Pharmacokinetic* approach, the *Biological* approach and the *Pharmaceutic* approach [5]. The *Pharmacokinetic* approach involves alteration in chemical structure of drug. However this approach has several drawbacks, as it is very expensive, time consuming, requires repetition of clinical trials and regulatory approval. The *Biologic* approach is based on changing the route of administration from oral to parenteral where the drug is directly administered into systemic circulation. The disadvantage with this approach is that it

reduces the patient compliance. Hence the *Pharmaceutic* approach which involves modification of the formulation, manufacturing process or physicochemical properties of drug without changing the chemical structure, is the most preferred. The attempts, whether optimizing the formulation, manufacturing process or physicochemical properties of drug, are mainly aimed at enhancement of dissolution rate of drug as it is the rate-limiting step in absorption of most drugs.

One of the dosage form design consideration is that the delivery system should be capable of releasing the drug at its site of absorption to ensure bioavailability. In case of drugs with limited absorption site, special consideration on selection of excipients capable of attaining this is essential to ensure bioavailability. The formulation strategies need to be explored for drugs which undergo physical changes in the dosage form on co-processing with excipients or contact with physiological fluids. Rational choice of excipients, which address these intricate issues, is essential to ensure bioavailability. However the existing excipients cannot address the complex problems arising out of the physicochemical and biopharmaceutical properties of specific drug molecules. Further the adverse drug-excipient interactions restrict the choice of excipients. The use of alternative excipient or blend of excipients is often sought to address these limitations. At times these approaches result in compromising the bioavailability.

The objective of the present investigation is to develop a new excipient ensuring site specific delivery, enhancing dissolution without drug inactivation and capable of stabilizing the physical form of drug during co-precipitation and in solid state, thus ensuring bioavailability.

This chapter highlights the importance of dosage form factors especially the influence of excipients on oral bioavailability of drugs. The drug-excipient interactions affecting bioavailability, limitations of existing excipients, restricted choice of excipients and its influence on formulation development, need for excipients having added functionality and the considerations in development of new excipients are described. More specific literature related to the facets of excipient development, blends of excipients and their use for attaining rapid, sustained and site specific release dealt with in each chapter, is included appropriately.

1.2. THEORY AND REVIEW OF LITERATURE

1.2.1. Biopharmaceutic considerations in dosage form design

Drugs obtained from any source such as plant, animal or mineral sources or synthesized chemically are rarely administered in their pure chemical form. They are combined with number of inert substances (excipients / adjuvants) and transformed into convenient dosage form that can be administered by suitable route [7]. Earlier it was believed that therapeutic response to drug is an attribute of its intrinsic pharmacologic activity. But, today it is well established that dose response relationship obtained after drug administration by different routes like oral and parenteral, are not the same. Variations are observed when the same drug is administered in different dosage forms or similar dosage form but different compositions [5]. These variations largely depend on the physiochemical properties of drug, the excipients present in dosage forms and method of formulation of the drug.

The therapeutic effectiveness of the drug depends on the ability of the dosage form to deliver the drug to its site of action at a rate and amount sufficient to elicit desired therapeutic response. This attribute of the dosage form is referred to as physiologic availability, biologic availability or simply bioavailability. For most drugs the pharmacologic response can be related directly to the plasma levels of the drug. Thus the term 'Bioavailability is defined as the rate and extent (amount) of absorption of unchanged drug from its dosage form [5]. A drug that is completely but slowly absorbed may fail to show therapeutic response as plasma concentration for desired effect is never achieved.

The rate or rapidity with which the drug is absorbed is an important consideration when rapid onset of action is desired, also the slower absorption rate is desired if the aim is to prolong the duration of action. An oral drug delivery system providing a uniform drug release can only partly satisfy the therapeutic and biopharmaceutical needs, as it does not take in to account site-specific absorption rates within the gastrointestinal tract [8]. A drug delivery system guaranteeing site and rate specific delivery is needed to release locally effective drugs at their target site, to

achieve either a prolonged effective plasma level or to provide a pulsed release. For oral therapeutic use this means the creation of dosage form, delivering the drugs during their gastrointestinal transit at the right time and at right site at therapeutically optimal rate [8]. Drug absorption at right rate means, reaching the effective plasma level within an acceptable short time period, avoiding overshoot in rapidly absorbed drugs and finally, maintaining the effective plasma level. To supply drug at the right site means on one hand delivering locally effective drugs like antibiotics, anti inflammatory or cytostatic agents only at their target site, or releasing drugs with restricted absorption at their absorption window (Digoxin, Ampicillin, Ciprofloxacin, Cefuroxime axetil, Levodopa, Metformin and Captopril etc) [8, 9, 10].

To attain the desired therapeutic effectiveness without alteration in drug bioavailability, the design and evaluation of delivery systems for gastrointestinal tract requires the knowledge of three inter-related topics, *the drug*, *the delivery system* and the *destination intended* [11]. Each of these is inter-related to the other and it is essential to consider all aspects and constraints for successful development of new system ensuring the bioavailability and therapeutic efficacy.

The series of events arising after the oral administration of dosage forms like tablet or capsule are shown in Fig. 1.1 The drug has to dissolve at the absorption site and unless the drug goes into solution it cannot be absorbed into systemic circulation.

"Drug absorption" is defined as the process of movement of unchanged drug from site of administration to systemic circulation [5]. The principle mechanism for the drug absorption is passive diffusion. The other mechanisms include pore transport, facilitated / carrier mediated diffusion, active transport, ion pair transport and endocytosis. The driving force for the passive diffusion is the difference in drug concentration across the cell membrane and 90 % of the drugs are absorbed by this mechanism and it is the major process for absorption [5]. The rate determining steps in drug absorption are shown in Fig.1.2.

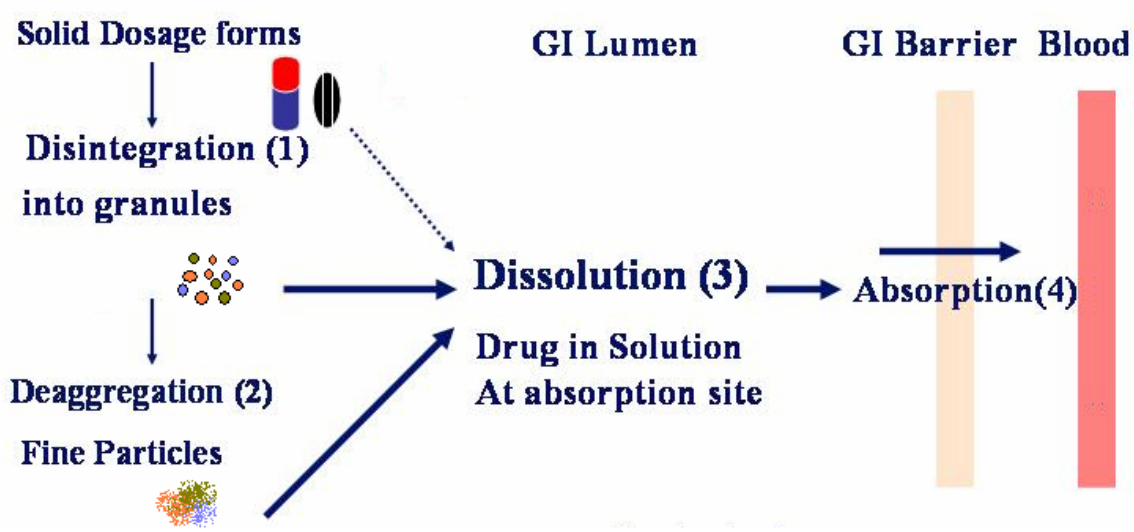

Fig.1.1. Series of events arising after the oral administration of a dosage forms ***adapted from Ref [5].***

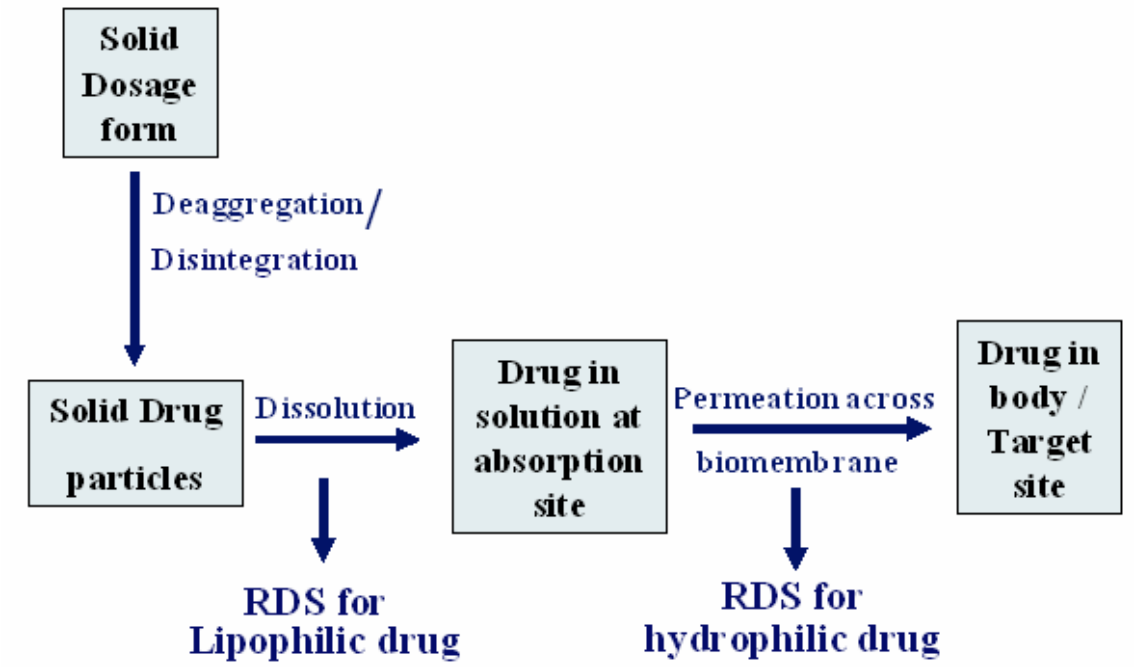

Fig.1.2. Rate - determining steps in absorption of drugs administered orally ***adapted from Ref [5]***

1.2.2. Factors affecting systemic absorption

The therapeutic effect of a drug depends on the concentration of drug at the site of action. The absorption of the drug into the systemic circulation is a prerequisite to reach the site of action for all drugs, except those drugs that are applied at the site of action, or those that are intravenously injected. After oral administration, many factors determine the bioavailability. Since only dissolved drug can pass the gastrointestinal membrane, dissolution is one of the critical factors [5]. However, drug metabolism in the intestinal lumen, the intestinal wall and the liver may also reduce its bioavailability. In general it can be stated that the rate of absorption, therefore the onset and extent of the clinical effect, is determined by the dissolution of the drug and the subsequent transport over the intestinal membrane and passage of the liver. These two aspects form the basis of the Biopharmaceutical Classification System (BCS), which is incorporated in the guidelines of the Food and Drug Administration (FDA) [4].

1.2.2.1. Biopharmaceutical classification (BCS) of drugs

Amidon and co-workers [12-14] put forth that the fundamental parameters controlling the rate and extent of oral drug absorption were the aqueous solubility of the drug and gastrointestinal permeability. They devised a Biopharmaceutics Classification System (BCS) that categorized drugs into four classes according to solubility and permeability (expressed as the extent of oral drug absorption) as depicted in Table 1.1. At its core, the BCS is an experimental model, centrally embracing permeability and solubility, with qualifications related to pH and dissolution [14]. The background of this classification is the understanding that dissolution from the dosage form depends considerably on the solubility of the drug and that absorption from the GI tract is dependent on permeability properties of the drug. However, dissolution is also affected by the biopharmaceutical characteristics of the formulation and absorption from the intestine may be influenced by certain ingredients (e.g. those modifying GI transit or membrane permeability) [13].

Table 1.1 Drug classification according to BCS

Class	Solubility	Permeability
I	High	High
II	Low	High
III	High	Low
IV	Low	Low

1.2.2.2. Strategies to increase drug absorption

From the classification it is evident that, depending on the class of the drug, different strategies can be applied to increase or accelerate the absorption of a drug: either increasing the permeability of the absorbing membrane or increasing the amount of dissolved drug that is in contact with the absorbing membrane (ergo the driving force for the absorption process). The examples of various drugs based on this classification are given in Table 1.2.

Class I

Class-I drugs dissolve rapidly in an aqueous environment and are rapidly transported over the absorbing membrane. Hence do not need any formulation strategies to increase their absorption. When the release of the active from the formulation is slower than the gastric emptying rate, good in-vitro-in-vivo-correlation (IVIVC) can be expected [15].

Class II

The strategy to enhance absorption (rate) of class-II drugs having dissolution limitations but no permeation limitations is to increase the amount of dissolved drug molecules at the absorption site. This has proven to be effective in many studies. This strategy is useful as long as permeation is not limiting. The absorption can be enhanced by accelerating dissolution. Class-II drugs show IVIVC as long as the *in-vivo*

dissolution rate is same as *in-vitro*. However, because the dissolution rate is critical for class-II drugs, the in-vivo absorption can be affected by several physiological fluctuations, like the volume and pH of the intestinal juices, the presence of bile salts, food, enzymes, and bacteria, the motility of the gut and the viscosity in the gut lumen [15].

Class III

For Class-III drugs, the permeation across the membrane is rate limiting. The strategy for class-III drugs is to increase the permeability of the absorbing membrane. Rapid dissolution is particularly desirable in order to maximize the contact time between the dissolved drug and absorption mucosa. Therefore, the duration of dissolution should be at least as stringent for class III drugs as for class I drug. Furthermore, Class III drugs exhibit a high variability in rate and extent of absorption, but if dissolution is fast such that 85% of drug dissolves in 15 minutes, the variation could be attributed to GI transit, luminal contents, and membrane permeation rather than dosage form factors [15].

Class IV

For a class-IV drug, both dissolution as well as permeability must be increased. However, increasing dissolution is more effective than increasing the permeability because in practice the amount of dissolved drug at the absorption site varies over six orders of magnitude (0.1 µg/l to 100 mg/l) whereas permeability varies over only a 50-fold range. Therefore, the potential to increase the absorption by increasing the drug concentration is greater, and it is more practical to increase the solubility even if permeability is further compromised. For Class-IV drugs, no IVIVC can be expected. It is up to the formulation scientist to increase the extent of absorption and also to improve the IVIVC. This will reduce the patient-to patient variability and improve the bioavailability and the predictability of pharmacokinetic parameters.

Table 1.2 BCS classification of drugs

Class	**Examples** *[ref 14,16, 17]*
I	Abacavir, Ketorolac, Albuterol, Ketoprofen ,Acetaminophen, Labetolol, Allopurinol, Levamisole, Amitryptyline, Chlorpheniramine, Levodopa, Antipyrine, Lidocaine, Buspirone, Meperidine, Caffeine, Metoprolol, Chloramphenicol, Metronidazole, Midazolam, Codeine, Minocycline, Colchicine, Misoprostol, Cyclophosphamide Morphine, Desipramine, Nifedipine, Dexamethasone, Phenobarbital, Diazepam Phenylalanine, Diltiazem, Prednisolone, Diphenhydramine, Primaquine, Disopyramide Promazine, Doxepin, Promethazine, Enalapril, Propranolol, Ergonovine, Pyranzinamide, Ergotamine, Quinidine, Ethinyl estradiol Quinine, Fluoxetine, Rosiglitazone, Hydralazine Theophylline, Imipramine Valproic acid, Isoniazid Verapamil, Isosorbid dinitrate Zidovudine
II	amiodarone HCl, atazanavir sulfate, atorvastatin, azithromycin, benazepril HCl, bicalutamide, candesartan cilexetil, carbamazepine, carisoprodol, carvedilol, celecoxib, clarithromycin, diazepam, divalproex sodium, docetaxel, donepezil HCL, efavirenz, etodolac, ezetimibe, fenofibrate, finasteride, gemfibrozil, glimepiride, glyburide, ibuprofen, indapamide, indomethacin, irbesartan, ketoconazole, lansoprazole, loratadine, lovastatin, meclizine HCL, metaxalone, moxifloxacin HCl, mycophenolate mofetil, nabumetone, nelfinavir mesylate, olmesartan medoxomil, pioglitazone HCl, prednisone, raloxifene HCl, risperidone, ritonavir, rofecoxib, simvastatin, spironolactone, tacrolimus, temazepam, valdecoxib, valsartan, ziprasidone HCl.
III	albuterol, alendronate sodium, amlodipine besylate, amoxicillin, atenolol, baclofen, buspirone HCl, captopril, carboplatin, ceftriaxone, ciprofloxacin, ciprofloxacin hcl, colchicine, fluconazole, folic acid, gabapentin, gemcitabine HCl, granisetron HCl, hydrochlorothiazide, hyoscyamine sulfate, lamivudine, lamotrigine, levetiracetam, levofloxacin, ciprofloxacin, lisinopril, metformin HCl, metronidazole, minocycline HCl, morphine sulfate, niacin, oxaliplatin, oxycodone HCl, oxycontin, penicillin VK, progesterone, ranitidine, risedronate sodium, rosiglitazone, sumatriptan, terazosin HCl, thalidomide, timolol maleate, topiramate, valacyclovir HCl, zoledronic acid, zolpidem.
IV	acyclovir, aspirin, cefdinir, cefprozil, cephalexin, clindamycin HCl, doxycycline hyclate, famotidine, felodipine, furosemide, glipizide, linezolid, methocarbamol, methotrexate, nifedipine, nitrofurantoin, olanzapine, oxcarbazepine, phenobarbital, sildenafil citrate, tadalafil, temozolomide, tetracycline, theophylline

1.2.3. The difference between absorption and bioavailability

Literature reveals that the terms drug absorption and bioavailability are very closely associated and both are used in discussions on drug administration. Although strongly interrelated, the two are essentially different. Absorption refers to transport over the absorbing membrane at the site of administration, whereas bioavailability is related to drug concentration in the systemic blood circulation. When the concentration in the blood plasma is measured as a function of time, the area under the curve represents the absolute bioavailability. The relative bioavailability, often reported in drug absorption studies, is calculated based on comparison with the bioavailability after intravenous injection. Bioavailability is affected by the intestinal and hepatic blood clearance of the drug. When the rate of clearance is linearly dependent on the blood concentration, absorption and bioavailability are proportionally related. However, when clearance processes take place via active secretion or via enzymatic metabolism, they can become saturated. In that case, intestinal and hepatic clearance depends on the blood concentration in a non-linear way or change in time, which results in non-linear pharmacokinetics. When, in this situation, the absorption of a drug is increased to a certain extent, the bioavailability can increase more than proportional. Therefore, doubling the absorption can result in a more than double bioavailability.

1.2.4. Consequences of low bioavailability

The scientists involved in search of new drugs are often challenged to attain and optimize oral bioavailability, just as they optimize efficacy and safety. Complete oral bioavailability is desirable for both clinical and economic reasons [18]. Low oral bioavailability is associated with greater intersubject variability of plasma concentrations and, hence, poorer control of the effects of the drug. To achieve systemic bioavailability, the drug must also avoid pre-systemic intestinal and hepatic metabolism and hepatic extraction to the bile. Much of the drug is wasted if bioavailability is low, thus presenting a certain economic disadvantage for costly drugs. The optimization of oral bioavailability begins at the compound selection stage, a process that includes

evaluation of the potential for oral bioavailability in humans. The optimization process includes evaluation of the influence of formulation on bioavailability, beginning with the dosing vehicle used for the initial animal studies and continuing throughout formulation development. The effects of salt and physical form on absorption are also important considerations. For a drug to be absorbed from the GI tract, the dose must dissolve or be in solution in the GI fluids, and the drug must be capable of permeating the intestinal epithelial membrane.

1.2.5. Factors influencing bioavailability

The various factors affecting the rate and extent of drug absorption include the pharmaceutic and patient related factors [5]. The patient related factors are anatomical, physiological characteristics such as age, gastric emptying time, gastrointestinal pH, pathological / disease state, gastrointestinal contents and pre-systemic metabolism. The patient related factors are subject to variation and beyond control. However the pharmaceutical factors related to the physicochemical properties of drug and dosage form can be altered to enhance the drug absorption and bioavailability.

1.2.5.1. Physicochemical properties of drug

f) Drug solubility and dissolution rate

The events that follow oral administration of an immediate release dosage form are shown in Fig.1.1.The two possible rate determining processes in absorption of orally administered drug are

1) rate of dissolution, and
2) rate of drug permeation through biomembrane

The aqueous solubility of a drug is an important factor affecting its bioavailability. For a drug to pass through biological membrane it must be soluble in water. If the solubility and rate of dissolution of an enterally administered drug are too low, it will result in excretion of major portion of the drug without its passage from the

gastrointestinal tract into the systemic circulation [19]. The slow dissolution rate exhibited by poorly water-soluble drugs is a major challenge in the drug development process. Following oral administration, these drugs generally show erratic and incomplete absorption which may lead to therapeutic failure [20]. Poor oral bioavailability for many drugs is thus attributed to poor solubility in the gastrointestinal fluids, poor gut membrane permeability and/or extensive hepatic first-pass elimination [21]. The virtual insolubility of gliquidone in water results in poor wettability and dissolution characteristics, which may lead to a variation in bioavailability [22]. Griseofulvin is a poorly soluble drug and efforts have been made to improve its wettability to enhance its dissolution and oral bioavailability [20] Solubility must be considered in combination with permeability and dose. Some very poorly soluble compounds are well absorbed because their permeabilities are high and the dose is low.

In case of hydrophobic drugs, it is the dissolution process, which acts as the rate-controlling step and therefore, determines the rate and degree of absorption. Consequently, these drugs show erratic and incomplete absorption from the gastrointestinal tract of animals and humans. Thus, one of the major challenges to drug development today is poor solubility, as an estimated 40% of all newly developed drugs are poorly soluble or insoluble in water [23]. In addition, up to 50 % of orally administered drug compounds suffer from formulation problems related to their high lipophilicity [24]. As a result, much research has been conducted on methods of improving drug solubility and dissolution rates to increase the oral bioavailability of hydrophobic drugs.

g) Particle size / effective surface area of drug

Surface are and particle size of drug are inversely related. The absolute surface area is the total area of solid surface of any particle and the effective surface area is area of the solid surface exposed to dissolution media. According to Noyes-Whitney equation the dissolution rate is directly proportional to the effective surface area of drug and hence influences the dissolution and absorption rate [25]. Particle size reduction results in subsequent increase in surface area of drug contributing to faster dissolution.

Myriad of methods for size reduction are adopted to increase the dissolution ergo the absorption and bioavailability.

h) Salt form of drug

Most drugs are either weak acids or weak bases [5]. The most favored means to enhance the solubility and dissolution of these drugs is to convert them to salt forms. The principle of in-situ salt formation is exploited to enhance the dissolution and absorption of drugs like aspirin and penicillin. Buffered tablets of these drugs result in enhanced bioavailability. Selection of appropriate salt form for enhanced dissolution is paramount. In case of theophylline the choline and isopropanolamine salts show 3-4 times rapid dissolution than ethylenediamine salt and exhibit better bioavailability.

i) Drug stability

During the shelf life or in GIT the drugs may destabilize. Two major stability problems resulting in poor bioavailability of orally administered drug are degradation of drug into inactive form and interaction with one or more components either of dosage form or those present in GIT [5]. This results in complexation of drug contributing to poor dissolution and reduced absorption. The destabilization of the drug is discussed in detailed in the formulation factors affecting bioavailability in section 1.2.5.2.

j) Polymorphism

Often a chemical substance exists in different ordered states [26]. This is referred to as polymorphism. The polymorphic form, in which the drug is present, is often influenced by the processing techniques. It is well known that differences due to polymorphism and pseudo polymorphism observed in drugs, are critical because physical and chemical properties of different crystalline form influence their bioavailability. Although polymorphs of a substance share the same chemical formula, difference in crystalline structure can affect the physiochemical parameters of the

substance such as, solubility, dissolution rate, density which in turn affect its important pharmaceutical properties such as bioavailability, stability as well as choice of formulation technology for developing dosage forms [27-31]. Drugs like Carbamazepine are better absorbed in anhydrous and amorphous form and the conversion to the crystalline, dihydrate form leads to lower solubility and also lower bioavailability [31, 32]. The order of dissolution of the different solid forms of drug is amorphous > metastable > crystalline.

k) Lipophilicity and drug absorption

The absorption of the drug across the biomembrane is influenced by the dissociation constant (pKa). As the value of pKa increases, a proportional increase in amount of drug absorbed is seen [5]. The degree of ionization of a drug at physiological pH is governed by its pKa value. An unionized drug if sufficiently lipid soluble, is absorbed into systemic circulation. For optimum drug absorption, sufficient aqueous solubility along with adequate lipid solubility is prerequisite. The rate of dissolution of a drug can be altered by changing the physical properties like particle size, crystalline structure. However, the permeability is promoted by modification in chemical structures *e.g*. prodrugs.

Cefpodoxime proxetil (CP) is a prodrug, third generation cephem type broad-spectrum antibiotic, administered orally. It exhibits a pH dependent solubility behavior, with highest solubility in acidic pH conditions, and the solubility falls as the pH increases. CP is absorbed from the intestinal tract after oral administration and hydrolyzed to its parent moiety cefpodoxime acid by nonspecific esterases in the intestinal wall/plasma. The drug is absorbed throughout the GIT, and shows relatively more bioavailability in fed conditions than fasted conditions [33]. Yet the bioavailability is 50 % as compared to the intravenous administration of sodium salt. Hence various formulation aspects are being explored to enhance the oral bioavailability of this drug.

1.2.5.2. Dosage form factors affecting drug bioavailability

I) Dosage form design: factors to be considered

A variety of dosage forms are available these days. Differing physical properties of actives and excipients often leads to an uneven distribution and alteration in drug delivery to the target site [34]. This entails the consideration of following factors in dosage form design to ensure bioavailability of the drug.

The First-pass effect

Bioavailability is significantly impaired if the release rate is retarded for drugs that suffer from an extensive first pass effect.

The absorption site

If the absorption site is limited, absorption is likely to decrease, and variable bioavailability will result for typical prolonged-release dosage forms.

Adverse reactions

Undesirable adverse reactions may develop by prolonging drug release.

Drug-excipient interaction

Preformulation studies should be undertaken to avoid the undesirable drug-excipient interactions resulting in alteration of drug structure and its bioavailability.

II) Nature and type of dosage form

A 2 to 5 fold difference in bioavailability of drug is observed depending on the nature and type of dosage form. This difference is attributed to the relative rate at which the particular dosage form releases the drug in the biological fluids. The relative rate at which the drug is released in the body fluids, is governed by the complexity of the dosage form. As the complexity of the dosage form increases, the nature of rate limiting step will differ and lead to different bioavailability problems.

The bioavailability of a drug from various dosage forms decrease in the following order: solutions> emulsions> suspensions> capsules> tablets> coated tablets> enteric coated tablets> sustained release products [5]. However there are certain exceptions to this sequence and at times the physicochemical properties of drug influence its dissolution from dosage form. In case of the poorly wettable drug Proquazone, dissolution from tablet at all drug loads is faster than from capsule formulation [34]. Normally the absorption of drug is fastest from solution with least bioavailability problems whereas absorption is slowest from sustained release product with greatest potential for bioavailability related problems. As exceptions, some highly specialized controlled release products boast of enhanced bioavailability e.g. OROS® osmotic technology. ALZA Corporation pioneered the transformation of the standard pharmaceutical tablet into an advanced drug delivery system with its OROS® osmotic technology. By targeting specific areas of the gastrointestinal tract, OROS® technology is capable of providing more efficient drug absorption and enhanced bioavailability. L-OROS® technology is capable of enhancing the bioavailability of drugs with low solubility (http://www.alza.com/alza/oros).

III) Disintegration time

The *in-vitro* disintegration of the drug is not a measure of its bioavailability. However if the dosage form does not comply the disintegration test, it portends the bioavailability problems as the subsequent drug dissolution would be slowed and affect the rate of absorption. The dissolution rate of a drug from a tablet is influenced by

physico-chemical properties of the drug itself and the disintegration of the tablet [36]. Najib and Jalal reported that dissolution is a direct function of tablet disintegration [37]. Abrahamsson et al. put forth that delay in tablet disintegration was responsible for the slower dissolution of drugs [38]

IV) Manufacturing and processing variables

In case of conventional solid dosage forms, the drug dissolution is the single most important factor in drug absorption. The factors that affect the influence the drug dissolution from these dosage forms include the effect of granulation method, compression force in case of tablets and the intensity of packing in capsules. The excipients used such as binders, lubricants, disintegrants and film forming or coating polymers also influence the drug dissolution and stability.

a) Method of granulation

Different methods are used for granulation and each technique has appreciable effect on the drug release profile which was ranked in the order direct compression< dry granulation< wet granulation (alcohol) < wet granulation (water) by Thapa et al [39]. The wet granulation affects the dissolution since causes association of residual water with drug particles in the solid state. This residual water may i) lead to formation of crystal bridge ii) initiate chemical reactions such as hydrolysis affecting drug stability iii) necessitate longer drying periods not desirable for the thermolabile drugs [5, 40].

b) Compression force

The compression force employed during the tableting process affects the density, porosity, hardness, disintegration time and dissolution of the tablets. Marcos et al reported that effect of compression force was profound on the dissolution efficiency of Furosemide tablets than the amount of polymer used [41]. The higher compression

force increases the density, hardness of tablet with reduction in porosity, inhibiting the penetration of fluids all contributing to slower dissolution.

c) Intensity of packing

The diffusion of gastric fluids into the capsule creates high pressure within it resulting in rapid bursting with subsequent drug dissolution. If very fine particles are very intensely packed they cause poor drug release due to lower wetting and poor penetration of gastric fluids.

d) Formulation factors: effect of excipients

A pharmaceutical dosage form generally consists of a drug substance combined with a varying number of excipients that have been added to the formulation to facilitate its preparation and function as a drug delivery system [42]. Many new drug candidates exhibit poor solubility and stability. The function of excipients is to define a formulation that is physically and chemically stable, manufacturable, and bioavailable [43]. The excipients may function as a stability enhancer and therefore they should protect, support, or enhance stability or bioavailability of formulation [44].

Excipients are also known as promoters of the degradation of drug. Functional groups or residues in excipients can have the propensity to interact with drug molecules [42]. Physical changes induced by excipient interactions in the formulation lead to altered dissolution or other delivery properties of the final dosage form [42]. Until the 1960s, new drug substances were formulated by pharmaceutical scientists into seemingly good dosage forms, which often turned out to degrade chemically during storage. Surprises regarding these changes in the drug's form often led to serious issues regarding bioavailability and stability. Ever since these changes in drug induced by drug-excipient interactions became apparent, considerable investigation is carried out before the formulation of dosage form, to identify key problems. This early, drug-excipient interaction and dosage form characterization work became known as preformulation [34]. Preformulation studies play significant part in anticipating formulation problems,

identifying the limits and interactions between drug and excipients [42]. Drug-excipient interaction study at an early stage of product development is an important exercise in the development of a stable dosage form [45].

1.2.6. Pharmaceutical Excipients: *influence on dissolution, absorption & bioavailability*

The International Pharmaceutical Excipients Council (IPEC) has defined pharmaceutical excipients as any substance other than the active drug or prodrug which has been appropriately evaluated for safety and are included in a drug delivery system to either 1) aid processing of system during its manufacture, or 2) protect, support or enhance stability, bioavailability, or patient acceptability, or 3) assist in product identification, or 4) enhance any other attribute of the overall safety and effectiveness of the drug during storage or use [46]. Pharmaceutical excipients for solid dosage forms are classified (IPEC) according to the function they perform in a pharmaceutical dosage form, although many excipients perform multiple functions [42]. The quality of the final product will be as dependent on the way in which the components are combined as it is on the components selected. Principal excipient classifications according to their functions are the following:

- Binders
- Disintegrants
- Fillers (diluents)
- Lubricants
- Glidants (flow enhancers)
- Compression aids
- Colors
- Sweeteners
- Preservatives
- Flavors
- Film formers/coatings
- Printing inks
- Suspensing/dispersing agents/surfactants

1.2.6.1. Drug- excipient interactions

Excipients have been traditionally thought of as being inert. However experience has taught that they can interact with a drug affecting its absorption and bioavailability [47]. Indeed, some excipients are added to a formulation specifically to take advantage of the interaction when it influences the bioavailability of the drug but this is not always the case. Crowley [48] has stated that excipients are better known as promoters of degradation than as stabilizers of drug. This is not surprising since functional groups or residues in excipients have the propensity to interact with labile active ingredients, with attendant loss of molecular integrity or other changes in quality.

Drug substances at times are fragile entities and environmental stresses and those associated with converting a drug into dosage form, all have the potential to cause changes that compromise quality. Such stresses cause molecular composition of drug to change to some extent. This reduces the amount of active ingredient in the dosage form and generates new molecular entities that could compromise safety. Physical changes can lead to altered dissolution or other delivery properties. Sedimentation in liquid products, consequent to altered solubility, could present safety as well as efficacy problems. Preformulation studies should identify propensity for change on the part of the drug substance and clarify the strategy for development of the dosage form. Drug–excipient compatibility studies might further constrain or clarify the options for formulation. Those found to inactivate the drug can be excluded. ***Such 'avoidance' tactics might suffice for many dosage form development programs, but not in all cases*** [48].

1.2.6.2. General considerations: Excipient-drug interaction

The potential for excipients to prevent or retard degradation will be determined by the factors that cause the molecular transformation of drug substances and these include [48]:

- environmental components, such as water vapour and sunlight;

- stresses during conversion to the dosage form, such as size reduction, compaction or sterilizing processes
- interactions between adjacent molecules of a drug, or between functional groups on the same molecule

For the excipients to act as stabilizers they must obviate or attenuate such effects.

1.2.6.3. Processes affected by drug–excipient interactions

Most of the drug-excipient interactions affect the processes of disintegration and / or dissolution and in case of extremely adverse interactions the biological activity of the drug may be altered affecting the bioavailability.

a) Disintegration

A drug–excipient interaction that results in inadequate or very slow disintegration of a drug product will reduce the bioavailability of the drug if disintegration is a rate-limiting step in its absorption. Kaojarern et al [49] investigated the bioavailability of six commercial formulations of the antihelmintic agent praziquantel. Of the six formulations investigated, one of the generic products showed only 69 % bioavailability and this was attributed to failure of disintegration and subsequently poor dissolution. The effect of 30 % reduction of bioavailability may lead to unacceptably high rates of treatment failure and such. Formulation of sulphadimidine with disintegrants like Primogel, Veegum, Amberlite resulted in decrease in disintegration time and dissolution rate and this was found proportional to the binding efficiency of sulphadimidine with these disintegrants [48, 50]. Slow dissolution of Oxymorphone was observed in formulation containing croscarmelose sodium resulting from interaction between the two [51].

b) Dissolution

Drug–excipient interactions that alter dissolution have a significant impact on absorption especially in case of lipophilic drugs where dissolution is the rate-limiting step [48]. *In-vitro* dissolution test on ten formulations of phenylbutazone showed that the dissolution of two formulations was adversely affected by the interaction of drug with excipients. This resulted in low bioavailability for the drug. Interaction of indomethacin and warfarin with Eudragit E causes delayed release of these drugs [52, 53]. Chitosan interacts with salicylic acid forming a salicylate salt causing delayed release of salicylic acid [54].

c) Loss of biological activity: consequence of drug degradation

Acetyl salicylic acid is degraded by magnesium stearate forming salicylic acid, salilsalicylic acid and acetyl salilsalicylic acid [55, 56]. The proton pump inhibitor Omeprazole was found to degrade in presence of enteric polymers due to interaction with the acidic groups from polymer. Riedel and Leopold [57] arranged the polymers in the order of the interaction exhibited with omeprazole as Eudragit L-100> HPMCAS-HF>shellac. The formulation of H_2 – receptor antagonist, Cemitidine with excipient mannitol resulted in reduced transit time in small intestine leading to reduced bioavailability [58].

1.2.6.4. Mechanisms of drug–excipient interactions

The key to a successful formulation is to understand the API, the excipients and the process, and in particular, their limitations. Excipient functionality is linked inextricably to the formulation and process, and all formulations are different, functionality per se is a matter for the excipient user and supplier. The excipient functionality may benefit one formulation but the same be regarded as dysfunctionality in another formulation [59].

Excipients form the greater mass in usual oral formulation and they contain functional groups that may give rise to chemical and physical transformations. The interactions normally occur between the excipient and drug rather than amongst the excipients used [60]. The physical interaction modifies the speed of dissolution or the uniformity of the dosage of formulation. Indeed some excipients are used to adsorb the drugs to enhance their wettability and dissolution rate. The contrary effect may be encountered when the forces of attraction are strong in which case the drug is released with difficulty and absorption is compromised. The most common example is use of lipophilic lubricant magnesium stearate which when finely dispersed with drug slows down the dissolution and therefore bioavailability [60]

a) Complexation

Complexing agents interact, usually reversibly, with a drug to form a complex [61]. The drug complex will dissociate upon coming into contact with GI fluids, releasing the drug substance, which can then be absorbed across the GI membranes. Complexing agents such as cyclodextrins are often used to increase the rate and extent of drug dissolution, ergo the bioavailability of poorly water soluble or unstable drugs [62].

Complexation of a drug is also reported to cause decreased bioavailability [47]. The antibiotic tetracycline forms an insoluble complex with calcium carbonate, which results in slower dissolution and lower absorption. The anti-epileptic drug phenobarbital forms an insoluble complex with PEG 4000. This causes decreased dissolution and decreased absorption to approximately one-third of that for phenobarbital alone [47].

b) Adsorption

Adsorption of drugs onto the excipients results in increased dissolution and bioavailability. There are also incidences where the dissolution is retarded and hence the bioavailability is reduced. Dicumarol a weakly acidic drug, on adsorption to magnesium oxide and hydroxide forms a more readily absorbable magnesium-chelate

[63]. Adsorption of drug molecules can render the drug unavailable for dissolution and diffusion and this might, in turn, reduce bioavailability [61]. Colloidal magnesium aluminum silicate, aluminum hydroxide, starch and talc when used in dicumarol formulations a decrease in absorption of dicumarol was attributed to the adsorptive properties of these excipients [63] Potential bioavailability problems were identified for chlorpromazine due to adsorption of chlorpromazine to the surface of talc and kaolin resulting in reduced membrane permeability [64].

c) Chemical interaction

Several different types of chemical drug–excipient interactions have been reported in the literature. These interactions can have a profound effect on the safety, efficacy and bioavailability of the drugs. At times these interactions cause complete inactivation of drugs severely affecting bioavailability and sometimes leading to severe toxicity. The potential consequences of drug-excipient interaction are evident from the misadventures in 1960s in Australia due to Phenytoin toxicity [2, 47]. The change from one formulation of Phenytoin containing calcium sulfate as major excipient to other formulation containing lactose, resulted in severe toxicity. This shows that careful consideration must be given to reformulating an established drug, and judicious selection of excipients is essential, especially for drug having a narrow therapeutic index.

Addition of silica gel to vitamin formulations containing ascorbic acid resulted in decomposition of ascorbic acid possibly as a consequence of the trace metals such as iron and copper present in silica gel, which catalyze the decomposition of ascorbic acid in solution. Chlordiazepoxide can exist in cationic form and forms an ion pair with the anionic surfactant sodium lauryl sulfate, resulting in decreased membrane permeability [47]. As seen in most of the cases disclosed above the drug-excipient interactions affected the rate of dissolution. In fact, an interaction between a drug and an excipient that alters the dissolution of some hydrophobic drugs has been shown to have a marked

impact on the absorption and bioavailability of that drug. This is certainly the case where dissolution is the rate-limiting step in absorption.

1.2.7. Physical stability of drug in dosage form: *causes for transformations & role of excipients as stabilizers*

The solid-state form of drug not only affects the solubility and dissolution rate but the choice of form such as amorphous, different polymorphs or solvates has marked influence on bioavailability [65]. Although pharmaceutical amorphous solids often have desirable properties, like faster dissolution rates over their crystalline counterparts, they are not marketed as widely as the crystalline forms. This is due to their lower chemical stability and their inherent tendency to crystallize [66]. Thus, molecular crystals of solid drugs, form major part of marketed pharmaceutical dosage form [67]. The instabilities within the drug or excipient need be explored and efforts to stabilize are essential to develop a pharmaceutically acceptable, stable formulation. By investigating the intrinsic stability of the drug, it is possible to advise on formulation approaches and indicate types of excipient, specific protective additives and packing, which are likely to improve the integrity of the drug and product. Morris et al have suggested use of excipients in the formulation as inhibitors of phase transitions [68].

a) Processing induced transformations (PITs)

Pharmaceutical active principles / solids existing in different physical forms; crystalline or amorphous, offer unique challenges in product development and manufacturing processes [68, 69]. Process-induced transformations (PITs) are phase transformations, which occur as a result of mechanical or thermal stress imposed upon a system during manufacture processing or after exposure to solvent [70]. During the processing of pharmaceutical solids the most important phase transitions are 1) transformation, like polymorphic transformations, crystallization of the amorphous form and vice versa, incongruent melting (melting followed by crystallization of a more stable form), solution-mediated polymorphic transformations; 2) physical interactions,

like the formation of eutectic mixture or solvate/hydrate formation; 3) physical decompositions, like desolvation [68].

Polymorphism is often characterized as the ability to exist as two or more crystalline forms of the same compound that have different arrangements and/or conformations of the molecules in the crystal lattice [71]. Different polymorphs or pseudopolymorphs have different physical properties e.g., powder flow and compactability, solubility and dissolution rate that relate to stability and bioavailability. Generally, the unsolvated form exhibits better dissolution behavior than the hydrated / solvated form. The most stable polymorphic form of a material is often used because it has the lowest potential for conversion from one polymorphic form to another, while the metastable form may be used to enhance the bioavailability.

However, a metastable pharmaceutical solid form can change crystalline structure or solvate or desolvate in response to changes in environmental conditions, processing, or over time. It is necessary to ensure that polymorphic differences (when present) are addressed via design and control of formulation and process conditions to physical and chemical stability of the product over the intended shelf life and bioavailability. Because an amorphous form is thermodynamically less stable than any crystalline form, inadvertent crystallization from an amorphous drug substance may occur. Amorphous material could crystallize e.g. during storage, especially on exposure to heat and humidity [67]. The combination of solvent and drying conditions provides a suitable environment for the generation of new polymorphs [70]. Whenever a wet suspension containing a drug substance is dried, the possibility exists that a change in its crystal state will take place. When a particular physical form is selected for formulation, ensuring that this form in the final product remains unchanged is critical. Monitoring of the solid-state form during the manufacturing process is especially important if dissolution or stability of the product is sensitive to solid phase changes [72].

b) Moisture induced transformations

Since API and excipients in the formulation may have different moisture sorption properties, they can interact and produce unpredicted PITs. The interaction of moisture with pharmaceutical solids is highly crucial to an understanding of water-based processes, e.g. manufacturing processes or prediction of dosage form stability and shelf life [73, 74]. At the same time, since moisture sorption by amorphous and crystalline materials is usually quite different, this can be utilized when designing dosage formulation. The amorphous drug substances have higher mobility and ability to interact with moisture and hence are also more likely to undergo solid-state reactions.

Metastable forms are expected to dissolve more rapidly than their corresponding stable forms [75]. However, a metastable form could also transform from the metastable to the stable form in the dissolution medium and thus the dissolution rate could be much lower than the predicted values. Because the solubility of the metastable form is determined by kinetic processes, it is dependent on the variables that control dissolution and crystallization rates: solubility, interaction between solute and solvent molecule, total solid surface area (mass and specific surface area), hydrodynamic conditions and temperature [76]. Besides during processing, during storage or dissolution metastable forms can also crystallize and transform to a more thermodynamically stable form [77 78].

c) Temperature induced transformations

Amorphous solids are generally less stable physically than their corresponding crystals [67]. The important factor is the T_g, above which the molecular mobility and the rate of solid-state reactions increases significantly [79].

1.2.7.1. Effects of excipients on the physical stability of the formulation

Although polymorphs of a drug substance share the same chemical formula, difference in crystalline structure affect the physiochemical parameters of the substance such as, solubility, dissolution rate, density which in turn affect their important

pharmaceutical properties such as bioavailability, stability of drug as well as formulation technology of dosage form. As the awareness of these effects has increased formulators are charged with the responsibility to formulate a product, which is physically and chemically stable

Instability of active pharmaceutical ingredient / drug and excipients is broadly classified as chemical (like hydrolysis, oxidation and deamidation) or physical instability (like polymorphism, pseudopolymorphism or crystallization). Many drugs in the solid-state undergo significant physico-chemical change in the presence of certain solid excipients: an increased rate of chemical degradation; a reduction in the degree of crystallinity; and the formation of molecular complexes [65, 73]. Metastable crystalline polymorphs may be less chemically stable than the most physically stable crystalline form [80]. The factors that could cause the molecular transformation of drug in the formulation include: environmental components, such as water vapor and sunlight; stresses during conversion to the dosage form, such as a compaction process; or interactions between adjacent molecules of drug or between functional groups on the same molecules [44].

Optimizing the selection of excipients in the formulation could reduce PITs during manufacturing and storage of final dosage forms. An excipient's effect depends on the amount present, and hence, the amount of moisture it brings into the drug-excipient interaction, as well as the relative ability of each solid to uptake and retain water at a particular temperature and RH [73].

1.2.7.2. Correlation between dissolution, bioavailability and polymorphism

It is well known that differences due to polymorphism and pseudo polymorphism observed in drugs are critical because physical and chemical properties of different crystalline forms influence their bioavailability. Most drugs exhibit structural polymorphism, and it is preferable to develop the most thermodynamically stable polymorph of the drug [80]. The physically more stable polymorphic form has lowest energy state, highest melting point and least aqueous solubility. The other forms are the metastable forms, which have higher energy, low melting point and greater

solubility [30]. These are special situations, which require a faster dissolution rate or higher drug concentration in order to achieve rapid absorption and efficacy. Since the metastable forms have greater solubility and hence greater bioavailability, they are preferred in the formulations [69]. Amorphous materials are thermodynamically unstable and will tend to revert to the crystalline form spontaneously or on storage (devitrification); such behavior has been well documented for a number of drugs [81, 82]. Crystallization has deleterious effects on dissolution performance of the dosage form, which in turn adversely affects the bioavailability of drugs [83]. Technologies have been developed to suppress the crystallization of the amorphous drugs and dispersion of drug into polymeric matrices to form solid dispersions is widely investigated.

1.2.7.3. Stabilization of drug in polymeric matrix: Solid dispersions

The purpose of formulating the drug substances as solid dispersion is to enhance the drug solubility, retain the physical stability of the drug form and hence enhance the bioavailability. Drugs can be stabilized in solid dispersions whereby the drug is dispersed in a polymer matrix [84]. The drug can be dispersed molecularly, in amorphous particles (clusters) or in crystalline particles in the polymeric matrix to enhance the dissolution. The different arrangements in which the drug can molecularly dispersed are shown in Fig 1.3. Knowledge about the molecular arrangement will enlarge comprehension of the properties and behavior of solid dispersions and it will facilitate optimization of their properties required for accelerated dissolution of hydrophobic compounds. The dissolution behavior of solid dispersions must remain unchanged during storage. The best way to guarantee this is by maintaining their physical state and molecular structure. For optimal stability of amorphous solid dispersions, the molecular mobility should be as low as possible [85]. However, solid dispersions, partially or fully amorphous, are thermodynamically unstable [86]. The presence of few crystalline particles will act as nuclei that can be the starting point for further crystallization. It has been shown that such solid dispersions show progressively poorer dissolution behavior during storage [87]. The physical stability of amorphous

solid dispersions should be related not only to crystallization of drug but also to any change in molecular structure including the distribution of the drug. Moreover, the physical state of the matrix should be monitored, because changes therein are likely to alter the physical state of the drug and drug release as well [88]. Physical changes are depicted in Fig 1.4.

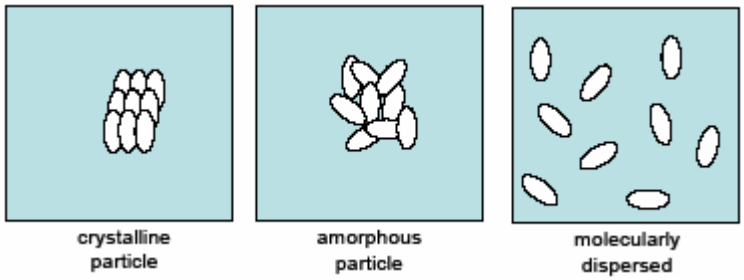

Fig.1.3. Schematic representation of three modes of incorporation of the drug in solid dispersion

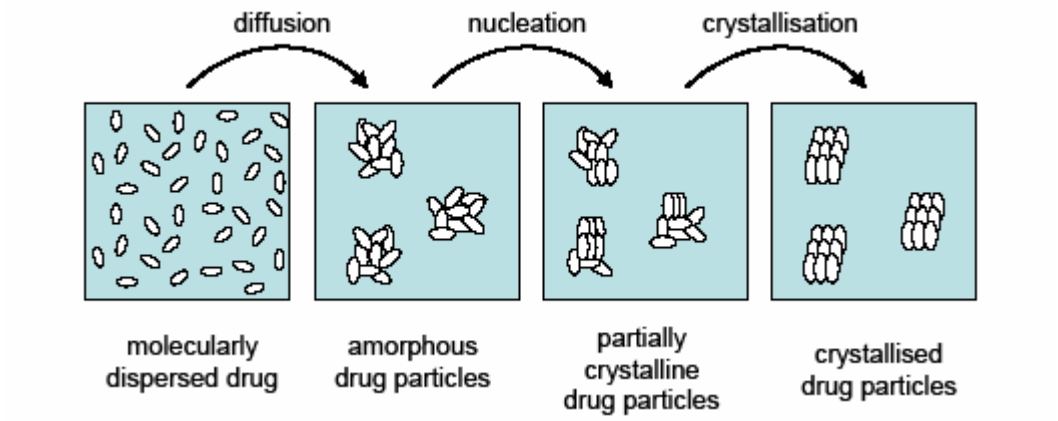

Fig.1.4. Physical changes in solid dispersions resulting in crystallization

1.2.7.4. Molecular mobility in drug-polymer matrix: Antiplasticization approach

Amorphous materials have a glass transition temperature (T_g) above which, the molecular mobility increases significantly and hence, crystallization is more likely to occur [86, 89]. The molecular mobility in amorphous materials determines the physical stability and reactivity [85]. The molecular mobility is related to macromolecular

properties like viscosity but is generally quantified in terms of mean relaxation time τ. The relaxation time is defined as the time necessary for a molecule or chain segment to diffuse across the distance of one molecule or chain segment [90, 91]. The relaxation time varies with temperature. Typical relaxation times at T_g are 100-200 seconds. Relaxation times at the storage conditions will be indicative for shelf life. The viscosity and relaxation time decrease more rapidly in fragile materials and unfortunately, most pharmaceutical amorphous systems show moderately fragile to fragile behavior. This implies that glasses will be more stable and devitrification or crystallization proceeds slower unlike in fragile materials.

The process of devitrification of the amorphous state, either during solid-state stability or solubilization process, pushes it toward the ordered crystalline form with consequent loss of the solubility advantage. This can be prevented by judicious qualitative and quantitative selection of stabilizing excipients for formulating the solid dispersion [90].

The polymeric matrix acts as antiplasticizer for the drug molecules inhibiting its molecular mobility [87]. By addition of the polymeric matrix having a higher T_g, than the drug, the T_g of the solid dispersion is elevated compared to that of the drug alone. Accordingly, the molecular mobility of the drug is reduced. This implies that the T_g of the matrix should be as high as possible in order to obtain a solid dispersion with a high T_g and thus a low molecular mobility [87, 90, 92].

Most of the solid dispersions are made from hydrophilic polymeric matrices and they have a tendency to pick up moisture. Hence the plasticizing effect of water absorbed in solid dispersions should be taken into account [89, 93]. Such matrices are hygroscopic and water will be homogeneously distributed through the solid dispersion. The T_g of the matrix is subsequently decreased to below storage temperature and the material becomes prone to devitrification. The plasticizing capacity of water is huge due to its low T_g, i.e. 135(K). The T_g of a homogeneous solid dispersion determines its stability. The T_g of these solid dispersions can be predicted from the Gordon-Taylor equation [94]:

$$T_{g\,MIX} = \frac{T_{gD} \cdot w_D + T_{gC} \cdot K \cdot (1 - w_D)}{w_D + K \cdot (1 - w_D)} \qquad \textit{Eq 1}$$

in which $T_{g,MIX}$ is the glass transition of the solid dispersion, $T_{g,D}$ and $T_{g,C}$ are the T_g´s of drug and matrix respectively and w_D is the weight fraction drug. The constant K according to the Simha-Boyer rule is given by:

$$K = \frac{\rho_D \cdot T_{gD}}{\rho_C \cdot T_{gC}} \qquad \textit{Eq 2}$$

in which ρ_D and ρ_C the density's of drug and matrix, respectively. Brinke and co-workers [94] assumed that the change in specific heat of glass and rubber (ΔCp) was inversely proportional to temperature resulting in a different definition of the constant K:

$$K = \frac{\Delta C_{pC}}{\Delta C_{pD}} \qquad \textit{Eq 3}$$

From these it is evident that the stability of amorphous solid dispersions that consist of two phases is determined by the mobility in those two phases. Hence in an amorphous solid dispersion containing amorphous clusters of drug molecules, the diffusion of drug in the matrix is determined by the T_g of the matrix, whereas crystallization of molecules within the clusters will be mainly determined by the T_g of the drug. The polymer matrix is capable of stabilizing the drug at the cluster-matrix interface. T_g of a homogeneous solid dispersion is a function of the composition (See Eq. 1). When the drug has a lower T_g than the matrix, high drug content depresses the T_g of the solid dispersion, increasing the risk for phase separation. This reduces the distance between drug molecules and hence facilitates crystallization. At times when the hydrophobic drug is dispersed in hydrophilic matrix, higher loading of the drug reduces the amount of water that can plasticize the solid dispersion on exposure to particular relative humidity, thereby decreasing molecular mobility [93]. Therefore, higher drug content can not only reduce the T_g of the dry solid dispersion but also decrease the plasticizing effect of water. Which one of the two competing effects has a larger contribution is difficult to predict. Another reason for increased stability with increasing drug loading, is the inhibition of crystallization of the matrix above a certain drug loading, when drug molecules sterically block the migration of matrix molecules.

1.2.7.5. Excipient (polymer) molecular weight: Influence on drug stability

To develop a stable solid dispersion, the molecular mobility should be minimized [85, 87]. As seen in the discussion above, a high T_g of polymer matrix is preferred. The T_g of an amorphous polymer matrix increases with increasing molecular weight [89]. Higher temperatures are required before transition takes place from the glassy, low mobility state to the rubbery state in which drug molecules can diffuse and crystallize. The selection of high molecular weight polymer matrices is therefore preferred because the free volume is smaller implying that molecular motions are restricted [90]. The relation between high molecular weight and high physical stability is well acknowledged in solid dispersion literature. At T_g, a significant change in volume is expected that results in increased molecular mobility, reactivity, and propensity to crystallize. Hence higher T_g of polymer matrix is beneficial [95]. The T_g has a certain maximum value, depending on the monomer composition in polymer. The relation between T_g and molecular weight is described by the Fox-Flory equation [96]

$$\frac{1}{T_g} = \frac{1}{T_g^{\infty}} + \frac{K}{DP} \qquad Eq\ 4$$

In which T_g^{∞} is the T_g at infinite chain length, *K* is a constant that depends on monomer geometry and interactions and DP is the degree of polymerization. The correlation between increase in molecular weight and decrease in chain ends is well established. With increase in molecular weight the number of chain ends is reduced and this restricts the segmental motion of polymers, which is reflected in increased T_g for high molecular weight polymers [89, 93]. The increased molecular weight of the polymer restricts the segmental motion of the polymer chains and retains the smaller drug molecules entrapped in the same form without its conversion to crystalline form [92, 95]. It was found that low molecular weight PVP did not prevent crystallization, whereas longer chains did [92]. Therefore, low molecular weight matrices are mixed with large matrix molecules to obtain high physical stability.

All the approaches to retain the drug in the same physical form in the solid state are aimed at ensuring rapid dissolution of the drug from the polymer matrix to ensure rapid absorption and hence ensure bioavailability.

1.3. BACKGROUND AND MOTIVATION

Advanced drug delivery systems are primarily aimed at providing better therapeutic efficacy and patient compliance. The primary concern for drugs exhibiting lower bioavailability and restricted absorption window is designing the delivery systems, which release the drug at the desired site thus enhancing their absorption (in turn bioavailability) [9,11,34]. Designing of novel drug delivery systems to meet these requirements has attracted considerable attention of investigators working in the field of drug delivery systems. In the last two decades the new technological advances have brought many innovative drug delivery systems like the floating tablets, pulsed release, osmotic delivery systems to the market and others are close to commercialization. Polymers play an important role in the design of these advanced drug delivery products. Polymeric excipients have been used in formulations for a variety of reasons, including release modification, taste masking, protection and stabilization of the drug, etc [7]. The synthetic and naturally occurring polymers are being used in the form of matrix, hydrogels, micro particles, nanoparticles, films and sponges in the drug delivery system. The applications of polymers either synthetic or natural are continuing and increasing in the field of drug delivery [7]. Polymeric excipients are no more recognized as cheap adjuvant in the dosage form design but play a major role in enhancing the product performance and are more or less solely responsible for affecting the drug release [60, 97].

There has been a myriad of efforts by the formulation scientist to develop dosage forms with enhanced performance in terms of efficacy and patient compliance. Varied polymers or blend of polymers are used to attain these objectives. Development of modified, controlled, sustained and delayed release products to enhance therapeutic benefits has been successfully undertaken [6]. These delivery systems further enhance patient compliance in terms of reduction in dosing frequency. The more recent developments in enhancing the patient compliance include the development of chewable, rapidly disintegrating, quick dissolve tablets providing ease of administration and rapid onset of action [98-102]. Formulation development of drugs especially to enhance patient compliance in case of pediatric and geriatric patients who find it

difficult to swallow solid dosage form is challenging. Most of the drugs for these patients are administered as liquid orals [103]. Development of chewable and quick dissolve tablets, suspensions and solutions entails the use of special agents to mask the taste of the drugs to enhance the patient compliance.

The excipients used for taste masking are hence entrusted with the enhancing the palatability ensuring the drug release at site of absorption which is a prerequisite to ensure bioavailability. However the task is daunting especially in case of drugs with limited absorption window. The limited absorption window or local site of action often necessitates use of excipients capable of delivering the drugs at the desired site. The complexity of the formulation gets amplified if the drug has a propensity to interact with functional groups of the excipient causing deactivation.

1.3.1. Drugs with limited absorption site / local site of action: *limitations of existing excipients influencing bioavailability*

For drugs with limited absorption region, spatial and temporal release formulations have been developed in past [104, 105]. Drugs, which are better absorbed from the intestine, are coated using the enteric polymers, which release the drug at the desired site due to the influence of pH on polymer dissolution. Formulation of drugs which exhibit limited/ restricted absorption window till upper gastric region is more challenging. The bioavailability of such drugs (Cefuroxime axetil, Ciprofloxacin HCl) is adversely affected once they reach the intestine due to lower absorption.

i) Cefuroxime axetil

Cefuroxime axetil (CA) is a second-generation cephalosporin antibiotic administered orally and is known to have extremely bitter taste [106]. Extensive efforts have been made in the past to develop oral suspension based on CA. Cellulose acetate trimellitate (CAT), hydroxypropyl methylcellulose phthalate (HPMCP), Eudragit E (EE) and Eudragit L (EL) have been evaluated as possible excipients to encapsulate the drug [107,108]. Lorenzo-Lamosa et al. [108] reported that the CA-EE microspheres

exhibited the desired release profile, but the drug was degraded in the presence of the polymer. Also in the presence of CAT, the degradation of CA led to unacceptably high proportions of impurities [107].

Donn et al. [109] studied the bioavailability of CA from tablets and suspension (based on wax coated CA granules). The tablets and suspension were not bio-equivalent as reported by Donn et al. [109]. The lower bioavailability of CA from suspension than tablet was attributed to wax coating on CA granules. The wax coating causes relatively delayed release of CA as the release takes place only on forming stearate salt in alkaline pH due to interaction between sodium ions and stearic acid [106]. On the contrary Dantzig et al. [110] showed that CA is hydrolyzed to cefuroxime in the intestinal lumen by the esterases. This lowered CA concentration in the lumen resulting in reduced absorption and low bioavailability in humans [110]. Similar findings were reported by Campbell et al. [111] and Ruiz-Balaguer et al. [112]. The literature reported above implies that excipients like wax coatings and enteric polymers which are known to release the drug in intestine are not ideal carriers for this drug. CA has a low oral bioavailability of 37-52 % [113, 114] and hence any further reduction in the bioavailability due to inappropriate choice of excipient should be avoided.

The physiochemical properties of CA constrain the options of excipients for formulation. CA has a limited absorption window restricted to upper gastric region. In addition CA has a tendency to gel in presence of moisture at physiological temperatures (37°C) leading to poor dissolution and reduced absorption [115]. It falls under the Class IV type of drugs as per BSC classification [16]. As reported in literature earlier the preferred way to increase bioavailabilty of such drugs is at discretion of formulation scientist and enhancement in dissolution is preferred [15]. The physicochemical and pharmacokinetic properties of this difficult to formulate drug warrants the use of hydrophobic polymer coating, releasing it in gastric region without its inactivation. Further the polymer should be capable of taste masking CA.

ii) Ciprofloxacin HCl

One of the approaches to enhance oral bioavailability of the drugs is to deliver them at the site of absorption. Ciprofloxacin is a Class III drug as per the BCS classification [15, 16, 17]. These drugs are associated with lower permeability but high solubility. Since permeability is rate limiting the rapid dissolution is particularly desirable in order to maximize the contact time between the dissolved drug and absorption mucosa to enhance the oral bioavailability [15]. This is substantiated by the successful development of Cipro® OD, a gastroretentive floating drug delivery system based on hydrogels [117, 118].

Ciprofloxacin HCL is a bitter drug better absorbed from gastric region, but it is associated with extremely bitter taste. The pediatric formulations are hence required to mask the bitter taste. Ideally a reverse enteric polymer should be used to taste mask and release it in gastric region to ensure better bioavailability. Eudragit E the commonly used reverse enteric polymer is soluble below pH 5 and permeable above it. Ciprofloxacin is a highly water soluble drug and hence requires a coating which is completely impermeable to water. Literature reveals use of enteric polymers to mask the bitter taste [119, 120]. This provides the taste masking but compromises the release in gastric region. To overcome this there is a need to develop a highly hydrophobic gastric soluble polymer, which addresses these needs of the molecule.

iii) Clarithromycin

Literature reports evaluation of Clarithromycin for the treatment of *Helicobacter pylori* and hence requires to be administered in the gastric region [121-124]. The bacterium is found in highest concentrations in the gastric pits of the antrum, but it can also be found on metaplastic epithelial cells with gastric characteristics in other parts of the gastrointestinal tract such as the duodenum. The activity of Clarithromycin decreases below pH 7.5 and Clarithromycin monotherapy produces an unacceptably low eradication rate of only 42% [124]. One of the explanations for the absence of a truly successful *H. pylori* eradication regimen includes the drug delivery

problems associated with directing antibacterial agents. Clarithromycin is unstable at low pH, and the instability of these drugs at the normal gastric pH (pH 1–2) affects their delivery to the sites where *H. pylori* resides in the stomach [123, 124].

One of the approaches to enhance the drug concentration at site of action was development of intragastric buoyant sustained release tablets of Amoxicillin to treat *H. pylori* infection [125]. Similarly mucoadhesive microspheres of clarithromycin for enhancing the treatment of *H. pylori* for have been reported [123]. The complex of clarithromycin with polyacrylic acid has been investigated for the same. However this complexation retards the release of Clarithromycin at gastric pH. The study on degradation kinetics of Clarithromyycin showed it has a half live of 1.47 hr in acidic pH [123]. The slow release of Clarithromycin from the complex affected its therapeutic efficacy as slow dissolution caused degradation of Clarithromycin. Hence a rapid release would be preferred to overcome this limitation.

Clarithromycin is investigated for its treatment of *H. Pylori* infections in pediatric patients [121, 122]. Clarithromycin is extremely bitter and hence to improve patient compliance it has to be taste masked. To overcome bitterness it is complexed with carbomer (polyacrylic acid derivative) and enteric coated [125]. Such formulations are of little use in *H. pylori* infection as these do not release the drug at the desired local site of action. To taste mask this drug, there is a need of highly hydrophobic polymer as leaching of even small quantities gives perception of bitter taste. Eudragit E is soluble below pH 5 and permeable above it and hence it is not ideal for this application. The use of enteric polymer with carbomer does not release in gastric pH at site of action. Hence there is a need of new polymer which address to these issues.

iv) Solid-state stability of drugs: influence on bioavailability

a) Celecoxib

Celecoxib is a cyclooxygenase-2 (COX-2) inhibitor [90].The amorphous form of Celecoxib, a BCS class II drug, was found to provide an initial increase in solubility over its crystalline form, but a rapid devitrification, [127, 128] both on storage and

during dissolution, resulted in a loss of solubility advantage. Selection of a stabilizer for the amorphous form should retard self-association of drug molecules into its crystalline form. Apart from the dissolution media, the residual solvent used for the preparation of solid dispersions results in its rapid solvent-mediated reversion to the crystalline form with significant loss of solubility [129]. The dissolution of amorphous form of Celecoxib is retarded from the dosage form in the gastric fluids due to rapid conversion to crystalline form [126]. The reasons for the same are described in literature review section 1.2.7. This necessitates the need of excipient, which prevents the conversion of Celecoxib from disordered molecular conformation into a thermodynamically stable, ordered crystalline form during the storage and also in presence of gastric fluids. This warrants the use of hydrophobic material, which shows rapid dissolution at gastric pH. So the utility of hydrophilic polymer polyvinyl pyrrolidone otherwise extensively used in stabilization of amorphous drugs, is questionable. Hence there is a need to develop high molecular weight, hydrophoic polymer rapidly dissolving at gastric pH.

1.3.3. Summary

Various pharmaceutical compositions which achieved a specific attribute such as taste masking, site specific delivery and solid state drug stabilization but compromised on the release and bioavailability, were analyzed. The restrictions faced by formulation scientists in formulation development due to non-availability of polymers having specific functionality are described. One of the areas where the polymers are most extensively used is the taste masking of the drugs and solid dispersion for physical stabilization. The limitations of the existing polymers (either delayed release or complete deactivation of drug) have restricted the formulation development of these drugs affecting their gastric absorption and altering the bioavailability. This has educed the need to develop a polymer, which is capable of catering to these formulation needs. It can be envisaged that new biomaterials would be needed to address these complex situations arising out of the physicochemical and pharmacokinetic characteristics of drugs.

1.3.4. Need for new excipients: *general considerations*

Better utilization of existing excipients, improved understanding of their functional behavior and development of modified, newer excipients, are some of the important areas of future research in drug delivery. This is because most of these materials used in drug delivery were not designed for medical purposes. For example, some of the materials used in the artificial heart and vascular grafts were originally used as clothing [130]. The excipients industry to date has been an extension of the food industry [131]. Excipients are of various origin: animal (e.g. lactose, gelatin, stearic acid), plant (e.g. starches, sugars, cellulose, arginates), mineral (e.g. calcium phosphate, silica) and synthesis (e.g. PEGs, polysorbates, povidone, etc. [60].

There are many types of drug delivery devices, each with its own particular requirements for its constituent material. For example, reservoir devices require a biocompatible membrane, which will control the diffusion of drug through the system. Other devices control rate by the swelling properties of the polymer. Non-erodible matrix devices control diffusion through the polymer composition and pore structures created in the polymer. Osmotic devices generally require a selective osmotic membrane, which will allow only certain substances to pass through [130]. The majority of the excipients that are currently available fail to live up to these functionality requirements, thus creating the opportunity for the development of new high-functionality excipients [132].

Joshi and Dureiz [133] in an article titled “Added Functionality to Excipients: An Answer to Challenging Formulations” have stressed the need of excipients with enhanced functionality to meet the formulation challenges for orally disintergrating tablets (ODT). The excipients have to provide better mouth feel, taste masking with good flow and compressibility and yet providing low friability. Many bulk excipients commonly used for conventional tablets do not fulfill the development requirements of an ODT, thus necessitating the use of specific excipients and technologies to mask the drug’s unacceptable taste and improve the ODT’s overall mouthfeel. This requires the

development of new added functionality excipients. For attaining these objectives the physicochemical properties of existing excipients are modified.

The development of new excipients to date has been market driven / technology-driven (i.e., excipients are developed in response to market demand) rather than marketing-driven (i.e., excipients are developed first and market demand is created through marketing strategies) and has not seen much activity as shown by the fact that, for the past many years, not a single new chemical excipient has been introduced into the market [132]. The primary reason for the lack of new chemical excipients is the relatively high cost involved in excipient discovery and development and regulatory considerations. However, with the increasing number of new drug moieties with varying physicochemical and stability properties, there is growing pressure on formulators to search for new excipients to achieve the desired set of functionalities.

Some of the other factors driving the search for new excipients are:

- the ability to modulate the solubility, permeability, or stability of drug molecules
- the growing performance expectations of excipients to address issues such as disintegration, dissolution, and bioavailability
- the lack of excipients that address the needs of a specific patients such as those lactose and sorbitol sensitivity
- shortcomings of existing excipients *e.g.* loss of compaction of microcrystalline cellulose (MCC) upon wet granulation, high moisture sensitivity, and poor die filling as a result of agglomeration
- inability of excipients to match improved machinery performance *eg*. tableting machinery's increasing speed capabilities, which require excipients capable of maintaining good compressibility and low weight variation even at short dwell times

1.3.4.1. Development of new tailor made excipients

There have been considerable advances in materials science and close corroborations with the medical fraternity has led to large contributions from

biomedical engineering permit the design and development of a new series of excipients with 'tailormade' characteristics for particular formulations and manufacturing processes. Apart from the vast and rapid contributions from the scientific community working in area of biomaterials, the introduction of delivery systems and the advance in biopharmaceutics have led to a new interest in the role and functionality of the excipients [97].

Three main approaches are followed by the industry to obtain excipients with improved functionality: physical or minor chemical manipulation of materials already known, combination of two or more marketed excipients in order to reduce unwanted defects [97, 134].Any new excipient under development must go through various stages of regulatory approval aimed at addressing issues of safety and toxicity, which is a lengthy and costly process. This can be cut down by undertaking the generic development (ANDA filings). The approach has already been successfully applied in the intravenous delivery field, in which CyDex and Pfizer worked collaboratively to obtain the approval of a solubilizer [135]. The combined expertise of pharmaceutical and excipient companies can lead to the development of tailor-made innovative excipients.

1.3.4.2. Requirements of excipients

The quality of medicines depends not only on the active principles and production processes, but also the performance of the excipients. The traditional concept of the excipient as any component other than the active substance has undergone a substantial evolution from an 'inert' and cheap vehicle to an essential constituent of the formulation. Excipients are now chosen to perform a variety of functions to guarantee the stability and bioavailability of the drug substance from the drug product and its manufacturability on a production scale. Beyond the dosage form necessities, excipients are required to perform important and specific technological functions, particularly in the case of oral dosage forms *e.g.* The polymers used for taste masking have to enhance the palatability of the formulation ensuring the release of drug in stomach sans leaching in mouth and in aqueous media yet retaining its stability.

Fundamental requirement for excipients are quality, safety and performance with respect to the formulation type as shown in Fig. 1.5.

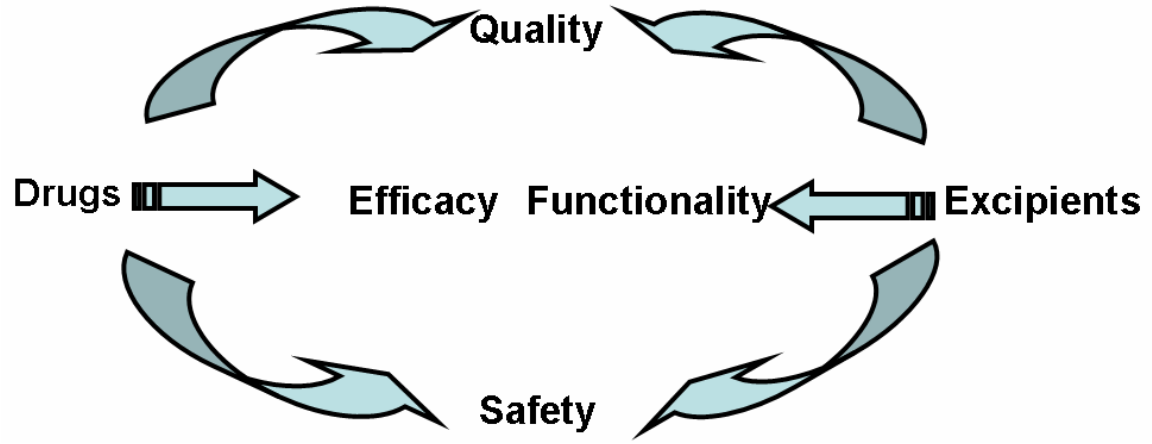

Fig.1.5. Requirements of excipients *(adapted from ref [97])*

1.3.4.3. Recent trends in excipient development

Developing new grades of existing excipients by modification of mere physicochemical properties of existing excipients has been the most successful strategy for the development of new excipients in past three decades [132], a process that has been supported by the introduction of better performance grades of excipients such as pregelatinized starch, croscarmellose, and crospovidone. However, functionality can be improved only to a certain extent because of the limited range of possible modifications. New combinations of existing excipients are an interesting option for improving excipient functionality because all formulations contain multiple excipients. Many possible combinations of existing excipients can be used to achieve the desired set of performance characteristics. Over the years, the development of single-bodied excipient combinations at a subparticle level, called *coprocessed excipients*, has gained importance [134]. Some of the new excipients introduced in market to enhance the product and manufacturing performance include: Starch 1500®, LycatabPGS®, Fast-

Flo® lactose, FlowLac 100®, Elcema®, Avicel®, Vitapur® Cellactos®, Ludipress® and Prosolv® etc.

1.3.4.5. Safety of new excipients

Since excipients form a major part of the drug delivery systems their safety essential and hence use of new excipients is often a concern. Many excipients are also food ingredients hence excipient manufacturers have tended to rely on food regulations (food additive status or generally recognized as safe [GRAS] determination) as an initial safety review and as an indication of eventual acceptability of their products. However, this option may not be appropriate for many new excipients [136, 137].

In the current system in the United States, an excipient would be considered acceptable if it is referenced in, and part of, an approved new drug application (NDA) for a particular function in that specific drug product. At present, recognition of an ingredient as GRAS is the only mechanism available for the pre-NDA evaluation of a new excipient [136, 137]. GRAS status is no guarantee that the material will be approved as an excipient in a drug product - such approval can only take place within the context of an NDA. GRAS status indicates a measure of FDA review to a pharmaceutical manufacturer and eliminates some of the uncertainty associated with use of a new excipient. IPEC (International Pharmaceutical Excipients Council) has been formed and is concerned for establishing regulatory mechanism in which a new excipient can be assessed centrally for safety and quality. IPEC is working to overcome the hesitation of the pharmaceutical industry to use new excipients, which in turn could prevent the advancement of pharmaceutical technology.

The implementation of a global DMF (drug master file) system to handle confidential information for excipients is considered. As per this, new excipients could be evaluated with a base set of data for general acceptance similar to the programs established by the Flavor and Extract Manufacturers Association for flavor ingredients and the Cosmetic Ingredient Review for cosmetic ingredients. Finally, the use of a new excipient still would be subject to final approval as part of a drug product, and specific-use information would be supplied with the drug product submission. So the new

excipient will have to pass through the safety evaluations normally used for the new drugs. Due to lack of concrete guidelines for safety evaluation of the new excipients most of the biomaterials investigated use the in-vitro and in-vivo safety evaluations disclosed in the USP as a preliminary screening method for the toxicity of the materials.

1.4. CONCLUDING REMARKS

The literature survey reveals that a clear understanding and consideration of biopharmaceutic characteristics of drugs is crucial in the design and execution of a successful development program for bioavailability enhancement. Therefore right tools to identify the barriers that limit oral bioavailability of drugs and development of innovative drug delivery platforms to overcome these challenges are essential. The solubility of a molecule contributes critically toward its "drugability", by influencing the dissolution and bioavailability (BA), especially in the case of biopharmaceutics classification system (BCS) class II and IV drugs. Hence drug delivery systems incorporating excipients to enhance the dissolution of these drugs are preferred. The limitations of the existing polymers due to restricted functionality making them unsuitable for development of difficult to formulate drugs (complex physicochemical and biopharmaceutical properties) should be identified. It is important to identify the mechanisms of drug degradation in presence of excipients causing their inactivation with loss of biological activity. Further the role of polymer architecture in stabilization of metastable forms of poorly dissolving drugs needs to be explored to convert unstable drugs into viable products. The number of drugs in market is exceptionally large compared to the number of approved excipients and further new drug molecules are investigated and many are on way to market. Limited excipients, drug-excipient interactions, often restrict choice of excipients by formulators leading to development of products, which compromise efficacy and bioavailability. It is therefore necessary to develop new excipient which will help overcome these limitations. Development of new reverse enteric polymer that can overcome the above mentioned limitations was undertaken.

1.5. REFERENCES

1) Asean Guidelines For The Conduct Of Bioavailability And Bioequivalence Studies, 21 July 2004 Note For Guidance On The Investigation Of Bioavailability And Bioequivalence"(The European Agency For The Evaluation Of Medicinal Products, London, 26 July 2001, Cpmp/Ewp/Qwp/1401/98
2) A.D. Bhatt, A.B. Vaidya, J. Postgrad. Med. 1992, 38, 130-134.
3) D.J. Greenblatt, T.W. Smith, J.W. Koch, Clin Pharmacokinetics 1976,1, 36-51.
4) Guidance for Industry Bioavailability and Bioequivalence Studies for Orally Administered Drug Products General Considerations *http://www.fda.gov/cder/guidance/index.htm*
5) S.B. Jaiswal and D.M. Bramhankar in Biopharmaceutics and Pharmacokinetics a Treatise, 1st Ed., Vallabh Prakashan, Delhi, India, 1995
6) Controlled Drug Delivery : Fundamentals And Applications, Robinson, J. R. Ed, Lee, V.H.L. Ed., Swarbrick, J. SED, 2nd Edition, Marcel Dekker Inc, New York, 1987
7) R. C. Rowe in: A. T. Florence (Ed.), Materials Used in Pharmaceutical Formulations, Critical Reports on Applied Chemistry, V 6, Published by Society of Chemical Industry, 1984 pp 1-35.
8) K. Klokkers-Bethke, W. Fischer, J. Controlled Rel 1991, 15, 105-112.
9) S.S. Davis, Drug Discovery Today, 2005,10, 249-257.
10) V. F. Patel, N. M. Patel, AAPS PharmSciTech 7 (1) Article 17, 2006; E1-E7 (http://www.aapspharmscitech.org).
11) Davis SS, The design and evaluation of controlled release systems for the gastrointestinal tract. J. Controlled Rel 1985; 2; 27-38.
12) G.L. Amidon, H. Lennernas, V.P. Shah, J.R. Crison, Pharm. Res. 1995,12, 413–420.
13) H. H. Blume , B.S. Schug, Eur. J. Pharm. Sci. 1999, 9, 117–121.
14) C.Y. Wu, L. Z. Benet, Pharm. Res. 2005, 22, 11-23.
15) J. Emami, J Pharm. Pharmaceut. Sci. 2006, 9, 169-189.

16) S.Turner, J. Ravishankar, R. Fassihi, USPTO 20060068010, 30 March 2006 in http://www.scolr.com/documents/MicrosoftPowerPoint-novelAlternativestoSolubilityEnhancement-SCOLR-4.pdf

17) N. A. Kasim, M. Whitehouse, C. Ramachandran, M. Bermejo, H. Lennernas, A. S. Hussain, H. E. Junginger, S.A. Stavchansky, K. K. Midha, V. P. Shah, G.L. Amidon, Mol. Pharma. 2004, 1, 85-96.

18) J. Aungst, Drug development, 2006, 84-86.

19) W. L. Jorgensen, E. M. Duffy, Adv. Drug Deliv. Rev. 2002, 54, 355–366.

20) S.M. Wong, I.W. Kellaway, S. Murdan, Int. J. Pharm., 2006, 317, 61-68.

21) L. Z. Benet, C.Y. Wu, M. F. Hebert, V. J. Wacher, J. Control. Rel. 1996, 39, 139-143.

22) S. Sridevi, A.S. Chauhan, K.B. Chalasani, A.K. Jain, P.V. Diwan, Pharmazie. 2003, 58, 807-810.

23) A. Naseem, C.J. Olliff, L.G. Martini, A.W. Lloyd, Int. J. Pharm. 2004, 269, 443–450.

24) R.N. Gursoy, S. Benita, Biomed. Pharmacother. 2004, 58, 173–182.

25) V.N.P. Le, P. Leterme, A. Gayot, M.P. Flament, Int. J. Pharm. Article in press, 2006 "Influence of granulation and compaction on the particle size of ibuprofen—Development of a size analysis method"

26) P. Di Martino, M. Scoppa , E. Joiris , G. F. Palmieri, C. Andres, Y. Pourcelot , S. Martelli, Int. J. Pharm. 2001, 213, 209–221.

27) J.K. Haleblain, W. Mc Crone, J. Pharm. Sci., 1969, 58, 911- 929.

28) S. Byrn, R. Pfeiffer, M. Ganey, C. Hoiberg, G. Poochikian, Pharm. Res., 1995, 12, 945-954.

29) G.G.Z. Zhanga, D. Lawa, E.A. Schmittb, Y. Qiub, Adv. Drug Deliv. Rev. 2004, 56, 371– 390.

30) D. A. Snider, W. Addicks, W.Owens, Adv. Drug Deliv. Rev., 2004, 56, 391–395.

31) R. Nair, S. Gonen, S. W. Hoag, Int. J. Pharm., 2002, 240, 11–22.

32) E.O. Machiste, P. Giunchedi, M. Setti, U. Conte, Int. J. Pharm., 1995, 126, 65-72.

33) V.K. Kakumanu, V. Arora, A.K. Bansal, Int. J. Pharm. 2006, 317, 155–160.

34) C.H. Dublin, Drug Deliv. Tech. 2006, 6 (4), 22-27.

35) J. V. Orelli, H. Leuenberger, Int. J. Pharm. 2004, 287, 135–145.

36) S. Anwar, J.T. Fell, P.A. Dickinson, Int. J. Pharm., 2005, 290, 121-127.

37) N. Najib, I. Jalal, Int. J. Pharm., 1988, 44, 43-47.

38) B. Abrahamsson, T. Albery, A. Eriksson, I. Gustafsson and M. Sjoberg, *Eur. J. Pharm. Sci.* 2004, 22, 165–172.

39) P. Thapa, M. Ghimire, A.B. Mullen, H. N E. Stevens, Kathmandu University Journal Of Science, Engineering And Technology, 2005, 1, 1-10.

40) R. Jain, A. S. Railkar, A. W. Malick, C. T. Rhodes, N. H. Shah, Eur. J. Pharm. and Biopharm. 1998, 46, 177-182.

41) B. P. Marcos, C. Gutierrez, J. G. Amoza, R. M. Pacheco, C. Souto, A. Concheiro, Int. J. Pharm. 1991, 67, 113-121.

42) S. Airaksinen, Ph.D. Thesis, 2005, Role of Excipients in Moisture Sorption and Physical Stability of Solid Pharmaceutical Formulations, Faculty of Pharmacy, University of Helsinki, Finland

43) V. Joshi, 2004, Excipient Choice in Solid Dosage Forms. Drug Delivery Technology, Excipient Update, http://www.drugdeliverytech.com/cgi-bin/articles.cgi?idArticle=69, January 2004.

44) Crowley PJ (1999) Excipients as stabilizers. PSTT 2: 237-243.

45) R.K. Verma, S. Garg, J. Pharm. Biomed. Anal. 2004, 38, 633-644.

46) M. C. Gohel, P. D. Jogani, J. Pharm. Pharmaceut. Sci. 2005, 8, 76-93.

47) K. Jackson, D. Young, S. Pant, PSTT, 2000, 3, 336-345.

48) P.J. Crowley, PSTT, 1999, 2, 237-243.

49) S Kaojarern, S Nathakarnkikool, U. Suvanakoot, *DICP, The Annals of Pharmacotherapy*: 1989, 23, 29-32.

50) A.E. Aboutaleb, *Pharmazie,* 1983, 38, 473–475.

51) Y. Asakawa, Drug–disintegrant interactions: binding of oxymorphone derivatives. J. Pharm. Sci. 1981, 70, 709–711.

52) S.Y. Lin, C.L. Cheng, R.I. Perng. Eur. J. Pharm. Sci. 1994, 1, 313-322.

53) M. Lovrecich, G. Zingone, F. Nobile, F. Rubessa, Int. J. Pharm. 1996, 31, 247-255.

54) S. Puttipipatkhachorn, J. Nanthanid, K. Yamamoto, G.E. Peck. J. Control. Rel. 2001, 75, 143- 153.

55) S. Wissing, D.Q.M. Craig, S.A. Barker, W.D. Moore, Int. J. Pharm. 2000, 199, 141-150.

56) G.C. Ceschel, R. Badiello, C. Ronchi, P. Maffei. J. Pharm. Biomed. Anal. 2003, 32, 1067-1072.

57) A. Riedel, C.S. Leopold, Drug Dev. Ind. Pharm. 2005, 31, 151-60.

58) D.A. Adkin, *J. Pharm. Sci* 1995, 84, 1405–1409.

59) R. C. Moreton, Pharmaceutical Technology, MAY 2004, 98-119

60) G. Pifferi, P. Restani , Il Farmaco 58, 2003, 541-550

61) G.S. Banker, C.T. Rhodes Eds. *Modern Pharmaceutics* (4rd edn), Marcel Dekker, 1992

62) V.J. Stella, R.A. Rajewski, *Pharm. Res.* 1997, 1, 556–567.

63) M.J. Akers, J.L. Lach, L.J. Fischer, *J. Pharm. Sci.*1973, 62, 391–395.

64) Nakano, M. (1971). *J. Pharm. Sci.* 60, 571–575

65) L.F. Huang, W.Q. Tong, Adv Drug Deliv Rev. 2004, 56, 321-334.

66) S.R. Vippagunta, H.G. Brittain, D.J.W. Grant, Adv. Drug Deliv. Rev. 2001, 48, 3-26.

67) L. Yu, Adv. Drug Deliv. Rev. 2001, 48, 27-42.

68) K.R. Morris, Structural aspects of hydrates and solvates. In Polymorphism in Pharmaceutical Solids, Brittain HG (ed.). Marcel Dekker, Inc., New York, (1999) pp. 126-180.

69) D. Murphy, F. Rodriguez-Cintron, B. Langevin, R.C. Kelly, N. Rodriguez-Hornedo, Int. J. Pharm. 2002, 246, 121-134.

70) H.G. Brittain, E.F. Fiese, Effects of pharmaceutical processing on drug polymorphs and solvates. In Polymorphism in pharmaceutical solids, Brittain HG (ed.), Marcel Dekker Inc., New York, USA, 1999, pp. 331-361.

71) D.J.W. Grant Theory and origin of polymorphism. In Polymorphism in Pharmaceutical Solids, Brittain HG (ed.), Marcel Dekker, Inc., New York, 1999, pp.1-34.

72) G.G.Z. Zhang, D. Law, E.A. Schmitt, Y. Qiu, Adv. Drug Deliv. Rev. 2004, 56, 371-390.

73) C. Ahlneck, G. Zografi, Int. J. Pharm. 1990, 62, 87-95.

74) B.C. Hancock, G. Zografi, J. Pharm. Sci., 1997, 86, 1-12.

75) S. Debnath, R. Suryanarayanan, AAPS PharmSciTech, 2004,5(1): article 8.

76) Y.E. Hammouda, L.K. El-Khordagui, I.A. Darwish, A.H. El-Kamel, Eur. J. Pharm. Sci. 1999, 8, 283–290.

77) N. Rodriguez-Hornedo, D. Murphy, J. Pharm. Sci., 1999, 88, 651-660.

78) H. Zhu, C. Yuen, D.J.W. Grant, Int. J. Pharm. 1996, 135, 151-160.

79) B. Yu, B.Y. Shekunov, P. York, J. Cryst. Growth, 2000, 211,122-136.

80) D. Singhal, W. Curatolo, Adv. Drug Deliv. Rev. 2004, 56, 335-347.

81) M. D. Ticehurst, P. A. Basford, C. I. Dallman, T.M. Lukas, P.V. Marshall, G. Nichols, D. Smith Int. J. Pharm. 2000, 193, 247–259.

82) J. Berggren, G. Frenning, G. Alderborn, Eur. J. Pharm. Sci. 2004, 22, 191–200.

83) G. Sertsou, J. Butler, A. Scott, J. Hempenstall, T. Rades, Int. J. Pharm. 2002, 245, 99-108.

84) D. Mahlin, J. Berggren, U. Gelius, S. Engstrom, G. Alderborn, Int. J. Pharm., 2006, article in press. "The influence of PVP incorporation on moisture-induced surface crystallization of amorphous spray-dried lactose particles"

85) Y. Aso, S. Yoshioka, J. Pharm. Sci., 2006, 95, 318-325.

86) G. Van den Mooter, M. Wuyts, N. Blaton, R. Busson, P. Grobet, P. Augustijns, R. Kinget, Eur. J. Pharm. Sci. 2001, 12, 261–269.

87) I. Weuts, D. Kempena, A. Decorte, G. Verreck, J. Peeters, M. Brewster, G. Van den Mooter, Eur. J. Pharm. Sci. 2005, 25, 313–320.

88) S. Esnaasharia, Y. Javadzadeha, H. K. Batchelorb, B. R. Conwayb, Int. J. Pharm. 2005, 292, 227–230.

89) X. M. Zeng, G. P. Martin, C. Marriott, Int. J. Pharm. 2001, 218, 63–73.

90) P. Gupta, V. K. Kakumanu, A. K. Bansal, Pharm. Res., 2004, 21, 1762-1769.

91) S.H. Shamblin, G. Zografi, Pharm. Res., 15, 1998, 1828-1834.

92) K. Khougaz, S. Dorothe. E. Clas, Journal Of Pharmaceutical Sciences, Vol. 89, No. 10, October 2000 1325-1334

93) J. Berggren, G. Alderborn, Eur. J. Pharm. Sci. 2004, 21, 209–215.

94) T. Matsumoto, G. Zografi, Pharm. Res. 1999, 16, 1722–1728.

95) J. Berggren, G. Alderborn, Pharm. Res., 2003, 20, 1039 – 1046.

96) J.R. Fried, Polymer Science and Technology, Prentice Hall of India Private Limited, New Delhi 110001, 1999, Chapter 4, pp 132-164.

97) G. Pifferi, P. Santoro, M. Pedrani Il Farmaco 1999, 54, 1–14

98) J. Aurora, V. Pathak Drug Delivery Technology Vol. 5 No. 3 March 2005 http://www.drugdeliverytech.com/cgi-bin/issues.cgi?idIssue=33

99) E.L. Hamilton, E. M. Lutz, Vol. 5, No. 1, 2005 http://www.drugdeliverytech.com/cgi-bin/issues.cgi?idIssue=31

100) R. Stier, Vol. 4, No. 2, 2004, http://www.drugdeliverytech.com/cgi-bin/issues.cgi?idIssue=23

101) D. Brown, Vol. 3, No. 6, 2003, http://www.drugdeliverytech.com/cgi-bin/issues.cgi?idIssue=18

102) S. B. Borsadia, D. O'Halloran, J. L. Osborne, Vol. 3, No. 3, 2003, http://www.drugdeliverytech.com/cgi-bin/issues.cgi?idIssue=14

103) G. Mukherji, S. Goel, V. K. Arora, US Patent 6,565,877, May 20, 2003

104) M.V. Risbud, A.A. Hardikar, S.V. Bhat, R.R. Bhonde. J. Control. Rel. 2000, 68, 23–30.

105) N.J. Joseph, S. Lakshmi, A. Jayakrishnan. J. Control. Rel. 2002, 79, 71–79.

106) H. Robson, D. Craig, D. Deutsch, Int. J. Pharm. 1999, 190,183-192.

107) M. Cuna, M. Lorenzo-Lamosa, J. Vila-Jato, D. Torres, M. Alonso, Drug Dev. Ind. Pharm. 1997, 23, 259-265.

108) M. Lorenzo-Lamosa, M. Cuna, J. Vila-Jato, D. Torres, M. Alonso, J. Microencap. 1997, 14, 607-616.

109) K. Donn, N. James, J. Powell, J. Pharm. Sci. 1994, 83, 842-844.

110) A. H. Dantzig, C. Dale, L. Duckworth, B. Tabas, Biochimica et Biophysica Acta, 1994,1191, 7-13.

111) C. Campbell, L. Chantrell, R. Eastmond, Biochem. Pharmacol. 1987, 36, 2317–2324.

112) N. Ruiz-Balaguer, A. Nacher, V. Casabo M. Merino, Antimicrob. Agents. Chemother. 1997, 41, 445–448.

113) Ceftin Prescription Information, Physicians' Desk Reference; 2003, pp 1918-1921.

114) A. Finn, A. Straughn, M. Meyer, J. Biopharm. Drug Disposit. 1987, 8, 519-526.

115) D.S. Deutsch, J. Anwar, US Patent, 4,897,270, 1990.

116) N. Talwar, H. Sen, J.N. Staniforth, US Patent, US 6261601, 2001July 17.

117) N. Talwar, H. Sen, J.N. Staniforth, US Patent, US 6,960,356, 2005 Nov 1

118) M. Bucheler, R. Rupp, K. Benke, J. Michaelis, N. Pollinger US Patent 5695784 December 9, 1997

119) M. Bucheler, R. Rupp, K. Benke, J. Michaelis, N. Pollinger US Patent 6136347 October 24, 2000

120) V. Tolia, W. Brown, M. El-Baba, C.H. Lin, Pediatr. Infect. Dis. J. 2000 19, 1167-1171.

121) H. Shashidhar, J. Peters, C.H. Lin, R. Rabah, R. Thomas, V. Tolia, J. Pediatr Gastroenterol. Nutr. 2000, 30, 276-282.

122) M.K. Chuna, H. Sah, H.K. Choi, Int. J. Pharm. 2005, 297,172–179.

123) P. O. Erah, A. F. Goddard, D. A. Barrett, P. N. Shaw, R. C. Spiller, J. Antimicro. Chemother.1997, 39, 5–12.

124) T. Tokumura, Y. Machida, J.Control. Rel., 2006,110, 581–586.

125) M.Y.F. Lu, S. Borodkin, US Patent 4,808,411 28 February, 1989.

126) M.J. Hageman, H.E. Xiaorong, T. T. Kararli, A.L.Mackin, P.J. Miyake, B.R. Rohrs, PCT Patent Application WO 01/41536 14 June 2001.

127) B. C. Hancock, M. Parks, Pharm. Res. 2000, *17*, 397-404.

128) P. Gupta, G. Chawla, A. K. Bansal, Molecular Pharmaceutics, 2004, 1, 406-413.

129) P. Gupta, R. Thilagavathi, A.K. Chakraborti, A.K. Bansal, Molecular Pharmaceutics, 2005, 2, 384-391.

130) R. Langer, L. G. Cima, J. A. Tamada, E. Wintermantel, Biomaterials, 1990, 11, 738-745.

131) M. Steinberg, L. Blecher, A. Mercill, Pharm. Technol. 2001, 25, 62–64.

132) S.K. Nachaegari, A. K. Bansal, Pharmaceutical Technology, 2004, 52-64.

133) A. A. Joshi, X. Duriez, Pharmaceutical Technology, 2004, 12-19.

134) R.C. Moreton, Drug Dev. Ind. Pharm. 1996, 22, 11–23.

135) CyDex, "Captisol,"www.cydexinc.com/CaptisolProductApprovals.pdf

136) C.C. DeMerlis, Pharmaceutical Technology, 2002, 36-44.

137) C.C. DeMerlis, J. M. Goldring, Pharmaceutical Technology, 2003, 102-108.

CHAPTER 2

Objective & Scope of Work

2.1. PREAMBLE

Drugs often exhibit poor solubility and stability, and excipients are used to define a formulation that is physically and chemically stable, manufacturable, and bioavailable. The excipients also function as stability enhancer and therefore they should protect, support, or enhance stability or bioavailability of formulation. Excipients are traditionally thought of as inert but they can have a tremendous impact on the ultimate pharmacological availability of a drug substance when added to a formulation**.** Often drug-excipients interactions lead to degradation of drug substances. The functional groups or residues in excipients are responsible for these adverse interactions. Physical changes in the formulation arising out of drug-polymer interaction lead to altered dissolution or other delivery properties of the final dosage form.

There is a growing performance expectation from the existing excipients in developments of new drug delivery systems. Often the existing excipients fail to live up to the functionality requirements of these new drugs. The literature survey revealed that there are drugs, which need new excipients with better performance in terms of the release characteristics, drug compatibility and physical stability for enhancing the drug absorption. There is a need to develop new excipient with enhanced functionalities to address the formulation needs of new drug molecules with varying physicochemical properties.

2.2. OBJECTIVE AND SCOPE OF WORK

The major focus of this work is to develop formulations with enhanced bioavailability of drugs by 1) ensuring dissolution of drugs at target site / site of absorption 2) avoiding inactivation of drug and retaining it in biologically active form 3) providing immediate and / or sustained release with taste masking 4) retaining physical stability of metastable drug form and inhibiting its crystallization thereby enhancing its dissolution and absorption. We therefore undertook design and evaluation of new reverse enteric polymer, its physicochemical characterization and screening for pharmaceutical

applications (process adaptability, film formation etc), toxicity and drug release characteristics. The objectives of this investigation were as follows

9. To understand the effect of polymer architecture of existing excipients on physiochemical properties like pH dependent behavior, glass transition temperature and its interactions with other excipients and drugs causing its inactivation. Apply this understanding for the development of new reverse enteric polymer (NREP), which would overcome these limitations.

10. To develop series of copolymers and ter-polymers which will dissolve rapidly at gastric pH but remain insoluble or exhibit negligible swelling at pH > 4. Characterize these polymers for dissolution / swelling at pH relevant to product performance. Screen the suitable co-monomer composition and optimize its ratio to yield stringent pH dependent behavior needed for the formulation development. To undertake take physicochemical characterization of polymers by FTIR, NMR, GPC and DSC to meet the performance requirements specified above.

11. To evaluate the effect of co-monomer composition and polymer structure on T_g, its interaction with drugs and biocompatibility. To evaluate the *in-vitro* and *in-vivo* biological reactivity of polymer as per USP 26 NF XXI.

12. To investigate the utility of polymer for encapsulating the drugs and evaluate the drug release pattern at both gastric and near neutral pH. More specifically encapsulate the drugs Cefuroxime axetil, Clarithromycin and Ciprofloxacin HCL and using various techniques.

13. To assess the taste masking ability of polymer with immediate gastric release. To evaluate the *in-situ* morphological changes occurring in microspheres using the environmental SEM (ESEM). To compare the performance of NREP coating with a standard commercial product.

14. To assess the effect of basicity / pKa value of monomers DMAMEA and 4-VP on the stability of CA by HPLC analysis.

15. To undertake the physicochemical investigation of interactions between Cefuroxime axetil with Eudragit E and use this as reference to interpret the nature of CA interaction with NREP. These interactions would be evaluated using different analytical tools such as DSC, FTIR, NMR and HPLC analysis.

16. To undertake detailed investigation of Cefuroxime axetil-NREP interactions by techniques such as DSC, FTIR, NMR and HPLC analysis. These investigations were aimed at ensuring the retention of CA in biologically active form.

17. To evaluate the utility of NREP for attaining the sustained gastric release. To undertake the mechanistic investigations for determining the miscibility of NREP with other polymeric excipients like enteric and pH independent polymers. To review the nature of interactions by FTIR analysis. To assess the polymer-polymer miscibility by thermal analysis using MDSC. The T_g data treatment by various theoretical models such as Fox, Couchman and Schneider equation is proposed.

18. To encapsulate CA as a model drug having site-specific absorption in blends of NREP with other polymers. To investigate the effect of polymer-polymer interactions on drug release pattern. To assess the drug release pattern using the commonly employed mathematical model derived by Ritger and Peppas. To employ SEM analysis for correlating the morphological changes in the microspheres with kinetic parameters derived from Peppas equation.

19. To undertake mechanistic investigations of blends of Eudragit E with excipients other polymeric excipients like enteric and pH independent

polymers. To investigate the influence of co-monomer composition, charge density, basicity and polymer architecture on miscibility and polyelectrolyte salt formation. To identify ways of attaining controlled hydrogen bonding in polymer blends to avoid complexation. To review the nature of interactions by FTIR analysis. To assess the extent of polymer-polymer interactions by thermal analysis using MDSC. The T_g data treatment by various theoretical models such as Fox, Couchman and Schneider equation is proposed.

20. To evaluate hydrophobic blends of NREP with fatty acids to enhance the release of drugs Cefuroxime axetil and Ciprofloxacin at gastric pH. To evaluate the taste masking ability of these blends by encapsulation of drugs using emulsification solvent evaporation technique; hot melt granulation and spray drying.

21. To evaluate the co-precipitates of Cefuroxime axetil and Celecoxib with high and low molecular weight NREP for enhancing dissolution. To consider various approaches to enhance the molecular weight of polymer. To characterize the polymer for molecular weight by GPC and intrinsic viscosity. Evaluate the effect of molecular weight of NREP on inhibition drug crystallization in presence of residual solvent, thereby enhancing dissolution. To establish the correlation between the physical state and drug release using XRD analysis and *in-vitro* dissolution test.

CHAPTER 3

A New Reverse Enteric Polymer for Immediate Gastric Release: Design & Evaluation

3.1. INTRODUCTION

The merits of oral drug delivery systems over other routes are well established. In case of oral dosage forms dissolution precedes absorption and any change in the drug release or dissolution process influences drug absorption. In general, drugs, which are slightly soluble in water, are known to exhibit low bioavailability since they have low solubility and low dissolution rate in the gastrointestinal tract. For drugs which have site specific absorption the carrier system should release the drug at the site of absorption. A wide range of excipients has been used for temporal and spatial release of drugs by the oral route. In addition to enhancing bioavailability, excipients also help deliver drugs to patients in forms that facilitate administration.

Tablets and capsules are widely preferred for solid oral dosage forms. However pediatric and geriatric patients often experience difficulty in swallowing them. Drugs are therefore administered to such patients as solutions, suspensions and emulsions. This often leads to perception of bitterness [1, 2] and patient non-compliance [2-4]. The choice of taste masking technique to overcome this problem, is governed by the physicochemical and pharmacokinetic parameters of the drug and the type of dosage form. Wide range of excipients like wax, hydrophobic, enteric and reverse coatings is used for enhancing the palatability. However, many a times the drug dissolution at site of absorption is hampered due to these coatings affecting the bioavailability.

For drugs like Cefuroxime axetil (CA) and Ciprofloxacin hydrochloride, which are better absorbed from upper gastric region, a reverse enteric coating is ideal. However drug-polymer interactions adversely affect drug stability and release. Wax and enteric as well as reverse enteric polymers have not been able to effectively mask the taste without adversely affecting bioavailability of CA. The use of Eudragit E led to inactivation of CA and use of cellulose acetate trimellitate generated impurities above the acceptable levels [5, 6]. One of the major concerns in dispersing microspheres in suspensions form is diffusion of drug into aqueous media leading to perception of bitter taste. Also the slow permeation of moisture from film coat into the CA core results in gelation of CA core, leading to poor dissolution, reduced absorption and bioavailability

[7]. CA has a limited absorption window restricted to upper gastric region and is hydrolyzed by esterase enzyme in intestine to Cefuroxime, a form which cannot be absorbed orally [8]. Hence a polymer capable of releasing it in stomach is desirable. The limitations of existing excipients have educed the need for a new reverse enteric polymer, which can be used for taste masking and sustained gastric release.

pH sensitive polymers are useful as biomedical materials like drug carriers and have been evaluated for properties and possible applications [9]. The new polymers synthesized should meet the criteria for biocompatibility and biodegradability for successful applications. However, for oral drug delivery biodegradability is not critical [9]. Further the polymer should exhibit desired pH dependant behavior, adaptability to high temperatures like those encountered during coating process and biocompatibility to make it suitable for pharmaceutical applications.

In this chapter we report the design, synthesis and physicochemical and biological characteristics of the new reverse enteric polymer. The polymer composition was evaluated to yield the desired dissolution profile at gastric pH and minimal swelling at pH > 4 to provide taste masking and facilitate reconstitution of suspensions. The optimization of the polymer composition and screening of polymers to meet these requirements is described. The screening of polymer and its composition optimization is covered in two parts. Part A describes the screening of monomer compositions for polymer synthesis and the Part B describes the composition optimization of polymer to meet stringent performance requirements for immediate gastric release with taste masking ability.

3.2. PART A: SYNTHESIS OF POLYMERS AND SCREENING FOR REVERSE ENTERIC BEHAVIOR

The pH sensitive polymers in the present investigation were obtained by varying the composition of monomers essentially comprising of the hydrophobic monomer and basic monomers and optionally hydrophilic monomers. This variation in composition was done to attain the desired pH sensitive behavior exhibiting swelling / dissolution in acidic pH and deswelling at neutral and near neutral pH.

In the subsequent section we have discussed the screening of the monomers for the desired pH dependent behavior. The monomers were selected from the list given below. Always there is a concern about the safety and regulatory approval for use of new biomaterials. Taking into account the safety of the materials to be used, the monomers were selected such that their homopolymers or copolymers or derivatives have already acquired the GRAS Status. Synthesis of monomers and polymers is also discussed.

Hydrophobic monomers

The hydrophobic monomer was selected from the group consisting of methacrylic acid esters [10] like methyl methacrylate and butyl methacrylate. The hydrophobic monomers were included in polymer composition to avoid permeation of moisture from coatings to ensure drug stability and prevent drug leaching at pH of saliva.

Basic monomers

The basic monomers were selected from the group consisting of amino alkyl methacrylic acid esters and alkenyl pyridines like dimethyl amino ethyl methacrylate, piperidine ethyl methacrylate and 4-vinyl pyridine. The basic functional monomers were incorporated to impart pH dependent behavior.

Hydrophilic monomers

The hydrophilic monomers were selected from methacrylic acid esters like 2-hydroxy ethyl methacrylate and 2-hydroxyethoxy ethyl methacrylate. These monomers were preferred as their use for preparation of hydrogels in pharmaceutical applications has been described in past [11]. The hydrophilic monomers were included in polymer composition to optimize the pH dependent behavior in presence of minimum amount of functional monomer.

3.2.1. Materials and methods

3.2.1.1. Materials

Methyl methacrylate (MMA), 2-hydroxy ethyl methacrylate (HEMA) and 4-vinylpyridine (4-VP), dimethylamino ethylmethacrylate, butyl methacrylate and 1-piperidine ethanol were purchased from Sigma-Aldrich. Benzoyl chloride, hydroquinone and triethylamine were purchased from Merck. Azobisisobutyronitrile was obtained from local suppliers. All other chemicals were analytical grade. Potassium carbonate and sodium sulphate were purchased from Merck. Tetrahydrofuran for chromatography was purchased from Merck. Deuterated chloroform ($CDCl_3$) was purchased from Sigma Aldrich.

3.2.1.2. Synthesis of 1-piperidine ethyl methacrylate (PEMA)

Step 1: Synthesis of methacryloyl chloride

In a 500 ml round bottom flask (RBF) a mixture of 100 ml methacrylic acid (1.1 mole) and 250 ml benzoyl chloride (2.3 mole) in 1:2 ratio was taken. To this 4.5 g hydroquinone (inhibitor) was added. This mixture was refluxed for 1.5 hr at 90^0 C using a reflux condenser. The above reaction mixture was cooled and 1 g hydroquinone was added to it. This reaction mixture was distilled at 100^0 C and the final product, methacryloyl chloride was collected on an ice bath and stored in refrigerator.

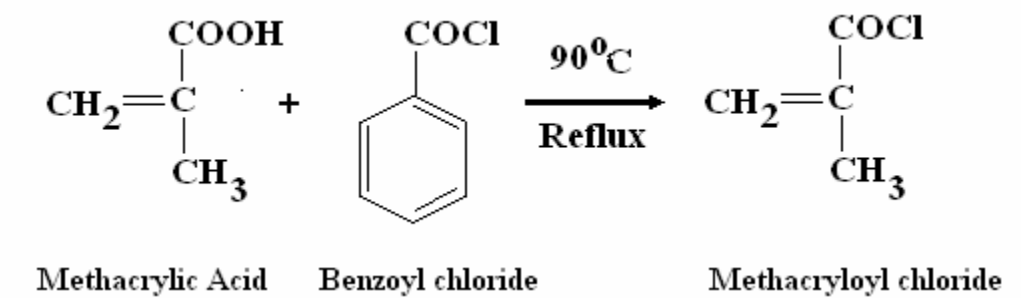

Scheme 1: Synthesis of methacryloyl chloride

Step 2: Esterification of methacryloyl chloride with 1-piperidine ethanol

1-piperidine ethyl methacrylate was synthesized by esterification of methacryloyl chloride and 1-piperidine ethanol. The esterification was carried out in a 250 ml RBF, a mixture of 50 ml of chloroform, 0.012 moles of alcohol and 0.012 moles of TEA were taken and kept on ice bath. In this mixture, 0.12 moles methacryloyl chloride, dissolved in 20 ml chloroform was added drop wise over a period of 2 to 3 hr using addition funnel and with constant stirring. After the complete addition of the acryloyl chloride, stirring was further continued for another 60 min to ensure complete esterification. This mixture was filtered to remove triethylamine hydrochloride salt (TEA HCl) and the filtrate was taken in a separating funnel and extracted 2 to 3 times with 1:2 volume of distilled water and chloroform. The water layer was discarded, and the chloroform layer that contained the product was collected in a 100 ml conical flask. 20 g of anhydrous Sodium sulphate was added and the mass was kept overnight in a refrigerator. Then it was filtered to remove salt and collected in a 100 ml RBF. Chloroform was evaporated from the RBF using rotavapor at reduced pressure (75 mbar) at room temperature and 1-piperidine ethyl methacrylate obtained was stored in refrigerator till further use.

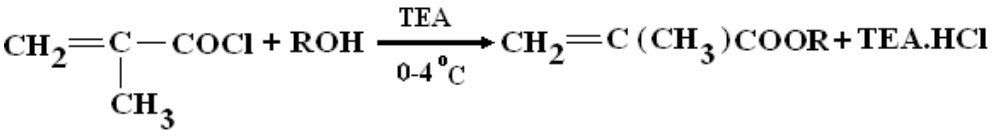

Scheme 2: Synthesis of methacrylate monomer

3.2.1.3. Synthesis of 2-hydroxyethoxy ethyl methacrylate (HEEMA)

The synthesis of HEEMA was carried out as described by Korytkowska et al. [12]. In a 1000 ml RBF, a mixture of methyl methacrylate 214 ml, diethylene glycol 143 ml (3:4 mole ratio) and toluene 262 ml (63 wt %) was taken. To this mixture anhydrous potassium carbonate 29 g (8 wt%, as catalyst) and hydroquinone 5 g

(inhibitor) was added. This mixture was refluxed for 2 hrs at 100^0 C by using reflux condenser. The above reaction mixture was cooled and then filtered. The filtrate was taken and washed with 2:1 vol. ratio of distilled water. The aqueous layer was extracted with 3 portions of DCM in a 3:2 v/v ratio. The water layer was discarded, DCM layer was collected in a 1000 ml conical flask and to this 150 g of anhydrous sodium sulphate was added and kept overnight in a refrigerator. The salt was removed by filtration. The filtrate was collected in a 1000 ml RBF and DCM was evaporated under reduced pressure of 75 mbar using rotavapor at room temperature. The crude product was collected and kept in refrigerator till further use.

To the crude product, 2 mg of hydroquinone was added and distilled under vacuum (1 mbar), the fraction that distilled at 100^0C was hydroxyethoxy ethylmethcrylate and was collected and stored in refrigerator.

3.2.1.3. Characterization of monomers

FTIR

HEEMA and PEMA were characterized neat on Shimadzu FT-IR 8300 at 4 cm^{-1}.

^{1}H NMR

HEEMA and PEMA were characterized H^1 NMR on FT NMR AC 200 operating at 200 MHz and MSL500 FT NMR operating at 500 MHz.

3.2.1.4. Synthesis of polymers

Compositions of various monomers, solvent and initiator used for polymerization are given in **Table 3.1**.

All polymerizations were carried out by free radical mechanism [16] using solution polymerization technique. Dimethyl formamide (DMF) was used as solvent for polymerization. Azobisisobutyronitrile was used as free radical initiator. DMF, AIBN and specific molar quantities of monomer as mentioned below in the **Table 3.1**, were used for polymerization. This mixture was agitated for 5 min. Nitrogen gas was slowly

purged in to this reaction mixture for 5-10 min. Polymerization was carried out at 65^0 C over night (15-16 hrs) in thermostatted water bath. Thereafter the polymer solution was concentrated at 60^0C in a 100 ml RBF using rotavapor at reduced pressure of 22 mbar.. This concentrate was precipitated in water. The precipitated polymers were dried at room temperature under vacuum and stored in desiccators till further use.

3.2.1.5. Characterization of polymers

^{1}H NMR

The polymer composition was determined by H^1 NMR using FT NMR AC 200 operating at 200 MHz and MSL500 FT NMR operating at 500 MHz. The polymer composition was determined by integrating the signals pertaining to each monomer.

GPC

The molecular weight was determined by the GPC. Weight average molecular weight of the polymer was determined by GPC (Waters 590 programmable HPLC pump, Waters 410 differential refractometer) using polystyrene standard (Polysciences Inc. USA) as reference. 3 mg polymer sample was dissolved in 1 ml of tetrahydrofuran and eluted through Styragel columns at a flow rate of 1ml / min at 25 °C.

3.2.1.6. Fabrication of polymer film

The polymer film was cast using the solvent evaporation technique by spreading the polymer solution (12 % w/v) in chloroform on a Teflon surface (casting area 19.64 cm^2). The solvent was allowed to evaporate at room temperature for 48 h. After solvent evaporation the film was cautiously pulled off from the Teflon surface. The film was stored in desiccator at room temperature till further use. The film thickness was measured using a micrometer screw and average film thickness was 0.06-0.07 mm.

3.2.1.7. pH dependent dissolution / swelling

Film of approximately 10 mm x 15 mm size was cut, weighed and immersed in 15 ml water and buffers of pH 1.2, 4.5 and 5.8 at room temperature. The dissolution of polymer film was observed at pH 1.2 at 10, 15, 30, 45 and 60 min. The polymer film immersed in water, pH 4.5 and 5.8 was removed daily, blotted with tissue paper and weighed. This procedure was repeated for 7 days. The buffers used for the study were hydrochloric acid buffer pH 1.2 (USP 26 NF XIII), phosphate buffer pH 5.8 (USP 26 NF XIII) and citric acid-trisodium citrate buffer pH 4.5. The citric acid-sodium citrate buffer was prepared by adjusting the pH of tri sodium citrate solution 0.03 M (9.5 g in 100 ml distilled water) to 4.5 by drop wise addition of citric acid 0.3 M (6.34 g in 100 ml distilled water) using pH meter. The equilibrium swelling was calculated as the ratio of difference between the weight of the swollen polymer film (W_s) and the dry polymer film (W_d) to that of the swollen polymer film (W_s).

$$\textbf{(\%) Equilibrium swelling} = \frac{(W_s - W_d)}{W_s} \times 100 \qquad \textbf{Eq 1}.$$

Table 3.1 Polymer compositions

S. No.	Polymer Composition	Monomer wt/wt %	Solvent [a]	Initiator [a]	Mol. wt
C1	MMA-*co*- VP	70 30	68.75	0.25	79,602
C2	MMA-*co*-DMAEMA	70 30	68.71	0.25	2,218
C3	BuMA -*co*-VP	70 30	55.44	0.25	1,14,393
C4	MMA-*co*-HEMA-*co*-DMAEMA	43 42 15	69.06	0.25	52,370
C5	MMA-*co*- HEMA -*co*-PEMA	43 42 15	62.09	0.5	13,152
C6	MMA -*co*-HEMA-*co*-VP	43 42 15	70.86	0.5	1,57,226
C7	MMA-*co*-HEEMA-*co*-VP	43 42 15	72.64	0.5	59,966
C8	MMA-*co*-HEEMA-*co*-DMAEMA	43 42 15	71.31	0.5	7,228
C9.	MMA-*co*-HEEMA-*co*-PEMA	43 42 15	70.70	0.5	14,589
C10	MMA-*co*-BuMA-*co*-VP	43 42 15	43.54	0.25	33,788
C11	MMA-*co*-BuMA-*co*-DMAEMA	43 42 15	44.29	0.25	1,86,456
C12	MMA-*co*-BuMA-*co*-PEMA	43 42 15	43.47	0.25	51,611

Where: a: % by weight of monomer MMA = methyl methacrylate, BuMA = butyl methacrylate, DMAEMA = dimethyl aminoethyl methacrylate, HEMA = hydroxy ethyl methacrylate, VP = vinyl pyridine, HEEMA= hydroxyethyl ethyl methacrylate, PEMA = piperidine ethyl methacrylate, MOL. Wt = molecuclar weight

3.2.2. Results and discussion

An ideal reverse enteric polymer has to retard the drug release at the pH of saliva (5.8-7 for humans) [13] and release the drug in the gastric region (pH <3) to ensure maximum bioavailability. The candidate polymer has to have the lowest possible dissolution pH above which, it should neither dissolve, nor swell. This entails use of cationic monomers. At the acidic pH, the polymer should dissolve rapidly so as to release the drug without any delay. In order to prevent the release of the drug by diffusion and / or protect the drug, the polymer should preferably be hydrophobic. The polymer should exhibit negligible swelling at pH of saliva and also in water to prevent leaching of drug and thus avoid perception of bitter taste. In the following sections we report the physicochemical characteristic of polymers and their screening based on response to different pH environment, to meet the requirements of an ideal reverse enteric polymer. The polymer composition exhibiting rapid swelling / dissolution at acidic pH with minimum swelling at pH 4.5 and 5.8 was taken up for further evaluation to match the desired pharmaceutical characteristics.

3.2.2.1. Characterization of monomers

FT-IR spectrum of PEMA (neat)

3410 cm^{-1} due to N-H stretching, 1720 cm^{-1} due to C=O stretching in ester, 1637.5 cm^{-1} due to C=C stretching, 1452 cm^{-1} due to C-N stretching, 1165 cm^{-1} C-C(=O)-O stretching. 997.1 cm^{-1} due to =C-H bending.

FT-IR spectrum of HEEMA (neat)

3427 cm^{-1} due to O-H stretching, 1716 cm^{-1} due to C=O stretching in ester, 1637.5 cm^{-1} due to C=C stretching, 1172 cm^{-1} C-C(=O)-O stretching, 1132 cm^{-1} due to C-O stretching, 997.1 cm^{-1} due to =C-H bending.

^{1}H NMR in ($CDCl_3$) PEMA:

6.07 δ and 5.57 δ due to protons from $=CH_2$ group, 4.35 δ due to protons of $–C(O)O–CH_2–$ group, 2.65 δ due to protons of –NH group, 2.44 δ due to protons of $–N(CH_2–)$ group, 1.91 δ due to protons of $CH_3–C=C–$ group and 1.41 δ due to protons of $–CH_2–$ groups.

^{1}H NMR in (DMSO d_6) HEEMA

6.07 and 5.57 δ due to protons of $=CH_2$ groups, 4.21 δ due to protons of $–(O)O–CH_2–$ groups, 3.65 δ due to protons of $–CH_2–O–CH_2–$, 3.49δ due to protons of $–CH_2–OH$ group and at 1.88 δ due to protons of $–CH_3$ groups.

3.2.2.2. Characterization of polymers

The molecular weight of the polymers is shown in **Table 3.1.** Polymer composition was determined by NMR.

^{1}H NMR spectra of polymers

The ^{1}H NMR Spectra of all the polymers have some common signals at 0.83 and 0.90 δ for protons of $–CH_3$ in methacrylate groups, at 1.23 or 1.39 δ for protons of $–CH_2–$ groups of carbon–carbon backbone in polymer, at 3.56 or 3.58 δ due to protons of $–C(O)O–CH_3$ groups and at 4.08.or 4.11 δ due to protons of $–C(O)O–CH_2–$ groups.

^{1}H NMR ($CDCl_3$) of poly(MMA-*co*-VP)

1.55 δ for protons of –CH– groups, 6.9 δ due to protons adjacent to nitrogen of 4 vinyl pyridine in aromatic ring, 8.38 δ for protons adjacent to nitrogen of 4 vinyl pyridine.

^{1}H NMR ($CDCl_3$) of Poly (MMA-*co*-DMAEMA)

2.27 δ due to protons of $–CH_2–N$, 2.68 δ for protons of $(CH_3)_2$-N groups of DMAEMA.

^{1}H NMR ($CDCl_3$) of Poly (BuMA-*co*-VP)

1.55 δ due to protons of –CH– groups, 1.33 δ due to protons of $–CH_2–$ groups of BuMA, 6.9 δ and 8.38δ due to protons adjacent to the nitrogen of pyridine ring.

^{1}H NMR ($CDCl_3$) of Poly (MMA-*co*-HEMA-*co*-DMAEMA)

1.81 δ for protons due to –OH groups, 3.8 δ for protons due to $–CH_2–OH$ of HEMA, 2.27 δ due to $–CH_2–N$ protons, 2.58 δ due to protons from $(CH_3)_2$ N groups of DMAEMA.

^{1}H NMR ($CDCl_3$) of Poly (MMA-*co*-HEMA-*co*-PEMA)

1.39 δ for protons due to $–CH_2–$ groups, 1.57 δ for protons due to –CH– groups of piperidene, 1.82 δ for protons due to –OH proton and 3.81 δ for protons due to$–CH_2–$ OH of HEMA, 2.43 δ for protons due to NH group and 2.58 δ due to protons from $CH_2–N–$groups of PEMA.

^{1}H NMR ($CDCl_3$) of Poly (MMA-*co*-HEMA-*co*-VP)

1.52 δ for protons due to –CH– groups, 8.41 δ due to protons adjacent to nitrogen of pyridine ring, 3.58 δ for protons of OCH_3 groups of methyl methacrylate and 3.82 δ for protons of OCH_2 groups of HEMA.

^{1}H NMR ($CDCl_3$) of Poly (MMA-*co*-HEEMA-*co*-VP)

1.65 δ for protons of –CH– groups, 6.14 and 8.0 δ for protons adjacent to nitrogen in pyridine ring. The signals for the protons from HEEMA were seen at 1.96 δ due to –OH, 3.87δ due to $–CH_2–OH$ and 3.59δ due to $–CH_2–O–CH_2–$ groups.

^{1}H NMR ($CDCl_3$) of Poly (MMA-*co*-HEEMA-*co*-DMAEMA)

1.82 δ due to –OH group protons, 3.73 δ due to protons of $–CH_2–OH$ groups of HEMA, 2.26 δ due to $–CH_2–N$ group protons and 2.56 δ due to $(CH_3)_2N$ group protons of DMAEMA and at 3.68 δ due to protons of $–CH_2–O–CH_2–$ groups in HEEMA.

^{1}H NMR ($CDCl_3$) of Poly (MMA-*co*-HEEMA-*co*-PEMA)

1.43 δ due to protons of $–CH_2–$ groups and 1.57 δ for –CH– groups of piperidine. 1.82 δ due to protons of –OH groups and 3.81δ due to protons of $–CH_2–OH$ groups and 3.68 δ due to $–CH_2–O–CH_2–$ groups of HEEMA, 2.43 δ due to NH group protons, and 2.58 δ due to $CH_2–N$ protons of PEMA.

^{1}H NMR ($CDCl_3$) of Poly (MMA-*co*-BuMA-*co*-VP)

1.55 δ for protons of –CH– groups, 1.33 δ due to protons of $–CH_2–$ groups of BuMA, 6.9 δ due to protons adjacent to nitrogen of 4 vinyl pyridine in aromatic ring, 8.38 δ for protons adjacent to nitrogen of 4 vinyl pyridine.

^{1}H NMR ($CDCl_3$) Poly (MMA-*co*-BuMA-*co*-DMAEMA)

2.27 δ for protons due to $–CH_2–N$ groups and 2.68 δ due to protons of $(CH_3)_2N$ groups of DMAEMA.

^{1}H NMR ($CDCl_3$) of Poly (MMA-*co*-BuMA-*co*-PEMA)

0.94 δ due to protons of CH_3 groups and 1.4 δ due to protons of $–CH_2$ groups of BuMA, 2.43 δ due to protons of NH groups, 2.58 δ due to protons of $CH_2–N$ groups of PEMA

Polymer screening based on response to buffers of different pH

The screening was based on the response of the polymers towards the buffer media. Due to presence of the cationic monomer most polymers showed dissolution at acidic pH. Polymers, which dissolved at acidic pH and remained deswelled at pH 4.5 and 5.8 for extended period were considered ideal. The compositions C1 to C12 were evaluated for this. The composition showing ideal behavior was taken up for further optimization. The response of the compositions C1-C12 for different buffers is shown in **Table 3.2, 3.3 and 3.4**.

Table 3.2. Swelling / Solubility behavior of polymer in acidic buffer pH 1.2

S. No	Observed behavior	Comments
C1	The polymer film started thinning from the sides and it almost completely dissolved in 30 min with only a small part remaining which solubilized in 60 min.	Dissolution rate needs to be enhanced
C2	Initially the polymer film showed some swelling in 10 min and later started thinning and major portion solubilized in 30 min and the remaining part in 60-80 min.	Dissolution rate needs to be enhanced
C3	The polymer film swells upto 30 min and then solubilized almost completely in 50 min	Dissolution rate needs to be enhanced
C4	The polymer showed swelling of 30 % attained in 30 min and it remained in a deformed shape till 120 min.	Not suitable, very slow dissolution
C5	The polymer film showed an equilibrium swelling of 14.8% attained in 15 min and remained same till 120 min.	Not suitable very slow dissolution
C6	The edges of the polymer film started thinning. The film solubilized almost completely in 30 min.	Desirable
C7	The polymer film dissolved in 15 min.	Desirable
C8	The polymer film dissolved in 15 min.	Desirable
C9	The polymer film dissolved in 15 min.	Desirable
C10	The polymer film showed swelling of 12.1 % attained in 30 min and remained so till 120 min.	Dissolution needs to be enhanced
C11	The edges of the polymer film started to thin from the sides and the film showed high swelling in 20 min followed by complete dissolution in 40 min.	Dissolution needs to be enhanced
C12	The polymer film showed high swelling in 15 min followed by complete dissolution in 30 min.	Desirable

Table 3.3 Swelling / Solubility of polymer in buffer pH 4.5

S. No	Observed behavior	Comments
C1	The polymer film does not show any swelling on the first day. On day 2 fall of 1.43 % in weight was observed indicating dissolution	Need to increase hydrophobicity without affecting dissolution at pH 1.2
C2	The polymer film goes in solution in 2 hrs on day 1.	Not desirable, it has to be insoluble
C3	The polymer film does not show any swelling from day 1 to day 7.	Desirable
C4	The polymer does not show any swelling in 2 hrs on day 1 but swells upto 33.3 on day 3 and it solubilizes from day 4 onwards to 11 % on day 7.	High swelling is not desirable. Hydrophobicity needs to be increased
C5	The polymer film does not show swelling till day 3 but starts to solubilize 1.4% on day 4 and 3 % on day 7.	Hydrophobicity needs to be increased
C6	The polymer film does not show swelling on day 1 and till day 3 but slight dissolution from day 7.	Initial behavior is acceptable. Further increase in hydrophobicity needed.
C7	The polymer film shows high swelling 49 % in one hr on day 1. Followed by deformation in shape with complete dissolution on day 5.	Not desirable, it has to be insoluble
C8	The polymer film goes into solution partially, in one hour and complete dissolution in second hour on day 1.	Not desirable, it has to be insoluble
C9	The polymer film shows high swelling and deformation in shape in one hour on day 1 and goes in to solution on day 2.	Not desirable, it has to be insoluble
C10	The polymer film does not show any swelling from day 1 to day 7.	Desirable
C11	The polymer film swells and deforms on day 1 and goes into solution on day 2.	Not desirable, it has to be insoluble
C12	The polymer film does not show any swelling on day 1 but swells upto 10.2 % on day 5 and it goes into solution 6.9 % on day 7.	Not desirable, it has to be insoluble

Table 3.4 Swelling / Solubility behavior of polymer in buffer pH 5.8

S. No.	Observed behavior	Comments
C1	The polymer film did not show any swelling in 2 hr on day 1 with 3.82 % swelling on day 2. Later it started to solubilize from day 4, measured in terms of fall in weight (5 %).	Need to increase hydrophobicity without affecting dissolution at pH 1.2
C2	The polymer film showed a swelling of 6.2 % in one hour followed by solubilization and it broke into pieces on day 2 and solubilized on day 4	Not desirable, it has to be insoluble
C3	The polymer film does not show any swelling from day 1 to day 7.	Desirable
C4	The polymer film does not show swelling on day 1 but swells upto 4.3% on day 7.	Hydrophobicity needs to be increased
C5	The polymer film does not show any swelling from day 1 to day 7.	Desirable
C6	The polymer film does not show any swelling till day 5 but swells to 1.3 % on day 7.	Initial behavior is accepatable further increase in hydrophobicity needed
C7	The polymer film shows a swelling of 41.28% in one hr. on day 1, is later deformed in shape and remains as such till day 7.	High swelling is not desirable Hydrophobicity needs to be increased
C8	The polymer film goes in solution in 2 hrs on day 1.	Not desirable, it has to be insoluble
C9	The polymer film shows high swelling and deformation on day 1 in 2 hrs and the polymer solubilizes partially till day 7.	Not desirable, it has to be insoluble
C10	The polymer film does not show any swelling from day 1 to day 7.	Desirable
C11	The polymer film swells on day 1, breaks into pieces on the second day and solubilizes on day 3.	Not desirable
C12	The polymer film does not show swelling till 2 days but later it swells and is completely deformed. The polymer does not dissolve in 7 days.	High swelling is not desirable Hydrophobicity needs to be increased

The compositions C1 and C2 both had higher content of the hydrophobic monomer and showed slow dissolution at pH 1.2. The composition C2 dissolved at pH 4.5 within 2 hr and exhibited high swelling followed by slow dissolution at pH 5.8. Since dissolution or swelling at higher pH is not desired, the hydrophobicity needs to be increased but the polymer had shown slow dissolution at acidic pH hence this does not seem feasible. The composition C1 showed slight dissolution at pH 4.5 on day 2 and after day 5 in pH 5.8. Hence the increase in hydrophobic nature would overcome this limitation. So this copolymer composition was considered for further optimization. Another copolymer C3 with BuMA and VP was attempted replacing the MMA in C1 to impart the hydrophobic nature. The replacement of MMA by BuMA in C3 imparted the hydrophobic nature to the polymer as desired and the dissolution at pH 4.5 and 5.8 as observed in C1 was overcome in C3. All the compositions C1 to C3 showed slow dissolution in acidic pH 1.2 and hence to enhance the dissolution addition of hydrophilic monomer was considered and a series of ter-polymers C4 to C12 were synthesized as shown in **Table 3.1.**

The monomers HEMA and HEEMA were considered for imparting hydrophilic nature to the polymers. The inclusion of HEMA would impart glassy nature to the polymer as compared to the inclusion of HEEMA, which would result in imparting rubbery nature to the polymers. The compositions C4, C5 and C6 are based on MMA, HEMA copolymerized with basic monomers DMAEMA, PEMA and VP. The compositions C4 and C5 showed swelling at pH 1.2 without dissolution upto 2 hr. This behavior can be attributed to rubbery nature of these polymers due to presence of DMAEMA and PEMA. This causes rapid relaxation in polymer due to further fall in T_g due to plasticization of polymer chains by diffusion of the buffer media. This causes swelling of the polymers initially and then the polymer slowly goes into solution. The composition C6 containing VP shows rapid dissolution at pH 1.2 as desired. The composition C6 did not show swelling at pH 4.5 and 5.8 upto 3-4 days, which is desirable. The slight swelling shown on day 7 can be reduced by further optimization of the polymer composition. This polymer composition with MMA, HEMA and VP was therefore considered for further investigations.

The compositions (C7, C8 and C9) containing MMA, HEEMA copolymerized with VP, DMAEMA and PEMA were synthesized. The inclusion of highly hydrophilic monomer HEEMA in these polymers causes rapid dissolution of these polymers at acidic pH 1.2. However the inclusion of HEEMA resulted in dissolution of these compositions at pH 4.5 and swelling followed by dissolution at pH 5.8.

In order to increase the hydrophobicity, the hydrophilic monomer was replaced with BuMA. The inclusion of BuMA would impart the rubbery nature to the polymer. This would lower of the T_g of the polymer. The diffusion of the buffer media would further lower the T_g of the polymer causing the polymer chains to undergo relaxation and aid in its dissolution at pH 1.2. Also the inclusion of BuMA along with MMA would retard the swelling at pH 4.5 and 5.8. Compositions C10, C11 and C12 containing MMA, BuMA copolymerized with VP, DMAEMA and PEMA were synthesized. The compositions C11 and C12 showed swelling and dissolution at pH 4.5 and 5.8, which was not desired. The composition C10 did not show any swelling at pH 4.5 and 5.8, which was desirable. However the polymer showed slow dissolution at pH 1.2.

Amongst all the compositions investigated, the polymer based on monomer VP showed minimal swelling at pH 4.5 and 5.8 so this basic monomer was preferred over DMAEMA and PEMA as inclusion of these monomers caused the polymers to swell at higher pH. The hydrophilic monomer HEMA was preferred over HEEMA. The inclusion of HEEMA was found to impart swelling at pH 4.5 and 5.8. The hydrophobic monomer MMA was preferred over BuMA as the T_g of homopolymer of BuMA is 20°C and its presence in the compositions investigated here imparted rubbery nature to the polymers, which was not desirable. Higher T_g is preferred so that the polymer does not cause tackiness at elevated temperatures involved during coating and drying process. Hence the various compositions of copolymers MMA-*co*-VP and terpolymers based on MMA-*co*-HEMA-*co*-VP were considered for further optimization of the dissolution behavior.

3.3. PART B: COMPOSITION OPTIMIZATION OF NEW REVERSE ENTERIC POLYMER

3.3.1. Materials and methods

3.3.1.1. Materials

Methyl methacrylate (MMA), 2-hydroxy ethyl methacrylate (HEMA) and 4-vinylpyridine (4-VP) were purchased from Sigma-Aldrich. Tetrahydrofuran for chromatography was purchased from Merck. Deuterated chloroform ($CDCl_3$) was purchased from Sigma Aldrich. Azobisisobutyronitrile was obtained from local suppliers. All other chemicals were analytical grade.

3.3.1.2. Synthesis of the pH sensitive polymer

The trace impurity of EGDMA was removed from HEMA before polymerization to yield soluble polymer. Freshly distilled monomers MMA and 4-VP were used for polymerization. In a 250 ml round bottom flask MMA, HEMA and 4-VP were added to 80 ml of dimethyl formamide. Solution polymerization of the monomer mixture was carried out using azobisisobutyronitrile as initiator at 65°C for 18 h. The polymer solutions were concentrated on a rota-evaporator. The polymers were dissolved in (1:1) dichloromethane-methanol mixture and precipitated in water to remove unreacted monomers. Polymers were dried at 27°C under vacuum for 72 h. The polymer compositions are given in **Table 3.5.**

3.3.1.3. Polymer characterization

3.3.1.3.a. ^{1}H NMR analysis

The polymer composition was determined by ^{1}H NMR spectroscopy. The spectra were recorded on a 500 Mz Bruker DRX spectrometer. The solvent used was

deuterated chloroform ($CDCl_3$). The polymer composition was determined by integrating the signals pertaining to each monomer.

3.3.1.3.b. Gel permeation chromatography (GPC)

Weight average molecular weight of the polymer was determined by GPC (Waters 590 programmable HPLC pump, Waters 410 differential refractometer) using polystyrene standard (Polysciences Inc. USA) as reference. The polymer sample 3 mg was dissolved in 1 ml of tetrahydrofuran and eluted through Styragel columns at a flow rate of 1ml / min at 25 °C.

3.3.1.3.c. Glass transition temperature (T_g)

The polymer glass transition temperature was determined by modulated differential calorimetry (MDSC) using Q100 DSC (Q^{TM} series), TA Instruments using MDSC heat-only method. The modulation amplitude was $\pm$ 0.53°C every 40 s. Indium was used to calibrate the enthalpy and temperature values. 2.1 mg of sample was placed in the crimp sealed aluminium pan and scanned at 5°C / min over the temperature range 10-200°C. Nitrogen gas was used at a purge flow of 50 ml / min.

3.3.1.3.d. FTIR spectroscopy

NREP was analyzed by FTIR using a Perkin Elmer, Spectrum One (diffused reflectance mode). 2-3 mg of sample was thoroughly mixed and triturated with potassium bromide (100 mg) and placed in the sample holder. The sample was scanned from 4000 to 450 cm^{-1}. The measuring conditions were resolution, 4.0; sample scans; 16.

3.3.1.3.e. Fabrication of polymer film

The same procedure was repeated as described in section 3.2.1.6.

3.3.1.3.f. pH dependent dissolution / swelling

The same procedure was repeated as described in section 3.2.1.7.

3.3.2. Biological reactivity *in-vitro* and *in-vivo*

3.3.2.1. Cell line and culture media

L-929 mammalian fibroblast cells (source ATTC) were used for the in-vitro biological reactivity test supported with minimum essential medium (MEM) supplemented with Foetal Bovine Serum as culture media.

3.3.2.2. Animals

10 healthy albino mice, not previously used, (5 for test and 5 for control) weighing 17–23 g were used for study. Animals were housed in polypropylene cages with stainless steel top with paddy husk bedding under standard conditions of temperature 23 $\pm$ 1°C. The animals were fasted overnight prior to test and 3-4 hrs post medication and thereafter fed from the commercial feed and potable water was given *ad libitum*.

3.3.2.3. In-vitro biological reactivity test

The *in-vitro* cytotoxicity test was conducted using test on extracts method using the polymer sample as per USP 26 NF XXI (2003) [14]. The polymer extract was compared against the negative control and positive control; Ultra high molecular weight polyethylene and diluted phenol respectively. The polymer extract was prepared by incubating polymer sample (0.1g/ml) in serum supplemented mammalian cell culture media at 37 $\pm$ 2 °C for 24 $\pm$ 1 h in 5 $\pm$ 1 % carbon dioxide environment and the extract was filtered through 0.22 µ membrane. The serum supplemented mammalian cell

culture medium was preferred as it simulates more closely to the physiological conditions. 100 % extract was used as such and other samples were prepared by diluting to 50 % and 25 %.

The extracts of polymer, negative control and positive control in triplicate as well as their dilutions were placed on confluent monolayer of L-929 mouse fibroblast cells. The cells were incubated with extracts at 37± 2 °C for 24 ± 1 h. The cell culture was examined microscopically for cellular response.

3.3.2.4. In- vivo biological reactivity test

The *in-vivo* biological reactivity test was conducted using systemic injection test intravenous and intraperitoneal injection of NREP extracts as per USP 26 NF XXI (2003).

3.3.2.4.a. Systemic injection test (intravenous)

The NREP extract was compared against the control; sodium chloride injection containing 0.9% sodium chloride NaCl. The NREP extract (2.0 g / 10 ml) was prepared by extracting the sterilized polymer in duplicate, in 10 ml each of sodium chloride injection, containing 0.9% sodium chloride NaCl at 70 ± 2 °C for 24 ± 1 h. The portions of test and control extract were subjected to check the pH. The NREP extract was injected intravenously (lateral tail vein) to 5 mice at a dose of 50 ml / kg body weight. Similar procedure was repeated on 5 mice for control by injecting sodium chloride injection at same dose. The animals were observed immediately after injection and at 4, 24, 48 and at 72 h for any abnormalities, weight loss or death.

3.3.2.4.b. Systemic injection test (intravenous)

NREP extracts were prepared in duplicate by extracting sterilized 2.0 g of polymer in 10 ml of cotton seed oil at 70 ± 2 °C for 24 ± 1 h and 10 ml of cotton seed oil alone was used as control. 10 animals not previously used, were grouped in to two

lots of 5 for control and 5 under test. The rest of the test procedure was performed as described for the intravenous systemic injection test as described above.

3.3.3. Results and discussion

Apart from pH dependent behavior, the candidate polymer should have other features like good film forming characteristics and high T_g as to ensure ease of processing during various formulation stages like coating and heat-sealing. A blend of excipients has often to be used to achieve desired drug release profiles. The polymer should therefore be compatible with the drug as well as other excipients and be non-toxic. In the following sections we show how the copolymer designed by us meets the requirements of an ideal reverse enteric polymer.

3.3.3.1. Monomer choice for reverse enteric copolymer

The reverse enteric polymer is intended for immediate / sustained release of drugs in the gastric region (pH<3) and inhibit the same in reconstitution media pH $\geq$ 3.5. Polymers containing cationic groups are soluble in acidic medium. We chose 4-vinyl pyridine as the cationic monomer. The pK_a of 4-VP is 5.45 - 5.65. The T_g of poly (4-VP) is 148°C and hence copolymer based on 4-VP would have higher T_g. This would ensure ease of processing and storage. In order to minimize the charge on the polymer and yet ensure dissolution at gastric pH, 4-VP was copolymerized with MMA and HEMA. This approach is similar to that adopted by Lynn and Langer [15] who synthesized a series of Michael addition polymers, which are equally efficient in gene delivery but are not as toxic as polyethylene imines.

The charge density on the copolymer is tailored to ensure pH dependent behavior but low enough to avoid interactions with drugs and other polymers. This is also expected to cause lower cell damage and ensure lack of biological reactivity.

3.3.3.2. Composition optimization

Reverse enteric polymer for oral suspension should exhibit immediate drug release at the gastric pH. Yet the drug release should be minimal at reconstitution pH so that it does not lead to perception of bitterness.

The release of the drug from the polymer depends upon the relative rates of the sorption and diffusion of the penetrant and the diffusion of the drug. In the case of the drug encapsulated in a reverse enteric polymer, two conditions have to be met. The reconstitution medium should not penetrate the polymer so that the release of the drug is inhibited. A hydrophobic / glassy polymer will ensure this. At the gastric pH, the medium should penetrate the polymer and cause rapid dissolution of the polymer without appreciable swelling. This will ensure that the drug does not undergo polymorphic transformation / gelation which inhibits its release resulting in lower bioavailability.

Sorption of liquids into glassy polymers results in either bulk scale changes or case II transport. In the former case, quasi equilibrium swelling is followed by a slow approach to final true equilibrium. Polymers, which undergo bulk scale changes, will obviously be not suitable, if the drug undergoes gelation or polymorphic transformation in presence of moisture [16].

If the sorption of the penetrant medium follows case II transport and the swollen layer undergoes rapid dissolution, the drug immobilized in the glassy polymer region will be protected, while that in the swollen layer will be released as a result of dissolution. The copolymer composition was optimized to achieve this end result as discussed below.

The polymers listed in **Table 3.5** were screened for pH dependent behavior by exposing the polymer films to buffers of pH 1.2, 4.5 and 5.8. The results of swelling studies of these polymers at buffer 4.5 and 5.8 are shown in **Figs. 3.1 and 3.2** respectively. Copolymer of MMA and 4-VP containing 95 % w/w of MMA in feed, was synthesized. At pH 1.2, the copolymer did not solubilize even after 4-5 hrs. This can be attributed to high MMA content. The resulting polymer was glassy and hydrophobic and the penetration of the buffer medium in the polymer film was very slow. To

enhance the rate of penetration of the buffer and also the rate of dissolution, a copolymer (P1) containing 83 % MMA and 17 % of 4-VP was synthesized.

On exposure to buffer pH 1.2, the copolymer film (P1), became translucent with gradual dissolution. Under acidic conditions this copolymer swelled in the buffer more rapidly because of higher 4-VP content. The swelling of the film leads to the formation of a glassy core and swollen outer shell. As time proceeds the glassy core recedes inwards, while the swollen shell dissolves. Thus overall dimensions of the film decrease with time leading eventually to the complete dissolution of the film after 60 min. On exposure to buffer pH 4.5, the film dissolved after 24 hrs and at pH 5.8 it showed water uptake followed by dissolution after 3 days. Increase in 4-VP content enhanced the rate of dissolution of the polymer film at pH 1.2 but also led to dissolution of the polymer at pH 5.8. Such a polymer would be of little use as a reverse enteric polymer for oral suspension. To enhance the rate of penetration of buffer at pH 1.2 without enhancing the rate of dissolution / swelling at pH 5.8, incorporation of neutral hydrophilic monomer *viz* HEMA was considered. A series of ter-polymers P2 to P9 were synthesized and the composition was optimized to ensure rapid dissolution at acidic pH and minimal swelling at pH 4.5 and above.

To enhance the dissolution in acidic pH further, polymer P2 was synthesized. The MMA content was lowered to 61 % w/w, HEMA was increased to 21 % w/w and 4-VP content 18 % w/w was unaltered. The incorporation of HEMA resulted in rapid and complete dissolution of P2 at pH 1.2 in 30 min as compared to 60 min for P1. However the presence of hydrophilic component HEMA resulted in dissolution of the polymer at pH 4.5 and 5.8 after 2-3 days. To impart hydrophobic character to the polymer, compositions P3 and P4 were synthesized with higher content of MMA (69, 68 % w/w) and lower content of 4-VP (11 and 9 % w/w) maintaining the HEMA content at 21 % as in P2.

Both polymers P3 and P4 containing higher percentage of MMA showed very low uptake of water as compared to polymer P2 at pH 4.5 and 5.8 respectively. However the increase in content of MMA with reduction in 4-VP as compared to P2 imparted a hydrophobic character. This delayed its dissolution rate and complete dissolution at pH 1.2 occurred after only 45 min. In order to enhance the dissolution rate

at acidic pH, compositions P5 and P6 containing higher HEMA (37 and 32 % w/w respectively) and lower MMA (52 and 56 % w/w respectively) content than P3 and P4 were synthesized.

As expected, the increase in content of HEMA in compositions P5 and P6 resulted in rapid dissolution at acidic pH 1.2 as compared to polymer P3 and P4. With increase in HEMA content, these films showed swelling at pH 4.5 and 5.8 followed by dissolution on day 3 of exposure. To ensure minimal drug leaching at pH 4.5 and 5.8, enhanced polymer hydrophobicity at this pH was desired. Composition P7 containing 61 % w/w of MMA, 30 % w/w of HEMA and 9 % w/w of 4 VP was synthesized. The polymer dissolved rapidly (15min) at pH 1.2. It did not dissolve at pH 4.5 and 5.8 but swelled significantly. Swelling would contribute to diffusional release of drug, in the swollen layer and render the reconstituted suspension bitter, over a period of time. To suppress the swelling at pH 4.5 and 5.8, compositions P8 and P9 with slightly higher MMA (64 and 62 % respectively) and lower HEMA content (24 and 27 % w/w) as compared to polymer P7 were synthesized. Both P8 and P9 showed rapid dissolution at pH 1.2 and minimal swelling on exposure to buffer pH 4.5 and 5.8 for period of 7 days, as seen in **Figs. 3.1 and 3.2.** Thus an optimum polymer composition, which showed minimum swelling at pH 4.5 and above but rapid dissolution at pH 1.2 was arrived at. This composition P9 taken up for further investigation would be referred to as NREP in subsequent discussion.

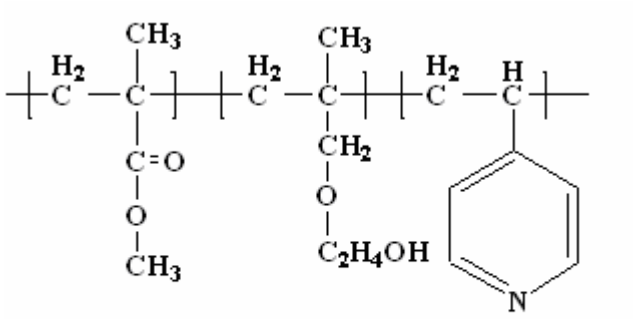

New Reverse Enteric Polymer

Scheme 3. Structure of new reverse enteric polymer

Table 3.5 Polymer composition: optimization

Polymer	MMA:HEMA:4VP % W/W (by NMR)	pH 1.2 dissolution time (min)	pH 4.5	pH 5.8
			Soluble /swells	
P1	83: 0: 17	(Upto 60)#	(S, day 2)*	(S, day 4)*
P2	61: 21:18	(Upto 30)≈	(S, day 4)*	(S, day 4)*
P3	69 :20 :11	(Upto 45)#	(IS and low Sw)≈	(IS and low Sw)≈
P4	68: 23: 9.0	(Upto 45)#	(IS and low Sw)≈	(IS and low Sw)≈
P5	52:37: 11	(Upto 15)≈	(S, day 4)*	(S, day 4)*
P6	56:32: 12	(Upto 15)≈	(S, day 4)*	(S, day 4)*
P7	61:30: 9.0	(Upto 15)≈	(IS and high Sw)*	(IS and high Sw)*
P8	65:24: 11	(Upto 15-30)≈	(IS and low Sw)≈	(IS and low Sw)≈
P9	62:27: 11	(Upto15-30) ≈	(IS and low Sw)≈	(IS and low Sw)≈

S: soluble, IS: insoluble, Sw: swelling, # slow dissolution, * solubility/swelling not desired, ≈ acceptable behavior

Table 3.6 NREP characteristics

Monomer Compositions %			Molecular Weight	Polydispersity	T_g
	Feed	By NMR			
MMA	60	62			
HEMA	25	27.0	58,550	1.6	121.2°C
VP	15	11			

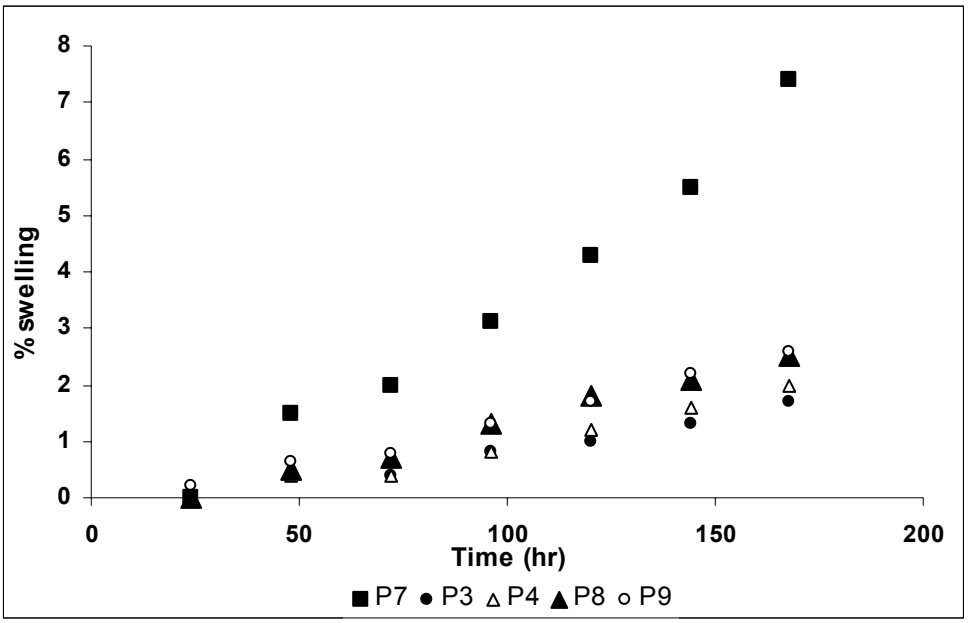

Fig.3.1. Swelling studies at pH 4.5

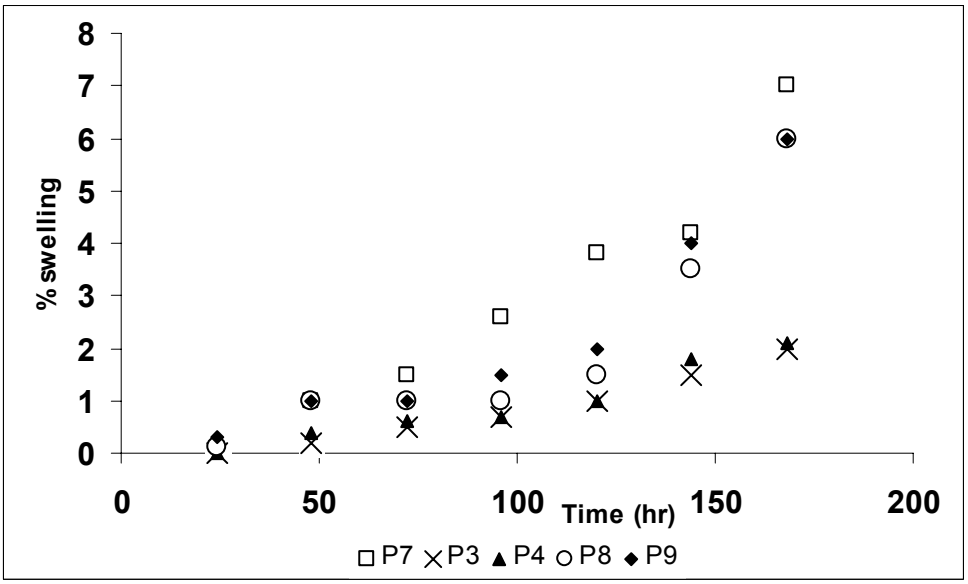

Fig.3.2. Swelling studies at pH 5.8

3.3.3.3. NREP characterization

3.3.3.3.a. ^{1}H NMR analysis

Fig. 3.3 shows the NMR spectrum for the polymer. The signals for ^{1}H NMR spectrum of NREP are assigned as follows: ($CDCl_3$, ppm): 8.43 δ (2H) protons adjacent to nitrogen of 4 vinyl pyridine in aromatic ring; 7.03 δ (2H) adjacent to nitrogen of 4 vinyl pyridine in aromatic ring; 4.11 δ (2H) protons for CH_2 group in HEMA; 3.84 δ (2H) protons for CH_2 group in HEMA; 3.61 δ (3H) protons for OCH_3; 2.96 δ (1H) of CH methine group; 2.01 δ (OH) protons of C_2H_4-OH; 1.5~2.0 δ (2H) protons for CH_2 backbone in polymer chain; 0.8~1.2 δ (3H) of CH_3 group; signal at 2.17 δ indicates the presence of acetone solvent. The monomer composition in the polymer was calculated by integration of all protons. The polymer composition was MMA 62 % w/w, HEMA 27 % w/w and 4-VP 11 % w/w. Comparison with the feed ratios is summarized in **Table 3.6** and the structure of NREP is shown in Scheme 1. For the system MMA-HEMA the monomer reactivity ratios are $r_1 = 0.58$ and $r_2 = 0.75$ [17], for the system MMA- 4-VP $r_1 = 0.57$ and $r_2 = 0.79$ [18] and for HEMA- 4-VP, $r_1 = 0.72$ and $r_2 = 1.09$. [19]. The lower degree of incorporation of 4-VP observed could be due to the fact that the reactivity ratios in ternary polymerizations are different than those observed in copolymerization and / or under the copolymerization conditions used in our work, the monomer reactivity ratios are very different from those reported above. However, we did not investigate the reasons for the lower reactivity of 4-VP any further.

3.3.3.3.b. FTIR spectrum of NREP

The FTIR spectrum for NREP is shown in **Fig. 3.4**. The peak assignments for polymer are summarized below; IR (KBr, cm^{-1}): 3541 (OH, free OH groups); 1726 (C=O, ester); 2844-2990 (Methyl C-H asym / sym stretch); 1448 -1482 (Methyl C-H asym / sym bend); 1190-1270 (C-O stretch); 1558-1601, 990 (characteristic for pyridine ring)

NREP is a terpolymer comprising MMA, HEMA and 4-VP and contains both proton accepting and donating groups. The carbonyl groups from MMA and HEMA act as proton acceptors and are capable of interacting with the proton donating groups. The nitrogen from the pyridine ring also acts as proton acceptor and is capable of forming hydrogen bonds. The hydroxyl group of HEMA is a proton-donating group. It is expected that such a polymer should exhibit self-association by hydrogen bonding between hydroxyl-carbonyl or hydroxyl-hydroxyl and hydroxyl–pyridine nitrogen groups.

The band at 3285 cm^{-1} in NREP corresponds to hydrogen-bonded hydroxyl of HEMA comonomer. This band shows a shoulder at 3541 cm^{-1} corresponding to free hydroxyl group. The maximum at 3285 cm^{-1}, corresponds to intramolecular associated hydroxyl groups in NREP.

The band corresponding to carbonyl from MMA and HEMA in NREP is seen at 1726 cm^{-1}. In addition a shoulder is seen at lower wave number (1636 cm^{-1}). This indicates contribution of carbonyl group of NREP to intramolecular hydrogen bonding. The self association due to hydrogen bonding between carbonyl and hydroxyls in poly(HEMA) is reported [20].

The most intense bands corresponding to pyridine ring are those located at 1557, 1597 and 993 cm^{-1} [20, 21]. NREP shows bands corresponding to pyridine at 1601 and 1558 cm^{-1} and 990 cm^{-1}. The spectrum of NREP shows a shift in the position of the pyridine band at 1597 cm^{-1} to 1601 cm^{-1}, indicating hydrogen bonding between pyridine nitrogen and hydroxyls from HEMA, contributing to self-association in the polymer. Similar shifts for hydrogen-bonded pyridine have been reported [21, 22]. FTIR spectrum of NREP shows that both carbonyls from MMA and HEMA comonomer and pyridine nitrogen are involved in hydrogen bonding with hydroxyl groups of HEMA, which contribute to self-association and rigidity as reflected in enhanced T_g of the polymer (121.2°C). The polymers, which are associated or crosslinked, exhibit lower reactivity towards cells as this imparts rigid structure to the polymer [23, 24].

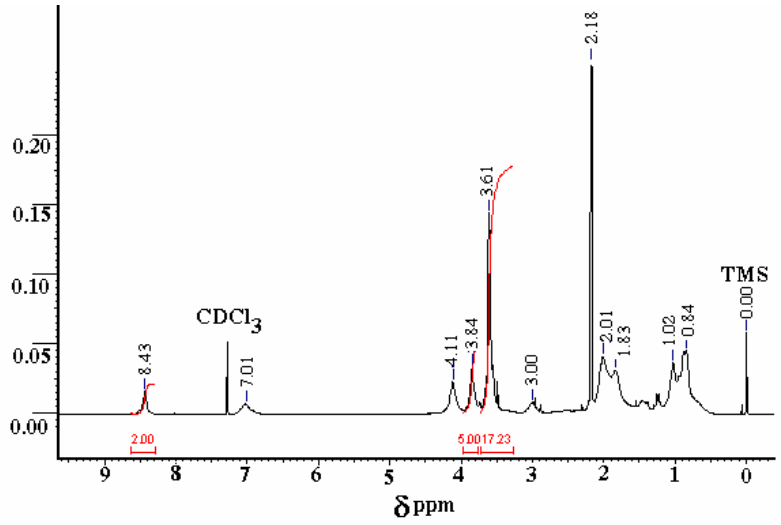

Fig.3.3 NMR spectrum of NREP

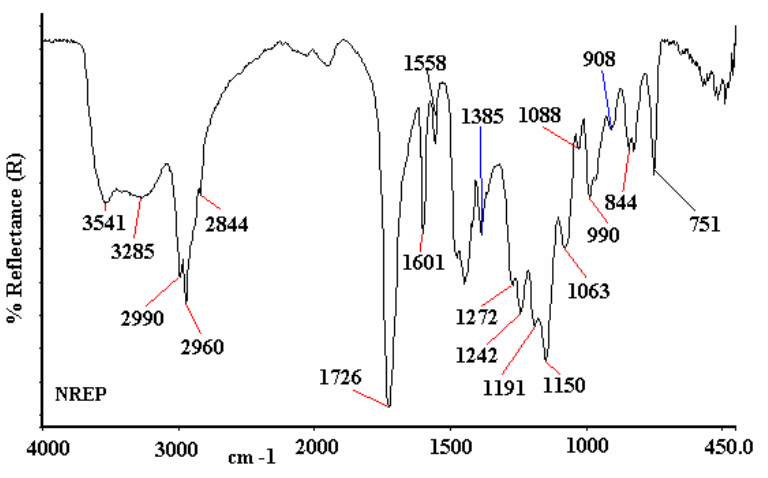

Fig.3.4. FTIR spectrum of new reverse enteric polymer

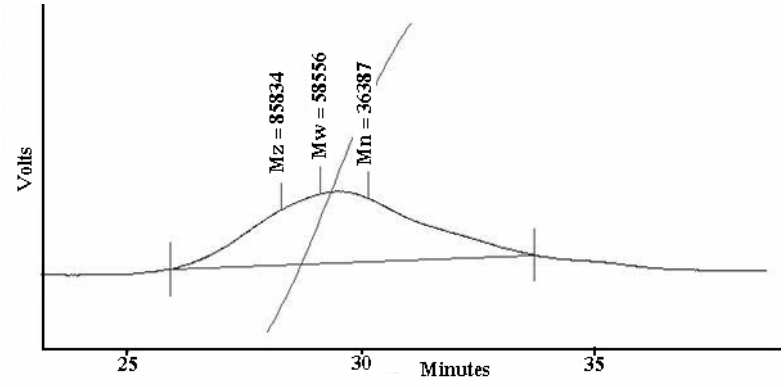

Fig.3.5. Molecular weight distribution for the NREP

3.3.3.3.c. Gel permeation chromatography (GPC)

Fig. 3.5 shows the molecular weight distribution for the NREP. Polymers with high molecular weight are known to undergo slow dissolution [25]. At the molecular weight of 58,550, NREP exhibits fast dissolution in acidic pH (15-30 min) and is insoluble at pH > 4.5. Polydispersity, the ratio of the weight average molecular weight to number average molecular weight was found to be 1.6 indicating a narrow molecular weight distribution. This is desirable since polymer samples with high polydispersity index are known show variable dissolution pattern than the monodisperse samples [26] Presence of low molecular weight components ($<5x10^3$) has deleterious effects on mechanical properties of the polymer film [27].

3.3.3.3.d. pH dependent dissolution

NREP film dissolves completely in the buffer pH 1.2 in 30-45 min. but does not solubilize at pH 4.5 and 5.8. **Fig. 3.6** shows equilibrium swelling at the pH 4.5 and 5.8 and in distilled water.

The comonomer composition influences the response of NREP towards different buffers. Poly (4-VP) is a weak base and solution pH influences its charge [28, 29]. Presence of 4-VP in NREP facilitates its rapid dissolution at pH 1.2 and it is reported in the past that poly (4-VP) is fully protonated in strong acidic solutions [29]. At low pH ionization of amino groups occurs due to protonation of nitrogen present in the aromatic ring of 4-VP. The tertiary amine group of 4-VP has pK_a value of 5.45 -5.62 [30, 31] so its pK_a > pH 1.2. This causes the protonation and subsequent dissolution of the polymer in the acidic environment. Pinkrah et al [32] reported the swelling of microgels based on poly(4-VP) at pH below the apparent pK_a of 4-VP. Kirsh et al. [33] studied the ionic equilibria of poly(4-VP) and represented the interactions between HCL-poly(4-VP) and ionized pyridine with chloride ions as shown in Scheme 2.

The uptake of water by NREP films at pH 4.5 and 5.8 is very low for 2-3 days with a slight increase thereafter. The ionization of cationic polymers decreases with increase in pH, reducing the hydration and decrease in swelling of polymer [34] and our

findings are consistent. At pH 4 the degree of protonation of polyvinyl pyridine is zero and limits its solubility [28, 29]. The swelling of the polymer is governed by the ionization rate. In case of polyacids the ionization occurs when the pH is above the pK_a of the ionizable group. Converse holds for the polybases containing pendant amine groups, which ionize at pH lower than the pK_a of the ionizable group [35, 36]. Ionization occurs in presence of acidic protons. As the pH increases from 1.2 to 4, the difference between the pK_a value and pH falls and hence the ionization is suppressed. This observation is similar to that reported by Pinkrah et al. [32]. Said et al. [34] also reported lowest swelling at pH values ranged 3-4, for copolymer of acrylic acid and cationic dimethylaminoethyl methacrylate. Further NREP contains higher proportion of MMA, which contributes to its hydrophobic nature and retards hydration. The poor swelling of hydrogels based on poly(MMA-co-HEMA) due to highly hydrophobic nature of MMA and moderate hydrophilicity of HEMA is reported in the past [37]. NREP composition is such that at pH 4.5, 4-VP is not protonated and MMA contributes for hydrophobic nature as is evident from the swelling studies showing very little uptake of water at this pH.

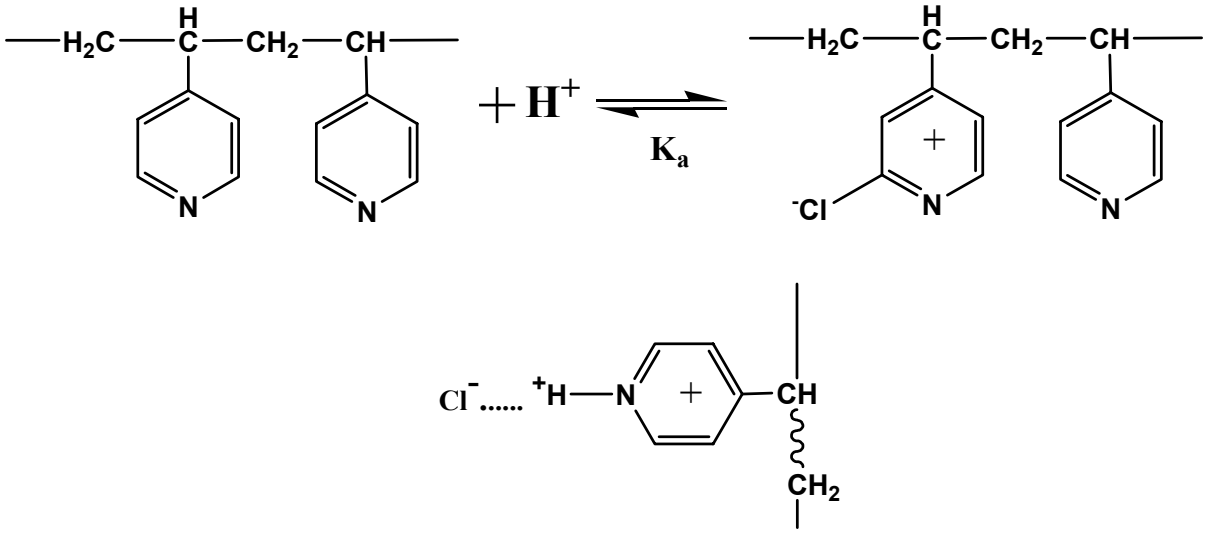

Scheme 4. Protonation of poly(4-VP) in presence of HCl

The swelling of NREP at pH 5.8 was slightly greater than that observed at pH 4.0. Unlike the complete deprotonation of 4-VP at pH 4, significant but incomplete deprotonation of poly(4-VP) occurs at pH 4.8 [28,29, 38]. The pH (5.8) is very close to the pK_a value of 4-VP (5.45-5.62) and so the extent of swelling is lower as compared to that at acidic pH 1.2 but slightly more than that at pH 4.5. The deprotonation of tertiary amine group in 4-VP at higher pH and the presence of methyl methacrylate contribute to the hydrophobicity of the polymer. The polymer therefore remains deswollen at higher pH. The swelling of poly (4-VP) films on exposure to hydrochloric acid vapor and subsequent deswelling by regaining hydrophobic nature on treatment with base has been reported by Harnish et al. [39]. Eudragit E dissolves at pH $\leq$ 5, but swells at pH > 5 [40]. NREP on the other hand dissolves at pH < 4 and does not swell at pH > 4.5. This distinctive pH dissolution profile of NREP is attributed to the difference in pK_a values of 4-VP (5.45-5.65) and DMAEMA (8.4) monomers [41] and the T_g of the two polymers is 121.2° C and 45° C respectively.

The pH interval in which the dissolution transition occurs is narrow and sensitive to the monomer selection and composition. The dissolution characteristics of NREP make it ideal for the gastric delivery of drugs. The gastric pH is < 3 [42] and the dissolution pH of NREP is < 4. Hence it would be useful as reverse enteric polymer. The hydrophobic nature of NREP, rapid dissolution at gastric pH and insolubility at near neutral and neutral pH make NREP ideal for the development of taste-masked products, especially liquid oral preparations like dry syrup

NREP does not exhibit swelling / dissolution in distilled water as seen from **Fig. 3.7.** The ESEM analysis of NREP film exposed to water shows no change in surface morphology of the film.

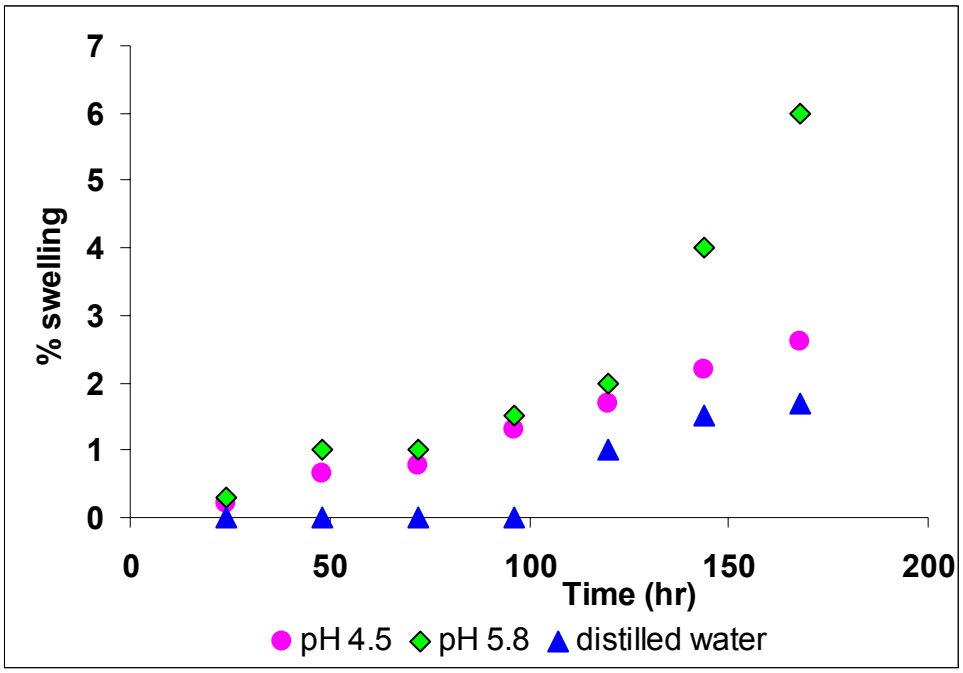

Fig.3.6. Swelling studies for NREP (P9)

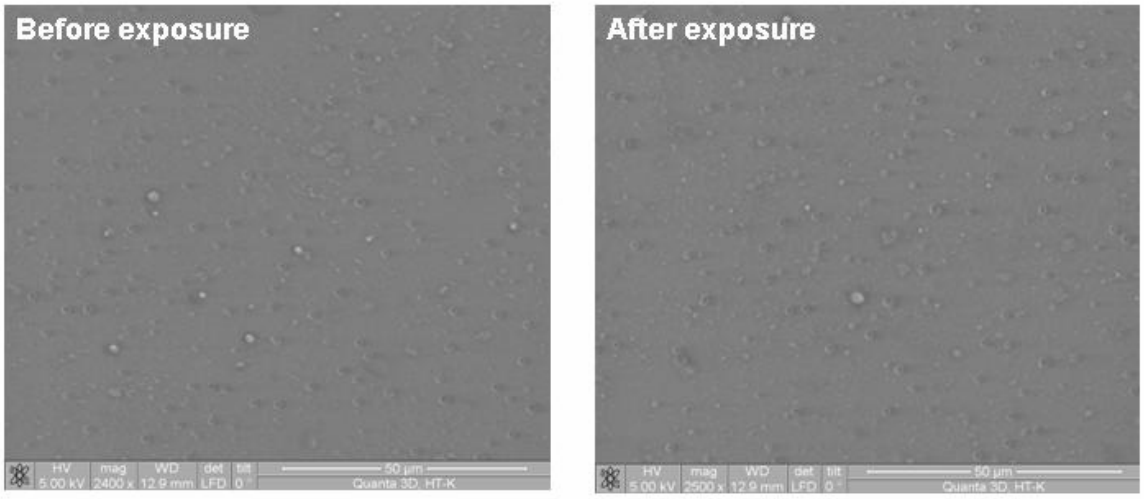

Fig.3.7. Morphological changes in NREP on exposure to distilled water. (a) before exposure. (b) after exposure of 7 days

3.3.3.3.e. Glass transition temperature (T_g)

The polymers used in pharmaceutical dosage forms have to withstand high temperatures encountered during the coating, drying and heat-sealing process. The T_g is an indicator of tackiness encountered during such processes. High T_g of hydroxypropylcellulose, hydroxypropyl methylcellulose and ethylcellulose (120°C, 180°C and 140°C) makes these polymers ideal in this respect [43]. Eudragit E, shows caking at temperature above 25°C and has to be stored at or below room temperature because of its low T_g (45°C).

The T_g of NREP was evaluated from reversible heat flow of thermograms obtained by MDSC. The T_g induction point is 115°C and the transition occurs at 121.2 °C. The monomer composition in random terpolymer NREP was so chosen as to yield high T_g yet retain the solubility at acidic pH. The T_g of homopolymer DMAEMA has a T_g of 19 °C and incorporation of such a monomer would reduce the T_g of polymer. The T_gs of homopolymers poly(MMA) (105 °C), poly(HEMA) (87.5 °C) and poly(4-VP) (148 °C) are high [22, 44]. The monomer selection is done in such a way that the T_g values of the respective homopolymers lie above and below the desired T_g of the polymer [45]. The higher content of HEMA monomer would impart lower T_g and more hydrophilic nature to NREP and this was not desired as NREP is expected to show hydrophobic nature at higher pH. The increase in content of MMA would impart high T_g and also the hydrophobic character to polymer, which was desired and hence higher concentrations of MMA were considered. Homopolymer of 4-VP has highest T_g and its higher content is expected to impart high T_g to NREP. The T_g of the binary mixture is given by the following equation [46]

$$T_g = T_{g1}\, w_1 + T_{g2}\, w_2 \qquad \textit{Eq 1}$$

or multi component systems the equation can be written as

$$T_g = \sum_{i=1}^{N} T_{gi} w_i \qquad \textit{Eq 2}$$

So for the terpolymer NREP the equation becomes

$$T_g = (T_{g1}\, w_1 + T_{g2}\, w_2 + T_{g3}\, w_3) \qquad \textit{Eq 3}$$

Where w_1, w_2 and w_3 are weight fractions and T_{g1}, T_{g2} and T_{g3} are the glass transition temperatures of the homopolymers. The experimental value (121.2 °C) is higher than the value arrived at (103 °C) from above equation. The high T_g of the NREP eliminates the need to store it at lower temperatures and avoids tackiness during processes involving heat. This enhancement of T_g over the calculated value can be attributed to the intramolecular hydrogen bonding in NREP demonstrated earlier by IR studies. The self-association between the hydroxyls from HEMA with carbonyl of MMA and nitrogen of 4-VP enhances T_g over the theoretical values. Increase in T_g as a result of restriction of polymer segment motion due to hydrogen bonding is reported in the past [47-49]. It has been reported that intramolecular crosslinking imparts rigid behavior to polymers preventing strong binding with cell membranes thereby reducing cell damage [23, 24]. The increase in T_g of NREP over weight average value suggests the restricted segmental movement of polymer chains. From these observations it can be presumed that NREP would not exhibit binding with cell membranes and thereby elicit low biological response.

3.3.3.4. Biological reactivity in-vitro and in-vivo

Biocompatibility is a critical consideration in the design and application of polymeric biomaterials [50]. Evaluation of *in vitro* cytotoxicity of biomaterial is the first step to establish biocompatibility. This is performed qualitatively using immortalized cell lines and the morphological examination of cell damage and growth when in direct or indirect contact with materials [51].

The monomer structure, charge density, molecular weight and nature of amine group are known to affect the cytotoxicity and all these factors were considered in designing NREP. One of the criteria for selection of HEMA, MMA and 4-VP for design of reverse enteric polymer was based on the influence of structure of monomers

affecting the cytotoxicity. Neutral and polyanionic polymers show less toxic effects than polycations and literature reveals that there has been a concern in applications of polycations due to their high positive charge [23, 50]. Cytotoxicity of polycations, acrylic and methacrylic acid derivatives has been extensively investigated [50, 52, 53].

4-VP was chosen as basic monomer since it is a tertiary amine and it has been reported in the past that the toxicity of tertiary amines is lower as compared to the primary and secondary amines [50, 54, 55]. The charge density on the polymer is considered a key parameter for interactions with cell membrane causing cell damage. Polymers with higher charge density are more cytotoxic [24, 56]. The ionization of polymer is related to pK_a value of functional monomer, which in turn influences charge density on polymer. Dimethylamino ethylmethacrylate having pK_a 8.4 is less toxic than poly(L-Lysine) as at physiological pH it is ionized 55 % as compared to poly(L lysine) which is ionized 90 % [57]. The pK_a of 4-VP is 5.45-5.62 and it can be expected that it will be less ionized at physiological pH. NREP would therefore exhibit lower toxicity. The charge density resulting from number and three dimensional arrangements of cationic residues affects biological response on the cell membranes and the same is reduced with increase in space between reactive amine groups in primary structure [23]. The NMR analysis revealed that the incorporation of 4-VP is 10.8%, which is sufficient to induce pH dependent behavior. The charge density of polymers is also affected by the three dimensional structure and flexibility of macromolecules. The intramolecular crosslinking imparts rigid behavior to polymers preventing strong binding with cell membranes thereby reducing cell damage [23, 24]. The FTIR spectrum revealed that pyridyl nitrogen is hydrogen bonded with hydroxyls from HEMA. This association results in higher T_g than that calculated by weight average formula suggesting restriction in segmental motion within polymer. With reduced flexibility within NREP we expect it to elicit lower biological response, if any.

Yoshii and Lawrence [52, 53] evaluated toxicity of series of esters of acrylic and methacrylic acids. Yoshii [52] ranked the order of toxicity for these materials as bisphenol A bis 2-hydroxypropylmethacrylate (bisGMA) > urethane dimethacrylate (UDMA) > triethyleneglycol dimethacrylate (3G) > 2-hydroxyethyl methacrylate (HEMA) > methyl methacrylate (MMA). All acrylates are more toxic than

methacrylates. The lower homologues are more toxic than the higher ones. The straight chain substituents are less toxic than the corresponding branched ones and simple aliphatic substituents are less toxic than those containing amine or hydroxyl functional groups. Both MMA and HEMA comonomers in NREP are linear methacrylate derivates and hence are expected to be less toxic as compared to esters of acrylic acid. The branched molecules are more efficient in neutralizing cell surface charge and cause disruption of cell than polymers with linear or globular structure [24]. 4-VP is a weakly basic heterocyclic monomer. We therefore expected NREP to exhibit lower toxicity.

3.3.3.4.a. In-vitro biological reactivity test

The determination of cell viability is an assay to estimate *in-vitro* cytotoxicity of biomaterials and the predictive value of toxicity is adjudged by effect of toxic materials on the basic cell functions [55]. These functions are common to all cells and hence toxicity can be measured by assessing the cellular damage. These tests are designed to determine the response of mammalian cell cultures following direct or indirect contact of elastomeric plastics and other polymeric materials with patients [14]. These tests are described as the Agar diffusion test, direct contact test and the elution test. The elution test is designed for extract of polymeric materials and is appropriate for dose response evaluations. The response of the NREP was compared with the positive control phenol and the negative control ultra high molecular weight polyethylene. The L929 mouse fibroblast cells are large spindle shaped adherent cells, which grow as confluent monolayer. The cellular responses were scored as 0, 1, 2, 3, and 4 according to none, slight mild, moderate and severe cytotoxicity based on USP 26 NF XXI, 2003. The sample meets the test requirements if the cultures treated with sample do not show reactivity greater than mild (Grade 2).

The extracts of positive control, dilute phenol gave severe cytotoxic response as expected. The L929 cells on treatment with phenol were grainy and lacked normal cytoplasmic space and large open spaces between the cells indicated cell lysis. The negative control gave no cytotoxic response. The cells were large, confluent and did not show lysis. The *in-vitro* cytotoxicity test measurements are based on microscopic

evaluations of morphological changes; the tests for NREP were conducted in triplicate to assure accurate judgment of biological response. The response of mouse fibroblast cells to NREP extracts is shown in **Fig.3.8.** On morphological examination the fibroblast cells after contact with 100 % extract of NREP at an extraction ratio of 0.1g / ml showed few loosely attached round cells without intracytoplasmic granules and were graded on the scale of 1 indicative of slight reactivity but within acceptable limits as per USP 26 NF XXI (2003). The cell cultures treated with 25 and 50 % NREP extract were confluent and showed discrete intracytoplasmic granules with no cell lysis and no morphological changes were observed. The absence of loosely bound or detached cells indicated no reactivity towards the cells. The responses for these were graded on the scale '0' indicating no reactivity. The cultures treated with NREP samples showed that the cells were viable and NREP did not exhibit reactivity greater than grade 1 but was always less than grade 2 and meets the requirements of the in vitro biological reactivity test as per USP 26 NF XXI (2003). The *in-vitro* cytotoxicity evaluation of NREP exhibited non-cytotoxic response towards the L929 cells and was therefore considered for *in-vivo* evaluation.

3.3.3.4.b. In- vivo biological reactivity test

The *in-vivo* biological reactivity test is designed to evaluate the response of animals towards polymeric materials in direct or indirect patient contact or by injections of extracts of specific material under test (USP 26 NF XXI, 2003). Three tests, the systemic injection test, intracutaneous test and implantation test are recommended for the elastomerics, plastics and other polymeric materials used for testing the suitability of materials intended for use in parenteral preparations, fabrication of containers and for use in medical devices, implants and other systems. The *in-vitro* cytotoxicity test is initial qualitative measure of biological reactivity, but to ensure safety, *in-vivo* biological reactivity tests were undertaken for NREP. We believe the comprehensive evaluation of NREP for biological reactivity both under *in-vitro* and *in-vivo* conditions would help establish better evaluation of polymer safety. This is essential to bring new materials from evaluation phase to real life applications.

The control and NREP extract in 0.9 % sodium chloride injection and cottonseed oil did not show presence of particulate matter and were visually clear. The pH of NREP extract in 0.9 % sodium chloride and control used in intravenous test was 6.49 and 5.92 respectively. The evaluation criteria for intravenous and intraperitoneal injection test were used. According to the pharmacopoeia (USP 26 NF XXI 2003) the polymeric sample does not meet the requirements of the test if death of two or more mice, abnormal behavior such as convulsions or prostration in two or more mice, or body loss greater than 2 g in three or more mice is observed.

None of the animals injected with the NREP extract in sodium chloride injection and cotton seed oil for intravenous and intraperitoneal injection test showed any abnormalities or loss in body weight during the observation period. The results suggest that NREP extracts in both media meet the requirements of the systemic injection test for intravenous and intraperitoneal application as per USP 26, NF XXI (2003).

3.4. CONCLUSIONS

In this chapter, the development and evaluation of a new reverse enteric polymer for drug delivery has been described. The rationale behind the choice of monomers has been discussed and validated experimentally. a series of reverse enteric co-polymers and ter-polymers containing hydrophobic, basic and hydrophilic monomers were synthesized. The screening of these polymers at pH 1.2, 4.5 and 5.8 revealed that the ter-polymer compositions containing monomers methyl methacrylate (MMA), 2-hydroxy ethyl methacrylate (HEMA) and 4-vinyl pyridine (4-VP) contributed to rapid acid solubility and hydrophobicity at pH > 4. The polymer could be used for taste masking of variety of dosage forms like tablets, granules and suspensions. The polymer can thus be used to release the drugs immediately from these dosage forms with prevention of drug leaching in aqueous media. The introduction of proton donating and accepting groups in NREP resulted in strong self associations. This contributed to compatibility with acidic drugs, enhanced biocompatibility and increase in T_g. The higher T_g (121.2^0C) of NREP over the weight average values ($103\ ^0$C) enhanced its biocompatibility and ability to withstand formulation processes involving heat like

coating and heat sealing without becoming tacky. The biological reactivity tests *in-vitro* and *in-vivo* indicate that the polymer is non-toxic. These results encourage development of oral drug delivery systems based on NREP. This has been discussed in Chapter 4.The blends of NREP with other polymers can be used for sustained release of drugs at gastric pH as well as the entire length of the GI tract and is described in Chapter 6.

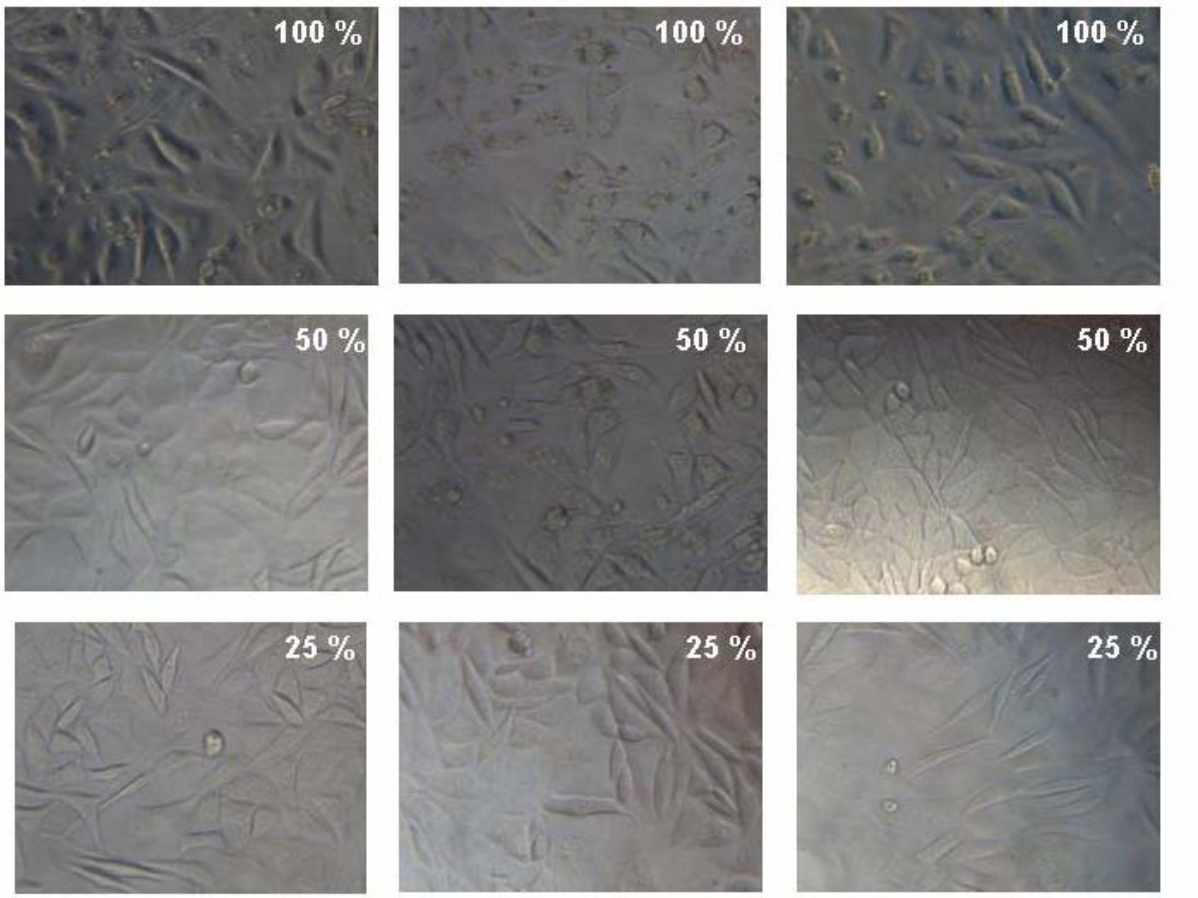

Fig.3.8. Morphological changes in L929 mouse fibroblast cells on exposure to 100 %, 50% and 25% extracts of NREP

3.5. REFERENCES

1) G. Mukherji; S. Goel; V. K. Arora, US Patent 6,565,877, May 20, 2003
2) D. R. Friend, J. Microencapsulation, 1992, 9, 469- 480.
3) G. M. Roy, Pharm. Tech. 1994, 18, 84–99.
4) B. Albertini, C. Cavallari, N. Passerini, D. Voinovich, M. L. Gonzalez-Rodriguez, L. Magarotto, L. Rodriguez, Eur. J. Pharm. Sci., 2004, 21, 295–303.
5) M. Cuna, M. L. Lorenzo-Lamosa, J. L. Vila- Jato, D. Torres, M. J. Alonso, Drug Dev. Ind. Pharm. 23, 1997, 259-265.
6) 7.M. L., Lorenzo-Lamosa, M. Cuna, J. L. Vila-Jato, D. Torres, M. J. Alonso, J. Microencap., 1997, 14, 607-616.
7) D.S. Deutsch, J. Anwar, US Patent, US 4,897,270, 1990, January 30.
8) A. H. Dantzig, D. C. Duckworth, L.B. Tabas, Biochimica et Biophysica Acta 1994, 1191, 7-13.
9) Yong Qiu, Kinam Park Advanced Drug Delivery Reviews, 2001, 53, 321–339
10) Yocum, R.H. E.d. and Hyouist E.B. Functional Monomers: Their preparation, polymerisation and application V 1 & V 2; Marcel Dekker INC, New York, 1973.
11) N.A. Peppas, P. Bures, W. Leobandung, H. Ichikawa Eur. J. Pharm. Biopharm. 2000, 50, 27-46
12) A. Korytkowska, I. Barszczewska-rybarek, M. Gibbs, Designed Monomers and Polymers, 2001, 4, 27-37.
13) L. I. Grossman, B.M. Brickman, J Dent Res., 1937, 16, 409-416.
14) USP 26 NF XXI (2003) US Pharmacopeial Convention, Rockville, MD,
15) D. M. Lynn, R. Langer, J. Am. Chem. Soc. 2000, 122, 10761-10768.
16) J. Crank, G.S. Park Edition, Diffusion in polymers, London Academic Press Inc, 1968
17) M. T. Iglesias, J. Guzmfin and E. Riande, Polymer, 1996, 37, 1443-1452.
18) T. Tamikado, J. Poly. Sci., 1960, 43, 489-500.
19) R. Saito, T. Tobe, J App. Poly. Sci. 2004, 93, 749-757.
20) Cesteros LC, Meaurio E, Katime I. Macromolecules 1993, 26, 2323-2330.

21) Cesteros LC, Velada JL, Katime L., Polymer 1995, 36, 3183-3189.

22) Ruokolainen J, Brinke G, Ikkala O., Macromolecules, 1996, 29, 3409-3415.

23) C. L. Gebhart, A. V. Kabanov, J. Control. Release, 2001, 73, 401–416.

24) D. Fischer, Y.L B Ahlemeyer, J. Krieglstein, T. Kissel, Biomaterials, 2003, 24, 1121–1131.

25) W J Cooper, PD Krasicky, F Rodriguez, Polymer, 1985, 6, 1069–1072.

26) J Manjkow, JS Papanu, DW Hess, DS Soane (Soong), Bell AT. J Electrochem Soc., 1987, 134, 2003–2007.

27) R. C. Rowe in: A. T. Florence (Ed.), Materials Used in Pharmaceutical Formulations, Critical Reports on Applied Chemistry, V 6, Published by Society of Chemical Industry, 1984 , pp 1-35.

28) T. Radeva, V Milkova, I Petkanchin, J. Colloid and Interface Science, 2004, 279 351–356.

29) E. Pefferkorn, A. Elaissari, Journal of Colloid and Interface Science, 1990, 138, 187-194.

30) J. S. Park, Y.B. Lim, Y.M. Kwon, B. Jeong, Y. H. Choi, S. W. Kim, Journal of Polymer Science: Part A: Polymer Chemistry, 1999, 37, 2305–2309.

31) R. H. Yocum Ed., E.B. Nyquist Ed., Functional Monomers Their preparation, polymerization and application, V 2, Marcel Dekker Inc, New York, 1974.

32) V. T. Pinkrah, M. J. Snowden, J. C. Mitchell, J. Seidel, B. Z. Chowdhry, G. R. Fern Langmuir, 2003, 19, 585-590.

33) Yu. E. Kirsh, O. P. Komarova and G. M. Lukovkin Eur. Poly. J., 1973, 9, 1405-1415.

34) A. El-Hag A. Said, Biomaterials, 2005, 26, 2733–2739.

35) A. R. Khare, N. A. Peppas, Biomaterials, 1995, 16, 559-567.

36) N.A. Peppas, P. Bures, W. Leobandung, H. Ichikawa Eur. J. Pharm. Biopharm. 2000, 50, 27-46.

37) L. Brannon-Peppas, N. A. Peppas, Biomaterials, 1990, 11, 635-644.

38) K. Prochazka, T. J. Martin, P. Munk, S. E. Webber, Macromolecules, 1996, 29, 6518-6525.

39) B. Harnish, J. T. Robinson, Z. Pei, O. Ramstrom, and M. Yan, Chem. Mater. 2005, 17, 4092-4096.

40) Eudragit: Technical literature from Internet: http: www.roehm.com, Specifications and test methods for EUDRAGIT® E 100, EUDRAGIT® E PO and EUDRAGIT® E 12,5 INFO 7.1/E from Internet: http: www.roehm.com , 2004-09

41) S. R. Van Tomme, M. J. V. Steenbergen, S. C. D. Smedt, C. F. V. Nostrum, W. E. Hennink, Biomaterials, 2005, 26, 2129–2135.

42) Y. Qiu, K. Park, Ad. Drug Del. Reviews, 2001, 53, 321–339.

43) A.B. Savage, in "Encyclopedia of Polymer Science and Technology 3," Mark, H.F., Gaylord, N.G.& Bikales, N.M. (eds), Interscience, New York, 1965, pp 476.

44) P. Peyser, In: J. Brandup and E.H. Immergut (Ed.), Polymer Handbook, VI/209, Wiley Interscience Publication, New York, 1989, pp 209-277.

45) E. Penzel, J.Rieger and H. A. Schneider, Polymer, 1997, 38, 325-337.

46) J.R. Fried, Polymer Science and Technology, Prentice Hall of India Private Limited, New Delhi 110001, 1999, Chapter 4, pp132-164

47) H.A. Schneider, Glass Transition (Theoretical Aspects), The Polymeric Materials Encyclopedia, CRC Press, Inc, 1996.

48) Jiang M, Li M, Xiang M, Zhou H. Adv. Polym. Sci., 1999, 146, 121-196.

49) M. Mayo-Pedrosa, C. Alvarez-Lorenzo, A. Concheiro, J. Thermal Analysis Calorimetry, 2004, 77, 681–693.

50) Y. X. Wang, J. L. Robertson, W. B. Spillman, Jr., R. O. Claus, Pharmaceutical Research, 2004, 21, 1362-1373.

51) A.P. Marques, R.L. Reis, J.A. Hunt, Biomaterials, 2002, 23, 1471–1478.

52) E. Yoshii, J. Biomed. Mater. Res., 1997, 37, 517-524.

53) W. H. Lawrence, G. E. Bass, W. P. Purcell, J. Autian, J Dent Res. 1972, 51, 526-535.

54) A. Agarwala, R. Unferb, S. K. Mallapragadaa, J. Control. Release, 2005,103, 245–258.

55) S. Mao, X. Shua, F. Unger, M. Wittmar, X. Xie, T. Kissel Biomaterials, 2005, 26, 6343–6356.

56) M. J. Bruining, H.G.T. Blaauwgeers, R. Kuijer, E. Pels, R. M.M.A. Nuijts, L.H. Koole, Biomaterials, 2000, 21, 595-604.

57) M.C Deshpande, M.C. Garnett, M. Vamvakaki, L. Bailey, S.P. Armes, S. Stolnik, J. Control. Rel., 2002, 81, 185–199.

CHAPTER 4

Taste Masked Compositions Comprising NREP & Bitter Drugs: Enhancing Bioavailability with Rapid Gastric Release

4.1. INTRODUCTION

Drugs are administered to patients in forms that facilitate administration and increase their efficiency. Drugs are administered by different routes, but oral route is by far the most preferred [1]. The majority of prescribed drugs are designed for oral application since they can be self-administered by the patient without hospitalization. The common oral dosage forms include: liquid mixtures like solutions, suspensions, solid dosage forms like tablets and capsules and liquid filled capsules etc. Pediatric and geriatric patients often experience difficulty in swallowing the solid dosage forms. Drugs are therefore administered to such patients as solutions, suspensions and emulsions. Formulating drugs in these dosage forms leads to perception of bitter taste [2]. The bitter taste of the drugs, which are orally administered, is disadvantageous in several aspects. Taste is an important parameter governing the compliance. The disagreeable taste of drugs causes difficulties in swallowing or causes patients to avoid their medication thereby resulting in low patient compliance [3-5]. Antibiotics are administered frequently to children and are often associated with unpleasant taste [3].

Taste masked formulations are designed to improve patient compliance. In the past Roy [4, 6] has discussed various methods for masking unpleasant taste. Use of sweeteners and flavors, complexation, barrier coating, viscosity modification and salt formation, functional group modification etc are some of the commonly used approaches for taste masking [5, 7, 8]. Conventional taste masking techniques such as use of sweeteners, amino acids, flavoring agents are often unsuccessful in masking the taste of the highly bitter drugs like quinine, barberin, etoricoxib, antibiotics like levofloxacin, ofloxacin, sparfloxacin, ciprofloxacin, cefuroxime axetil, erythromycin and clarithromycin. Thus taste-masking technologies are considered important and developed by many researchers.

Various methods for taste masking have been tried earlier, which include use of ion exchange resins, complexation of bitter drugs with pharmaceutically acceptable excipients and coating of drugs by lipids and various polymeric materials. Maximum taste masking effectiveness has been obtained by coating drug, whereby a physical barrier is created around the drug [5]. Amongst the polymers available currently, the

reverse enteric and enteric polymers are largely used for taste masking applications. Eudragit E, based on dimethylaminoethyl methacrylate and methacrylic esters is extensively used in taste masking applications. Enhancing the palatability of formulations is very challenging. Use of a particular taste masking technique is largely governed by the physicochemical and pharmacokinetic parameters of drug and also on type of dosage form. Ibuprofen is better absorbed in small intestine so its taste is masked using enteric polymer [9]. Often there is a concern that use of water insoluble polymer film may reduce the bioavailability of drugs [10]. Formulators have to strike a balance between taste masking and release characteristics desired. For drugs better absorbed in gastric region the drug has to be released at gastric pH (<3) [11] without delay and yet has to be restricted at pH of saliva (5.0 - 8.0) [12].

Cefuroxime axetil (CA) is a second-generation cephalosporin antibiotic administered orally and it is known to have bitter taste [7]. CA has a limited absorption window restricted to upper gastric region and is hydrolyzed by esterase enzyme in intestine to Cefuroxime, a form which cannot be absorbed orally [13-15]. Bioavailability of orally administered CA is low and reported to be 32-50 % [16]. Use of reverse enteric, enteric polymers and lipids for taste masking of CA, has been reported in past. Lorenzo-Lamosa et al. [17] studied the taste masking of CA using Eudragit E as one of the polymers. However Eudragit E caused significant degradation of CA due to negative interaction. Enteric coatings like Eudragit L, Cellulose acetate trimellitate, hydroxypropyl methylcellulose phthalate for taste masking of CA have been investigated in the past [17,18]. CA was found to degrade in presence of CAT [18]. The use of enteric polymers for taste masking of CA is of little use as they dissolve in intestinal region where CA is rendered inactive. Robson et al. [7] investigated the release of CA from stearic acid coated microspheres at alkaline conditions. The CA release was attributed to formation of water-soluble salt sodium stearate, resulting from reaction between stearic acid and sodium ions, present in Sorensons modified buffer. Donn et al. [19] studied the bioavailability of CA from tablets and suspension based on wax coated CA granules. The tablets and suspension were not found to be bioequivalent. The lower bioavailability of CA from suspension than tablet is attributed to wax coating on CA granules [19]. The wax coating causes

relatively delayed release of CA as construed from findings of Robson et al. [7]. Further absorption window of CA restricted to upper gastric region and its deactivation in intestine, account for lower CA bioavailability. None of the pH sensitive biomaterials available commercially satisfy the need to taste mask CA without affecting its bioavailability.

Clarithromycin is recommended for the treatment of H. pylori infection and needs to be released in the stomach at the site of infections [20]. Clarithromycin has a short half-life of 1.47 hr at acidic pH and is degraded at acidic pH. Chun et al [20] reported that if the rate of release of Clarithromycin is slow at acidic pH, most of it is degraded and not available for the treatment. However clarithromycin is extremely bitter and hence requires taste masking. Patent Application WO 02/092106 [21] discloses a taste-masked Clarithromycin composition comprising polycarbophil. This complex is further coated with an acid resistant polymer Eudragit L100 55, releasing the drug in the intestine. Many other formulations for clarithromycin are summarized in **Table 4.1.** Such formulations would therefore be of little use in treatment of H. pylori infections requiring the drug to be released in stomach.

Ciprofloxacin HCl is better absorbed from upper gastric region [22, 23]. It has bitter taste which needs masking [3]. Various approaches have been tried for that and are summarized in **Table 4.2.** All the polymers used are either water insoluble or enteric and hence would cause delayed release, which is not desirable due to limited absorption window.

We reported the development of new reverse enteric polymers in Chapter 2. In the present Chapter we have evaluated (NREP) based on methyl methacrylate (MMA), 2-hydroxy ethyl methacrylate (HEMA) and 4-vinyl pyridine (4-VP) for taste masking of Cefuroxime axetil, Ciprofloxacin HCl and Clarithromycin. More detailed investigations were undertaken for Cefuroxime axetil and the taste masking ability of NREP was compared with “Ceftum” containing wax coated CA granules, manufactured by Glaxo. The taste-masking test was done by evaluating the response and ranking done by human volunteers. The morphological changes occurring in the microspheres on exposure to the water, buffer media of pH 1.2 and 5.8 were examined under environmental scanning

electron microscopy (ESEM). NREP was found to effectively taste mask all the drugs and release them at the gastric pH.

Table 4.1: Literature survey for taste masking Clarithromycin

Company	Patent	Materials
Abbott	US 4808411 [24]	Carbomer and Hydroxyproplyl methylcellulose phthalate
	WO 9312771 [25]	Prolamine: Zein
	US 5599556 [26]	Prolamine and fatty acid
Gold, Oscar	EP 943341 [27]	Carbopol and Hydroxypropyl cellulose phthalate
Kotaro Kanppo	JP2001226293 [28]	Genugel, Genugum / Lecithin/ Carrageenan
EthyPharm	WO02072072 [29]	Fatty acid and Eudragit E
Biochemie	WO0172284 [30]	Hydroxypropyl methylcellulose, Eudragit L and Hydroxyproplyl methylcellulose phthalate
Bastian, Petra	WO03006066 [31]	Carbomer , Polymethacrylates (enteric) and Carboxymethylcellulose

Table 4.2: Literature survey for taste masking Ciprofloxacin HCl

Company	Patent	Polymer Used
Bayer	EP 551820 [32]	Eudragit NE30D,
	US 5695784 [33]	Eudragit L30D and
	US 6136347 [34]	Ethyl cellulose.
Bayer Yakuhin	JP 2000053563 [35]	Hydroxypropyl methylcellulose, Eudragit L, Ethyl cellulose dispersion
S.A.L.V.A.T. Spain	WO 0076549 [36]	Triglycerides of caprylic acid, ethyl cellulose,
Ranbaxy	WO 0135930 [37]	1) Aq. dispersion Eudragit NE
	WO 0076479 [2]	2) Eudragit L100 and HPMCP

4.2. TASTE MASKING OF CEFUROXIME AXETIL USING NREP

4.2.1. Microsphere preparation and characterization

4.2.1.1. Emulsification solvent evaporation

NREP solution was prepared in mixture of methanol: dichloromethane (2:1). CA was added to polymer solution under magnetic stirring. The drug polymer solution was dispersed slowly in light liquid paraffin containing 0.25 % of Span 85 under mechanical stirrer. The stirring was continued for 3-4 hr at 500 rpm. The microparticles were separated by filtration and washed with petroleum ether to remove paraffin oil. The microspheres so formed were dried under vacuum for 24 hr at room temperature. The composition of the microspheres is shown in **Table 4.3.**

4.2.1.2. Determination of drug content

The drug content was determined at 278 nm using Shimadzu UV160 IPC UV Visible spectrophotometer. Cefuroxime axetil content was determined by dissolving 50 mg of microspheres in 2 ml of methanol and sonicated for 5 min. Then the volume was made to 50 ml using 0.07 N HCl. The solution was filtered and diluted further for the analysis. Each sample was analyzed in triplicate.

Table 4.3 CA microspheres: content and efficiency of loading

Formulation	CA : polymer ratio	Loading Efficiency (%)	CA loading (%)
F1	1:5	90.0	15.0
F2	1:3	89.2	22.3
F3	1:2	89.4	29.8
F4	1:1	88.4	44.2
(CA=900mg)			

4.2.1.3. In-vitro dissolution test

The drug release from the microspheres was evaluated by placing the microspheres containing Cefuroxime equivalent to 125 mg in a basket containing 900 ml of 0.07 N HCl. The dissolution was carried out in Electrolab USP type II apparatus at 75 rpm at 37 $\pm$ 0.5°C. The samples were collected after 30, 60, 90, 120, 180 and 240 min. to follow drug release. The amount of drug released was estimated at 278 nm using Shimadzu UV Spectrophotometer. The dissolution tests were done in triplicate. The release in 0.07 N HCl from the microspheres was compared with that from a commercial wax coated preparation.

4.2.1.4. Gustatory test / taste evaluation

The microspheres equivalent to 4 doses of Cefuroxime (125 mg x 4) were suspended in syrup (85 % w/w sucrose) of pH 4.4 adjusted by addition of sodium citrate and citric acid buffer. The taste evaluation of reconstituted suspension was performed each day by placing few drops of the reconstituted suspension on tongue of four volunteers for 10-20 seconds and then spat out. The bitterness level was recorded and compared against the commercial sample, Ceftum. The volunteers were asked to grade the sample each day on the numerical scale of 0-4; the score '0' for sweet taste, '1' for acceptable, '2' for acceptable but slightly bitter, '3' for bitter and '4' for very bitter taste.

4.2.1.5. Scanning electron microscopy

Quanta ^{TM} SEM Series, FEI Company, environmental mode was used to record morphological changes occurring *in-situ* in microspheres on exposure to the dissolution medium 0.07 N HCl. The environmental mode was used to scan samples, as conventional SEM with gold coating cannot be used for recording in situ modifications in presence of buffer. The microsphere sample was introduced into the Quanta specimen chamber and 0.07 N HCl was introduced till the microspheres were immersed

completely. The acid medium was removed from the sample holder by applying vacuum. Changes occurring in individual microsphere were recorded by introduction of 0.07 N HCl drops onto the microsphere. The changes occurring in microspheres in the acidic medium were recorded for a span of 10 min. The integrity of the polymer coat on microspheres at pH 4.5 and 5.8 was examined. The samples were prepared by immersing the microspheres in buffer pH 4.5 and 5.8 for a period of 7 days. The samples were filtered and mounted immediately in the sample holder and examined for the surface modifications of microspheres.

4.2.2. Results and discussion

4.2.2.1. Dissolution studies

NREP coated microspheres were prepared by emulsification solvent evaporation technique. The CA loading efficiency of the microspheres was good as seen in **Table 4.3.** The compendial method for dissolution of Cefuroxime axetil immediate release tablets describes the use of 0.07 N HCl as dissolution medium [38](USP 26 NF XXI, 2003) and was chosen to investigate immediate release of CA. **Fig. 4.1** shows dissolution profile of CA. In the present investigations the composition F1 showed rapid dissolution of CA in 0.07 N HCl with 78 %, 84 % and 87 % being released in 30, 60 and 120 min. The release of CA was slightly faster in 30 min from F2, F3 and F4 compositions where the NREP loading was lower than that of F1. At end of 30, 60 min the composition F2 released 80 % and 95 % of CA. The composition F3 and F4 released 86 % and 88 % CA after 30 min respectively and 90% after 60 min. NREP shows rapid dissolution at acidic pH due to protonation of the tertiary nitrogen from pyridine ring and hence variation in polymer loading did not affect the release pattern from these compositions significantly.

Ceftum showed CA release of 40 %, 50 %, 65 % and 69 % in 0.07 N HCl at the end of 30, 60, 120 and 180 min. Ceftum contains microspheres of stearic acid with CA dispersed in it. The slow release is due to the insolubility of wax coating on microspheres in 0.07 N HCl. Donn et al. [19] studied the bioavailability of CA from

tablets and suspension based on wax coated CA granules. The tablets and suspension were not bio equivalent. The lower bioavailability of CA from suspension than tablet was attributed to wax coating on CA granules [19]. The wax coating causes relatively delayed release of CA as the release takes place only on forming stearate salt in alkaline pH due to interaction between sodium ions and stearic acid [7]. The mechanism by which wax coated microspheres release CA at gastric pH has not been explained. In contrast NREP is a pH dependent polymer, which goes into solution at acidic pH so the CA release from NREP coated microspheres is governed by dissolution.

Apart from wax coating, use of reverse enteric, enteric polymers for taste masking of CA has been reported in the past. Lorenzo-Lamosa et al. [17] studied taste masking of CA using Eudragit E. However Eudragit E caused significant degradation of CA due to negative interaction. Enteric coatings like Eudragit L, Cellulose acetate trimellitate, hydroxypropyl methylcellulose phthalate for taste masking of CA have been investigated in past [17,18]. CA was found to degrade in presence of CAT [18]. The use of enteric polymers for taste masking of CA is of little use as they dissolve in intestinal region where CA is rendered inactive.

In the present investigation the rapid dissolution of NREP contributes to immediate release of CA in 0.07 N HCl and since NREP is insoluble at pH of saliva it can be used effectively to taste-mask CA without compromising its bioavailability.

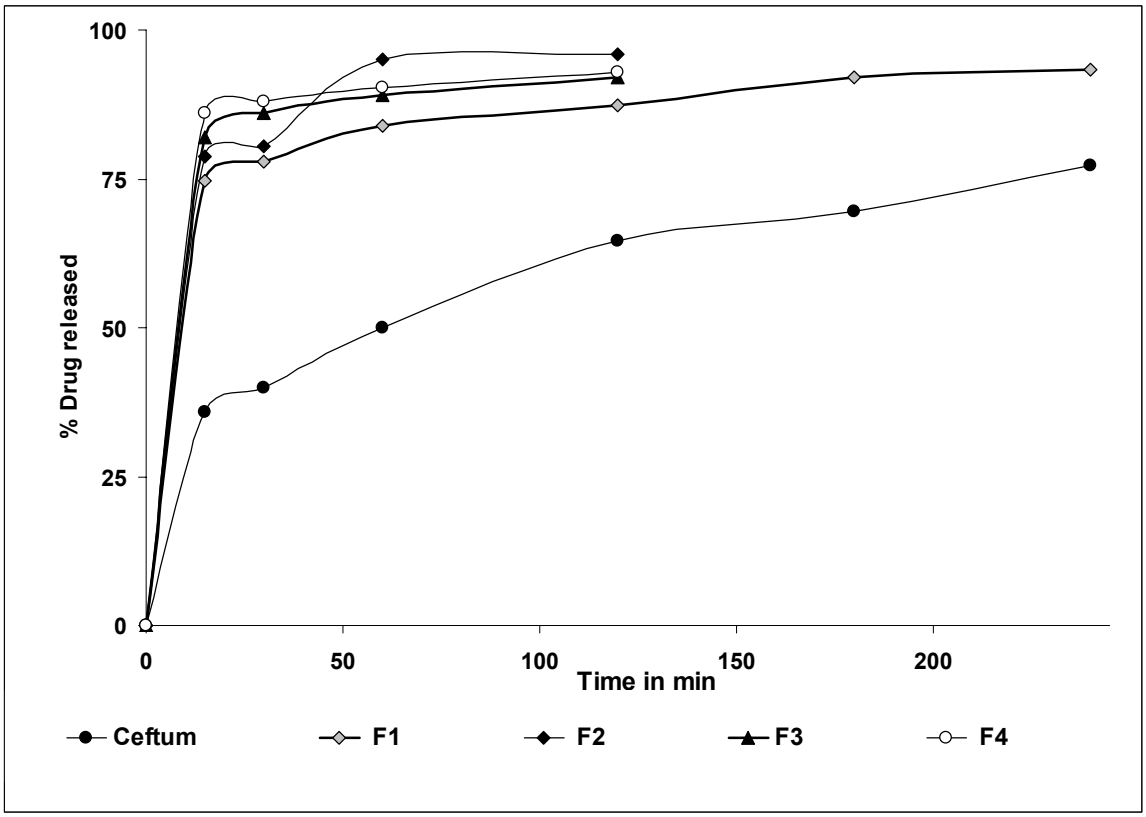

Fig.4.1. CA release from NREP microspheres and Ceftum in acidic pH 1.2

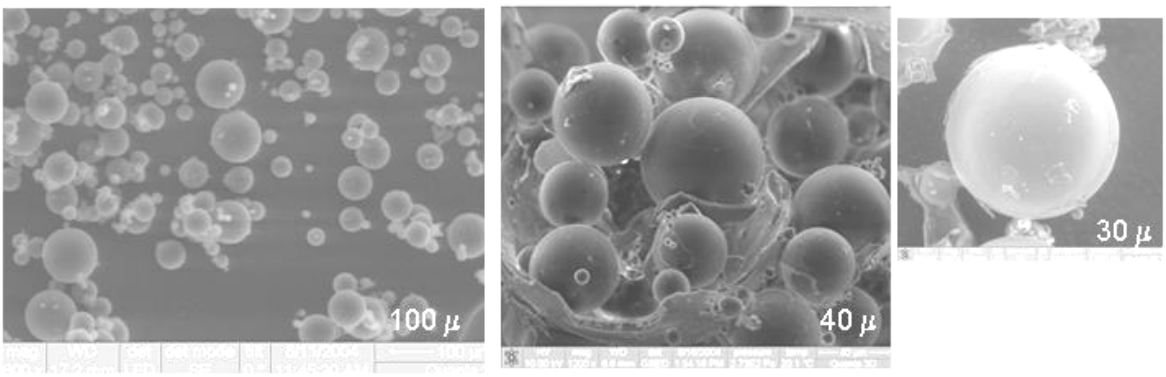

Fig.4.2.CA loaded Microspheres

4.2.2.2. Gustatory test / Taste evaluation

For the safety reasons minimum loading of synthetic polymers is preferred in formulating the drug delivery system. The recommended daily permissible amount for polymethacrylates is 2 mg / kg body weight [39] and hence compositions F3 and F4 containing lower NREP loading than that in F1 and F2 were considered for taste evaluations. The pH of Ceftum on reconstitution as per product information was 4.4. Also CA exhibits maximum stability in the pH range 3.5 to 5.5 [40]. Hence compositions F3 and F4 were reconstituted at pH 4.4 in syrup by adjusting the pH using citric acid-sodium citrate buffer. The equilibrium swelling studies show that NREP is practically deswelled at pH 4.5 since the degree of protonation of tertiary amine of pyridine is zero at pH~4 [41, 42]. It is expected that at this pH the compositions F3 and F4 would not release CA imparting bitter taste to syrup.

The palatability of the reconstituted suspensions was evaluated on the basis of numerical grading by the volunteers. The mean grading for the reconstituted taste masked CA microspheres and Ceftum is shown in **Table 4.4.** The compositions F3 and F4 showed a lower release at pH 4.4 and retained the palatability over seven days. The volunteers graded the formulations between 0-2 and rated the formulations as palatable. The taste of the reconstituted microspheres was better than the market formulation Ceftum initially for a period of 3 days and was comparable thereafter.

Table 4.4 Taste masking test

Day	Ceftum	F3	F4
1	0	0	0
2	0	0	0
3	1	0	0
4	2	0	0
5	2	0	1
6	3	1	1
7	3	1	1

0: Sweet, 1: acceptable, 2: acceptable but slightly bitter, 3: bitter, 4: very bitter

3.2.3. Scanning electron microscopy

The exposure of CA loaded microspheres to 0.07 N HCl, pH 4.5 and 5.8 was investigated using the environmental SEM. **Figs. 4.2 and 4.3** show the morphology of microspheres before and after suspending in buffer at pH 4.5 and 5.8 for 7 days. Morphological changes in CA loaded stearic acid microspheres on exposure to Sorenson buffer pH 7 were reported by Robson et al. [7].

The integrity of the polymer film at the pH of saliva and also at reconstitution pH 4.5 is crucial to retain the palatability of the formulations in which microspheres are incorporated. NREP is insoluble in water and also at pH 4.5 and 5.8 (**Fig 4.3**). The examination of microspheres recovered from the aqueous medium after 7 days does not show any drastic changes in the morphology. NREP coating remains insoluble and intact as seen in **Fig. 4.3**. This prevents leaching of CA at pH of saliva and masks its unpleasant taste as seen in the gustatory test. The integrity of the microspheres without any drastic morphological changes as exhibited by the ESEM is a consequence of pH dependent behavior of NREP.

The morphological changes occurring in 0.07 N HCl, were recorded by immersing the microspheres completely in the medium. Extensive changes in the surface of the microspheres were observed after immersion in the acid medium. Since NREP dissolves in acid the removal of the acid medium by applying vacuum resulted in formation of a blanket of polymer film over the microspheres as shown in **Fig. 4.4 (a) and (b)**. The removal of the film from the surface of the microspheres showed that the smooth surface of microspheres was distorted due to the deposits from the dissolved polymer. The change occurring in individual microsphere was monitored by isolating the microsphere with introduction of drops of 0.07 N HCl onto the sample and simultaneous recording of morphological changes. The effect of 0.07 N HCl on the microsphere after contact period of 1-2 minute is shown in **Fig.4.4 (c).** The microsphere developed small craters on exposure to the acid medium. **Fig. 4.4 (c)** shows the initiation of pore formation after 5 min. The microsphere showed the formation of distinct pores within 10 min. These morphological changes occurring in the microspheres help understand the rapid release shown by all compositions (F1 to F4) in

0.07 N HCl. These morphological changes confirm that the drug is released as a result of polymer dissolution.

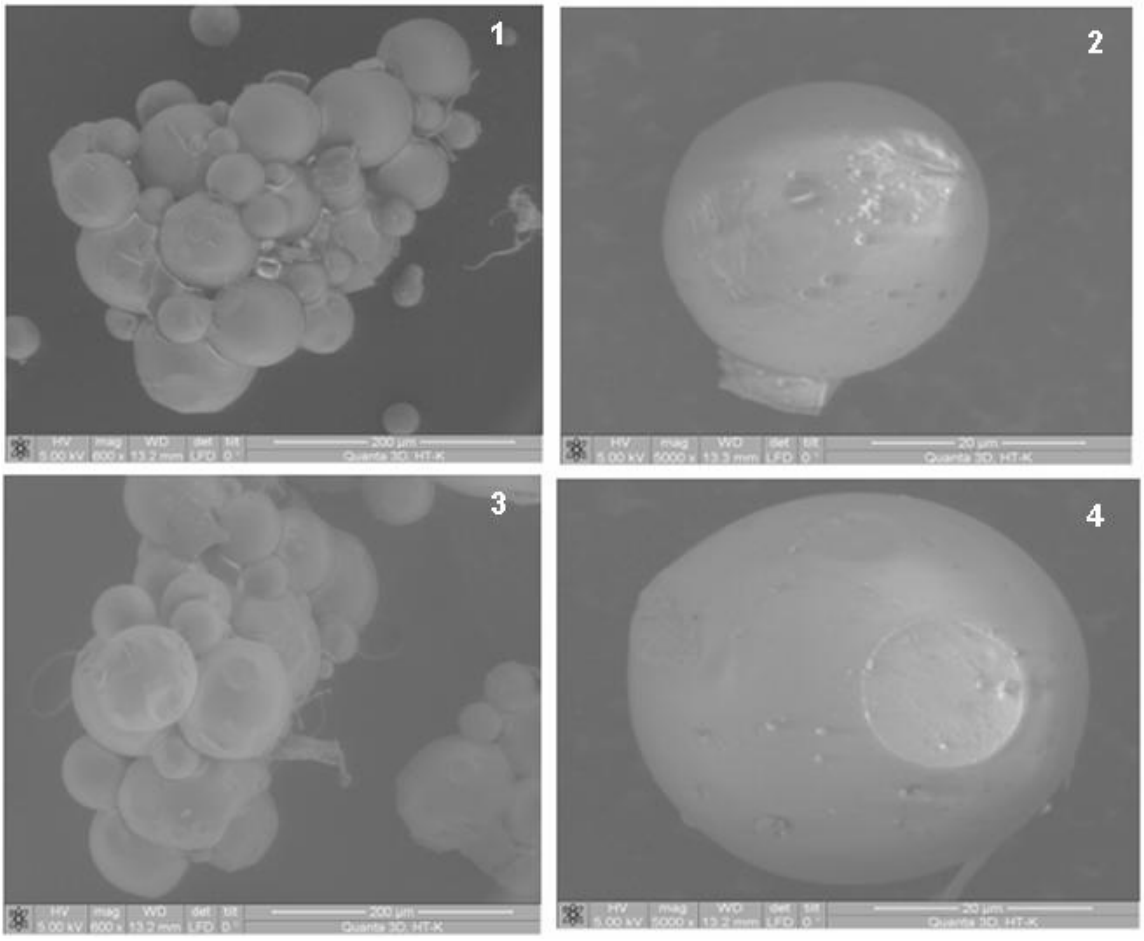

Fig.4.3. ESEM analysis of morphological changes in NREP microspheres on exposure to pH 4.5 and 5.8. (1 and 2; microspheres exposed to pH 4.5, 3 and 4; microspheres exposed to pH 5.8).

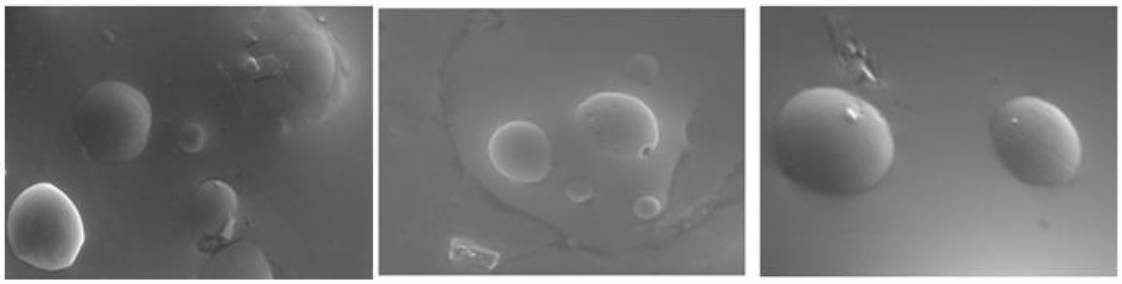

Fig.4.4a. ESEM analysis for morphological changes in NREP microspheres on immersion in buffer pH 1.2

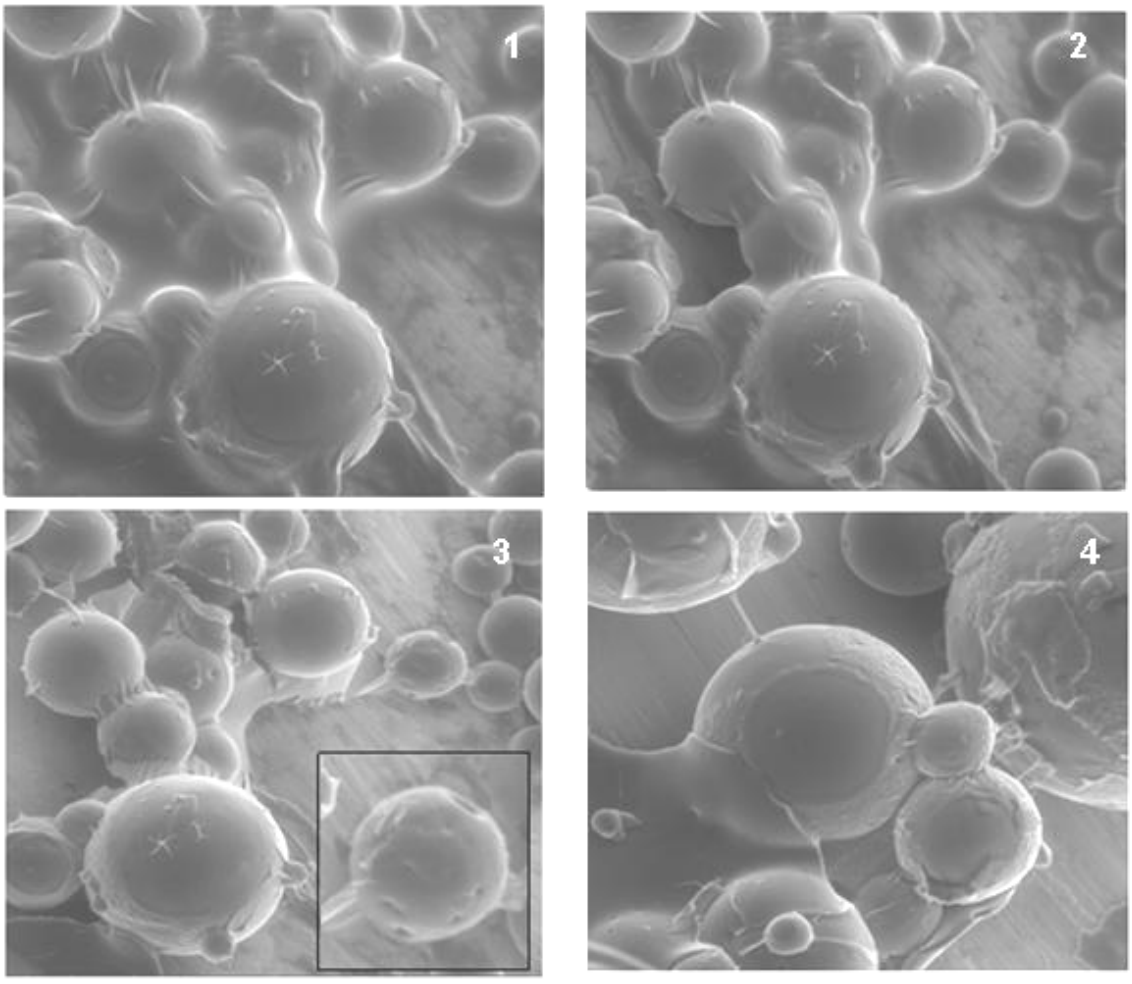

Fig.4.4b. ESEM analysis for morphological changes in NREP microspheres on exposure to pH 1.2 (1 and 2 NREP dissolution causes blanket on removal of buffer) (3 and 4 microsphere surface distorted due to deposition of dissolved NREP)

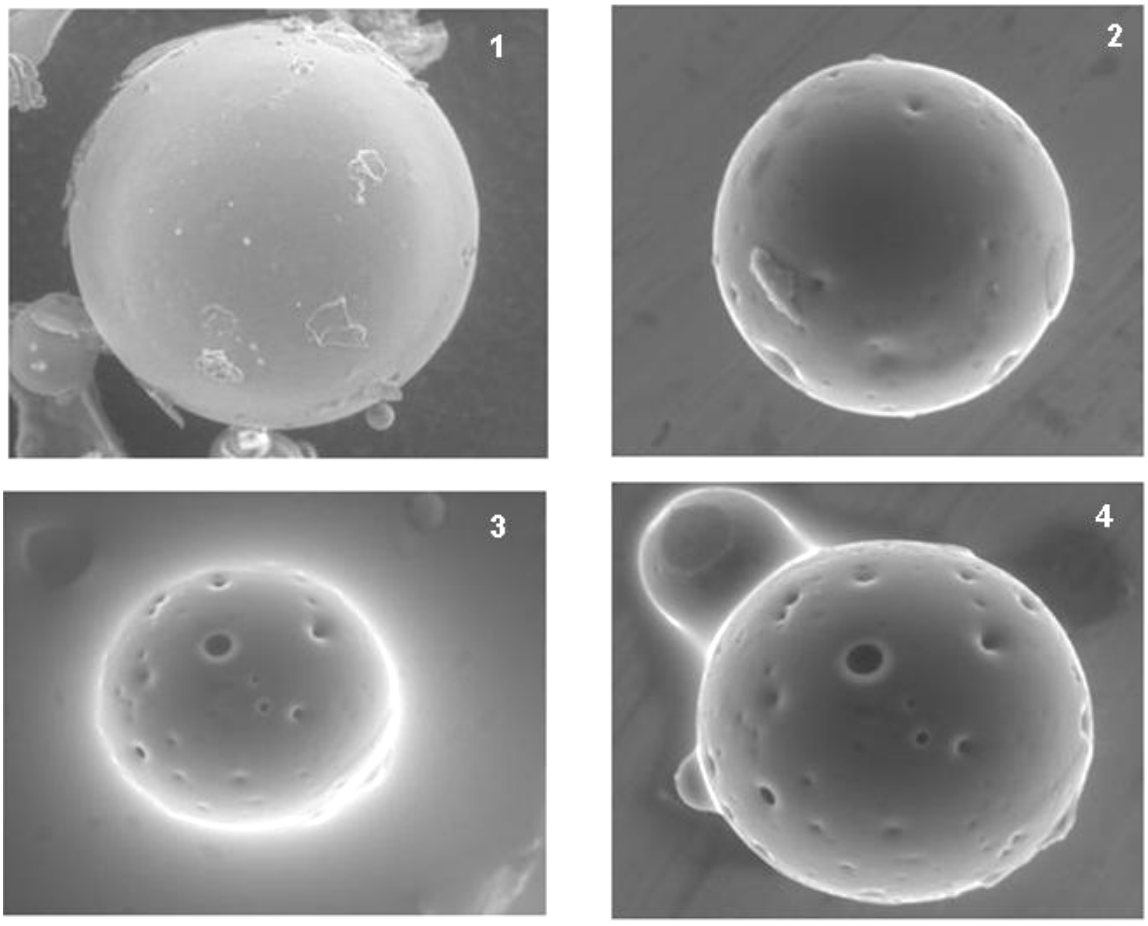

Fig.4.4c. ESEM analysis for morphological changes in NREP microspheres on exposure to pH 1.2 (1; before exposure, 2; after exposure for 2 min and removal of buffer, 3; after exposure for 5 min still immersed in buffer; 4; formation of pores after removal of buffer)

4.3. TASTE MASKING OF CIPROFLOXACIN HCL USING NREP

4.3.1. Microsphere preparation and characterization

4.3.1.1. Emulsification solvent evaporation

NREP solution was prepared in mixture of methanol: dichloromethane (2:1). Ciprofloxacin HCl was added to polymer solution under magnetic stirring. The drug polymer solution was dispersed slowly in light liquid paraffin containing 0.25 % of Span 85 under mechanical stirrer. The stirring was continued for 3-4 hr at 500 rpm. The microparticles were separated by filtration and washed with petroleum ether to remove the paraffin oil. The microspheres so formed were dried under vacuum for 24 hr at room temperature. The composition of the microspheres is shown in **Table 4.5.**

4.3.1.2. Determination of drug content

The drug content was determined at 276 nm using Shimadzu UV160 IPC UV Visible spectrophotometer. Ciprofloxacin HCL content was determined by dissolving 50 mg of microspheres in 2 ml of methanol and sonicating for 5 min. Then the volume was made to 250 ml using 0.01 N HCl. The solution was filtered and diluted further for the analysis. Each sample was analyzed in triplicate.

Table 4.5 Ciprofloxacin HCl microspheres: content and efficiency of loading

Formulation	Cipro: NREP ratio	Loading Efficiency (%)	Cipro loading (%)
F5	3.8 : 1	84.8	67.6
F6 (Cipro = 300mg)	1: 2.9	84.5	22.0

4.3.1.3. In-vitro dissolution test

Ciprofloxacin hydrochloride release from the taste masked particles was determined in 900 ml of 0.1 N hydrochloric acid buffer, at 37 ± 0.5°C, using USP type II apparatus rotated at 100 rpm. The samples were withdrawn at 15, 30, 45, and 60, min. The amount withdrawn each time was replaced with fresh media to maintain the sink conditions.

4.3.2. Results and discussion

4.3.2.1. Dissolution studies

NREP coated microspheres were prepared by emulsification solvent evaporation technique. The Ciprofloxacin HCl loading efficiency of the microspheres was good as seen in **Table 4.5.** The USP recommends the use of HCL buffer pH 1.2 to simulate the gastric conditions and hence the same was chosen to investigate immediate release of Ciprofloxacin HCL. **Table 4.6** shows dissolution profile of Ciprofloxacin HCl microspheres. The formulations F5 and F6 show rapid release of Ciprofloxacin HCl in at acidic pH. This is desired due to better absorption of ciprofloxacin from gastric region.

Table 4.6. Ciprofloxacin HCl release from microspheres

Time (min)	% Release	
	F5	**F6**
15	86.58	68.30
30	91.57	74.56
45	96.85	81.42
60	----	88.2

4.4. TASTE MASKING OF CLARITHROMYCIN USING NREP

4.4.1. Microsphere preparation and characterization

4.4.1.1. Emulsification solvent evaporation

NREP solution was prepared in mixture of methanol: dichloromethane (2:1). Clarithromycin was added to polymer solution under magnetic stirring. The drug polymer solution was dispersed slowly in light liquid paraffin containing 0.25 % of Span 85 under mechanical stirring. The stirring was continued for 3-4 hr at 500 rpm. The microparticles were separated by filtration and washed with petroleum ether to remove the paraffin oil. The microspheres so formed were dried under vacuum for 24 hr at room temperature. The composition of the microspheres is shown in **Table 4.7**.

4.4.1.2. Determination of drug content

Microspheres were weighed (50 mg) and transferred to 50 ml volumetric flask and drug extracted using methanol by sonication. The solution was filtered and 5 ml of this was diluted with glacial acetic acid to 25 ml. 1ml of this solution was transferred to 10 ml volumetric flask followed by the addition of 1ml of p-dimethylamino benzaldehyde (DAB) reagent (1% solution in methanol) and 3 ml of concentrated hydrochloric acid. After 10 minutes, volume was made up with glacial acetic acid and absorbance measured at 485 nm.

Table 4.7 Clarithromycin microspheres: content and efficiency of loading

Formulation	Clarithromycin : NREP ratio	Loading Efficiency (%)	Clarithromycin loading (%)
F7	1 : 2	93	31
F8	1.6 : 1	91	57
(Clari= 500mg)			

4.4.1.3. In-vitro dissolution test

Clarithromycin release from the taste masked particles was determined in 900 ml of acetate buffer pH 2.8, at 37 ± 0.5°C, using USP type II apparatus rotated at 100 rpm. The samples were withdrawn at 15, 30, 45 and 60 min. The amount withdrawn each time was replaced with fresh media to maintain the sink conditions.

4.4.2. Results and discussion

4.4.2.1. Dissolution studies

NREP coated microspheres were prepared by emulsification solvent evaporation technique. The Clarithromycin loading efficiency of the microspheres is shown in **Table 4.7**. Clarithromycin undergoes degradation in the acidic environment at pH 2 in HCl solution [20] so the dissolution was investigated at pH 2.8 in acetate buffer. In case of formulations developed based on the complex formed between polyacrylic acid and polyvinyl pyrrolidone Clarithromycin release was found to decrease with time. This decrease in release was attributed to degradation of drug at that pH. Further the degradation half-life of Clarithromycin at pH 2 in HCL solution was reported to be 1.47 hr. **Table 4.8** shows dissolution profile of Clarithromycin microspheres. The formulations F7 and F8 show rapid release of Clarithromycin at acidic pH 2.8. This is desirable for the treatment of H. pylori infections which are located in the stomach / gastric region.

Table 4.8 Clarithromycin release from microspheres

Time (min)	% Release	
	F7	**F8**
15	48.20	53.97
30	65.51.	69.40
45	72.80	76.32
60	82.59	85.59

4.5. CONCLUSIONS

NREP exhibits rapid dissolution at pH< 4 and remains insoluble at neutral and near neutral pH. The polymer can thus be used to release the drugs immediately at gastric pH from taste masked dosage forms with prevention of drug leaching in aqueous media. Bitter drugs Cefuroxime axetil (CA), Ciprofloxacin HCl and Clarithromycin were coated using NREP. CA was released rapidly at gastric pH. The release was inhibited at salivary pH. NREP prevented CA leaching in aqueous media. The NREP coated CA suspension formulation was compared against the marketed product "Ceftum". The CA compositions based on NREP showed a slower release at pH 4.4 and retained the palatability over seven days. The volunteers graded the formulations between 0-2 and rated the formulations as palatable. The taste of the reconstituted microspheres was better than the marketed formulation "Ceftum" initially for a period of 3 days and was comparable thereafter. The encapsulation of Ciprofloxacin and Clarithromycin using NREP showed rapid release of these drugs under gastric conditions. This ensured the release of Clarithromycin and Ciprofloxacin HCL at the target site and site of absorption. Thus encapsulation of these drugs by NREP provided site specific release along with taste masking ability. Further NREP can be used in variety of dosage forms like tablets, granules and suspensions. One of the approaches to enhance the bioavailability is the "*Pharmaceutic Approach*" involving formulation modification aimed at enhancing drug dissolution rate. We have adopted similar methodology by encapsulating the above drugs using NREP ensuring rapid drug dissolution. Interaction of Cefuroxime axetil with various polymers is reported. Taste masking without inactivation can be determined by investigating the nature of interactions between CA and NREP and this has been undertaken in the subsequent chapter.

4.6. REFERENCES

1) M. Diarra, G. Pourroyb, C. Boymondc, D. Musterd, Biomaterials, 2003,24, 1293–1300
2) G. Mukherji; S. Goel; V. K.Arora, US Patent 6,565,877, May 20, 2003
3) D.R. Friend, J.Microencapsulation, 1992, 9, 469- 480.
4) G.M. Roy, 1994. Pharm. Tech. Eur. 24-35
5) B. Albertini, C. Cavallari, N. Passerini, D. Voinovich, M. L. Gonzalez-Rodrıguez, L. Magarotto, L. Rodriguez Eur. J. Pharm. Sci. 2004, 21, 295–303.
6) G.M. Roy, Modifying Bitterness, Mechanisms, Ingredients and Applications, CRC Press LLC, 2002.
7) H.J. Robson, D.Q. M. Craig, D. Deutsch, Int. J. Pharm. 1999,190, 183-192.
8) A. Nanda, K. Raghupathi, S. Garg, Indian Journal of Pharmaceutical Science 2002, 64, 10-17.
9) G. Weil, A. Knoch, A. Laicher , F. Stanislaus , R. Daniels, Int. J. Pharm. 1995, 124, 97-105.
10) S. Pisal, R. Zainnuddin, P. Nalawade, K. Mahadik, S. Kadam, *AAPS PharmSciTech* 2004; 5 (4) Article 62 (http://www.aapspharmscitech.org).
11) Y. Qiu, K. Park Adv. Drug Deliv. Rev. 2001, 53, 321–339.
12) L. I. Grossman, B. M. Brickman J. Dent. Res. 1937, 16, 409-416.
13) A. Finn, A. Straughn, M. Meyer, J. Chubb, Biopharm. Drug Disposit. 1987, 8, 519-526.
14) C. J. Campbell, L. J. Chantrell, R. Eastmond, Biochem. Pharmacol. 1987, 36, 2317–2324.
15) N. Ruiz-Balaguer, A. Nacher, V.G. Casabo, M. Merino, Antimicrob. Agents. Chemother. 1997, 41, 445–448.
16) Ceftin Prescription Information, Physicians' Desk Reference 2003 pp 1918-1922
17) M. L., Lorenzo-Lamosa, M. Cuna, J. L. Vila-Jato, D. Torres, M. J. Alonso, J. Microencap. 1997,14, 607-616.

18) M. Cuna, M. L. Lorenzo-Lamosa, J. L. Vila- Jato, D. Torres, M. J. Alonso, Drug Dev. Ind. Pharm. 1997, 23, 259-265.

19) K. H Donn, N. C. James, J. R. Powell, J. Pharm. Sci., 1994, 83, 842-844.

20) M.K. Chun, H. Sah, H.K. Choi, Int. J. Pharm., 2005, 297, 172–179.

21) P. J. Ferguson, J. W. Piper, WO 02/092106, 09 May 2002.

22) N. Talwar, H. Sen, J.N. Staniforth, US Patent, US 6261601, 17 July 2001.

23) N. Talwar, H. Sen, J.N. Staniforth, US Patent, US 6,960,356, 1 Nov 2005.

24) M.Y. F. Lu; S. Borodkin; US Patent, US 4,808,411, 28 February, 1989

25) G.A. Meyer, T.B. Mazer; PCT Application WO9312771, 8 July 1993.

26) G.A. Meyer, T.B. Mazer; US Patent, US 5,599,556 4 February, 1997

27) Gold Oscar (AR) European Patent EP0943341 – 22 September 1999.

28) Sue, Kazuko Japanese Patent Application JP 2001226293, 21 August 2001.

29) L. Christophe; S. Sandrine, PCT Application, WO02072072, 19 September 2002.

30) F. X. Schwarz. PCT Application, WO0172284, 04 October 2001.

31) Bastian Petra, PCT Application WO03006066, 23 January 2003.

32) N. Poellinger, J. Michaelis, K. Benke, R. Rupp; M.D. Buecheler, European Patent EP0551820, 21 July1993.

33) N. Pollinger; J. Michaelis; K. Benke; R. Rupp; M. Bucheler; US Patent US 5,695,784, 9 December 1997.

34) N. Pollinger; J. Michaelis; K. Benke; R. Rupp; M. Bucheler; US Patent US 6,136,347, 24 October 2000.

35) T. Nishioka, Y. Yamanouchi, A. Yoshida, K. Ohta, Japanese Patent Application JP 2000053563, 22 February 2000.

36) C. M. Roig, A.P. Tubau, R.J. Julve, PCT Application WO0076549, 21 December 2000.

37) G. Mukherji, M. Kumar, H. Sen, R.K. Khar WO0135930, 25 May 2001.

38) United States Pharmacopoeia XXIII, 1995. United States Pharmacopeial Convention, Rockville, MD

39) A. H Kibbe, Handbook of Pharmaceutical Excipients, 3rd Edition, American Pharmaceutical Association 2000.

40) N. A. T. Nguyen, Pharm. Res, 1991, 8, 893-898.

41) T. Radeva, V Milkova, I Petkanchin, J. Colloid and Interface Sci. 2004, 279, 351–356.

42) E. Pefferkorn, A. Elaissari, J. Colloid and Interface Sci., 1990, 138, 187-194.

CHAPTER 5

Drug-polymer Compatibility Studies:

Implications for Drug Bioavailability

5.1. INTRODUCTION

Excipients form integral part of all pharmaceutical dosage forms. A major consideration in use of biomaterials for drug delivery is drug-polymer interaction, drug transformation and its degradation [1]. The drug-excipient interactions often modify the physicochemical characteristics of the drug [2]. These interactions could be either reversible or irreversible in nature and alter in most cases dissolution, bioavailability, safety and efficacy and in extreme cases even the stability of the drug [3-5]. Jenquin and McGinity, [6] reported both reversible and irreversible binding between salicylic acid and Eudragit RL and RS. The ionic interactions are reversible but formation of new covalent bond is an irreversible interaction. The methacrylic acid polymers Eudragit L and S interact with propranolol hydrochloride [7]. Acetyl salicylic acid is degraded by magnesium stearate forming salicylic acid, salilsalicylic acid and acetyl salilsalicylic acid [8,9].

Schmitt et al. [10] discussed factors affecting drug excipient compatibility and degradation kinetics of drugs. Crowley and Martini [11] reviewed the nature and extent of physical and chemical interactions and their influence on compatibility for a wide range of drug polymer systems. Sarisuta et al. [12] showed that protonation of amine group in erythromycin in presence of carboxylic acid present in Eudragit L and Shellac led to the formation of amine salt, but degradation of the drug was not observed.

Most of the drug–excipient interactions result in delayed release of the drug from formulations. Chitosan interacts with salicylic acid forming a salicylate salt causing delayed release of salicylic acid [13]. Interaction of indomethacin and warfarin with Eudragit E causes delayed release of these drugs [14, 15].

Preformulation studies are carried out during product development to identify and address the stability issues. The general principles for selection of excipients are not well-defined and excipients are often selected without adequate consideration of drug-excipient compatibility [2]. The modification of formulations necessitated by stability issues at a later stage, when the performance requirements are already met, are time consuming and costly. This could be avoided by preliminary evaluation of drug–excipient compatibility.

Cefuroxime axetil (CA) is a second-generation cephalosporin antibiotic administered orally and is known to have bitter taste [16]. Extensive efforts have been made in the past to develop oral taste masked formulation for CA. Cellulose acetate trimellitate (CAT), hydroxypropyl methylcellulose (HPMCP) and Eudragit E (EE) have been evaluated as possible excipients for drug coating. Lorenzo-Lamosa et al. [17] reported that the CA-EE microspheres exhibited the desired release profile, but the drug was degraded in the presence of the polymer. Also in the presence of CAT, the degradation of CA led to unacceptably high proportions of impurities [18]. CA has a limited absorption window restricted to upper gastric region as it is hydrolyzed by esterase enzyme in intestine to Cefuroxime, a form, which cannot be absorbed orally [19-22]. Bioavailability of orally administered CA is low (37-52 %) [23]. It is therefore essential that the drug be released in gastric region under acidic pH conditions so that its bioavailability is not affected. The enteric polymers dissolve in intestinal region due to ionization of the carboxylic acid groups. Use of these polymers to taste mask CA can therefore affect its bioavailability.

In the earlier chapter we have demonstrated the ability of NREP in taste masking of Cefuroxime axetil and other drugs with their release in the gastric region. Since CA has shown interaction with different polymers as listed above it was important to investigate its interaction with the polymer (NREP) synthesized by us. In this chapter we report the results of investigation of interactions between CA and the NREP as well as EE by differential scanning calorimetry (DSC), X ray diffraction (XRD), Fourier transform infrared spectroscopy (FTIR) and nuclear magnetic resonance spectroscopy (NMR) as well as high pressure liquid chromatography (HPLC) techniques. The results indicate that CA is stable in presence of NREP but is degraded by EE. The differences are shown to result from the fact that the polymer exhibits the desired dissolution profile when the degree of incorporation of 4-VP (10.8 %) was lower as compared to that of dimethylamino ethyl methacrylate (DMAEMA) in EE (50 %). Further the monomer 4-VP is weakly basic as compared to DMAEMA and does not hydrolyze CA to Cefuroxime.

5.2. MATERIALS AND METHODS

5.2.1. Materials

Cefuroxime axetil (CA) and its reference standard were a gift from Lupin Laboratories Ltd. Eudragit E (Degussa) was gift from Lupin Laboratories Ltd. $CDCl_3$ and Acetone d_6 solvents for NMR were purchased from Sigma-Aldrich. Ammonium di hydrogen phosphate and Acetanilide (HPLC) grade were purchased from Fluka. NREP was synthesized as disclosed by us earlier [24, 25]. The other solvents were purchased from Qualigens.

5.2.2. Preparation of CA-polymer physical mixtures

The physical mixture of CA with NREP and EE was prepared in weight ratio 1:1. The neat polymer and drug were weighed, mixed thoroughly in mortar and pestle. The mixture was used for further analysis.

5.2.3. Preparation of CA-polymer blends

CA: polymer in weight ratio 1:1 was used for preparing the drug-polymer blends. CA was added to the 5 % w/v polymer solution in dichloromethane: methanol (1:2). In a petri dish 10 ml of above solution was transferred and the solvent was allowed to evaporate at room temperature under vacuum. The dried material was collected and stored under vacuum till further use.

5.2.4. Physicochemical characterization

5.2.4.1. XRD analysis

The physical state of CA was determined by X ray diffraction analysis. For XRD analysis Rigaku D max 2500 X ray diffractometer with copper target (Cu

$K\alpha_1$ radiation) and 18 KW rotating anode type generator was used. The samples were scanned from 5 to 60° 2θ at a speed of 3° 2θ / min at ambient temperature. The X ray powder diffraction patterns for CA, polymers EE, NREP, physical mixtures and CA-EE and CA-NREP blends were measured.

5.2.4.2. DSC analysis

The pure drug CA, polymers EE and NREP, physical mixtures and CA-polymer blends were subjected to thermal analysis using TA Instruments DSC Q10 with nitrogen as purge gas at a flow rate of 20 ml/min. Indium was used to calibrate the enthalpy and temperature values. The experiments were conducted in hermetically sealed aluminium pans. The weight of each sample was in the range 5-6 mg and the heating rate was 10°C/ min from 30 to 180°C.

5.2.4.3. FTIR spectroscopy

The interactions between CA- EE and CA-NREP were examined by analyzing the samples by FTIR Perkin Elmer (diffused reflectance mode). 1-2 mg of samples were thoroughly mixed and triturated with potassium bromide and placed in the sample holder. The samples were scanned from 4000 to 450 cm^{-1}. The measuring conditions were resolution, 4.0; zero fitting, 2.0; sample scan, 32; acquisition, single sided. The peak assignments were made for the neat samples of NREP, EE and CA, and were compared with the peaks obtained for the polymer-drug physical mixtures and blends.

5.2.4.4. NMR spectroscopy

The CA-EE and CA-NREP interactions were also investigated by ^1H NMR spectroscopy. The spectra were recorded on a 500 MHz Bruker DRX spectrometer. The solvents used were deuterated chloroform ($CDCl_3$) and Acetone d_6. The samples analyzed were polymers; EE, NREP, CA and CA-polymer blend in solution. One drop of Acetone d_6 was added to the samples for complete dissolution of samples.

5.2.4.5. HPLC analysis

The CA-polymer interactions were also analyzed using HPLC, comprising Waters 510 pump and Waters 486 Tunable absorbance detector. The mobile phase was monobasic ammonium phosphate buffer and methanol (62:38 v/v) as per USP 23, 1995. The column used was Spherisorb S5C1, 25 cm x 4.6 mm, 5 μm particle size waters HPLC columns. Cefuroxime axetil content was estimated at 278 nm at a flow rate of 1 ml/min using Acetanilide as internal standard. The peak positions for the CA-polymer samples were compared against the CA reference standard and working standard.

5.3. RESULTS AND DISCUSSION

Extensive efforts have been made in the past to develop oral suspension formulations based on CA, which will mask bitter taste of the drug and release the drug in the upper gastric region. EE, cellulose acetate trimellitate (CAT) and hydroxypropyl methylcellulose (HPMCP) have been evaluated as possible excipients. Lorenzo-Lamosa [17] reported that the CA-EE microspheres exhibited the desired release profile, but the drug was degraded in the presence of the polymer. Also in the presence of CAT, the degradation of CA led to unacceptably high proportions of impurities. The impurities generated in the presence of HPMCP 55 were lower than those generated in the presence of HPMCP 50, but for solubility reasons it would release the drug at pH 5.2 onwards. CA is degraded by esterase enzyme in intestine and is better absorbed from upper gastric region [19-22]. It is therefore essential that the drug be released in gastric region under acidic pH conditions.

In the previous chapters we reported a new reverse enteric polymer based on methyl methacrylate, 2-hydroxy ethyl methacrylate and 4-vinyl pyridine [24-26]. The polymer dissolves in the acidic pH upto 3.5 and is insoluble at neutral and basic pH. The polymer composition was optimized to yield rapid dissolution of the polymer and release the drug within 30 minutes under gastric conditions. The swelling of the polymer and hence leaching of the drug was minimal during storage of reconstituted microparticles in suspension form. The polymer was found to be biocompatible and met

pharmacopoeial requirements as per USP 23 (1995) [26]. Comprehensive investigation of CA–NREP interactions was undertaken using XRD, DSC, ^{1}H NMR, FTIR and HPLC and the results were compared with those for the system CA–EE. The changes in physical state of the drug and chemical interactions in drug-polymer blends prepared in presence of solvents were evaluated. The results of present investigation indicate that CA is stable in the presence of NREP but is degraded in the presence of EE. This has been attributed to differences in composition of the two polymers (**Fig. 5.1**).

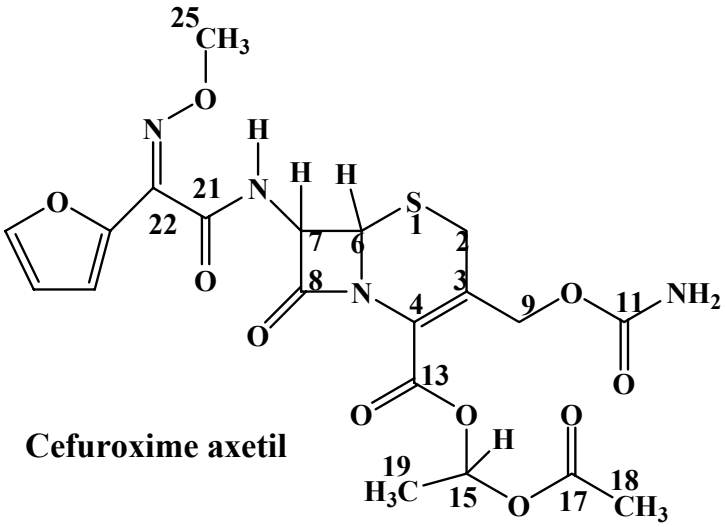

Cefuroxime axetil

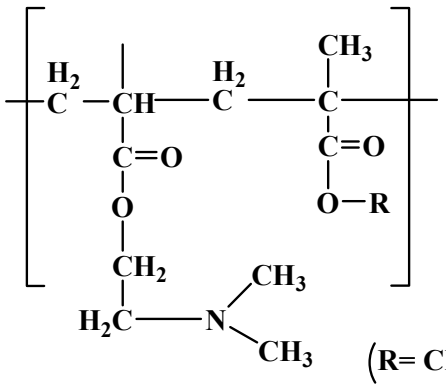

Eudragit E

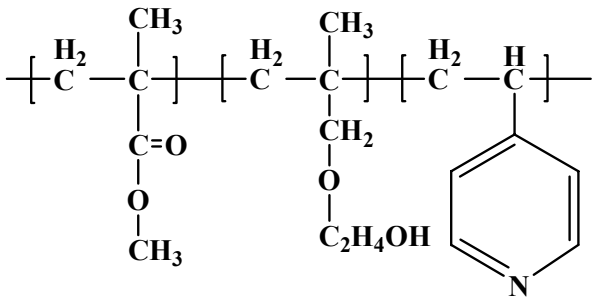

New Reverse Enteric Polymer

Fig.5.1. Molecular structures of Cefuroxime axetil, Eudragit E and NREP.

5.3.1. XRD analysis

Drugs exist in polymorphic forms. Often, a particular form of drug such as amorphous or crystalline is biologically active. In case of CA the amorphous form is more bioavailable [28, 29] and is chemically more stable during storage. A number of methods are disclosed in the past to obtain the amorphous form of CA [28, 30-35]. Efforts were made to convert crystalline drugs to amorphous forms and retain the same [36-43]

In the present investigation the conversion of amorphous CA to the crystalline form in the presence of the NREP was investigated by XRD and it was observed that the drug was retained in its amorphous form. It may be noted that in addition to the polymer composition, attributes such as molecular weight and the processing techniques play a critical role in inhibiting crystallization of the drug [24, 25]. See **Fig.5.2**. Since CA degraded in presence of EE, these blends were not investigated.

5.3.1.1. X-Ray diffractograms of CA, NREP, CA-NREP physical mixture and CA-NREP blend

The XRD patterns for the neat CA and NREP are shown in the curve (a) and (d) in **Fig. 5.2**. The polymer and the drug are both amorphous in nature as exhibited by the halo in the diffractogram. The physical mixture shows amorphous nature of the drug. The diffractogram for CA-NREP blend shows pattern similar to that exhibited by the physical mixture indicating that the drug is not transformed to a higher melting crystalline form.

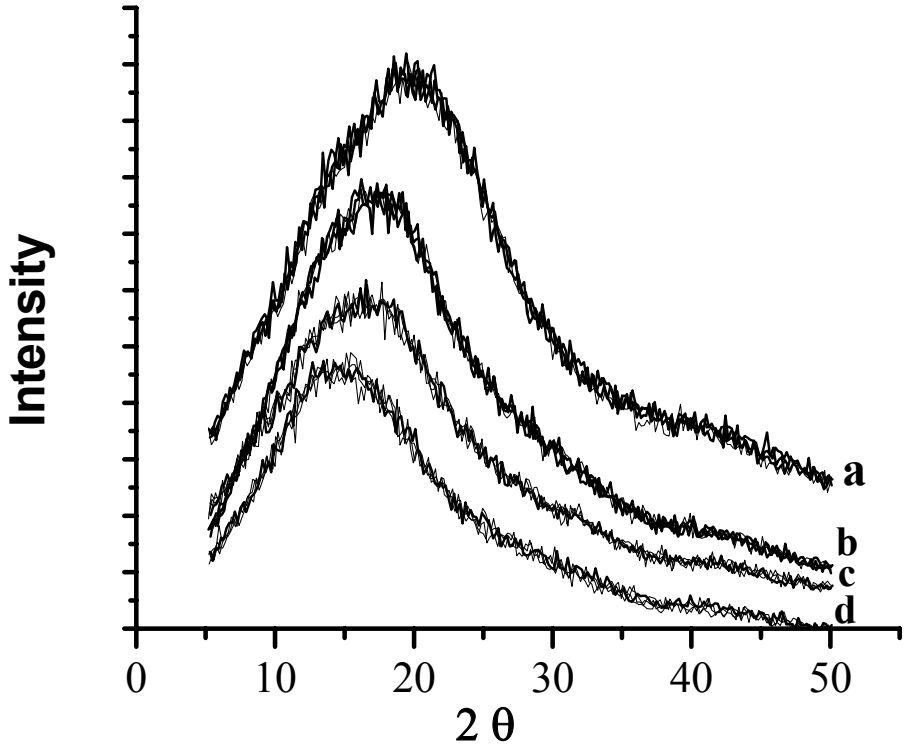

Fig.5.2. XRD pattern of Cefuroxime axetil and CA- NREP blends: Cefuroxime axetil (a); physical mixture of Cefuroxime axetil-NREP (b); CA-NREP blend (c) and NREP (d).

5.3.2. DSC analysis

DSC is employed in pharmaceutical industry for investigating physical stability, excipient compatibility, chemical stability and interactions involving macromolecules [44-46]. The thermal behavior of the drug and excipient is evaluated individually and compared against the drug-excipient binary mixture and blends. Ideally the endotherm of drug-excipient mixture should show the features of both the components. Any deviation for the drug-excipient physical mixture implies an interaction, which may or may not lead to incompatibility. The changes noted include the alteration in T_g and shift in endotherm or appearance of a new peak. In the past drug excipient interactions have

been studied by DSC by Holgado et al., Mura et al., Lloyd et al., McDaid et al. and Takka [7,47-50].

In the present investigation the DSC method is used to identify the changes in the T_g of the polymers and also the physical form of CA in presence of polymers. CA can exist in three polymorphic forms [51]. Crystalline CA shows melting point at 175-180°C and substantially amorphous high melting form exhibits melting point at 135-137°C and a low melting amorphous form having melting point in the range 70- 80°C [51, 52]. CA is more bioavailable orally from the amorphous form than from the crystalline form [28, 29].

5.3.2.1. Thermal behavior of CA, NREP and EE

The DSC thermograms are shown in **Fig. 5.3 and 5.4**. The scan for the CA is shown in curve **(a) Fig. 5.4**. In the present investigation thermal analysis of CA-NREP blends was very important to ensure that CA is retained in the same form in presence of NREP. Normally drugs exist in either amorphous or crystalline form. However in case of CA the drug is reported to exist in three polymorphic forms [51, 52]. Woo and Chang, 2000; and Jo et al.[51,52] reported crystalline form of CA which shows endotherm at 175-180°C, a substantially amorphous form (presence of some crystalline form) which exhibits endotherm at 135-137°C and another substantially amorphous form (presence of some crystalline form) which exhibits endotherm in the range 70-80°C. CA is more bioavailable orally from the amorphous form than from the crystalline form [28,29].

The gift sample obtained from Lupin Laboratories showed an endotherm at 71.4°C. Since CA exists in different forms and also these forms exhibit different bioavailability, we evaluated the nature of CA after blending with NREP. The purpose of this investigation was to validate any changes in the form of CA due to interaction with NREP. The retention of CA in a form similar to the plain drug without blending was preferred. In the subsequent section we describe the results of our investigation to substantiate this.

EE shows a T_g at 45.2°C (**Fig.5.3**). This value is in good agreement with the values in the range 45-50°C reported by Lovrecich et al., Lin et al., Eerikainen and Kauppinen, [15, 53, 54]. Eudragit EPO shows caking at temperature above 25°C and therefore has to be stored at or below room temperature [55]. Low T_g leads to tacky polymer coats in pharmaceutical processes involving high temperatures like drying and heat sealing [56].

The NREP shows a T_g at 123.3°C (**Fig. 5.3**), which is substantially higher than that of Eudragit E. The T_g of the polymers is affected by the monomer composition. The T_g of homopolymers of monomers in EE are: poly (butyl methacrylate (BuMA)) 20°C, poly (DMAEMA) 19°C and poly (MMA) 105°C respectively. The presence of DMAEMA and BuMA components in EE contributes to the lower T_g of this polymer. The T_g of the homopolymers poly (HEMA), 87.5°C and poly (4-VP), 142°C is high. The incorporation of these monomers in NREP contributes to higher T_g of this polymer. NREP polymer can be stored at higher temperature and can withstand higher processing temperatures normally employed in process like coating, spray drying etc. Thus in addition to effective taste masking, immediate release, NREP offers better processing attributes.

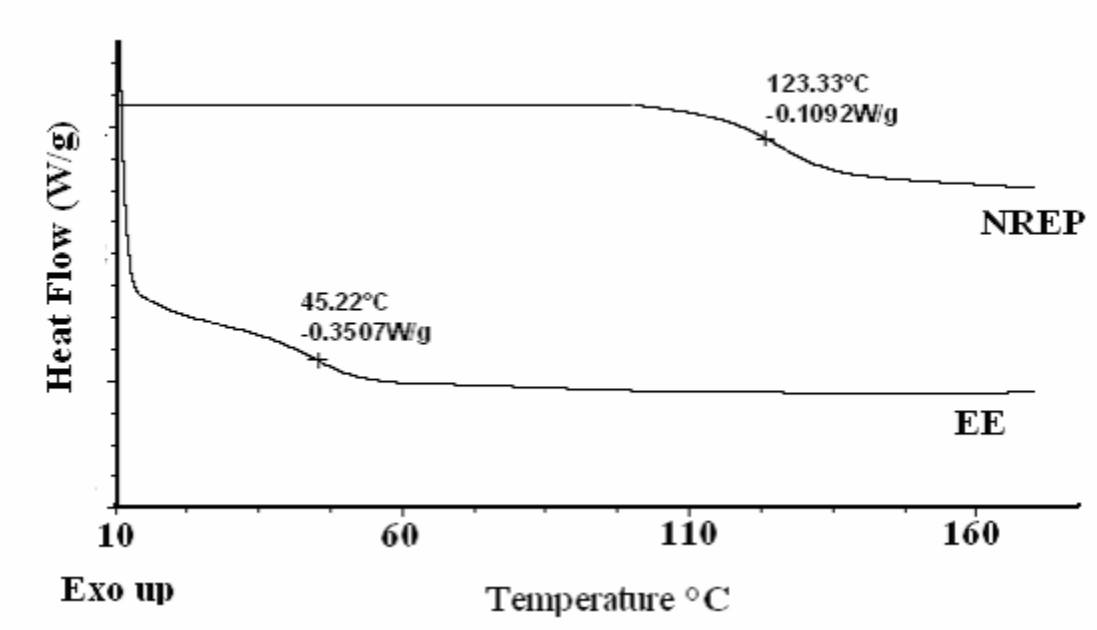

Fig.5.3. Glass transition temperatures for NREP and Eudragit E.

5.3.2.2. Study of interaction between CA -NREP

The physical mixture of CA and NREP shows a sharp endotherm at 69.15°C corresponding to CA as seen in **Fig. 5.4**. Thus characteristics of CA are retained in the physical mixture. The CA-NREP blend prepared by evaporation of the solvent shows the endotherm at 69.45°C corresponding to CA (**Fig.5.4**). The CA-NREP blend does not show the presence of higher melting form or the crystalline form. The characteristic endotherm of CA is found in both the physical mixture and also CA-NREP blend prepared by solvent evaporation. This indicates absence of interaction between CA and NREP.

The DSC curve for physical mixture as well as blend of CA-NREP shows T_g of the polymer at 108°C. The T_g of NREP is lowered by 15°C. Holgado et al., showed that Ephedrine complex with Eudragit L resulted in a fall in T_g of Eudragit L due to the plasticization of the polymer. The presence of small drug molecules between adjacent polymer segments results in an increased segmental mobility. This causes the shift in the polymer T_g to a lower value [57]. Takka, [7] also reported that drug polymer complexation in the system sodium carboxy methylcellulose (NaCMC) and Propranolol hydrochloride, resulted in a fall in T_g of NaCMC from 130.9 to 127.2°C.

5.3.2.3. Study of interactions between CA–EE

The scans for physical mixture show the features for both CA and EE. The characteristic endotherm corresponding to CA at 71.4°C is seen in **Fig. 5.5**. The T_g of the polymer in the mixture is identical to that of neat EE. The endotherm corresponding to higher melting or crystalline form is not seen. The physical mixture of EE and CA does not exhibit any interaction between the two.

The DSC scan for the blend differs from that for physical mixture in two aspects; 1) endotherm corresponding to CA is absent 2) the T_g of EE has shifted to a higher value. Often the disappearance of the DSC endotherm is indicative of the strong interaction. However it does not necessarily imply an incompatibility and further analysis to establish the same is required [48].

The DSC scan of CA-EE blend shows a shift in T_g of the polymer from 45.3°C to 90.5°C. This indicates a strong interaction between the CA and EE. The interactions between the drug and polymer are known to affect the T_g of the polymer [7]. The deviation from the ideal behavior is based on the degree of intermolecular interaction between the individual components in the blends [58]. If the interaction between the drug and polymer is strong then there is an increase in the T_g due to loss of the chain mobility in polymer [7, 47]. The characteristic endotherm for Cefuroxime axetil is retained in physical mixture of CA-EE, CA-NREP and CA-NREP blend indicating the absence of drug-polymer interaction. The T_g of NREP is 123.3°C. The value for the physical mixture as well as blend with CA is 108°C, which indicates plasticization by drug. The T_g of EE in CA-EE physical mixture is same as that of the neat polymer. In contrast the T_g is increased by almost 50°C when blended with CA. In subsequent sections we show that Cefuroxime axetil is converted to Cefuroxime in the presence of EE. The interaction between the dimethyl amino group in the polymer and the carboxylate of Cefuroxime results in the loss in the mobility of the polymer chain, leading to increase in T_g.

Takka, 2003 [7] investigated interactions between propranolol and Eudragit L and S. The characteristic endothermic peak of Propranolol hydrochloride was not found in complexes with polymers Eudragit S and L. The shift in T_g of the Eudragit L and S to a higher value was attributed to interaction between propranolol and the polymers. Holgado et al.[47] reported similar results for interaction between Carteolol and Eudragit L. The endothermic peak for Carteolol was absent in the thermogram for complex with Eudragit L. The T_g of polymer was found to increase by 30°C in the complex. The disappearance of the characteristic endothermic peak of Carteolol indicated an interaction between the drug and the polymer and a change in the physicochemical properties of complex as compared to the physical mixture.

CA-EE blends are also discolored during the process indicating the interaction between the two. Zajac et al. [59] reported similar observations. However this in itself is not an indication of drug polymer incompatibility. Verma and Garg, [5] reported color change for glipizide in presence of meglumine. The DSC results indicated an interaction between glipizide and lactose, meglumine and TRIS buffer. Further detailed

characterization of glipizide–excipient blends by FTIR and HPLC indicated absence of degradation products. Thus discoloration was a result of interaction between the excipient rather than the between drug and excipient. Similarly, Malan et al. [60] demonstrated interaction between niclosamide and excipients using DSC analysis. Yet this did not lead to incompatibility as shown by HPLC analysis. Since the nature of the interactions cannot be established by thermograms, CA–NREP and CA–EE blends were further characterized by FTIR, ^{1}H NMR and HPLC.

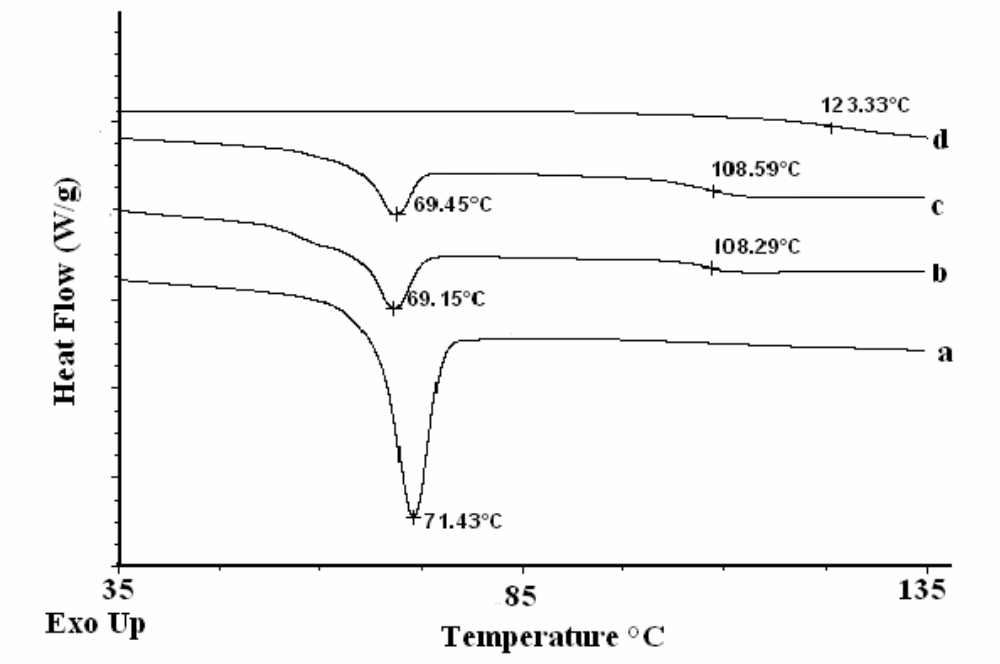

Fig.5.4. DSC thermograms for Cefuroxime axetil and NREP blend: Cefuroxime axetil (a); physical mixture Cefuroxime axetil –NREP (b); Cefuroxime axetil – NREP blend (c) and NREP (d).

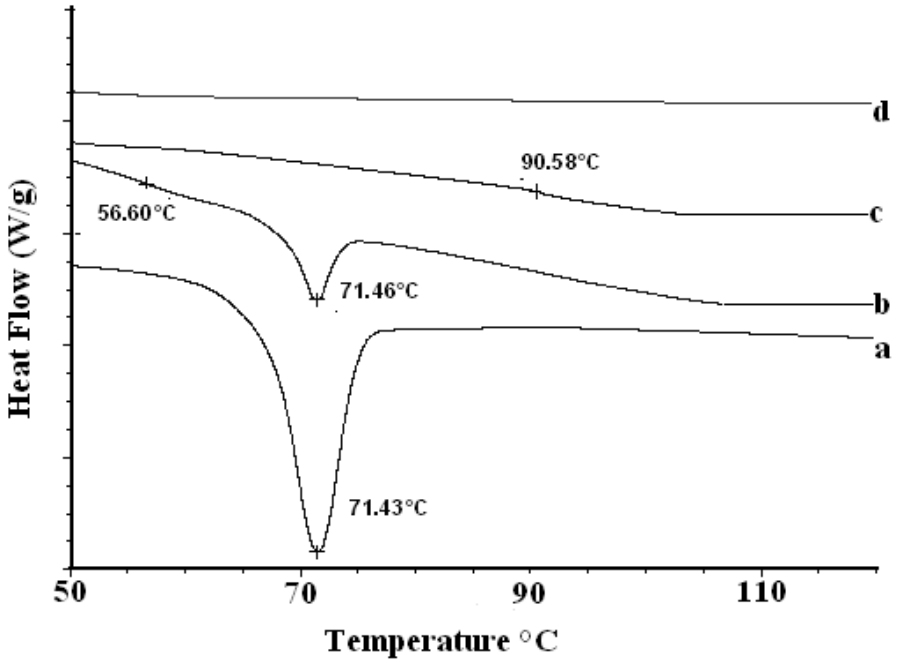

Fig.5.5 DSC thermograms for Cefuroxime axetil and Eudragit E blend: Cefuroxime axetil (a); physical mixture Cefuroxime axetil–Eudragit E (b); Cefuroxime axetil – Eudragit E blend (c) and Eudragit E (d).

5.3.3. FTIR spectroscopy

FTIR is a useful tool for analyzing the interactions in the drug-polymer blends and provides valuable information at the molecular level [58]. Drug polymer interaction results in the generation of additional bands or alteration in the band position and band broadening compared to the spectra of pure drug and polymer [6]. The drug polymer interaction could be caused by redox reaction, acid-base reaction, hydrolysis or combination of these and manifested in change in solubility, phase transition, polymorphic transition, and bioavailability etc [12].

The common inactivation associated with CA is conversion to Cefuroxime, Δ-2 isomer and anti isomers [61]. The conversion of CA to Cefuroxime occurs by conversion of 1-acetoxyethyl ester group at C_{13} position to carboxylic acid. The C-O, C-O-H and O-H vibrations are highly characteristic of carboxylic acids. The hydroxyl group in carboxylic acids forms stable dimeric hydrogen bonded structures with the

carbonyl group. The characteristic bands for the carboxylate functionality are seen in the region 1610-1550 cm^{-1}. A characteristic broad feature in the range 3300-2500 cm^{-1} and an absorption close to 2600 cm^{-1}, is observed for the hydrogen bonded O-H of most carboxylic acids. The hydrogen bonding results in significant band broadening and lowering in absorption frequency. The extent of this is a function of degree and strength of the hydrogen bonding [62].

In the present investigation the CA-NREP and CA –EE blends were studied by FTIR analysis and evaluated for following changes reflecting an interaction;1) generation of new bands 2) hydrogen bonding 3) band broadening and shifts.

5.3.3.1. FTIR spectra of CA, NREP and EE

The **Figs. 5.6, 5.7 and 5.8** show FTIR spectra for CA, NREP and EE. The peak assignment for CA is as follows IR (KBr, cm^{-1}): 3480-3210 (NH, NH_2 complex N-H stretch for primary and secondary amine at C_{11} and C_7 position); 1783 (β lactum); 1729 (C=O, C_{13}, C_{17} position CA); 1683 and 1535 (amido, C_7 position CA); 1729 and 1595 (carbamate, C_9 position CA); 1075-1010, 1156 (C-N stretching, C_{11}, C_{21} position CA); 1377 (C-N stretching, β lactum ring); 592 cm^{-1} (S-C, β lactum ring). These are in agreement with those reported in the literature [28, 30, 35].

The peak assignment for NREP is as follows IR (KBr, cm^{-1}): 1719 (C=O, ester); 2839 - 2992 (Methyl C-H asym / sym stretch); 1448 -1482 (Methyl C-H asym / sym bend); 1190-1270 (C-O stretch); 1558-1601 (aromatic ring stretch); 1388 (aromatic tertiary amine C-N)

The peak assignment for EE is as follows IR (KBr, cm^{-1}): 2949 – 2874 (Methyl C-H asym / sym stretch); 2821- 2770 (methylamino, N- CH_3, C-H stretch); 1728 (C=O, ester); 1454 (Methyl C-H asym / sym bend); 1273 -1240 (C-O stretch); 1149 (Aliphatic amine C-N stretch; C-O stretch, ester). The peaks assigned are comparable to those assigned by Lin et al.[53].

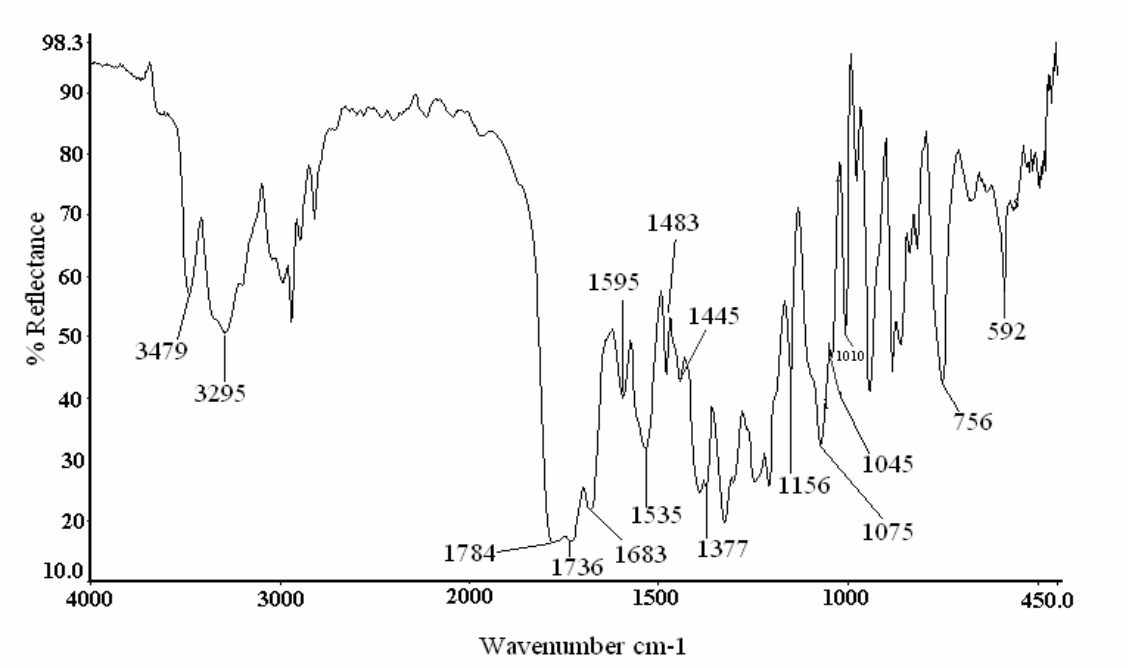

Fig.5.6. FTIR spectrum of Cefuroxime axetil in the range of 4000-450 cm^{-1}.

5.3.3.2. Study of CA-NREP interactions

Fig. 5.7 shows FTIR spectra for the physical mixture and blends of CA and NREP. The IR spectrum for CA-NREP physical mixture is additive in nature and exhibits absorption frequencies corresponding to CA and NREP at the respective wave numbers. The spectrum does not show any additional new bands, band broadening and alteration in frequency. This indicates that there is no interaction in the solid state between the two. The DSC results reported in the previous section showed that CA endotherm was retained in physical mixture indicating that drug was stable and that there is no interaction with the polymer. The FTIR analysis confirms this.

The CA-NREP blend was evaluated for interactions between the drug and polymer in presence of organic solvents. FTIR spectrum of CA-NREP blend is similar to that of CA-NREP physical mixture. The bands corresponding to the carbonyl functionality in the ester groups (C_{13} and C_{17} position in CA structure, **Fig. 5.1**) are intact in CA-NREP blends (as seen at 1729 cm^{-1}). The band for β lactum is retained and seen at 1783 cm^{-1} in CA-NREP blend. No new peak is seen in the region 1610-1550 cm^{-}

^{1} corresponding to carboxylate salt. The spectrum does not show band broadening or shift characteristic for hydrogen bonding. The interaction between anionic and cationic moiety has been studied in the past. Moustafine et al. [64] studied the interaction between cationic Eudragit E100 and anionic Eudragit L100. A strong band corresponding to carboxylate group at 1560 cm^{-1} was seen. The CA-NREP blend does not exhibit these features. This leads us to the conclusion that conversion of CA to Cefuroxime has not taken place in presence of NREP.

All the bands corresponding to the functional groups of CA and NREP are present in the CA-NREP blend. The FTIR study shows that there is no chemical interaction between CA and NREP and CA is physically entrapped in the blend. This is confirmed by the absence of the bands corresponding to carboxylate (1560 cm^{-1}) and hydrogen bonding (3300-2500 cm^{-1}). The DSC analysis showed that the endotherm for CA is retained in the CA-NREP blend indicating absence of interaction between the two. The FTIR analysis thus supports the findings of DSC analysis further.

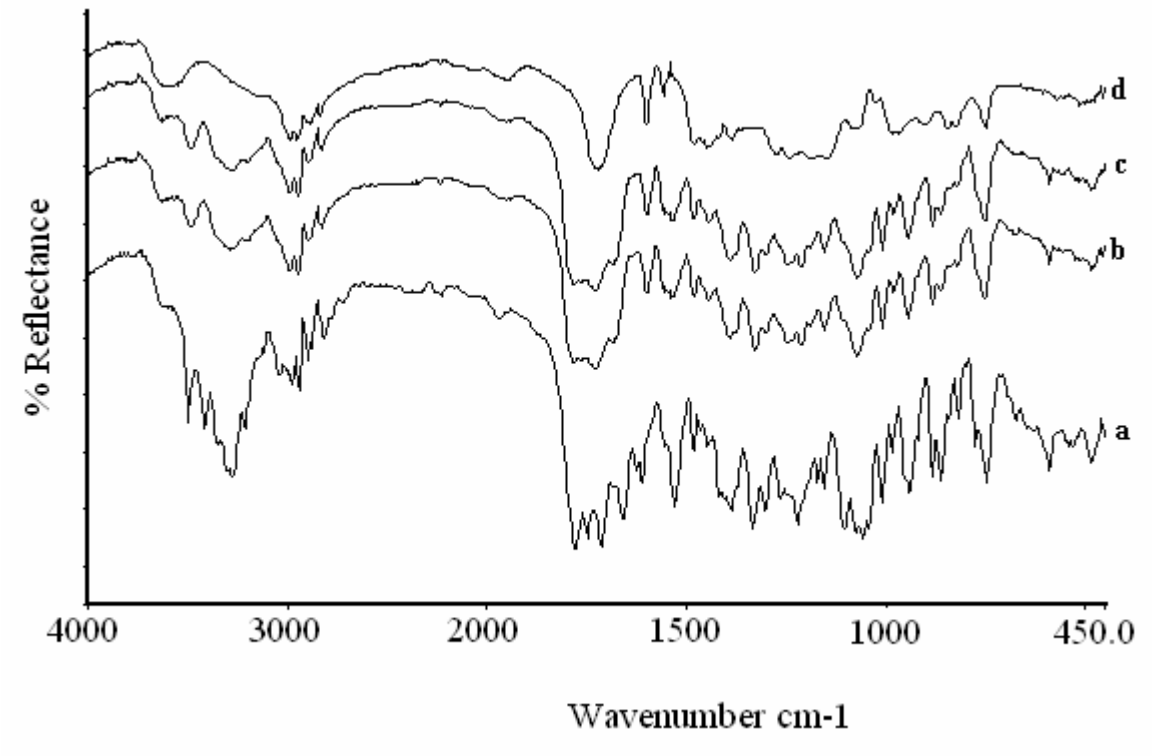

Fig.5.7. FTIR spectra of Cefuroxime axetil and NREP blends: Cefuroxime axetil (a); physical mixture of Cefuroxime axetil-NREP (b); Cefuroxime axetil-NREP blend (c); and NREP (d).

5.3.3.3. Study of interactions between CA-EE

The DSC scans for CA-EE blend showed interaction between CA and EE as exhibited by absence of endotherm for CA. The samples for blends and physical mixture were further analyzed by FTIR to investigate the nature of interaction at molecular level. The FTIR spectra for CA- EE physical mixture and CA-EE blend are seen in **Fig. 5.8**.

The physical mixture of CA-EE showed bands corresponding to both CA and EE. Band broadening is observed in the region 3200 to 3400 cm^{-1}. This indicates hydrogen bonding between the two. The spectrum does not show appearance of new bands in the region 1550-1600 cm^{-1}, corresponding to carboxylate group. This shows that CA is not transformed into Cefuroxime in physical mixture. This leads to the conclusion that physical mixture of CA-EE does not show any incompatibility. The DSC results too had shown the presence of endotherm corresponding to CA.

The FTIR spectrum of CA-EE blend showed some significant differences as compared to the physical mixture of CA-EE (**Fig. 5.8**). The major spectral change observed was appearance of new band and broadening. The other changes observed were lowering of band intensity and a shift to lower absorption frequencies. A new band appears at 1561 cm^{-1} (**Fig. 5.8**) in CA-EE blend. CA converts to Cefuroxime in presence of EE and the band at 1561 cm^{-1} is assigned to interaction between dimethylamino groups of EE and carboxylate groups from Cefuroxime, generated as a degradation product in presence of EE. Similar findings for interaction of cationic or anionic polymer with oppositely charged drug and polymer have been reported in the past. Takka, 2003 [7] observed a new absorption band between 1556-1550 cm^{-1} due to carboxylate salt formation, resulting from drug polymer interaction in the complexes of cationic drug Propranolol hydrochloride and anionic polymers Eudragit L and Eudragit S respectively. Sarisuta et al. [12] reported the presence of bands corresponding to carboxylate in the region 1550-1560 cm^{-1}. The carboxylate bands were attributed to the protonation of amine groups in erythromycin molecule by the carboxylic groups of Eudragit L 100. Moustafine et al. [65] reported similar findings for polyelectrolyte

complex of EE–sodium alginate wherein the carboxylate-groups of alginate form ionic bonds with dimethylamino groups of EE.

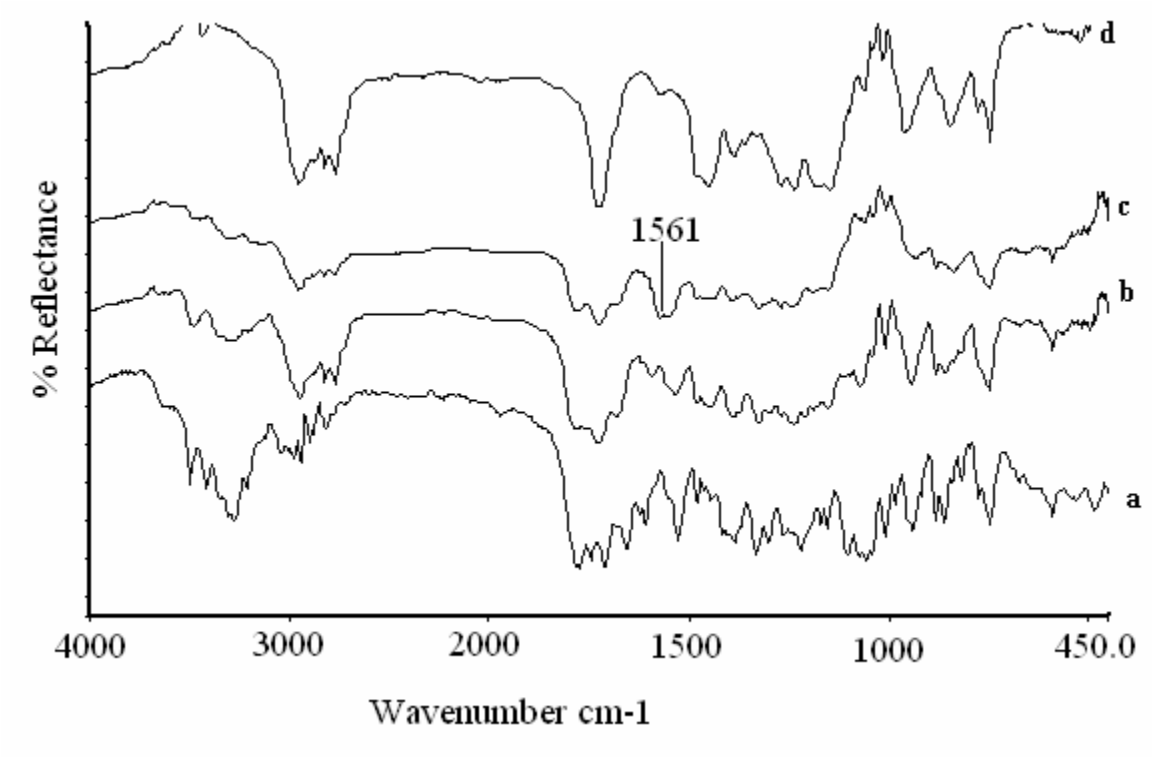

Fig. 5.8. FTIR spectra of Cefuroxime axetil (a); physical mixture of Cefuroxime axetil-Eudragit E (b); Cefuroxime axetil-Eudragit E blend (c); and Eudragit E (d).

The spectrum for CA-EE blend shows band broadening in the region 2400-2600 cm^{-1}. This band broadening is a result of interaction between dimethylamino groups of EE with the carboxyl groups of Cefuroxime obtained as degradation product of CA. This feature is common for hydrogen bonded carboxylic acids [62]. Moustafine et al. [64] observed a significant band broadening at 2548 cm^{-1} due to interaction between dimethylamino groups of EE and the carboxyl groups of EL100. Similar band broadening was observed at 2720, 2510 and 2480 cm^{-1} in the polyelectrolyte complex between cationic EE and anionic sodium alginate [65]. CA-EE blend shows significant band broadening and lowering of the absorption intensity in the region of 3200-3400 cm^{-1}. These findings indicate intermolecular hydrogen bonding between dimethylamino

groups of EE and carboxyl group of Cefuroxime. This also suggests the conversion of CA to Cefuroxime.

There is a significant lowering in the intensity for the band corresponding to the carbonyl group (1729 cm^{-1}) in the CA-EE blend as compared to that seen in EE and physical mixture of CA-EE. The absorption intensity for β lactum at 1783 cm^{-1} is significantly reduced in CA-EE blend. This frequency is unaltered in the CA-EE physical mixture. The position and intensity of the bands at 2821 and 2770 cm^{-1} in CA-EE blend, due to dimethylamino groups in EE has reduced. Moustafine et al. [65] reported that the ratio of the bands at 2773 and 2824 cm^{-1} had significantly changed due to interaction of EE and Eudragit L. Tatavarti et al. [66] too reported significant reduction in intensities for Verapamil hydrochloride formulation in presence of Eudragit L 100-55 and absence of bands (2250-2800 cm^{-1}) corresponding to Verapamil. The interaction between Verapamil hydrochloride and Eudragit L 100-55 resulted in brown coloration and retardation in drug release. In the present investigation the CA–EE blend turned brown in color. The overall intensities for the functional groups in CA-EE blend are greatly reduced in comparison to the CA-EE physical mixture. This confirms an interaction between EE and CA.

The FTIR spectra of CA-EE blend indicate the formation of Cefuroxime as a degradation product. The DSC scans had exhibited complete absence of the endotherm for CA in CA-EE blend indicating an interaction. The FTIR explains the reasons for incompatibility between the CA and EE. In contrast no such degradation was observed in CA–NREP blends. This has been further validated by ^{1}H NMR and HPLC analysis discussed in subsequent sections.

5.3.4. ^{1}H NMR spectroscopy

The bioavailability of the drug is directly related to its structure and physical state. The DSC and FTIR studies have confirmed interaction between CA and EE but the lack of it in the system CA-NREP. The interaction between the CA-EE and CA-NREP in presence of solvent was determined by ^{1}H NMR spectroscopy. The ^{1}H NMR

spectra of CA-EE and CA-NREP blend were evaluated for the signals corresponding to protons associated with 1-acetoxyethyl group attached to Cefuroxime.

5.3.4.1. ^{1}H NMR of CA, NREP and EE

The spectra for CA, EE, NREP, CA-EE blend and CA-NREP blend are shown in **Fig. 5.9 and 5.10**. The signals for ^{1}H NMR spectrum of CA are assigned as follows: ($CDCl_3$, ppm): 1.5 δ (d, 3H) for CH_3 at C_{19} position; 2.14 δ (d, 3H) for CH_3-CO-O group at C_{18} position; 3.45~3.63 δ (dd, 2H) for protons at C_2 position of the β lactum; 4.04 δ (s, 3H) for the N-O-CH_3 attached at C_{22} position; 4.7~4.9 δ (m, 2H) proton at C_9 position; 5.02~5.04 δ (m, 1H) proton at C_6 position; 5.04~5.07 δ (m, 1H) proton at C_9 position; 5.93 δ (m, 1H) proton at C_7 position; 6.44~6.45 δ (m, 1H) protons in the furan ring; 6.8~6.85 δ (m, 1H) protons in the furan ring; 6.9~7.1 δ (m, 1H) proton at C_{15} position; 7.47~7.48 δ (d, 1H) protons in the furan ring; 7.5~7.52 δ (d, 1H) proton of N-H group; signal at 2.07 δ indicates acetone solvent. Yoon et al. [30] reported similar assignments for the ^{1}H NMR of CA.

The signals for ^{1}H NMR spectrum of NREP are assigned as follows: ($CDCl_3$, ppm): 8.43 δ (2H) protons adjacent to nitrogen of 4 vinyl pyridine in aromatic ring; 7.03 δ (2H) adjacent to nitrogen of 4 vinyl pyridine in aromatic ring; 4.11 δ (2H) protons for CH_2 group in HEMA; 3.84 δ (2H) protons for CH_2 group in HEMA; 3.61 δ (3H) protons for OCH_3; 2.96 δ (1H) of CH methine group; 2.01 δ (OH) protons of C_2H_4-OH; 1.5~2.0 δ (2H) protons for CH_2 backbone in polymer chain; 0.8~1.2 δ (3H) of CH_3 group; signal at 2.17 δ indicates acetone solvent.

The signals for ^{1}H NMR spectrum of EE are assigned as follows: ($CDCl_3$, ppm): 4.07 and 3.95 δ (2H) protons for OCH_2 group; 3.59 δ (3H) protons for the -OCH_3; 2.96 and 2.89 δ (2H) of CH_2 backbone; 2.41 and 2.56 δ (1H) for CH methine group; 2.28 δ (6H) protons for CH_3 of methylamino group; 1.9~1.6 δ (2H) for CH_2 backbone in polymer; 1.4~1.2 δ (3H) methyl group; 1~0.8 δ (3H) protons for the terminal CH_3 for butyl methacrylate moiety. The signal at 2.17 δ ppm indicates acetone solvent.

5.3.4.2. Study of interactions between CA-NREP

The ^{1}H NMR for the CA–NREP blend (**Fig. 5.9**) is additive in nature and shows presence of signals corresponding to the protons of neat CA and NREP respectively in the blend. The spectrum does not show additional signals in the blend indicating the absence of interaction between the two. The signals corresponding to protons at C_{15}, C_{18} and C_{19} position of the 1-acetoxyethyl group in CA appear in the CA-NREP blend at the same position as seen in spectrum of CA. The signal at 2.14 δ (d, 3H) for CH_3-CO-O group at C_{18} position of CA is retained in CA-NREP blend. The signal at 1.5 δ (d, 3H) for CH_3 at C_{19} position is seen at 1.55 δ in CA-NREP blend. The signals due to proton at C_{15} position in CA appear at 6.9~7.1 δ (m, 1H). The spectrum confirms the presence of the 1-acetoxyethyl group in CA in presence of NREP. This confirms that CA has not transformed to Cefuroxime in presence of NREP. The ^{1}H NMR of CA-NREP shows the presence of signals corresponding to the protons for rest of the CA structure.

The protons in the furan ring of CA appear as three multiplets at the same position in CA-NREP blend. The signals at 3.45~3.63 δ (dd, 2H), for protons at C_2 position of the β lactum ring in CA are merged with signal for OCH_3 of NREP at 3.6 δ. The signals at 4.07 δ (3H) corresponding to protons of (N-O-CH_3) and 5.98 δ for protons at C_7 position are retained in the CA-NREP blend at the same position as seen in CA spectrum. The signal for proton at 6th position of the β lactum ring and for a proton at C_9 position appeared at 5.08 δ (1H+1H) and 4.87 δ (1H) as seen in the spectrum of CA.

The CA-NREP spectrum shows signals for the protons found in the 1-acetoxyethyl group of CA. From the FTIR analysis the absence of carboxylate salt was confirmed. The ^{1}H NMR analysis further substantiates that CA is not degraded to Cefuroxime in presence of NREP.

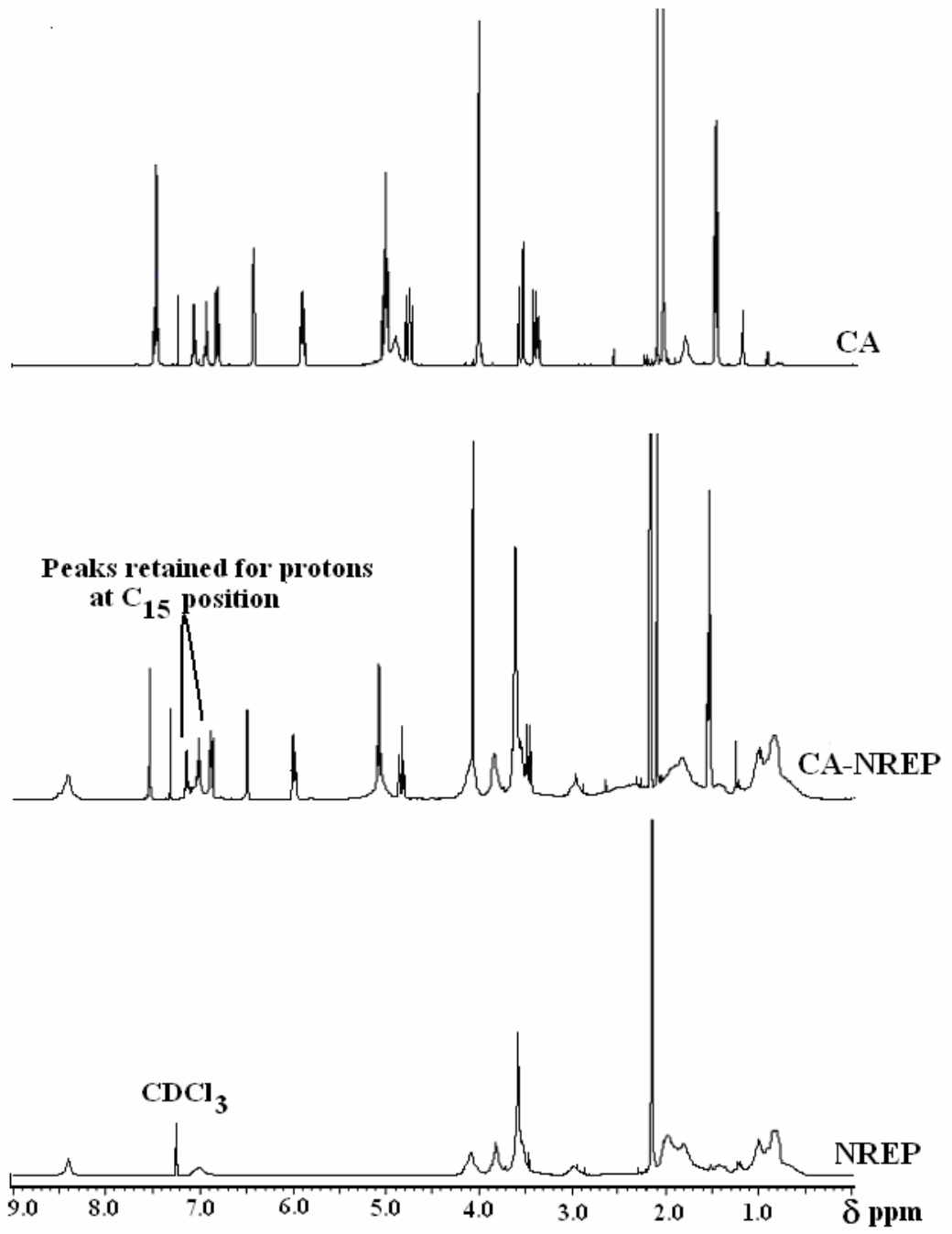

Fig.5.9. NMR spectra for Cefuroxime axetil and NREP blends; NREP; CA-NREP, CA, Cefuroxime axetil.

5.3.4.3. Study of interactions between CA-EE

The FTIR analysis showed the conversion of CA to Cefuroxime, which was evident from the appearance of bands corresponding to carboxylate salt. Cefuroxime has the same skeletal structure as CA, and contains "COOH" group at C_{13} position rather than the 1-acetoxyethyl group. So it is expected that if the major degradation product of CA in presence of EE is "Cefuroxime" then the ^{1}H NMR should show the features common for Cefuroxime structure except for the "1-acetoxyethyl ester" substitution at C_{13} position of CA. Stoeckel et al. [67] analyzed the degradation product Cefuroxime, obtained by exposure of CA to phosphate buffer. The peaks assigned for Cefuroxime were 3.44 and 3.71 δ for protons at C_2 position (CH_2), 4.02 δ for protons in N-O-CH_3 group, 4.69 and 4.88 δ for protons at C_3 position (-CH_2) and 5.25 and 5.83 δ for protons at C_6 (CH) and C_7 (CH) positions respectively. The three multiplets at 6.65, 6.92, and 7.71δ were assigned to three hydrogens of the furane ring.

The ^{1}H NMR of CA-EE blend (**Fig. 5.10**) shows peaks corresponding to (3H) for (N-O-CH_3) group at 4.05δ. The peak corresponding to the protons at the C_2 position of the β lactum ring at 3.45 and 3.6 δ has merged with the signal for OCH_3 of EE at 5.9δ. The signals for protons at C_6, C_7 and C_9 position appear at same position as CA. New signals appear at position 4.47, 4.60 and 4.65 δ suggesting the formation of new species due to the interaction between two. Additional new signals have been detected at 5.29, 5.35, 5.75, 7.63 and 7.74 δ. We have not attempted assignments of these new signals. The protons in the furan ring of CA appear as three multiplets at 6.48, 6.87 and 7.51 δ and are retained in the CA-EE blend. The peak height of signals due to proton at C_{15} position of the 1-acetoxyethyl ester moiety is significantly reduced from 0.65 and 0.06 in CA to 0.011 and 0.007 respectively in CA-EE blend. This indicates the change in the structure of 1-acetoxyethyl group at C_{13} position in CA structure. The peak height of signal at 2.10 δ due to the protons (3H) at C_{18} position in CH_3-CO-O group of CA is significantly reduced from 0.99 in CA to 0.244 in presence of EE. The signals due to protons (3H) of the methyl group at C_{19} position show a shift from 1.56 to 1.52δ. However the position of this signal is retained at 1.56 δ in case of CA-NREP blend.

The ^{1}H NMR study shows that the signals due to the protons at C_{15} position in 1-acetoxyethyl group in CA are altered in CA-EE blend. The ^{1}H NMR shows the generation of additional signals, not observed in the neat EE and CA. This confirms the degradation of CA in presence of EE, signifying the incompatibility between the two.

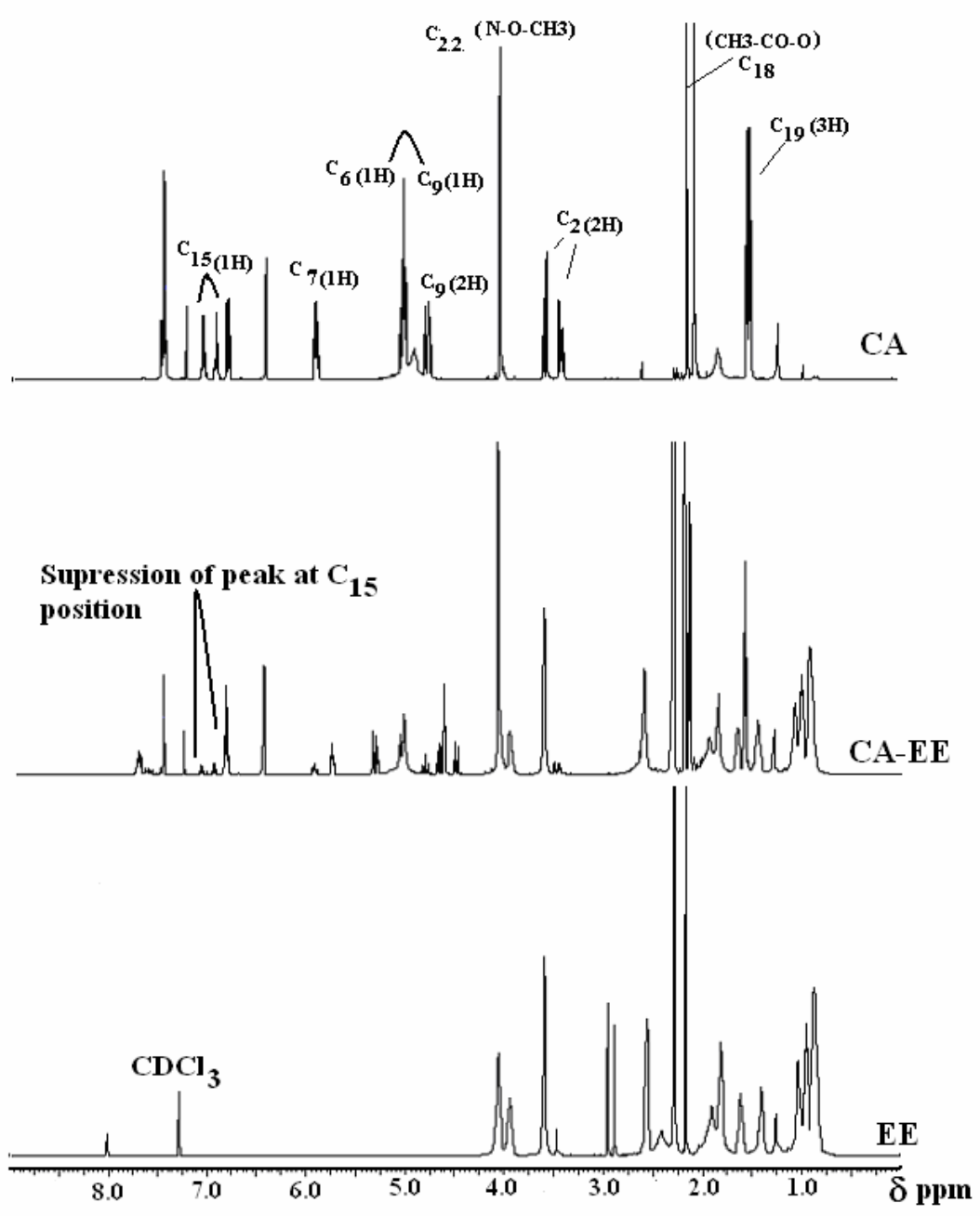

Fig. 5.10. NMR spectra for Cefuroxime axetil and Eudragit E blends EE, CA-EE, CA.

5.3.5. HPLC analysis

The stability and kinetics of degradation of CA has been studied by HPLC in the past [59, 61, 68-70]. The common degradation products identified are Δ-2 isomer, Cefuroxime, alpha, beta sulphoxides and anti isomers. The CA anti isomers are inactive against β lactamases. These geometrical isomers of CA have been separated by HPLC in the past [71]. Lorenzo-Lamosa et al. [17] showed that the main impurities were Cefuroxime and Δ-2 isomer. The inactivation of CA in presence of EE was ascribed to the interaction of the anionic drug with cationic polymer. Cuna et al. [18] reported that CA is unstable in presence of CAT and leads to generation of Cefuroxime, Δ-2 isomer and β sulphoxide. The content of Δ-2 isomer was very high.

The compendial requirements for CA are summarized below. The ratio of diastereoisomer A to the sum of diastereoisomer A and B (rA / rA+rB) should be between 0.48 to 0.55 and the resolution between the diastereoisomer A and B should not be less than 1.5. The Cefuroxime content should not be more than 0.5%, the Δ-2 isomer should not be more than 1.5%, anti Cefuroxime not more than 1.0 %, none of the individual impurity should be more than 0.1% and the total impurity should not be more than 3% (USP, 1995). The degradation of CA in presence of EE and NREP was studied by comparing the chromatograms of reference standard and working standard samples.

5.3.5.1. Method validation: CA

The mobile phase used was as per USP 23, (1995) but the flow rate was adjusted to 1 ml/min for system suitability. The reference standard and working standard were injected and the separation of diastereomer A and B was achieved. The resolution for diastereomers A and B was not less than 1.5 for the reference and working standard (**Fig. 5.11**). The ratio rA/ rA+rB was 0.51 and 0.52 for the reference and working standard respectively. This value for the working standard obtained in present estimation matched with the value reported in certificate of analysis given by Lupin Laboratories Ltd.

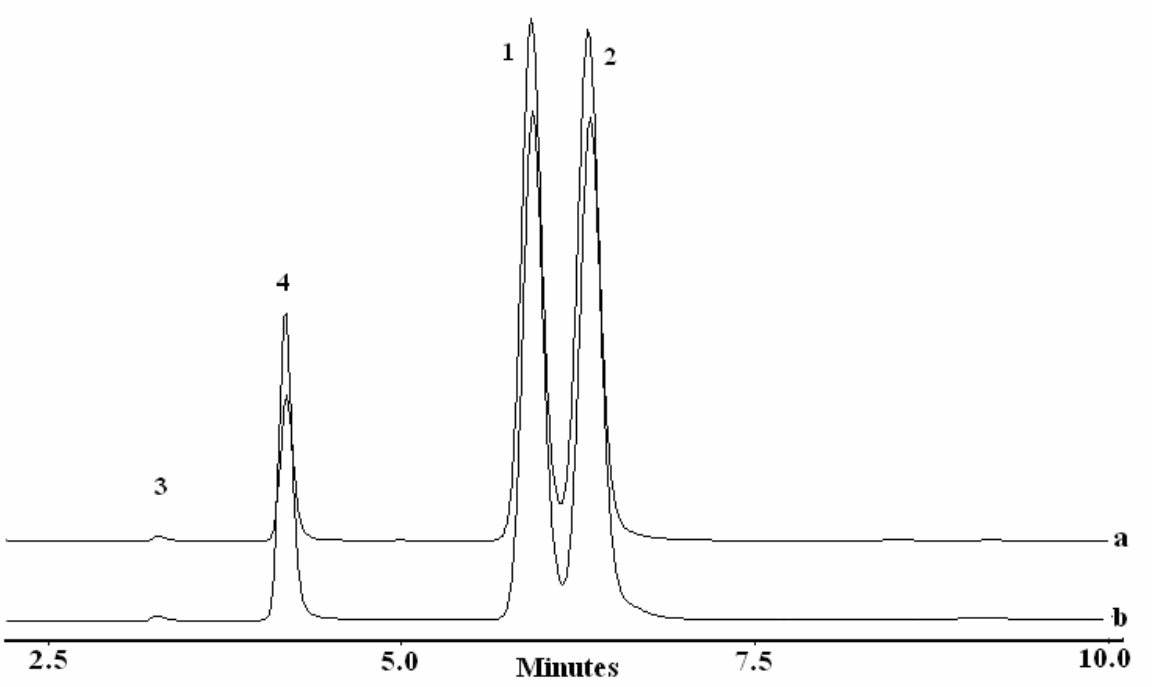

Fig.5.11.Chromatogram of Working standard (a) and Reference Standard (b) of Cefuroxime axetil: (1) Cefuroxime axetil isomer B; (2) Cefuroxime axetil isomer A; (3) Cefuroxime; (4) Acetanilide- internal standard.

5.3.5.2. Study of interactions CA-EE

The objective of our investigation was to identify degradation products and compare this data to interpret the nature of interaction if any between NREP and CA *vis a vis* EE. The chromatogram for physical mixture of EE and CA is significantly different than the chromatogram for CA (**Fig. 5.12**). The resolution between the diastereomer A and B has reduced to less than 1.5. The Cefuroxime content has doubled for the physical mixture in comparison to the neat CA. The resolution, % impurity and the diastereomer ratio are shown in **Table 5.1**. The Δ-2 isomer has appeared in CA-EE physical mixture, which was absent in the neat CA sample. The anti isomers are also seen in the chromatogram (**Fig.5.12**).

The CA-EE blend shows complete degradation of CA in presence of EE. The major degradation products are Cefuroxime and Δ-2 isomer. These findings are similar to those of Lorenzo-Lamosa et al. [17]. The peaks at retention time 3.11, 4.06, 4.58 and

4.93 correspond to other impurities generated. The other major degradation products are alpha sulphoxide and anti isomers (**Fig. 5.12**). The Cefuroxime content in CA-EE blend is more than 0.5 % and the resolution between the diastereomers falls from 0.973 in the physical mixture to 0.814 in blend. The ratio rA / rA+rB has reduced to 0.47 in CA-EE blend from 0.53 as seen in the physical mixture. Many other impurities have been generated as seen in the chromatogram.

Table 5.1 Compatibility between CA – NREP and CA-EE by HPLC analysis

Sample	**Resolution**	**$\frac{rA}{rA+rB}$**	**Cefuroxime %**	**Sulphoxide**	**Δ-2 isomer**
Reference std	1.67	0.51	0.34	$\alpha=2.6 \times 10^{-3}$ $\beta=2.1 \times 10^{-3}$	----
Working std	1.51	0.52	0.35	$\alpha= 9 \times 10^{-4}$ $\beta=2.1 \times 10^{-3}$	----
CA-EE physical mixture	0.97	0.53	0.47	$\alpha=1 \times 10^{-3}$ $\beta=2.4 \times 10^{-3}$	0.41
CA-EE blend	0.81	0.47	0.5	$\alpha= 0.12$	0.42
CA-NREP physical mixture	1.63	0.54	0.34	$\alpha=2.8 \times 10^{-3}$ $\beta=1.3 \times 10^{-3}$	----
CA-NREP Blend	1.66	0.54	0.34	$\alpha=2.6 \times 10^{-3}$ $\beta=1.5 \times 10^{-3}$	----
CA-NREP Blend after aging	1.64	0.55	0.46	$\alpha=1.1 \times 10^{-3}$ $\beta=7.8 \times 10^{-4}$	-----
CA - DMAEMA	0.91	0.58	0.54	$\alpha= 2.7 \times 10^{-3}$ $\beta=2 \times 10^{-3}$	0.11
CA - 4-VP	1.67	0.52	0.36	$\alpha= 1.9 \times 10^{-3}$ $\beta=1.3 \times 10^{-3}$	------

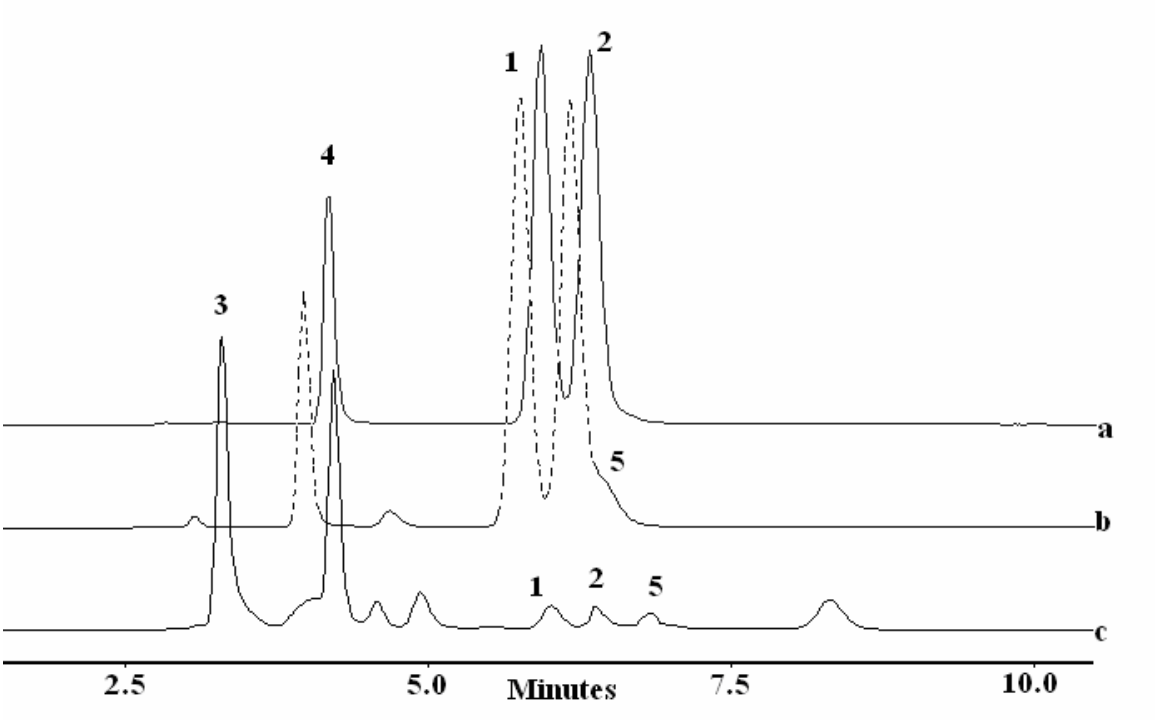

Fig. 5.12. Chromatogram of Cefuroxime axetil (a), physical mixture of Cefuroxime axetil –Eudragit E (b) and Cefuroxime axetil-Eudragit E blend (c): (1) Cefuroxime axetil isomer B; (2) Cefuroxime axetil isomer A; (3) Cefuroxime (4) Internal standard: Acetanilide and (5) Δ-2 isomer.

5.3.5.3. Study of interactions between CA-NREP

The chromatogram for CA-NREP physical mixture can be seen in **Fig. 5.13**. The physical mixture of NREP and CA shows a resolution of 1.63 and ratio of rA / rA+rB is 0.54. The Cefuroxime content was found to be 3.4 x 10^{-1} %. The chromatogram shows absence of Δ-2 isomer. The peak for α sulphoxide is seen in chromatogram and corresponds to 0.044 % of impurity. The total impurities generated are < 3 % and individual impurity < 0.1 %. This is within the acceptable limits as per USP, 1995.

The CA-NREP blends were analyzed for the stability of CA in presence of NREP. The blends of CA- NREP showed that resolution between diastereomer A and B

is more than 1.5 and the ratio rA / rA+rB is 0.54, which is acceptable as per pharmacopoeial limits (USP, 1995). The chromatogram for CA-NREP blend shows absence of Δ-2 isomer. This indicates that CA is not converted to its Δ -2 isomer in the presence of NREP. The content of alpha and beta sulphoxide impurities, is minimal, *viz.* 2.66×10^{-3} and 1.52×10^{-3} % respectively. The total content of the impurities is less than 3 % and within the pharmacopoeial limits (USP, 1995). The HPLC data show that CA is stable and does not interact with NREP. The chromatograms for CA-NREP show that the area for diastereomer B is reduced in the presence of NREP. This is seen from the change in the ratio rA / rA+rB from 0.52 for neat CA to 0.54 in presence of NREP. Since the ratio has changed, it was necessary to evaluate if this ratio further changes on aging.

The blends were therefore analyzed after six months. The chromatogram did not show significant deviation from that obtained for the CA-NREP blend after its preparation. The chromatogram did not show significant deviation from that obtained for the CA-NREP blend after its preparation (2 weeks). The chromatogram showed absence of Δ- 2 isomer impurity. It is therefore evident that CA in CA–NREP blends is not converted to Δ-2 isomer even after aging for six months. The content of cefuroxime in CA-NREP blend on aging was increased to 0.46 %. The other impurities generated were less than 1.15×10^{-3} in content. The resolution for aged sample was 1.64 and the ratio rA / rA+rB was maintained to 0.55, which is acceptable as per USP, 1995.

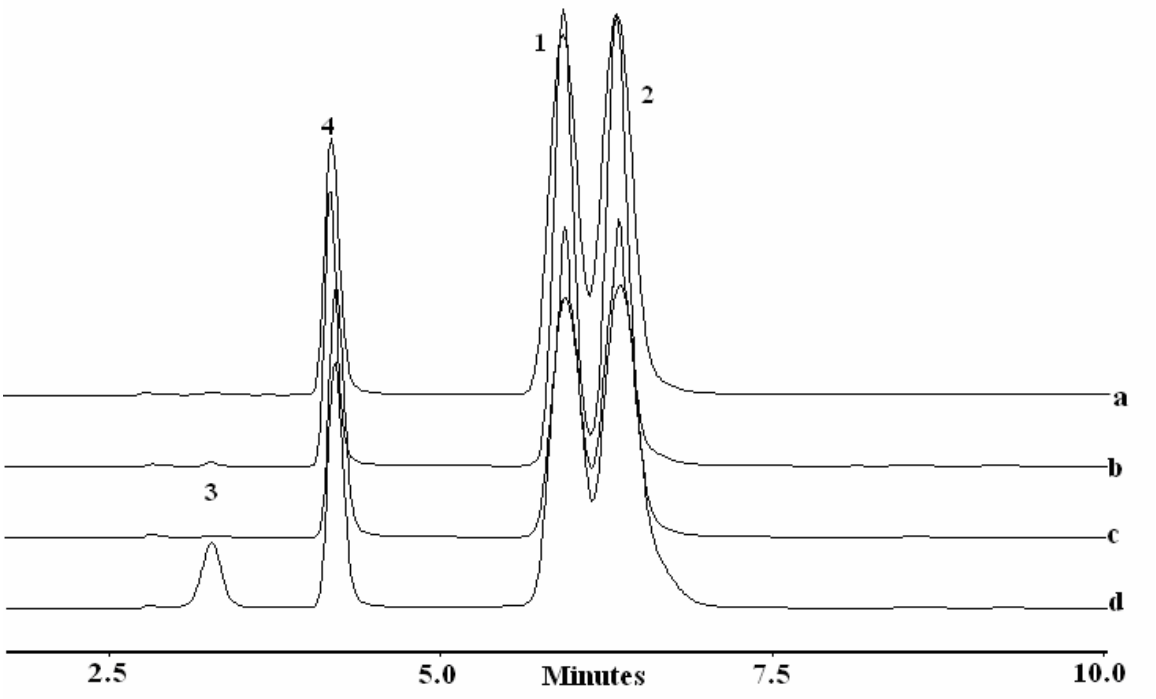

Fig. 5.13. Chromatogram of (a) Cefuroxime axetil working standard; (b) physical mixture of Cefuroxime axetil–NREP; (c) Cefuroxime axetil-NREP blend; (d) Cefuroxime axetil blend on aging here (1) Cefuroxime axetil isomer B; (2) Cefuroxime axetil isomer A; (3) Cefuroxime (4) Internal standard: Acetanilide.

5.3.5.4. Study of interactions between CA and basic monomers

Various analytical methods used in the present investigation revealed that CA is stable in presence of NREP and was degraded in presence of EE. Stability of CA in presence of basic monomers was investigated to confirm if the differences in the behavior of the polymer could be attributed to the differences in the presence of basic monomers 4-VP and DMAEMA. CA and basic monomers were taken in 1:1 ratio in methanol and this solution was used for HPLC analysis after 5-10 min.

The chromatogram for DMAEMA-CA solution is similar to that observed for CA-EE (**Fig. 5.14**). The major impurities observed were Cefuroxime and Δ-2 isomer. The chromatogram reveals generation of many other impurities. The resolution between the diastereomer A and B of CA has come down from 1.51 to 0.91 in presence of DMAEMA. Similar results were obtained for physical mixture of CA with EE and CA-EE blend (**Table 5.1**). The ratio rA/ rA+rB has increased to 0.58. This shows that the DMAEMA interacts with CA and the presence of this functional monomer in EE results in its interaction with CA.

The chromatogram for 4-VP-CA solution in methanol (**Fig. 5.14**) shows the peak for 4-VP at 4.9 min and the peaks corresponding to diastereomer A and B of CA. The content of cefuroxime is same as the working standard (0.34 %). The chromatogram does not show the generation of Δ-2 isomer. The resolution between the two diastereomers is 1.67 and the ratio rA / rA+rB is 0.52. The total impurities generated are negligible and below 3 %. This indicates that CA is stable in presence of monomer 4-VP. The stability of CA in presence of NREP containing 4-VP as functional monomer can be explained on the basis of absence of interaction between CA and 4-VP. The degree of protonation of polymers is proportional to pKa value of monomers. The pK_a value for 4-VP is is low (5.45). The low content of 4-VP in NREP (11 %) and also weak basic nature (pK_a = 5.45) along with self associations between pyridine nitrogen and hydroxyls from HEMA in NREP make it less amenable to interact with CA. Hence CA is stable in presence of NREP.

The degree of protonation of polymers is proportional to pKa value of monomers [72]. The pK_a values for DMAEMA and 4-VP are 8.4 and 5.45 respectively [72-74]. Since the pK_a value of DMAEMA is higher it is more prone to protonation. EE contains approximately 50 % DMAEMA [55]. Park et al. [72] reported copolymers with high DEAEMA content (N, N diethyl amino ethyl methacrylate, pK_a = 9.5) to be positively charged and highly protonated till neutral pH. The high content of functional monomer and the higher pK_a value of DMAEMA lead to protonation of EE up to pH 6. Moustafine et al. [65] reported the formation of polyelectrolyte complex between EE-EL and EE–sodium alginate, where EE is protonated and interacts with other anionic

polymers. In the present investigation highly protonated polymer (EE) of DMAEMA interacts with the anionic drug (CA) resulting in the formation of the carboxylate salt.

Further the content of 4-VP in NREP is only 11.82 % as compared to the content of DMAEMA (50 %) in EE. Since the pK_a value of 4-VP is less than DMAEMA, the degree of protonation of NREP is lower than EE. CA is stable in presence of NREP due to the lower basicity of the polymer as compared to Eudragit.

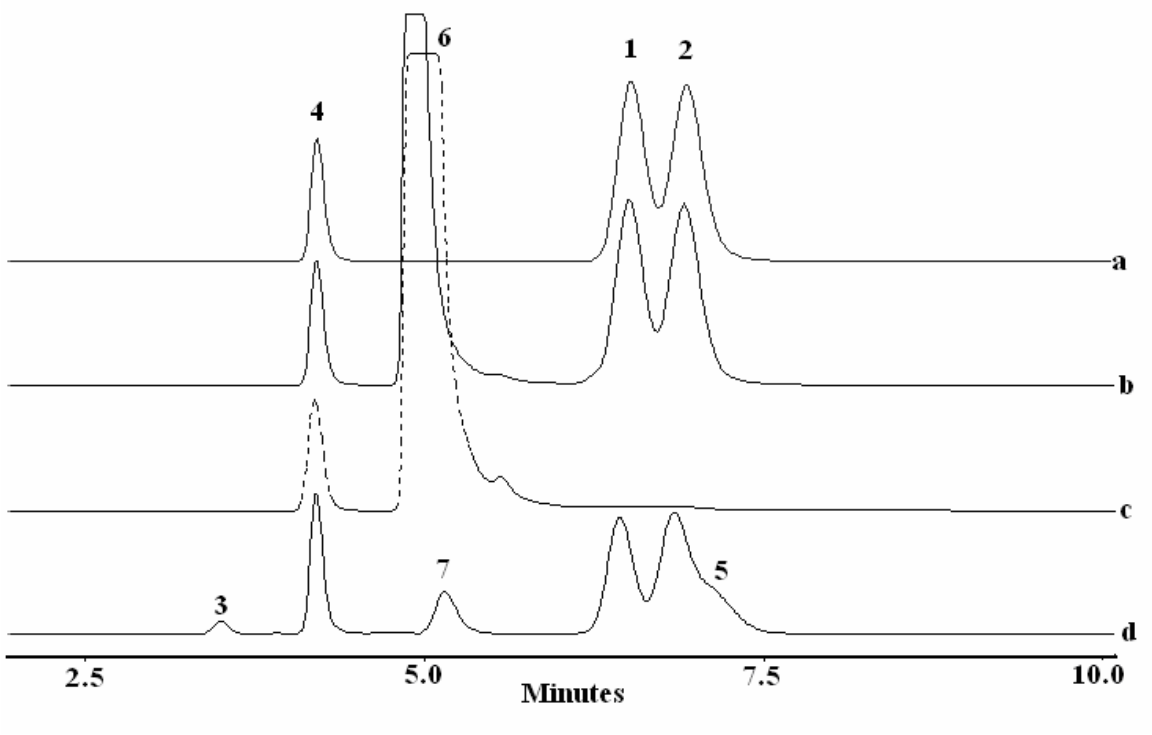

Fig.5.14. Chromatogram of Cefuroxime axetil (a); Cefuroxime axetil-4 vinyl pyridine (b); internal standard-4 vinyl pyridine (c) and Cefuroxime axetil-dimethylamino ethyl methacrylate (d): (1) Cefuroxime axetil isomer B; (2) Cefuroxime axetil isomer A; (3) Cefuroxime; (4) Internal standard: Acetanilide; (5) Δ-2 isomer; (6) 4-vinyl pyridine and (7) impurity.

5.4. CONCLUSIONS

Drug polymer interactions play a critical role in dosage formulation. Interactions between CA and NREP were investigated since CA undergoes polymorphic

transformations as well as gelation which limits its bioavailability and the reverse enteric polymer Eudragit E is known to be incompatible with CA. Physicochemical interactions of Cefuroxime axetil (CA) with Eudragit E (EE) and NREP were evaluated. CA was completely inactivated by EE. A detailed investigation of interactions between CA-EE was undertaken by DSC, FTIR, NMR and HPLC analysis. The FTIR and NMR showed the conversion of CA to Cefuroxime (acid form) due to interaction with EE. The HPLC showed generation of high level of impurities. The major impurities were Cefuroxime, Δ- 2 isomer and sulphoxides. The T_g of Eudragit E was enhanced in the presence of CA. This was due to formation of Cefuroxime resulting due to charge transfer in CA-EE blends causing the rigidisation of the donor chain (EE). These investigations were used as reference in interpreting the interactions between NREP-CA. XRD analysis showed that in presence of NREP, CA is retained in the amorphous form. The DSC analysis shows that the endotherm of CA is retained and that the NREP is plasticized by CA. This was further confirmed by IR and NMR analyses which show absence of interactions. The HPLC analysis for CA-NREP shows that the extent of impurities is low, the resolution between diastereomers is unaltered and the conversion of CA to Cefuroxime and Δ- 2 isomer, is very low and within acceptable limits. The fraction of diastereomer B in CA is within the pharmacopoeial limits. Aging studies up to six months showed that CA is compatible with NREP. The HPLC analysis of CA and its interaction with basic monomer 4-vinyl pyridine and dimethylamino ehtylmethacrylate showed that CA was inactivated in presence of DMAEMA immediately. However CA was found stable in presence of 4-VP. The absence of interaction between CA and NREP has been attributed to the low content of vinyl pyridine in the polymer as well as its weakly basic character. The other factor contributing to this is the self associations within NREP arising from hydrogen bonding between hydroxyls of HEMA and pyridine nitrogen. The judicious selection of the comonomer composition in NREP avoids its interaction with CA. This helped in ensuring the encapsulation of CA in biologically active form, providing taste masking with enhanced dissolution at gastric pH without its inactivation.

5.5. REFERENCES

1) R. Langer, L.G. Cima, J. A. Tamada, E. Wintermantel, Biomaterials, 1990, 11, 738-745
2) A.M. Serajuddin, A.B. Thakur, R.N. Ghoshal, M.G. Fakes, S.A. Ranadive, K.R. Morris, S.A. Varia, J. Pharm. Sci. 1999, 88, 696-704.
3) P. Mura, G.P. Bettinetti, M.T.Faucci, A. Manderioli, Parrini, P.L.. Thermochim. Acta 1998, 321, 59-65.
4) G.A.G Novoa, J.H. Ki, S. Mirza, O. Antikainen, A. I. Colarte, A. S. Paz, J. Yliruusi. Eur. J. Pharm. Biopharm. 2005, 59, 343–350.
5) R .K. Verma, S. Garg, J. Pharm. Biomed. Anal. 2005, 38, 633-644.
6) M.R. Jenquin, J.W. McGinity. Int. J. Pharm. 1994, 101, 23- 34.
7) S. Takka. Il Farmaco 2003, 58, 1051-1056.
8) S. Wissing, D.Q.M. Craig, S.A. Barker, W.D. Moore, Int. J. Pharm. 2000, 199, 141-150.
9) G.C. Ceschel, R. Badiello, C. Ronchi, P. Maffei. J. Pharm. Biomed. Anal. 2003, 32, 1067-1072.
10) E.A. Schmitt, K. Peck, Y. Sun, J.M. Geoffroy. Thermochem. Acta, 2001,380, 175-183.
11) P. Crowley, L. Martini, Pharm. Technol. Eur. 2001,13, 3, 26- 34.
12) N. Sarisuta, M. Kumpugdee, B.W. Muller, S. Puttipipatkhachorn. Int. J. Pharm. 1999,186, 109-118.
13) S. Puttipipatkhachorn, J. Nanthanid, K. Yamamoto, G.E. Peck. J. Contr.Release 2001, 75, 143- 153.
14) S.Y. Lin, C.L. Cheng, R.I. Perng. Eur. J. Pharm. Sci. 1994, 1, 313-322.
15) M. Lovrecich, G. Zingone, F. Nobile, F. Rubessa, Int. J. Pharm. 1996, 31, 247-255.
16) H.J. Robson, D.Q. M. Craig, D. Deutsch, Int. J. Pharm. 190, 1999, 183-192.
17) M.LL.Lorenzo-Lamosa, M. Cuna, J.L.Vila-Jato, D. Torres, M. J. Alonso. J. Microencap. 1997,14, 607-616.

18) M. Cuna, M. L. Lorenzo-Lamosa, J. L. Vila- Jato, D. Torres, M. J. Alonso. Drug Dev. Ind. Pharm. 1997, 23, 259-265.

19) A. Finn, A. Straughn, M. Meyer, J. Chubb. Biopharm. Drug Disposit. 1987, 8, 519-526.

20) G. Fischer, B.S. Daniel, L. Slot, A.M. Lademann, C. Jensen, WO 03/ 024426 A1, Mar 27, 2003.

21) C. J.Campbell, L. J. Chantrell, R. Eastmond. Biochem. Pharmacol. 1987, 36, 2317–2324.

22) N.Ruiz-Balaguer, A. Nacher, V.G. Casabo, M. Merino. Antimicrob. Agents. Chemother. 1997, 41, 445–448.

23) Ceftin Prescription Information, Physicians' Desk Reference 2003 pp 1918-1922

24) M.G. Kulkarni, A.R. Menjoge, US Patent US 20050137372 A1, 23 June 2005.

25) M.G. Kulkarni, A.R. Menjoge, US Patent US 20050136114 A1, 23 June,2005

26) A.R. Menjoge, M.G. Kulkarni, Novel Reverse Enteric Polymers: Evaluation and applications for taste masking technologies. 32nd Annual; meet and exposition controlled release society, 2005.

27) United States Pharmacopoeia XXIII, 1995. United States Pharmacopeial Convention, Rockville, MD pp. 315.

28) H.A. Crisp, J.C. Clayton, US Patent 4,820,833, 11 April 1989.

29) B. Tejchman, M. Jarominska, M. Horodecka, I. Oszczapowicz, Acta Polon. Pharm.-Drug Research. 1995, 52, 477-482.

30) G. Yoon, H. S. Jeong, S. S.Yim. WO 09843980A1, 08 Oct, 1998.

31) K. Karimian, M. Motamedi, S. Zinghini, US Patent US 5847118, 8 Dec, 1998.

32) J.K. Somani, S. Sethi, O. D. Tyagi. US Patent US 6060599, 9 May, 2000.

33) V.K. Handa, O.D. Tyagi, U.K. Ray, US Patent US 6384213, 7 May, 2002.

34) S.J. Hwang, G. H. Jo, J. H. Yun, D. H. Won. Preparation of amorphous form of Cefuroxime axetil using supercritical fluid processing American Association of Pharmaceutical Scientists (AAPS) Annual Meeting, November 10-14, 2002 Toronto, Canada, AAPS Pharm. Sci. 4, 4, Abstract W4300.

35) T.S. Hwang, C.Y. Ahn. WO 00216372 A1, 28 Feb, 2002.

36) 1999; I. Katzhendler, M. Friedman. US Patent US 5980942, 9 Nov, 1999.

37) C. Jingling, V. Zalman, WO 00/71098, 30 Nov, 2000.

38) M. Miyamoto, T. Oda, T. Bunrin, T. Okabe, T. Nishiyama, US Patent US 6171599, 9 Jan 2001.

39) M. Miyamoto, T. Oda, US Patent US 6462093 B1, 8 Oct 2002.

40) R.S. Vladyka, D.F. Erkoboni, P.R. Stergios, US Patent US 6497905, 24 Dec 2002.

41) O. Masato. WO 02/087588, 7 Nov, 2002.

42) G. Fischer, B.S. Daniel, L. Slot, A.M. Lademann, C. Jensen, WO 03/ 024426 A1, 27 Mar, 2003.

43) P. Gao, M.J. Hageman, W. Morozowich, R. J. Dalga, K.J Stefanski, T. Huang, A. Karim, F. Hassan, J.C. Forbes. US Patent US 2003/0045563 A1, 6 March, 2003.

44) F. Balestrieri, A.D. Magri, A.L.Magri, D. Marini, A. Sacchini. Thermochemi. Acta 1996. 285, 337-345.

45) S. Gaisford, G. Buckton. Themochem. Acta 2001, 380, 185-198.

46) A.A.S. Araujo, S. Storpirtis, L. P. Mercuri, F.M.S.Carvalho, M.S. Filho, J.R. Matos, Int. J. Pharm. 2003, 260, 303-316.

47) M.A Holgado, M.A. Arevalo, J.A. Fuentes, I. Caraballo, J.M. Llera, A.M. Rabasco. Int. J. Pharm. 1995, 114, 13-21.

48) P. Mura, A. Manderioli, G. Bramanti, S. Furlanetto, S. Pinzauti. Int. J. Pharm. 1995, 119, 71-79.

49) G.R. Lloyd, D.Q.M. Craig, A. Smith. J. Pharm. Sci. 1997, 86, 991–996.

50) F. M. McDaid, S.A. Barker, S. Fitzpatrick, C.R. Petts, D.Q.M. Craig. Int. J. Pharm. 2003, 252, 235-240.

51) J.S. Woo, H.C. Chang, US Patent US 6107 290, 22 Aug 2000.

52) G. H. Jo, J.H. Yu, J. H. Yun, S. J. Hwang, J.S. Woo, Preparation of amorphous form of Cefuroxime axetil using supercritical fluid processing. Controlled Release Society 29 th Annual Meeting Proceedings, 2002, Abstract 057.

53) S.Y. Lin, H.L Yu, M.J. Li. Polymer, 1999, 40, 3589- 3593.

54) H. Eerikainen, E.I. Kauppinen, Int J. Pharm. 2003, 263, 69–83.

55) Specifications and test methods for EUDRAGIT® E 100, EUDRAGIT® E PO and EUDRAGIT® E 12,5 Internet: www.roehm.com , INFO 7.1/E , 2004-09, pp1-4.

56) A.B. Savage, In: H.F. Mark, N.G. Gaylord, & N.M. Bikales, (Ed) Encyclopedia of Polymer Science and Technology, Vol 3, Interscience, New York, 1965, pp 476.

57) A.O. Okhamafe, P. York. J. Pharm. Pharmacol. 1989, 41, 1-6.

58) R. Nair, N. Nyamweya, S. G. Nen, M. L.J. Marinda, S.W. Hoag. Int. J. Pharm. 2001, 225, 83-/96.

59) M. Zajac, A. Jelinska, L. Dobrowolski, I. Oszczapowicz, J. Pharm. Biomed. Anal. 2003, 32, 1181-1187.

60) C.E.P Malan, M. M. Villiers, A. P. Lotter, J. Pharm. Biomed. Anal. 1997, 15, 549-557.

61) H. Fabre, H.I Bork, D.A. Lerner, J. Pharm. Sci. 1994, 83, 553-558.

62) J. Coates. Interpretation of infrared spectra a practical approach. In: R.A. Meyers (Ed.), Encyclopedia of analytical chemistry, John Wiley and Sons Ltd, Chichester, 2000 pp.10815-10837.

63) G. Yoon, H. S. Jeong, S. S.Yim. WO 09843980A1, 08 Oct 1998.

64) R.I. Moustafine, T.V. Kabanovaa, V.A. Kemenovab, G. Van den Mooterc. J. Contr. Release, 2005. 103, 191-198.

65) R.I. Moustafine, V.A. Kemenovab, G. Van den Mooterc. Int .J. Pharm. 2005b, 294, 113-120.

66) A.S. Tatavarti, K.A. Mehta, A.A. Augsburger, S.W. Hoag, J. Pharm. Sci. 2004, 93, 2319-2331.

67) K. Stoeckel, W. Hofheinz, J.P. Laneury, P. Duchene, S. Shedlofsky, R.A. Blouin. Antimicrob. Agents. Chemother. 1998, 42, 2602-2606.

68) N.T. Nguyen. Pharm. Res., 1991, 81, 893-898.

69) B. Tejchman, M. Jarominska, M. Horodecka, I. Oszczapowicz, Acta Polon. Pharm.-Drug Research. 1995, 52, 477-482.

70) B. Tejchman, I. Oszczapowicz, Acta Polon. Pharm.-Drug Research, 1997, 54, 7-12.

71) L. Zivanovic, I. Ivanovic, S. Vladimirov, M. Zecevic. J. Chromatogr. B, 2004, 800, 175-179.

72) J.S. Park, Y. B. Lim, Y.M. Kwon, B. Jeong, Y.H. Choi, S. W. Kim. J. Poly. Sci. Part A: Polymer Chemistry, 1999, 37, 2305–2309.

73) P.V. Wetering, N. J. Zuidam, Steenbergen, M. J. V., Houwen O. A. G. J. V., Underberg W. J. M, Hennink W. E., Macromolecules, 1998, 31, 8063-8068.

74) S.R.V. Tomme, M. J. V. Steenbergena, S. C. De Smedtb, C. F. V. Nostruma, W.E. Henninka, Biomaterials, 2005, 26, 2129–2135.

CHAPTER 6

Miscible Blends of NREP with Enteric & pH Independent Polymers for Sustained Gastric Release

6.1. INTRODUCTION

A wide range of natural, modified natural and synthetic polymers is used in the formulation of pharmaceutical dosage forms. [1, 2] The drug release needs to be tailored according to the pharmacokinetic characteristics of the drug. This is often limited by the physicochemical properties of the polymers. Designing new polymeric excipients to meet such requirements involves high development costs and uncertainties of regulatory approvals [3]. Variations in coating levels, incorporation of additives such as plasticizers, have been attempted in the past. However this is limited by the mechanical properties of the films [4, 5]. The limitation can be overcome by the use of polymer blends [5, 6].

Miscibility of wide range of polymers used in pharmaceutical dosage forms has been investigated in the past by a variety of techniques such as DSC, microscopy, light scattering, inverse gas chromatography, rheology and spectroscopy. Blends of hydroxypropyl methylcellulose (HPMC) with methylcellulose (MC), hydroxypropyl cellulose (HPC) and polyvinylpyrrolidone (PVP) [7], carbopol and poly(ethylene oxide; PEO) [8], poly(N-isopropyl acrylamide) blends with PVP and carbopol [9], chitosan with PAA (polyacrylic acid), HPMC, MC, PVP, PEO and PVA [10-12] have been investigated in the literature. However the influence of these on drug release was not investigated.

Blends of a) hydrophilic b) hydrophilic and pH independent c) hydrophilic and enteric d) pH independent e) pH independent and enteric and f) enteric polymers for regulating drug release have been reported in the past. Kim and Fassihi [13] investigated blends of hydrophilic polymers HPMC and pectin to control the release of Nifedipine, Prednisolone and Diltiazem hydrochloride, which have varying degrees of water solubility. The drug release from these matrices was shown to be erosion controlled and governed by the hydrodynamic stress and intensity of fluid flow. Blends of hydrophilic and pH independent polymers; ethylcellulose (EC)-HPMC have been investigated for developing porous drug delivery systems [4, 14]. Yamada et al. [15] achieved sustained release of Ketoprofen salt over twelve hours from microspheres coated by EC-carboxymethylcellulose (CMC); (1:1) blends. Samani et al [16]

investigated the release of Diclofenac sodium from HPMC and carbopol blends. The strong hydrogen bonding between polymers diminished release fluctuations. Also the total excipient loading required, was lower.

Blends of pH independent polymers Eudragit® RSPM and EC (Ethocel 100) were evaluated for sustained release of Didanosine in intestinal region [17]. Moderate swelling of Eudragit® RSPM and plastic properties of hydrophobic EC retarded the release in intestine. To enhance the release, addition of a third component, a canalizing agent was considered. The diffusion coefficient of Dexamethasone from PVA and cellulose acetate butyrate blends, could be controlled by adjusting the ratio of miscible and partially miscible blends [18].

Blends of pH independent polymer EC with enteric polymer Eudragit® (EL) and hydroxypropyl methylcellulose acetate succinate (HPMCAS) were evaluated for controlling Theophylline release in intestine [19]. Dashevsky et al. [20] reported the use of blends of polyvinylacetate (PVA) and Kollicoat MAE 30 DP to attain pH independent release of verapamil HCL. Khan et al. [21] used binary blends of enteric polymers EL and Eudragit® S (ES) to attain colon-targeted delivery.

In contrast, blends of reverse enteric polymer Eudragit® E (EE) and enteric polymers result in insoluble polyelectrolyte complexes. These cannot be used in film coating although the drug delivery from hydrogels has been reported [This is discussed in next chapter]. The NREP synthesized by us was found to be useful for taste masking and immediate release of Cefuroxime axetil in the gastric region [22, 23]. NREP did not exhibit adverse interactions leading to inactivation of CA [This has been discussed in Chapter 5] as observed in case of EE [24].

The literature reveals numerous investigations on phase behavior of polymer blends. Various permutations and combinations for blends of excipients have been investigated to attain desired release for drugs, macromolecules, proteins and peptides. However, systematic investigations, which characterize extent of interactions within the blend constituents responsible for blend miscibility and correlate the same with the release of the drug, are not reported.

In the earlier chapters we have shown the taste masking ability of NREP without inactivation of Cefuroxime axetil. Further NREP releases the drug immediately in

gastric pH. In the present investigation we have explored miscible blends of NREP with various enteric polymers and pH independent polymers for sustained gastric release of Cefuroxime axetil. The interactions contributing to miscibility have been investigated by FTIR spectroscopy. MDSC analysis has been used to evaluate the T_g behavior of blends. The variation in T_g has been further quantified in the framework of third power equation derived by Schneider 1989, 1996, 1997 [25-27]. The negative deviations from additivity rule are reflected in the values of fitting parameters K_1 and K_2. Based on the understanding of these interactions, blend compositions can be chosen for sustained release of Cefuroxime axetil over the gastric region [28]. Further the increase in K_1 has been correlated qualitatively with interactions as observed in FTIR spectroscopy. The value of K_2 increases with more favorable interactions resulting from conformational changes in polymer chain. These investigations also provide guidelines for selection of polymers based on extent of interactions, to modulate drug release over the entire length of GI tract.

Blends of reverse enteric polymer with enteric polymers capable of microencapsulating and film coating of the drug have not been reported till now, to our knowledge. The blending of polybases with polyacids results in complexation and these blends therefore cannot be used for encapsulation. In this chapter, we report mechanistic evaluation of NREP blends with enteric and pH independent polymers to develop sustained release of drugs. The unique feature of NREP is that it does not form inter polyelectrolyte complexes. The novelty of this work is it provides a new set of polymer blends containing reverse enteric and enteric polymers capable of film forming which can be investigated for tailoring varied drug release pattern. Encapsulation of Cefuroxime axetil in NREP resulted in dissolution-controlled release of CA at gastric pH over 30-45 minutes. The encapsulation in blends extended the release to up to 4 hours. The release was shown to be diffusion controlled depending upon the extent of interactions between NREP and other polymers constituting the blend.

6.2. MATERIALS AND METHODS

6.2.1. Materials

The film forming polymers: Eudragit® L 100 (EL), Eudragit® S 100 (ES) (Degussa / Rohm Pharma), Hydroxypropyl methylcellulose phthalate (HPMCP) (Eastman), Cellulose acetate phthalate (CAP) (Eastman) and Ethylcellulose (EC) were gift from Lupin Laboratories Ltd, India and Zein was purchased from Sigma-Aldrich. NREP was synthesized as disclosed in chapter 3. The solvents methanol (MeOH), dichloromethane (DCM) and chloroform ($CHCl_3$) were purchased from Qualigens.

6.2.2. Preparation of polymer blends

The polymer blends of EL, ES, CAP, HPMCP, EC and Zein with NREP were prepared by solution casting method using a mixture of methanol and chloroform (20:80). Films of NREP and above polymers were prepared in the weight ratio (25/75), (34/66), (50/50), (66/34) and (75/25). These blends were used for further physicochemical characterization.

6.2.3. Physicochemical characterization of polymer blends

6.2.3.1. FTIR spectroscopy

The interactions between NREP-EL, ES, CAP, HPMCP and Zein were examined by FTIR spectroscopy using Perkin Elmer, Spectrum One, in diffused reflectance mode. 2-3 mg of samples were thoroughly mixed and triturated with potassium bromide (100 mg) and placed in the sample holder. The samples were scanned from 4000 to 450 cm^{-1}. The measuring conditions were resolution, 4.0; zero fitting, 2.0; sample scan, 16; acquisition, single sided. The peak assignments were made for the neat polymer samples of NREP, EL, ES, CAP, HPMCP and Zein. These were compared with the peaks obtained for the polymer blends.

6.2.3.2. DSC analysis

The polymers NREP, EL, ES, CAP, HPMCP and Zein and blends of NREP-with the polymers listed, were subjected to thermal analysis using TA Instruments DSC Q100 V9.0 built 275, using MDSC heat-only method, with nitrogen as purge gas at a flow rate of 50 ml/min. The modulation amplitude was $\pm$ 0.53°C every 40 s. Indium was used to calibrate the enthalpy and temperature values. The experiments were conducted in hermetically sealed aluminum pans. The weight of each sample was in the range 1-2 mg and the heating rate was 5°C/ min from 10 to 200°C.

6.2.4. Encapsulation of CA using Polymer blends

6.2.4.1. Emulsification solvent evaporation

CA was encapsulated by emulsification solvent evaporation method. NREP-polymer blend solutions were prepared in mixture of methanol: dichloromethane (1:1) CA was added to polymer blend solution under magnetic stirring. The drug-polymer solution was dispersed slowly in light liquid paraffin containing 0.25 % of Span 85 under mechanical stirring. The stirring was continued for 3-4 hr at 500 rpm. The micro particles were separated by filtration and washed with petroleum ether to remove the paraffin oil. The micro particles so formed were dried under vacuum for 24 hr at room temperature.

6.2.4.2. Determination of drug content

The drug content was determined at 278 nm using Shimadzu UV160 IPC UV Visible spectrophotometer. Cefuroxime axetil content was determined by dissolving 50 mg of micro particles in 2 ml of methanol and sonicated for 5 min. Then the volume was made to 50 ml using 0.07 N HCl. The solution was filtered and diluted further for the analysis. Each sample was analyzed in triplicate.

6.2.4.3. Release studies of CA

The drug release from the micro particles was evaluated by placing the micro particles containing Cefuroxime equivalent to 125 mg in a basket of 900 ml of 0.07 N HCl. The dissolution was carried out in Electrolab USP type II apparatus at 75 rpm at 37 $\pm$ 0.5°C. The samples were collected after 15, 30, 60, 90, 120, 180 and 240 min. and the volume was made upto initial value by adding fresh dissolution medium. The amount of drug released was estimated at 278 nm using the Shimadzu UV Spectrophotometer. The dissolution tests were done in triplicate.

6.2.5. Scanning electron microscopy

The micro particle samples after dissolution were scanned to study the morphological characteristics by using Leica UK model Stereoscan 400. The samples were gold sputtered before scanning.

6.3. DRUG RELEASE FROM MISCIBLE POLYMER BLENDS: THEORETICAL CONSIDERATIONS

6.3.1. Miscibility of polymers

Polymer blends in general are immiscible, since entropy of mixing is small and does not compensate for unfavorable endothermic heat of mixing. Miscibility is achieved by incorporating functional groups in either or both components of blends [25]. The interactions between functional groups, which could be electrostatic, dipole-dipole resonance, proton transfer and hydrogen bonding, result in exothermic mixing leading to miscibility [29]. Depending on the extent of interaction the blends are categorized as immiscible, partially miscible and miscible. In the present investigation we demonstrate that the nature and extent of interactions between the polymers explains the mechanism as well as the extent to which the release of CA is sustained.

Miscibility of wide range of polymers has been investigated in the past by a variety of techniques such as DSC, microscopy, light scattering, inverse gas chromatography, rheology and spectroscopy [29]. The estimation of the T_g is the most widely used tool to evaluate miscibility in polymer blends. The immiscible blends exhibit two T_gs corresponding to the individual components. In partially miscible blends, the two values shift depending upon extent of miscibility. At the other extreme, when the interactions between the blend components are strong, inter-polymer complexes are formed which exhibit T_g values higher than individual component of the blend. The miscibility of the polymers resulting from weak interactions between components results in T_g intermediate to the values for individual polymers.

Fox equation [25], which assumes volume additivity of mixing, provides the simplest framework to correlate T_gs of blends. According to the equation

$$\frac{1}{T_g} = \frac{X_1}{T_{g1}} + \frac{X_2}{T_{g_2}} \qquad \textit{Eq 1}$$

where T_{g1} and T_{g2} represent T_gs of polymer 1 and polymer 2, respectively and X_1 and X_2, are weight fractions of polymers in blend. The T_gs of polymer blends may exhibit both positive and negative deviations from composition dependence predicted by Fox equation. Further, the deviations are often not monotonous. A large number of approaches to correlate composition dependence of T_g of blends have been proposed and have been reviewed by Schneider [25-27]. We have chosen to analyze the composition dependence of T_gs of blends investigated by us in the framework of Schneider equation [27] since it can account for both positive and negative deviations from the Fox equation as well as the sigmoidal T_g vs compositions curves. Also the physical significance of parameters K_1 and K_2 has been better understood over the years. The miscible polymer blends result from homo and hetero molecular contacts between the binary blend components. The number of each type of contact will depend upon the volume fraction of each component. Each of these contacts will make a different contribution to the T_g of blends.

In development of correlation for T_g of blends, Brekner et al [30] considered the parameter K_1 to account for the deviations from additivity due to the difference between

contributions of hetero and homo molecular contacts to the T_g of the blend. Further, these contacts also influence the free volume distribution in the vicinity of the contact. The effect of this redistribution on T_g determines the magnitude of the parameter K_2. Since this redistribution also influences the formation of contacts, the parameter K_1 depends both on the contribution of hetero contacts to T_g and the influence of changes in free volume in the neighborhood on the contribution of contacts.

Considering the effect of these two factors on the deviations from volume additivity behavior, and applying appropriate boundary conditions, following equation was arrived at to correlate the dependence of T_g on the blend composition

$$\frac{(T_g - T_{g1})}{(T_{g2} - T_{g1})} = (1+K_1)\phi - (K_1+K_2)\phi^2 + K_2\phi^3 \qquad \textit{Eq 2}$$

The condition $K_2 = 0$ assumes effects of molecular surroundings for all contacts to be identical. However, $K_1 = 0$ necessitates that $K_2 = 0$, which then leads to volume additivity.

Equation (2) when converted to the corrected weight fraction of the component having higher T_g, results in

$$\frac{(T_g - T_{g1})}{(T_{g2} - T_{g1})} = (1+K_1)W_{2c} - (K_1+K_2)W_{2c}^2 + K_2 W_{2c}^3 \qquad \textit{Eq 3}$$

Where $w_{2c} = [K' (T_{g1}/T_{g2}) w_2] / [w_1 + K' (T_{g1}/T_{g2}) w_2]$

In real life both positive and negative deviations from volume additivity are observed [27]. In some cases sigmoidal plots for T_g vs composition curves are obtained. These deviations are best quantified by estimating parameters K_1 and K_2. Further in view of the factors contributing to K_1 and K_2 the term (K_1-K_2) is a measure of deviations in T_g observed as a result of differences between the contributions from hetero and homo molecular contacts to the T_g of the blend. These values were tabulated by Schneider for a wide range of polymer blends and the blends were classified into

five categories depending upon the values of K_1 and (K_1-K_2) [27]. Negative deviations from additivity were reflected in $K_1<0$ and $(K_1-K_2) < 0$. This condition is satisfied in most of the cases that we have investigated. The negative deviations are characteristic of conformational entropic effects, which contribute to weaker interactions.

In the subsections that follow, we have discussed the T_g behavior of NREP blends. The deviations from the weight average behavior have been quantified in the framework of Schneider equation (3). Based on this, the polymers have been listed in the order of increasing interactions. The reasons for the observed order have been explained on the basis of interactions between the components of the blends investigated by FT-IR spectroscopy in the previous section.

6.3.2. Mathematical model for release from blends

The release data was treated with the general equation put forth by Ritger and Peppas 1987 [31] for the non swellable devices:

$$M_t / M_\infty = kt^n \qquad \textit{Eq 4}$$

Where, M_t / M_∞ is the fraction of drug released at time t, k is the proportionality constant which accounts for the structural and geometrical properties of the matrix, and n is the diffusional exponent indicative of the mechanism of drug release. This equation adequately describes the release of drugs from slabs, spheres, cylinders and tablets. In case of Fickian release, the exponent n has a limiting value of 0.50, 0.45 and 0.43 for release from slabs, cylinders and spheres, respectively. The values of release parameters, n and k, are inversely related and a higher value of k may suggest burst drug release from the matrix [32].

6.4. CONSIDERATION FOR SITE-SPECIFIC RELEASE OF CA

Modified release dosage forms of cephalosporins like Cefaclor, Cephalexin have been developed [33]. Controlled / sustained release formulations of beta lactam antibiotics are preferred in view of their short half-lives. Cefuroxime axetil, a second-generation cephalosporin antibiotic administered orally, has a half-life of 2 hrs [34]. A

sustained release formulation is hence desirable [35]. CA has a limited absorption window restricted to upper gastric region. It is hydrolyzed by esterase enzyme in the intestine to Cefuroxime, a form that cannot be absorbed orally [36-38]. Bioavailability of orally administered CA is reported to be 37-52 % [34]. Hence development of enteric / delayed release formulation would be of little use as this would further lower CA bioavailability.

For drugs with limited absorption region, spatial and temporal release formulations have been developed in the past [39-43]. Bordonnet et al [44] described varied approaches to attain gastro-retentive systems. Floating drug delivery systems based on hydrophilic polymers is reported in past [45-47]. However the physiochemical properties of CA pose a challenge to formulation scientist. It has a tendency to gel in presence of moisture at physiological temperatures (37°C). Also the slow permeation of moisture from film coat into the tablet core results in gelation of CA core, leading to poor dissolution and reduced absorption [48].

The physicochemical and pharmacokinetic characteristics of CA, necessitate the choice of hydrophobic polymers as encapsulant to attain sustained release.

6.5. RESULTS AND DISCUSSION

6.5.1. Blend Characterization

6.5.1.1. FTIR spectroscopy

Infrared spectroscopy is extensively used in the analysis of polymer blends [49]. While polymer blends are rendered miscible by various types of associations, hydrogen bonding is the most common [50]. The hydrogen bonding in polymer blends affects absorption bands in the region 3500-3600 cm^{-1}. The other regions largely affected by polymer miscibility include the C=O stretching (1734 cm^{-1}), $–CH_2$ symmetric stretching (2886 cm^{-1}) and the finger printing region (1300 - 650 cm^{-1}) [51]. In case of polyelectrolyte complexes resulting from interactions between polyacids and polybases,

a new absorption band in the region 1500 - 1600 cm^{-1} corresponding to carboxylate salt is seen [52, 53].

In the present investigation this technique has been used to correlate the effect of interaction in polymers on miscibility and its effect on drug release. The nature of interaction between the NREP and the other polymers affects the release pattern as the ionization of the pH dependent polymer is affected due to the extent of polymer interaction. It was observed that with increase in extent of interaction, the protonation of NREP is affected and this in turn affects the release pattern. The extent of interaction on thermal behavior and CA release pattern is discussed in subsequent section. The polymer blend interactions investigated for all the systems are summarized in **Table 6.1**.

6.5.1.1.a FTIR spectra of NREP

The peak assignments for NREP are summarized below; IR (KBr, cm^{-1}) see **Fig. 6.1**.

NREP: 3541 (OH, free OH groups); 1726 (C=O, ester); 2839-2992 (Methyl C-H asym / sym stretch); 1448-1482 (Methyl C-H asym / sym bend); 1190-1270 (C-O stretch); 1558-1601, 990 (characteristic for pyridine ring)

NREP is a terpolymer comprising MMA, HEMA and 4VP and contains both proton accepting and donating groups. The carbonyl groups from MMA and HEMA act as proton acceptors and are capable of interacting with the proton donating groups. The nitrogen from the pyridine ring also acts as proton acceptor and is capable of forming hydrogen bonds. The hydroxyl group of HEMA is a proton-donating group. It is expected that such a polymer should exhibit self-association by hydrogen bonding between hydroxyl-carbonyl or hydroxyl-hydroxyl and hydroxyl – pyridine nitrogen.

Hydroxyl stretching region (3100 - 3650 cm^{-1})

The spectrum of NREP shows bands at 3285 and 3541 cm^{-1}, which arise from several contributions corresponding to hydroxyl groups in different environments. The spectrum of poly(HEMA) shows broad band at 3370 cm^{-1} and a shoulder at 3524 cm^{-1} which correspond to free hydroxyls and inter and intramolecularly associated

hydroxyls. This feature is seen in most of the self associated polymers containing hydroxyl groups and poly(HEMA) is known to exhibit self association via hydroxyl-hydroxyl and hydroxyl-carbonyl bonding [54]. Similar absorption pattern in the region 3200-3600 cm^{-1} is observed in the case of NREP. The band at 3285 cm^{-1} in NREP corresponds to hydrogen bonded hydroxyl of HEMA comonomer. This band shows a shoulder at 3541 cm^{-1} corresponding to free hydroxyl group. The maximum seen at 3285 cm^{-1} corresponds to intramolecularly associated hydroxyl groups in NREP. The associations of hydroxyl groups with carbonyl and pyridine nitrogen from co-monomers MMA and 4VP in NREP are discussed in the next section.

Carbonyl stretching region (1650-1740 cm^{-1})

The spectrum of poly(MMA) shows frequency corresponding to C=O groups at 1730 cm^{-1} [55]. The band corresponding to carbonyl from MMA and HEMA in NREP is seen at 1726 cm^{-1}. In addition a shoulder is seen at lower wave number (1636 cm^{-1}). This indicates contribution of carbonyl group of NREP to intramolecular hydrogen bonding. The self association due to hydrogen bonding between carbonyl and hydroxyls in poly(HEMA) is reported by Cesteros et al. [54]. The participation of C=O of PMMA in hydrogen bonding with free OH groups is reported [56] which substantiates our assumption.

Pyridine ring modes (1540-1640 cm^{-1})

The most intense bands corresponding to pyridine ring are those located at 1557, 1597 and 993 cm^{-1} [54, 57]. The band at 1557 cm^{-1} in poly(4-VP) is unaffected by hydrogen bonding of nitrogen whereas the bands at 1590 and 993 cm^{-1} are known to show a shift. The preference of hydroxyl groups for interaction with nitrogen of pyridine ring over the carbonyl in the same polymer has been reported in the past [54]. NREP shows bands corresponding to pyridine at 1601 cm^{-1}, 1558 cm^{-1} and 990 cm^{-1}. In the past a shift from 1597 to 1603 cm^{-1} for hydrogen-bonded pyridine is reported [57, 58]. The spectrum of NREP shows a shift in the position of the pyridine band at 1597 cm^{-1} to 1601 cm^{-1}, indicating hydrogen bonding between pyridine nitrogen and hydroxyls from HEMA, contributing to self-association in the polymer. FTIR spectrum

of NREP shows that both carbonyls from MMA and HEMA comonomer and pyridine nitrogen are involved in hydrogen bonding with hydroxyl groups of HEMA, contributing to self-association.

Potential interactions with NREP

Poly(4VP) has been reported to undergo hydrogen bonding (nitrogen of pyridine acts as proton acceptor), co-ordination complexation (lone electron pair of nitrogen) and charge transfer (acid / base interactions) [59]. 4VP imparts basic character to NREP and hence should be capable of forming hydrogen bonds with polyacids. If the interaction between polyacids and polybases involves proton transfer, it could lead to salt formation [60]. The chemical structure of NREP indicates that the free hydroxyl from HEMA, carbonyl from HEMA as well as MMA and pyridine nitrogen could be expected to contribute towards hydrogen bonding. Since NREP exhibits self-association, it was of interest to investigate, if intermolecular associations with other components of the blends would overcome the intramolecular associations within the polymer.

A comprehensive analysis of spectral regions involving hydroxyl and carbonyl stretching and the pyridine ring modes was undertaken. Of special significance was the pyridine ring mode as it was expected to differentiate between strong and weak interactions. Complexation of pyridine to metal ions and sulfonic acid has been reported in the past [59, 61, 62]. The complexation involves conversion of pyridine to pyridinium by proton transfer. The protonation or coordination bonding of pyridine is associated with the appearance of new band in FTIR spectrum between 1618-1637 cm^{-1} and disappearance of band at 1597 and 1555 cm^{-1} [58, 61, 63, 64]. The weak interactions involving hydrogen bonding of nitrogen of 4VP are associated with a band shift of 5-6 cm^{-1} to higher wave number from 1597 cm^{-1} [58, 65]. In the present investigation the blends were examined for such changes in pyridine ring mode.

Table 6.1 Assignments for FTIR spectra

NREP	Implications
Hydroxyl stretching region (cm^{-1})	
3541	Free OH available for hydrogen bonding
3285	Hydrogen bonded hydroxyls; self association
Carbonyl stretching region (cm^{-1})	
1726 (shoulder at 1636)	Hydrogen bonded carbonyl ;self association
Pyridine ring mode (cm^{-1})	
990, 1558	Characteristic bands of pyridine ring
1601	Weak hydrogen bonding between Pyridine Nitrogen and OH groups ; self association
EC	
Hydroxyl stretching region (cm^{-1})	
3485	Free OH available for hydrogen bonding
NREP-EC	
Hydroxyl stretching region (cm^{-1})	
3483 (-2)	Free OH, shift due to blending
3285	Weak, hydrogen bonded hydroxyl, Intermolecular association
Carbonyl stretching region (cm^{-1})	
1727 (shoulder at 1635)	Hydrogen bonded carbonyl
Broad than Neat NREP but narrow than plain EC	Self association in EC overcome by intermolecular association with NREP
Pyridine ring mode (cm^{-1})	
1601 and 1558	both bands unaffected weak interactions between EC and NREP
EL	
Hydroxyl stretching region (cm^{-1})	
3565	Free OH, available for hydrogen bonding
3210	Hydrogen bonded hydroxyl, strong, bonding , self associations
Carbonyl stretching region (cm^{-1})	
1727 (broad with shoulder at 1635)	Hydrogen bonded carbonyl ; self association
NREP-EL	
Hydroxyl stretching region (cm^{-1})	
3543 (-20)	free OH , shift due to hydrogen bonding in blend
3253 (-30)	Hydrogen bonded hydroxyl , shift to lower wavenumber (intermediate strength bonds) Intermolecular association

Carbonyl stretching region (cm^{-1})	
1727 (with shoulder, narrow than EL and broad than NREP)	Hydrogen bonded carbonyl (Intermolecular association)
1703	
Pyridine ring mode (cm^{-1})	
1558	(unaffected)
1603 (shifts from 1601to + 2)	Nitrogen from pyridine ring hydrogen bonded (weak OH bonded, intermolecular associations) No presence of pyridinium units Moderate interaction
ES	
Hydroxyl stretching region (cm^{-1})	
3548	Free OH, available for hydrogen bonding
3224	Strong hydrogen bonded hydroxyl (self associations)
Carbonyl stretching region (cm^{-1})	
1727 (broad with shoulder at 1635)	Hydrogen bonded carbonyl ;self association
NREP-ES	
Hydroxyl stretching region (cm^{-1})	
3536	Free OH
3268, (shift to lower wavenumber by -17)	Weak hydrogen bonded hydroxyl (Intermolecular association)
Carbonyl stretching region (cm^{-1})	
1727 (with shoulder at 1703narrow than EL and broad than NREP)	Hydrogen bonded carbonyl (Intermolecular association)
Pyridine ring mode (cm^{-1})	
1558	(unaffected)
1603 (shifts from 1601to + 2)	Nitrogen from pyridine ring hydrogen bonded (weak OH bonded, intermolecular associations) No presence of pyridinium units Moderate interaction
HPMCP	
Hydroxyl stretching region (cm^{-1})	
3473	Free OH, available for hydrogen bonding
Carbonyl stretching region (cm^{-1})	
1725 (broad with shoulder)	Hydrogen bonded carbonyl (self association)

NREP-HPMCP	
Hydroxyl stretching region (cm^{-1})	
3511 shifts to lower wavenumber by (30)	Free OH
3297	Weak hydrogen bonded hydroxyl (Intermolecular association)
Carbonyl stretching region (cm^{-1})	
1725 (broad with shoulder at 1640)	Hydrogen bonded carbonyl (C=O liberated due to OH bonding of acid hydroxyls)Intermolecular association
Pyridine ring mode (cm^{-1})	
1598, 1557, 990	unaffected intensity lowered due to effect of blending
1601 (present but merged with other band of HPMCP)	(present but merged with other band of HPMCP)
1635	small band is emerged due to partial pyridinium units Strong interaction
CAP	
Hydroxyl stretching region (cm^{-1})	
3483	Free OH, available for hydrogen bonding
Carbonyl stretching region (cm^{-1})	
1725 (broad with shoulder)	Hydrogen bonded carbonyl ;self association
NREP-CAP	
Hydroxyl stretching region (cm^{-1})	
3526 (shifts to lower wavenumber by 15)	Free OH
3268 (shifts to lower wavenumber by17)	Weak hydrogen bonded hydroxyl
Carbonyl stretching region (cm^{-1})	
1725(broad with shoulder at 1740	Hydrogen bonded carbonyl (C=O liberated due to OH bonding of acid hydroxyls)
Pyridine ring mode (cm^{-1})	
1598, 1557, 990	unaffected intensity lowered due to effect of blending
1601	(present but merged with other band of CAP)
1635	small band is emerged due to partial pyridinium units Strong interaction

6.5.1.1.b NREP-Zein blends

ZEIN: IR (KBr, cm^{-1}); 1657 (amide I, C=O stretching vibrations); 1542 (amide II, N-H bending vibration) see **Fig. 6.2**. These assignments are similar to those described by Duodu et al. [65]. The broad band of amide I corresponds to two populations of carbonyl groups; those which are free and those involved in intramolecular associations with NH groups. Similar features for amide bands in poly (ether amide), were reported by Katime and Iturbe 1996 [66]. If these intramolecular associations are overcome, this polymer can form miscible blends.

Polyamides act as proton acceptors and are capable of hydrogen bonding with proton donor groups like carboxylic, hydroxyl and phenolic groups [9, 66]. Zein contains amide groups so it will act as proton acceptor like NREP. Both polymers are self associated and hence cannot be expected to show miscibility unless the self-association is overcome. There exists a possibility of interaction between hydroxyls from NREP and the amide carbonyl rendering the blends either miscible or partially miscible. The mixing of these polymers resulted in immediate phase separation. The NREP-ZEIN spectrum (**Fig. 6.2**) is additive in nature and the bands corresponding to the amide I and amide II of Zein appear unaffected in the NREP-Zein blend. The frequency for the free hydroxyl of NREP is unaltered in the blend. The absorption frequencies at 1601 and 1557 cm^{-1} corresponding to the pyridine groups are also unaltered. The bands for amide I and carbonyl of NREP appear in close proximity and hence hydrogen bonding between hydroxyl of NREP with carbonyl of amide group from Zein is difficult to establish. Similarly the bands for amide II and pyridine ring mode appear in close proximity. The amide bands are reported to shift as a result of hydrogen bonding [66-67]. However such changes are not observed blends suggesting that the amide groups are not involved in hydrogen bonding. The FTIR spectrum suggests absence of interaction between NREP-Zein.

The spectrum of NREP-Zein blend reveals that the two polymers do not exhibit significant interaction, as the frequencies corresponding to all functional groups are unaltered. It is expected that NREP-Zein blends would exhibit two T_gs owing to partial miscibility or immiscibility.

The FTIR spectroscopy revealed that Zein and NREP do not exhibit any interaction. The blends of NREP-Zein are expected to exhibit phase separation and their use in drug delivery would result in rapid release of CA at gastric pH, due to the protonation of pyridine nitrogen and subsequent dissolution of NREP. This was investigated from the CA release experiments in subsequent sections.

6.5.1.1.c NREP-EC blends

EC: IR (KBr, cm^{-1}); 3487 (broad band for OH groups); 2976, 2878 (methyl C-H asym / sym stretch); 1448, 1486 (methylene C-H bend); 1375 (C-H bending), 1131, 1064 (cyclic ether C-O stretch in C-O-C). These assignments are similar to those described in by Bugay and Findlay [68] and Suthar et al. [69].

The presence of cellulosic hydroxyls in EC enables it to participate in hydrogen bonding. The band corresponding to free hydroxyl group in EC is seen at 3485 cm^{-1} (see **Fig.6.3**). It does not show a shoulder at lower frequency corresponding to hydrogen-bonded hydroxyls. This is expected since the purpose of converting cellulose to ethylcellulose is to enhance solubility of EC, as strong hydrogen bonding within cellulose prevents its solubilization.

NREP can form miscible blends with EC via hydrogen bonding involving hydroxyl-hydroxyl, hydroxyl-carbonyl and hydroxyl-pyridine nitrogen, between EC and NREP respectively. The films of NREP-EC blends are clear and indicate miscibility between polymers. In the FTIR spectrum of the blend the band corresponding to the free hydroxyl group at 3483 cm^{-1} shows fall in intensity when compared to neat EC. Further it shows appearance of a shoulder at lower frequency (3285 $cm^{-1)}$ corresponding to hydrogen-bonded hydroxyl. Lee et al. [70] reported that hydrogen bonds arising in many blends differ in strength. Strong bands appear at 2800, 2500 and 1800 cm^{-1}, the moderate to intermediate strength bands at 3100-2800 cm^{-1} and weak structure less broad band at 3300 cm^{-1}. Since the hydrogen-bonded hydroxyl in NREP-EC shows absorption at 3285 cm^{-1} it is evident that the association between these polymers is weak.

The carbonyl frequency in NREP-EC blend shows maxima at 1727 cm^{-1} and a shoulder at lower frequency (1635 cm^{-1}). This shoulder is more profound in the blend than in neat NREP. This indicates the participation of carbonyl groups of HEMA and / or MMA from NREP in hydrogen bonding with hydroxyl groups from EC.

The bands characteristic of pyridine group are seen in the NREP-EC blend and do not show a fall in intensity. The appearance of the bands at 1601 and 1558 cm^{-1} indicates that the pyridine ring nitrogen is not involved in hydrogen bonding in NREP-EC blends (see **Figs. 6.3 (a) and (b)**).

The spectrum of NREP-EC blend shows that hydrogen bonding takes place in hydroxyl-hydroxyl and carbonyl-hydroxyl groups and the pyridine nitrogen is not involved in any interaction. From the interactions observed above, it may be expected that NREP-EC may exhibit a single composition dependent T_g as observed for miscible blends. Since the extent of interaction between NREP and EC is weak, only negative deviations from additivity would be expected. Also the blends exhibiting weak interactions would exhibit pH dependent behavior since the NREP-EC interactions would be overcome by the interactions between the acid buffer and pyridine of NREP. These assumptions are validated from the CA release experiments from NREP-EC micro particles.

6.5.1.1.c NREP-EL and ES blends

The peak assignment for EL and ES are as follows IR (KBr, cm^{-1}) see **Figs. 6.4 and 6.5**:
EL: 2500-3500 (OH groups); 2950-2997 (Methyl C-H asym / sym stretch); 2836 (Methoxy (CH_3-O-), C-H stretch); 1723 (esterified carboxylic acid, C=O); 1388, 1449, 1484 (Methyl C-H vibrations, asym / sym stretch), 1162, 1269 (ester vibrations).
ES: 2500-3500 (OH groups); 2950-2997 (Methyl C-H asym / sym stretch); 2839 (Methoxy (CH_3-O-), C-H stretch); 1728 (esterified carboxylic acid, C=O); 1388, 1449, 1484 (methyl C-H vibrations, asym / sym stretch); 1150, 1193, 1270 (ester vibrations). These values are similar to those assigned by Cilurzo et al. [71].

Both EL and ES are polyacids and contain acid hydroxyl groups. EL is expected to show stronger interactions with polybase than ES as it has higher content of

methacrylic acid than ES [72]. The spectra of EL and ES in the hydroxyl-stretching region show presence of free hydroxyl groups in region 3500-3550 cm^{-1} and a shoulder at lower frequency (3200 cm^{-1}), which is an indication of hydrogen bonded hydroxyls. The spectra of EL and ES in the carbonyl stretching region show maxima at 1727 cm^{-1} corresponding to C=O and a shoulder at lower frequency (1635 cm^{-1}). The presence of a shoulder indicates self-associations in these polymers arising from the hydrogen bonding between the acid hydroxyls (COOH) and the carbonyl from the acrylic groups. Existence of association between C=O and acid hydroxyls in Eudragit® L is reported in the past [73]. The salt formation of EL and ES results in two new bands at 1560 cm^{-1} and between 1400-1300 cm^{-1} [71]. The blends of these polymers with NREP were examined for the carboxylate salt formation.

The spectra for NREP-EL and NREP-ES blends are shown in **Fig. 6.4 and 6.5.** Blending of NREP with EL and ES is expected to show changes in the pyridine ring mode, hydroxyl and carbonyl-stretching region. If the interaction is strong as to result in polyelectrolyte complexes, then bands corresponding to pyridinium units are expected to appear accompanied by simultaneous disappearance of bands at 1558 and 1597 cm^{-1} characteristic of pyridine ring. The spectra of NREP-EL and NREP-ES blends showed presence of weak hydrogen bonding between pyridine nitrogen and acid hydroxyls but absence of bands corresponding to pyridinium units.

Hydroxyl stretching region

The differences in carbonyl stretching and hydroxyl stretching region of NREP-EL and NREP-ES blends are explained below. The band at 3540-3550 cm^{-1} corresponding to the free hydroxyl group is seen in neat NREP, EL and ES and this band in blends shows a decrease in intensity. Also the region 2500-3500 cm^{-1} in NREP-EL and NREP-ES blend shows significant band broadening.

According to Lee et al. [70], the band at 3100 cm^{-1} represents hydrogen bonding of intermediate strength and the broad structureless band at 3300 cm^{-1} corresponds to the weak hydrogen bonded hydroxyls. The band for free hydroxyl 3565 cm^{-1} in NREP-EL blend shows a maximum at lower frequency 3217 cm^{-1}. The appearance of this band at 3217 cm^{-1} in NREP-EL blend, is indicative of hydrogen bonding of intermediate strength.

The NREP-ES blends show a band corresponding to free hydroxyls at 3536 cm^{-1} with a shoulder showing maximum at 3268 $cm^{-1.}$ This indicates association of hydroxyls in hydrogen bonding. But the appearance of hydrogen-bonded hydroxyls at 3268 cm^{-1} as compared to 3217 cm^{-1} in NREP-EL, suggests weaker hydrogen bonding [70]. The interaction between NREP-ES is weaker than that in NREP-EL. This may be attributed to higher content of methacrylic acid in EL as compared to ES.

Carbonyl stretching region

The band at 1727 cm^{-1} in EL and ES is broader than the band at 1726 cm^{-1} for NREP. This indicates that intramolecular association between carbonyl and hydroxyl groups in EL and ES is very prominent than that seen in NREP. As compared to neat polymers EL and ES, the band for carbonyl group in the blends is narrowed but this band is broader than that seen for NREP. This is because self-association between the carboxylic carbonyl and hydroxyl within EL and ES is overcome and the carboxylic hydroxyl now participates in interpolymer association with NREP. This results in the liberation of carboxylic carbonyl from self-association and is reflected in the spectrum which shows maximum at 1726 cm^{-1} and shoulder at 1703 cm^{-1}. Similar results were reported by Lee et al. [70] for methacrylic acid and vinyl pyridine groups. Further no new bands were observed in the region 1560 cm^{-1} corresponding to the carboxylate group, confirming that no salt formation has occurred.

Pyridine ring mode

The 1599 cm^{-1} band for pyridine ring remains unaltered in the NREP-EL and NREP-ES blends. The band observed at 1601 cm^{-1} in neat NREP shifts to 1603 cm^{-1} in NREP-EL and NREP-ES blends. The shift to higher wave number from 1601 to 1603 cm^{-1} indicates participation of pyridine nitrogen in intermolecular hydrogen bonding. Similar shifts (5-6 cm^{-1}) for hydrogen bonded pyridine nitrogen in blends of poly(vinyl pyridine) with poly(vinyl acetate -co- vinyl alcohol), poly(HEMA), poly(mono methyl itaconate) and pentadecylphenol have been reported [54, 57, 58, 74]. The scale expanded spectra (**Fig. 6.4 (b) and 6.5 (b)**) show that no new bands generated in the region 1625-1637 cm^{-1}. Thus protonation of pyridine group to pyridinium has not occurred.

The intermolecular associations between NREP-EL and NREP-ES are of weaker magnitude, rendering the polymers miscible without leading to complex formation. Hydrogen bonding between these polymers results from the participation of acid hydroxyls of EL and ES and carbonyl, hydroxyl and pyridine of NREP. From the FTIR results it is expected that NREP-EL should exhibit single composition dependent T_g values with better fit to the Fox equation than NREP-ES blends. Unlike NREP-EC blends the NREP-EL/ES blends show hydrogen bonding with pyridine. However conversion to pyridinium units does not take place. Hence positive deviations from weight average are not expected.

The intermolecular associations between NREP-EL and NREP-ES are of weaker magnitude, rendering the polymers miscible without leading to complex formation. Hydrogen bonding between these polymers results from the participation of acid hydroxyls of EL and ES and carbonyl, hydroxyl and pyridine of NREP. From the FTIR results it is expected that NREP-EL and NREP-ES blends should exhibit single composition dependent T_g values.

Unlike NREP-EC blends the NREP-EL and NREP-ES blends show hydrogen bonding with pyridine. However, conversion to pyridinium units does not take place and hence positive deviations from weight average values are not expected. The interaction between NREP-EL is stronger than that seen in NREP-EC. Thus these blends are expected to show slower release of CA than that seen in NREP-EC. These predictions are validated from the CA release data from NREP-EL and NREP-ES blends.

6.5.1.1.d NREP-CAP and NREP-HPMCP blends

The peak assignments for CAP and HPMCP are as follows IR (KBr, cm^{-1}) see **Figs. 6.6 and 6.7**.

CAP: 3570-3200 (OH group); 2980, 2883 (methyl C-H asym / sym stretch); 1750, 1725, 1701 (C=O ester, carboxylic acid); 1599 (C=C conjugated vinyl, aromatic ring); 1492 (methylene C-H bend); 1284 (ester bond C-O-C), 1140- 1071 (cyclic ether C-O stretch in C-O-C); 746 (monosubstituted aromatic ring).

HPMCP: 3460 (O-H groups); 2989, 2884 (methyl C-H asym / sym stretch); 2938 (methylene C-H asym / sym stretch); 2828 (methoxy O-CH_3), 1725 (C=O, ester); 1599 (C=C conjugated vinyl, aromatic ring); 1448, 1486 (methylene C-H bend); 1285 (ester bond C-O-C); 1128,1067 (cyclic ether C-O stretch in C-O-C); 949 (aromatic C-H in plane bend), 746 (monosubstituted aromatic ring). These assignments are similar to those described by Bugay and Findlay [68].

Both CAP and HPMCP contain cellulosic hydroxyls in addition to acid hydroxyls. The carboxylic groups in CAP and HPMCP are attached to the aromatic ring and are therefore more amenable to dissociation due to stabilization effects of the ring. Propyl and methyl groups in HPMCP contribute to steric hindrance, limiting its interaction with NREP. We believe that CAP with only acetate groups attached to cellulose structure, would exhibit stronger interactions than HPMCP with NREP. These presumptions are validated by the values of parameters of Schneider equation discussed in the next section

The FTIR spectra for NREP-CAP and NREP-HPMCP blend are shown in **Figs. 6.6 and 6.7**. FTIR spectra of CAP and HPMCP show bands for free hydroxyl groups at 3483 and 3473 cm^{-1} respectively. The carbonyl band appears at 1725 cm^{-1} for both CAP and HPMCP and shows a shoulder at lower frequency. This is an indication of self-association in these polymers arising out of hydrogen-bonded carbonyl with acid hydroxyls or cellulosic hydroxyls. Similar feature was observed in carbonyl stretching region of ES and EL.

Hydroxyl stretching region

In the spectrum for neat CAP, band corresponding to free hydroxyl at 3483 cm^{-1} does not show a prominent shoulder at lower wave number. However, the free hydroxyl group at 3526 cm^{-1} in NREP-CAP blend shows a maximum at 3268 cm^{-1}. This additional band corresponds to hydrogen-bonded hydroxyls resulting from hydrogen bonding between CAP and NREP. In neat NREP this band appears at 3285 cm^{-1} and shifts to lower wave number in CAP-NREP blend to 3268 cm^{-1}. This shift indicates that the later is stronger amongst these [70].

For steric reasons HPMCP was expected to exhibit weak interaction than CAP with NREP. This is reflected in spectrum of NREP-HPMCP in hydroxyl stretching

region. The blend shows free hydroxyl band at 3511 cm^{-1} and a slight shoulder at 3297 cm^{-1}. The neat NREP shows distinct band for hydrogen bonded hydroxyls at 3285 cm^{-1} whereas the NREP-HPMCP blend shows the same at 3297 cm^{-1}. The shift to higher wave number shows its weak nature. This suggests that HPMCP shows weaker hydrogen bonding with NREP compared to CAP.

Carbonyl stretching region

The carbonyl stretching region of NREP-CAP blend is narrower than that seen in neat CAP but broader than that seen in neat NREP. This shows that the self-association between C=O and hydroxyls of CAP is overcome. The carbonyl groups from phthalic acid in CAP are liberated as the hydroxyl groups participate in the intermolecular associations with NREP. The shoulder to the carbonyl frequency (1725 cm^{-1}) at higher wave number (1740 cm^{-1}) further substantiates the liberation of C=O from self-association in CAP. This indicates that the acid hydroxyls of CAP participate in hydrogen bonding with NREP.

The carbonyl band in the NREP-HPMCP blends is narrower than that seen in HPMCP but broader than that in neat NREP. This shows that the self-association in HPMCP between C=O and acid hydroxyls is overcome and the carbonyl group is liberated. The hydroxyls in carboxylic groups from HPMCP participate in the intermolecular associations.

Pyridine ring mode

Both CAP and HPMCP show bands at 1599 and 1579 cm^{-1}. These bands overlap with the vibrations exhibited by the pyridine ring of NREP at 1601 and 1557 cm^{-1}. Hence the interpretation of the spectra of these blends for changes manifested by the association of pyridine nitrogen in hydrogen bonding is difficult.

The spectra of NREP-CAP and NREP-HPMCP, in the region 1700-1450 cm^{-1} showed three bands at 1598, 1577 and 1557 cm^{-1} as seen in **Fig. 6.6 (b) and 6.7 (b)**. The band corresponding to pyridine at 1601 cm^{-1} is merged with the band at 1599 cm^{-1} of HPMCP and CAP respectively. However, the second band at 1577 cm^{-1} corresponding to HPMCP and CAP and the third band at 1557 cm^{-1} due to pyridine ring are resolved. The other band corresponding to pyridine ring is seen at 990 cm^{-1} in NREP. This band

is present in both NREP-CAP and NREP-HPMCP blends at 988 and 991 cm^{-1} respectively. However its intensity is reduced as compared to that in neat NREP.

It has been reported in the past that conversion of pyridine to pyridinium is associated with disappearance of bands at 1599 and 1558 cm^{-1} and appearance of new band between 1635-1625 [58, 61, 63, 64]. Since bands at 1601 and 1599 cm^{-1} in NREP, CAP and HPMCP are too close to resolve, the band at 1557 cm^{-1} was examined. The scale expanded spectra of the NREP-HPMCP and NREP-CAP blends show a clear band at 1558 cm^{-1} and slight emergence of a new band at 1638 cm^{-1}. Since the content of pyridine in NREP is too low, the absorption of this band is not evident without scale expansion. This feature is weaker in NREP-HPMCP blends than in NREP-CAP blends as a result of steric hindrance encountered in the former case. The coexistence of the band at 988, 991 and 1558 cm^{-1} and emergence of weak new band at 1636 cm^{-1} in NREP-CAP and NREP-HPMCP blends respectively suggests partial conversion of pyridine groups to pyridinium. Partial protonation of pyridine in blends of poly(2-VP) with poly(monomethyl itaconate) and poly(ethylene -co- methacrylic acid) has been reported in the past [70, 57].

The complete conversion of pyridine to pyridinium would result in complex formation. The partial conversion observed in the present case might be attributed to presence of a) nonionic structural defects in NREP b) lower content of pyridine and / or c) low pKa value of 4VP. In the past it has been reported that blends of poly(4VP) with poly(HEMA) do not result in complexation [54]. The presence of nonionic structural defects in polyacids or polybases restricts complex formation with oppositely charged polymer [50, 70, 60, 75]. NREP contains 2-hydroxyethyl methacrylate, which may act as a structural defect, thereby avoiding the complex formation between the NREP-CAP and NREP-HPMCP. The proportion of these structural defects also affects the inhibition of complex formation. The introduction of HEMA in NREP perhaps inhibits complexation. NREP is a random terpolymer containing 62.2% of MMA, 27 % of HEMA and 10.8 % of 4 VP. The concentration of the carbonyl and the hydroxyl groups is more in NREP when compared to the nitrogen of the pyridine ring. Complexation between pyridine and phenolic units was inhibited by low content of 4VP and the presence of intercalated styrene units [76].

From the FTIR studies it was concluded that NREP-CAP blends exhibited stronger interaction than NREP-EC, NREP-EL, NREP-ES and NREP-HPMCP blends. We therefore believe that NREP-CAP blends would show maximum retardation of CA release. This was validated from the CA release experiments.

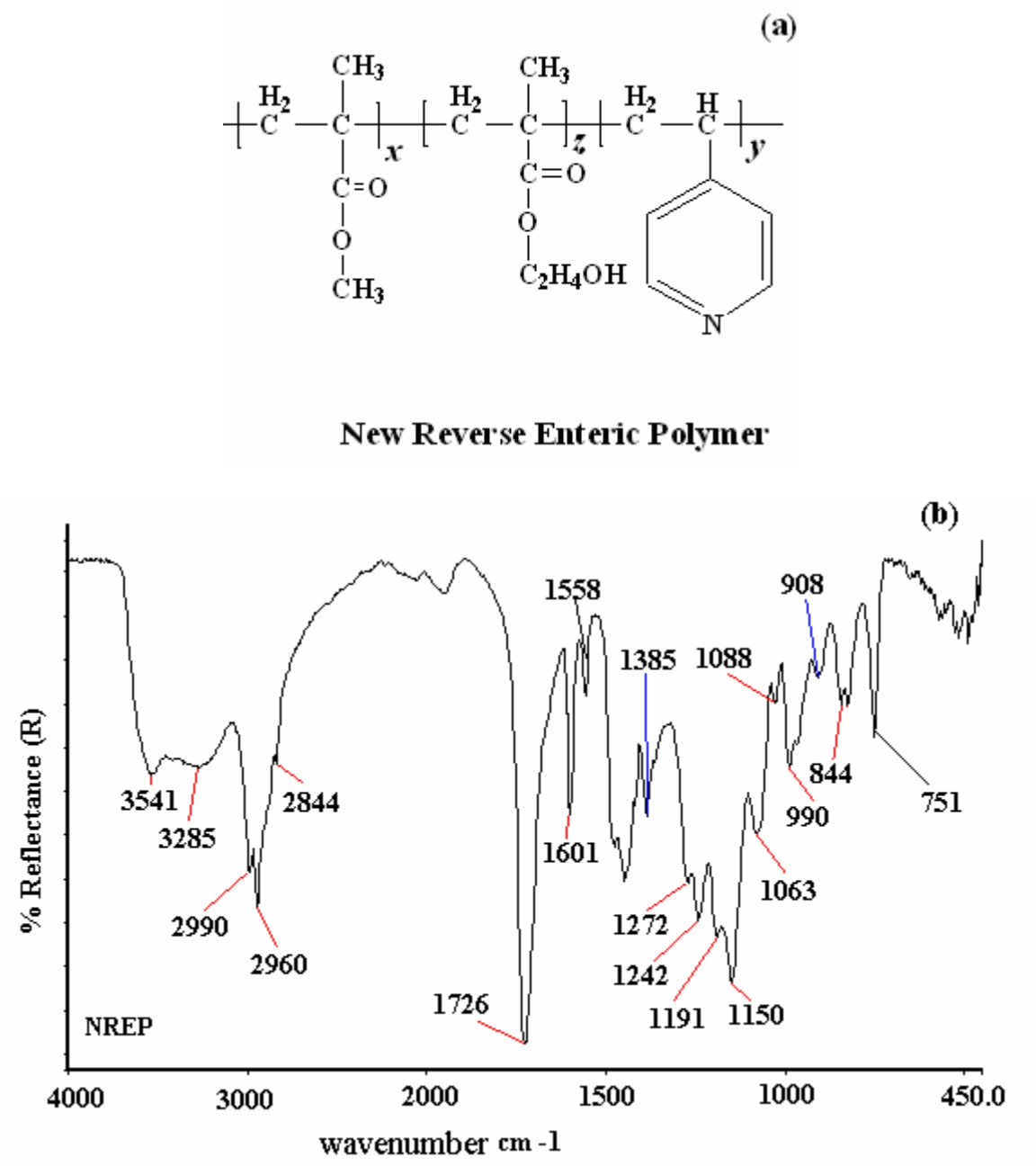

Fig. 6.1. New reverse enteric polymer: (a) structure (b) FTIR spectrum

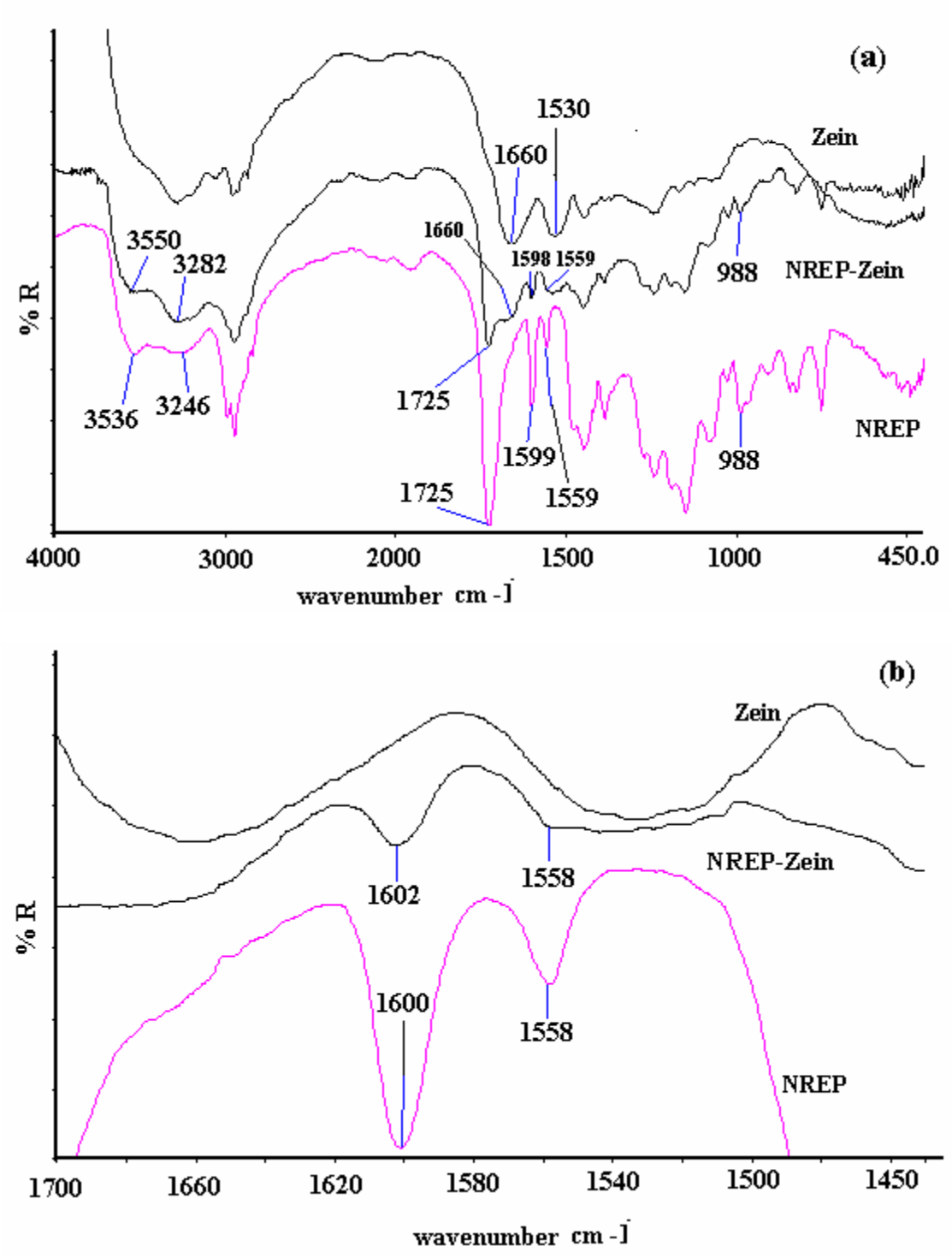

Fig. 6.2. FTIR spectra of NREP-Zein blends: (a) Overlay of NREP-Zein blends. (b) Scale expanded spectra.

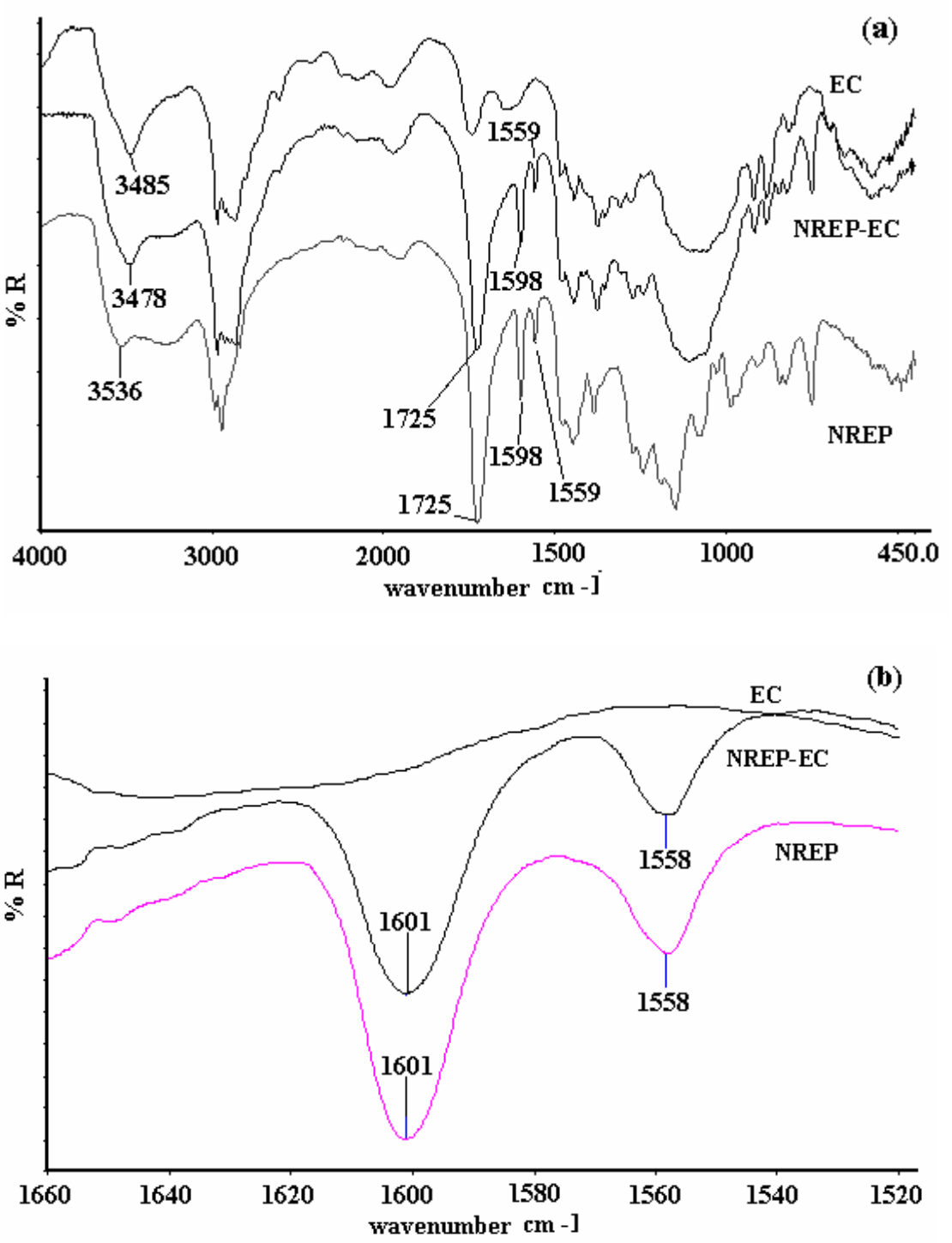

Fig 6.3. FTIR spectra of NREP-EC blends: (a) Overlay of NREP-EC blends. (b) Scale expanded spectra.

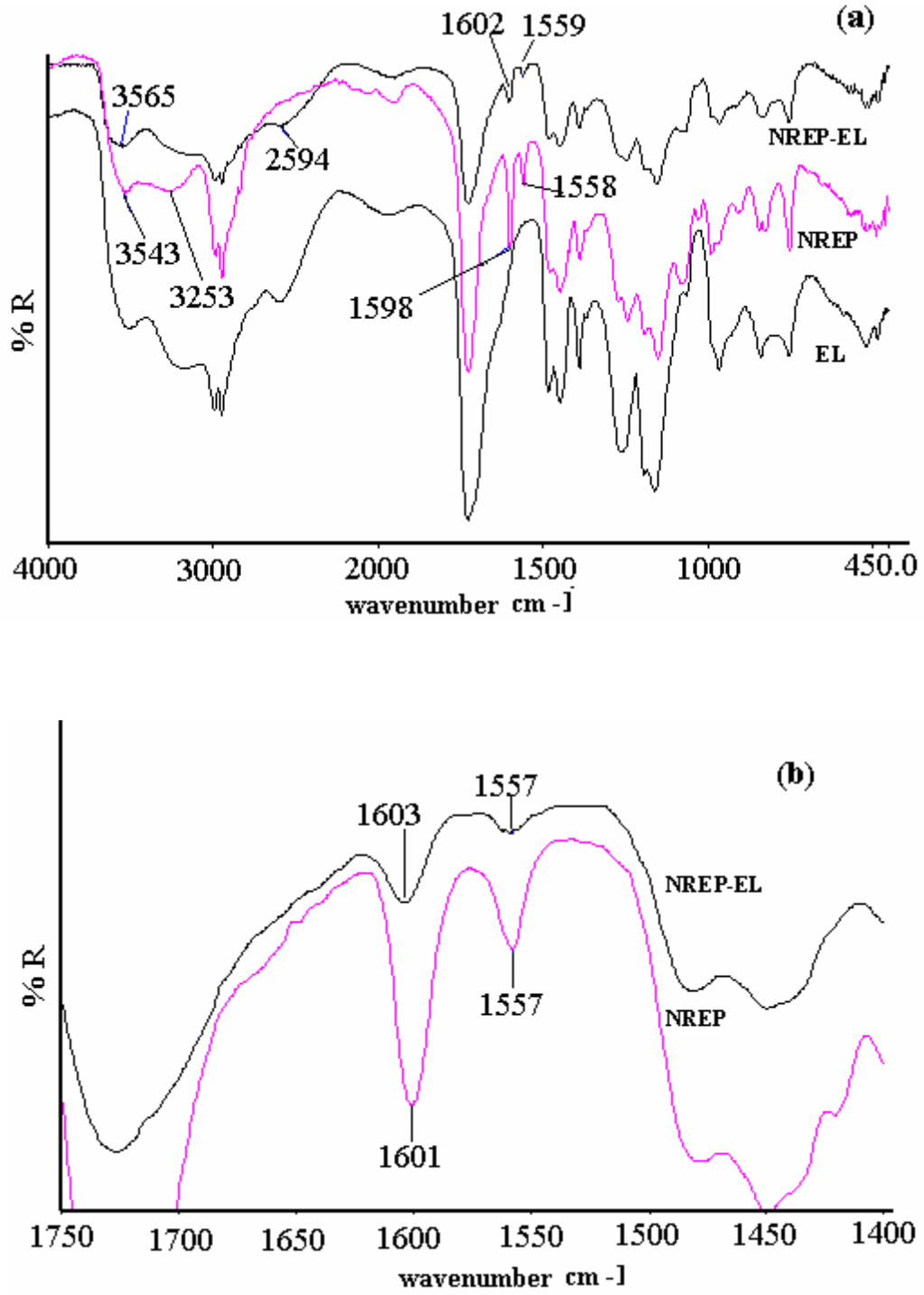

Fig. 6.4. FTIR spectra of NREP-EL blends: (a) Overlay of NREP-EL blends. (b) Scale expanded spectra.

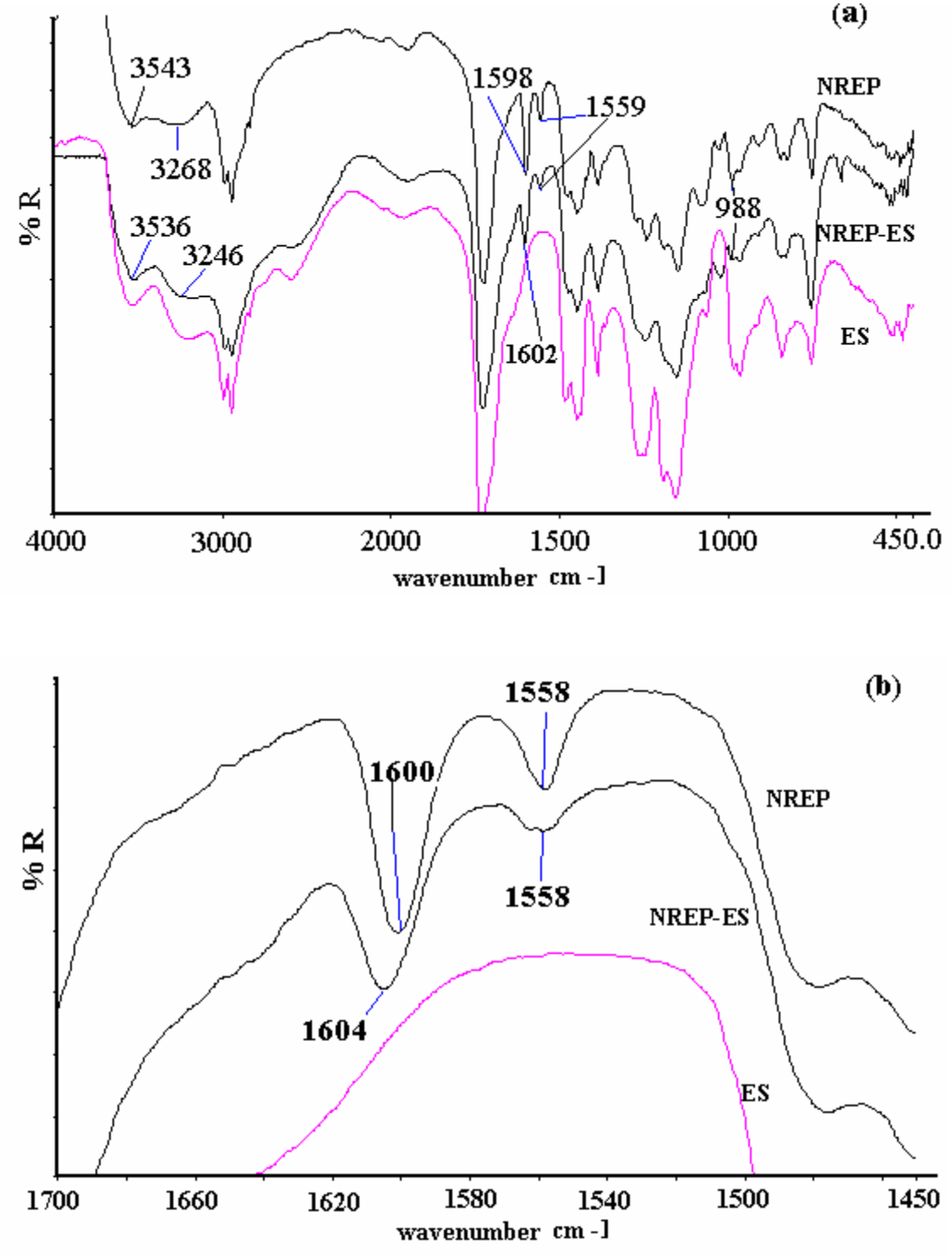

Fig. 6.5. FTIR spectra of NREP-ES blends: (a) Overlay of NREP-ES blends. (b) Scale expanded spectra.

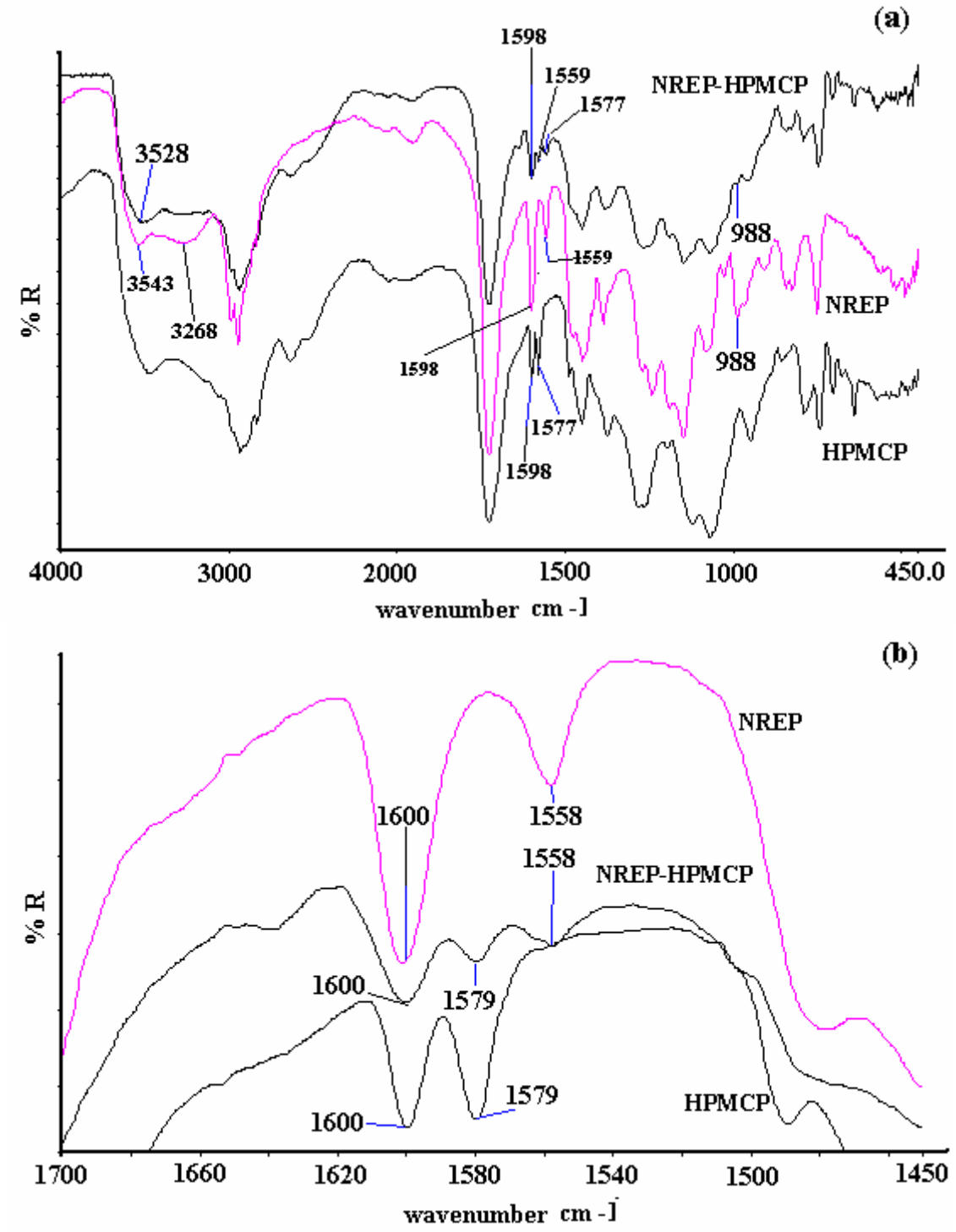

Fig. 6.6. FTIR spectra of NREP-HPMCP blends: (a) Overlay of NREP-HPMCP blends. (b) Scale expanded spectra.

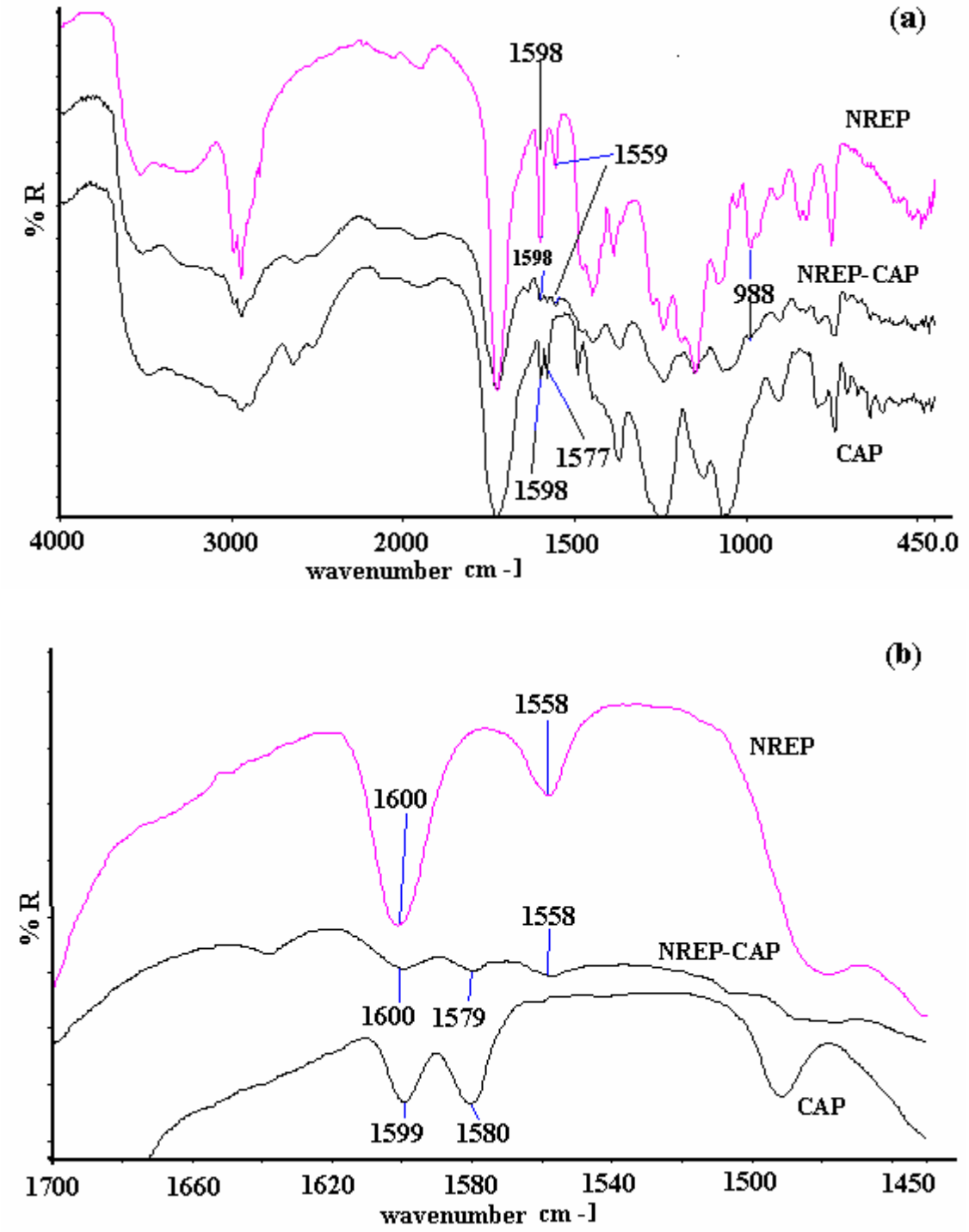

Fig. 6.7. FTIR spectra of NREP-CAP blends: (a) Overlay of NREP-CAP blends. (b) Scale expanded spectra.

6.5.1.2 Thermal analysis

The T_g of neat polymers is shown in **Table 6.2** and the observed T_gs are in good agreement with those reported in the past. In this section we have investigated the miscibility of the polymer blends and have investigated the extent of polymer-polymer interaction by fitting the data in the third power equation derived by Schneider (equation 3). The extent of interaction between NREP and other polymers was found to affect the release pattern. If the polymers are phase separated, then a burst release can be expected due to dissolution of one polymer. However, it was observed that as the extent of interaction increased (quantified in terms of K_1 value) the release mechanism was diffusion controlled (discussed in section 6.5.2).

6.5.1.2 a NREP-Zein

The films cast from NREP-Zein blends showed distinct transparent and opaque regions indicating phase separation and this was reflected in thermal analysis with appearance of two T_gs for all compositions as seen in **Fig. 6.8 (a)**. The lower T_g corresponding to the NREP rich phase and the higher one for phase rich in Zein was observed. The T_g *vs* composition plots (**Fig. 6.8 b**) did not show consistent composition dependence. T_g for Zein shifted to a higher value (169-170°C) from 164.4°C while opposite results were observed for the NREP rich phase wherein the T_g shifted to a value lower than 121.2°C. The shift in T_g of amorphous Zein films from 165°C to higher value (~170°C) due to conformational change from random coil to α and β form leading to partial crystallization is reported in the past [77]. Presence of moisture cleaves the intra and / or intermolecular bonding in Zein contributing to these effects. The fall in T_g of NREP could be due to the presence of Zein molecules in between the polymer chains. Since both Zein and NREP are proton-accepting polymers they do not interact, which results in immiscibility.

The thermal analysis revealed that NREP-Zein exist in phase separated forms. So the use of NREP-Zein blends for drug delivery would show pH dependent behavior at all compositions investigated. This would result due to the protonation of pyridine

nitrogen in acid buffer indicating a possibility of burst release. Hence to attain the sustained gastric release of CA, large amounts of Zein would be required along with NREP. The other option would be incorporation of a third polymer exhibiting better miscibility with NREP. This was investigated from the CA release experiments.

Table 6.2 Glass transition temperatures of neat polymers

Polymer	T_g observed (° C)	T_g reported (° C)	Reference No.
EL	164	157,160, 162	[71,73, 83]
ES	172.8	163, 171, 179	[71, 83, 84]
EC	135.8	133.4, 125	[1, 85, 86]
NREP	121.2	----	
HPMCP	137	~150	[87]
CAP	153.75	140, 160-170	[56, 88-91]
Zein	164.4	156,164,165	[77,92,93]

Table 6.3 Parameters of the Schneider equation

Blend	$K=T_{g1}/T_{g2}$	K_1	K_2	(K_1-K_2)
NREP-EC	0.89	-0.62	0.52	-1.14
NREP-ES	0.70	-0.08	0.47	-0.55
NREP-EL	0.72	-0.07	0.74	-0.75
NREP-HPMCP	0.88	0.01	1.78	-1.79
NREP-CAP	0.79	1.05	2.45	-1.40

6.5.1.2 b NREP-EC

The NREP-EC blends at all compositions show a single T_g as seen in the **Fig. 6.9 (a)**. The experimentally obtained values of T_g show large negative deviations from the values of T_g calculated by Fox equation (**Fig. 6.9 (b)**). T_gs for all blend compositions are within 3^0C and do not vary with composition. The extent of interactions was quantified by fitting the data in Schneider equation (**Fig. 6.9 (c)**) and the values of parameters K_1 and K_2 obtained were -0.62 and 0.59 respectively (see **Table 6.3**). The negative deviation from additivity reflects weak intermolecular interactions between blend components and is reflected in $K_1 < 0$. Since EC contains only cellulosic hydroxyl groups, weak interactions with polybase, NREP, are only to be expected. The polymer chains undergo conformational redistribution to establish hetero contacts responsible for miscibility, which is reflected in $K_2 > 0$. This conformational redistribution leads to change in entropy with increase in free volume resulting in fall in T_g of the blend compositions in comparison to the predictions based on volume additivity. The parameter K_2 is difference in effects of redistributions predominantly in environment of component 1 and component 2 respectively. $K_2 > 0$ reflects more conformational changes occurring in NREP than in EC. This is expected from bulky / rigid cellulosic structure of EC compared to NREP. The FTIR spectrum of the blend shows weak hydrogen bonding between EC and NREP. The spectrum reveals hydrogen bonding between cellulosic hydroxyls of EC with hydroxyls from HEMA and carbonyls from HEMA and MMA comonomers in NREP. These interactions between NREP and EC suggest that blends would exhibit pH dependent dissolution behavior at all compositions. Under acidic conditions dissolution of NREP would result due to ionization of tertiary nitrogen, as the intermolecular hetero interactions between these polymers are weak.

The thermal analysis revealed that the extent of interaction between NREP-EC was lower as seen from the K_1 value. So the use of these blends for drug delivery would show pH dependent behavior at all compositions investigated. This would result due to the protonation of pyridine nitrogen in acid buffer. Also alteration in blend composition

would not affect the initial release pattern, as the extent of interaction is lower. This was validated from the CA release experiments.

6.5.1.2 c NREP-EL and NREP-ES blends

The NREP-EL and NREP-ES blends formed clear films at all compositions in MeOH–$CHCl_3$ (1:2 v/v) solution indicating miscibility. Normally interactions between polyacids and polybases result in charge transfer with polyelectrolyte salt formation. The T_g *vs* composition curves for such systems result in large positive deviations from additivity [50]. As seen in **Fig. 6.10 (a)** the NREP-EL blends show a single composition dependent T_g located between the values of T_g for the pure components. The T_g values obtained experimentally show negative deviations from the weight average values of T_gs reflecting weak interaction between the two polymers (**Fig. 6.10 (b)**).

The data treatment by Schneider equation (**Fig. 6.10 (c)**) for NREP-EL blends resulted in K_1 and K_2 values of -0.07 and 0.748 respectively (**Table 6.3**). The value $K_1 < 0$ is expected since negative deviations for blend T_gs are observed from volume additivity. The value $K_1>0$ is seen in miscible polymer blends where the strong interactions within blend components overcome the cohesive forces within components [27]. The intramolecular interactions contribute to stiffening of the flexible bonds [27]. Both EL and NREP exhibit self associations which have to be overcome to effect favorable interactions between the two. From the FTIR spectrum for NREP-EL blend it was concluded that the hetero contact between the acid hydroxyl of EL and nitrogen of pyridine was established but was weak in nature and did not result in salt formation. The shift of band at 1601 cm^{-1} in NREP to 1603 cm^{-1} seen in NREP-EL was not observed in case of NREP-EC. The value of K_1 (-0.07) in NREP-EL is greater blend than in the case of NREP-EC (-0.62) due to stronger interaction exhibited by EL than EC with NREP.

The charge density influences formation of hetero contacts. NREP has low content of basic monomer as compared to the large number of carboxylic acid present in EL. Hence to establish miscibility, conformational redistribution has to take place in the environment of NREP component which is reflected in $K_2 > 0$. Also the strong

intramolecular association between hydroxyl of HEMA in NREP with pyridine nitrogen is overcome to establish the hetero contact with acid hydroxyl of EL. Although the hydroxyl groups in EL interact with the pyridyl nitrogen in NREP, the interaction is weak. The energetic interactions between NREP-EL are largely influenced by the entropy changes resulting from conformational rearrangements contributing to negative deviations from additivity. As a result, charge transfer and consequently stiffening of the donor chain does not take place. Similar observations for polystyrene and poly (α methyl styrene) were reported by Schneider [27]. The T_g of the blend did not show positive deviations from the Fox equation as observed in the case of EL-Eudragit® E as discussed in our next chapter. However $K_2 > 0$ indicates more conformational change in NREP environment than in EL. Hence T_g of the blend is greater than T_g for neat NREP. Weak interactions contribute to miscibility of NREP with EL and these blends are expected to exhibit pH dependent behavior. Since the interaction between EL and NREP is weak, it could be overcome by protonation of pyridyl nitrogen in acidic buffer, resulting in dissolution of NREP. The hetero interactions between NREP and EL in the blend delay ionization of NREP and slow down the overall rate of dissolution.

The NREP-ES blends show a single T_g for all compositions indicating a single phase behavior (**Fig. 6.11 (a)**). The experimentally obtained values of T_g show large negative deviation from the weight average T_gs calculated by Fox equation (**Fig. 6.11 (b)**). The values of T_g of NREP-ES blends do not exhibit variation with composition and lie within a narrow range of 121 to 123 ^{0} C. The content of methacrylic acid in ES (33%) is less than that in EL (50 %) [72] and hence weak interaction with NREP is expected than that exhibited by EL. The K_1 and K_2 values obtained for NREP-ES blends are -0.08 and 0.47 respectively (see **Fig. 6.11 (c)** and **Table 6.3**). The nature of hetero contact between NREP-ES is similar to that in case of NREP-EL as seen from the FTIR analysis and this is reflected in K_1 values, with K_1 slightly lower in ES blends(-0.08) than EL (-0.07). However, the lower charge densities on NREP and ES contribute to conformational redistributions to establish hetero contact for favorable energetic interactions. Since parameter K_2 reflects difference in effects of redistributions predominantly in environment of component 1 and component 2 respectively, the lower value compared to EL suggests substantial contributions from

component 2. The large negative deviations from additivity can be explained based on the conformational changes contributed by both components in NREP-ES blends and hence increase in free volume of these systems. The value of K_2 is low in case of NREP-ES blends than NREP-EL blends and this is again attributed to lesser conformational rearrangements undergone by EL as compared to ES due to higher charge density in the former.

Since the interaction between NREP-EL and NREP-ES is weak, it could be overcome by protonation of pyridyl nitrogen in acidic buffer, resulting in dissolution of NREP. However, the extent of interaction between NREP-EL and NREP-ES is greater than NREP-EC so the delay in ionization of NREP and slower rate of dissolution is expected than in NREP-EC blends. These assumptions were investigated from the CA release experiments (section 6.5.2).

6.5.1.2 d NREP-CAP and NREP-HPMCP blends

NREP at all compositions forms a clear film with CAP and HPMCP in MeOH-$CHCl_3$ (1:2v/v) solvent mixture. **Fig. 6.12 (a) and 6.12 (b)** show the DSC thermograms and T_g *vs.* composition plot for NREP-HPMCP. The NREP-HPMCP blends showed a single composition dependent T_g which increased with increase in HPMCP content indicating miscibility. As in earlier cases, the NREP-HPMCP blends too showed negative deviations from the weight average T_g values calculated by Fox equation reflecting weak interactions between these polymers. The FTIR showed partial protonation of pyridine to pyridinium in NREP-HPMCP blends. This interaction is stronger than that seen for NREP-EL systems. The data treatment in the frame work of Schneider equation (**Fig. 6.12 (c)**) yielded $K_1 = 0.01$ and $K_2 = 1.78$. This value of K_1 (0.01) is larger than that observed in case of NREP-EL (-0.07) indicating stronger interaction than in the case of NREP-EL blends and this is supported by the FTIR analysis (see **Table 6.1**). The positive value of K_1 reflects the favorable energetic interactions by hetero contact formation in NREP and HPMCP. However, this does not result in complete charge transfer. There is no stiffening of donor chain; the deviations of blend T_gs from predictions of Fox equation are still negative. The value of K_2 reflects

large contributions towards the blend T_g arising from the conformational redistributions in the polymer chains to establish the hetero contact. The positive values of K_2 (1.78) reflect the predominant contribution from NREP in conformational changes. This is expected as HPMCP is a bulky cellulosic structure with methyl and propyl substitution. NREP-HPMCP blends would not show rapid ionization at the acidic and basic pH due to stronger interactions. The compositions can be tailored to attain either burst or diffusion controlled release.

The NREP-CAP blends show a single composition dependent T_g indicating a single phase behavior (**Fig. 6.13 (a)**). The values of T_g observed experimentally (**Fig. 6.13 (b)**) are comparable to the values calculated by Fox equation and only a small negative deviation (less than 2°C) is seen at all compositions. The T_g values for CAP-NREP blends gave the best fit to Fox equation amongst all systems studied. The plots for data treatment by Schneider equation are shown in **Fig. 6.13 (c)** and **Table 6.3**. The FTIR spectrum shows formation of partial pyridinium in case of NREP-CAP and the value K_1 = 1.058, highest amongst all the systems investigated reflects that the interactions between the two components are most prominent amongst the systems investigated. The higher K_1 value as seen in case of NREP-CAP than NREP-HPMCP shows more interaction in NREP-CAP. This is expected as CAP does not have any side group substitutions like HPMCP contributing to steric hindrance. The K_2 value 2.45 shows the predominant contribution from NREP in conformational changes and this is expected as CAP has a bulky / rigid cellulosic structure as compared to NREP Since the interactions are strong, it appears that NREP-CAP blends would not show rapid ionization at the acidic and basic pH. Hence a diffusion-controlled release is anticipated.

As seen from **Table 6.3** the values of fitting parameters K_1 and K_2 were larger in case of NREP-CAP and NREP-HPMCP than those seen in case of NREP-EL, even though EL has high charge density. The structural symmetry due to presence of cellulose ring and aromatic ring in CAP / HPMCP and NREP respectively, helps in establishing better hetero contact between these systems than that in case of NREP-EL. The probability of charge transfer is influenced by favorable structural symmetry factors in polyacceptor / polydonor which contribute to increased hetero contacts [26, 27, 78].

The NREP-HPMCP and NREP-CAP blends have shown higher interactions than that seen in NREP-Zein, NREP-EC and NREP-EL and NREP-ES blends. Also these showed partial conversion of pyridine to pyridinium units, so it is expected that these blends would show slow ionization of NREP. This would retard the release of CA as compared to that seen from NREP-EC and NREP-EL blends. This was confirmed from the release experiments.

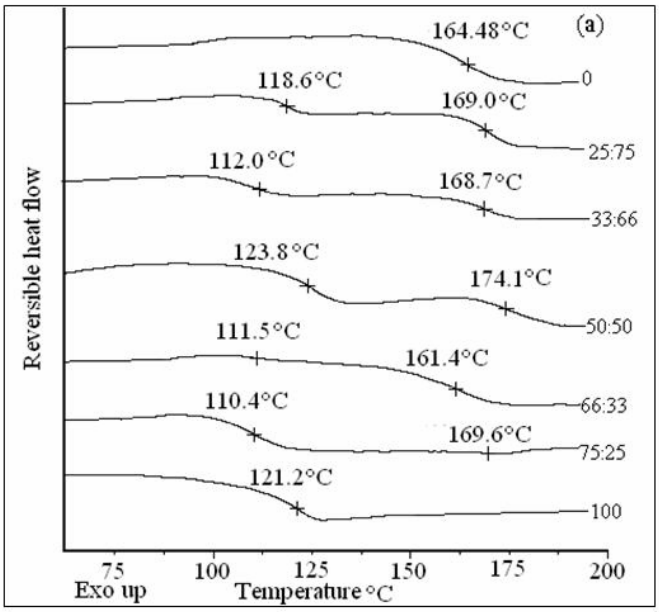

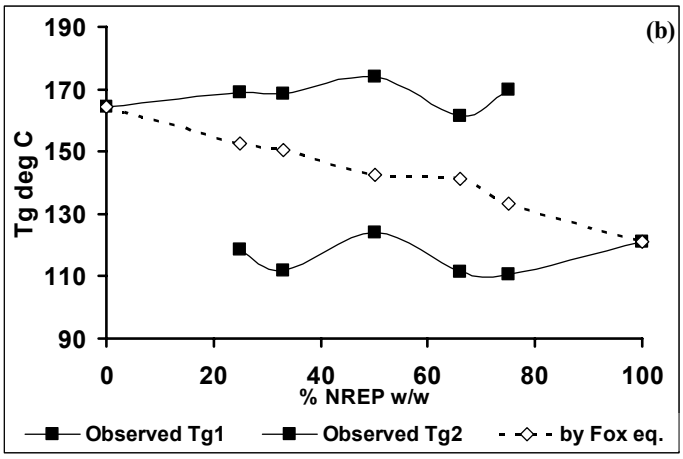

Fig.6.8. Thermal analysis of NREP-Zein blends: (a) Thermograms for NREP-Zein blends. (b)T_g *vs*. composition plot.

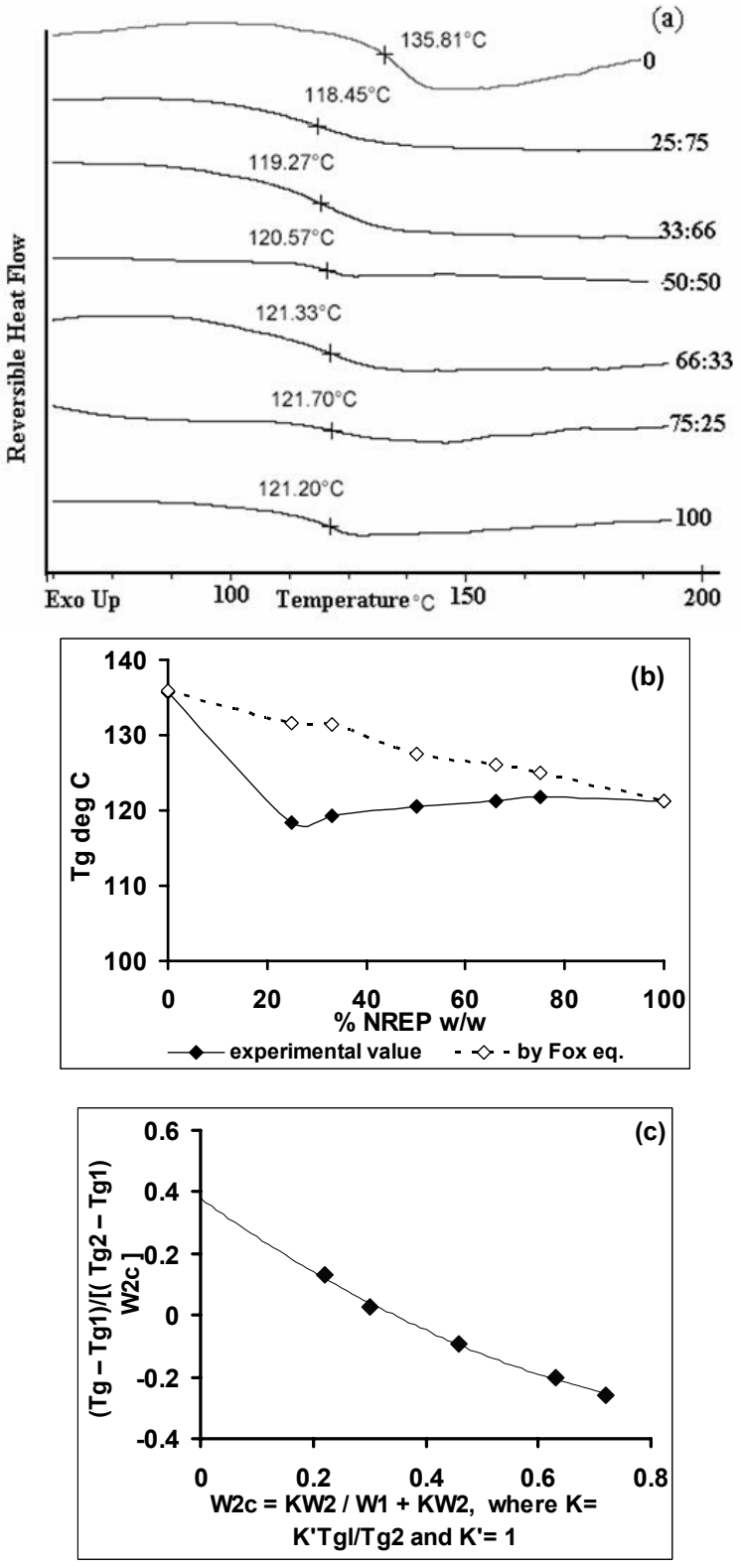

Fig.6.9. Thermal analysis of NREP-EC blends: (a) Thermograms for NREP-EC blends. (b)T_g *vs*. Composition plot. (c)T_g composition data as per equation 3.

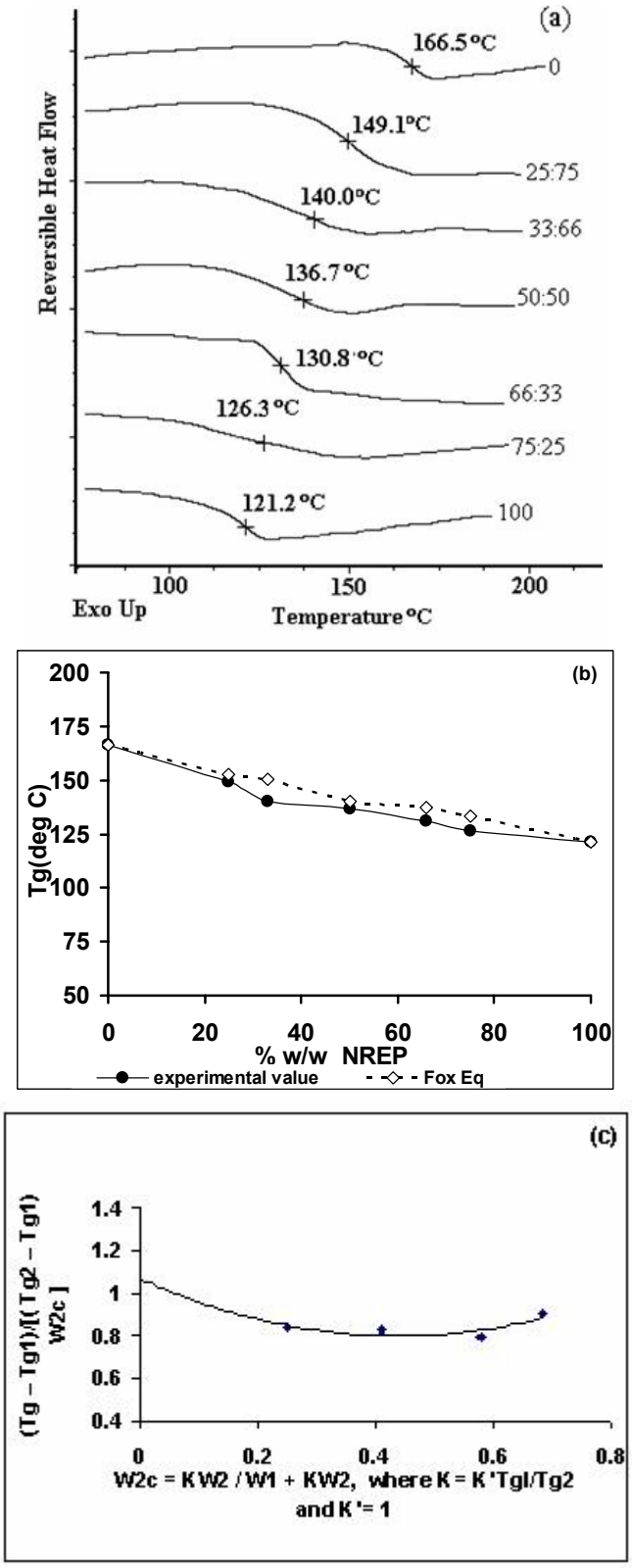

Fig.6.10 Thermal analysis of NREP-EL blends: (a) Thermograms for NREP-EL blends. (b)T_g *vs* Composition plot. (c)T_g composition data as per equation 3.

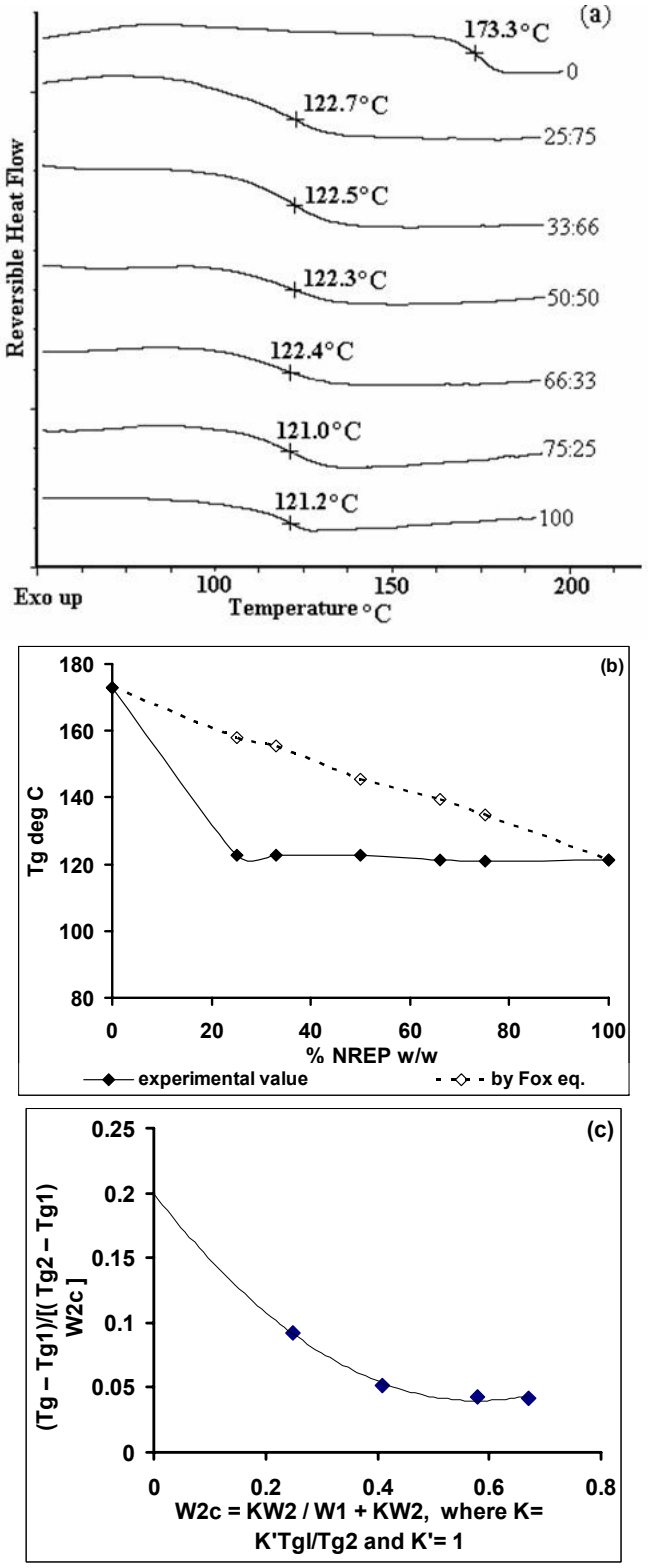

Fig.6.11Thermal analysis of NREP-ES blends: (a) Thermograms for NREP-ES blends. (b)T_g *vs* Composition plot. (c)T_g composition data as per equation 3.

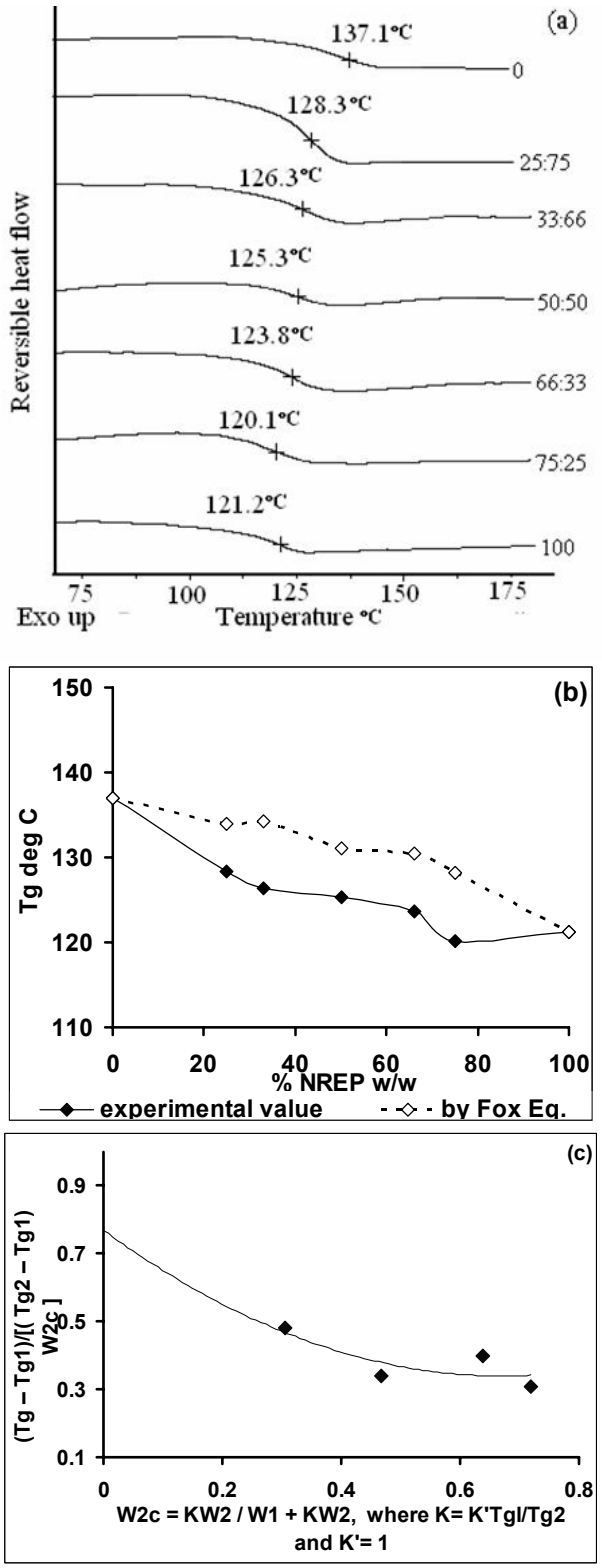

Fig. 6.12. Thermal analysis of NREP-HPMCP blends: (a) Thermograms for NREP-HPMCP blends. (b)T_g *vs* Composition plot. (c)T_g composition data as per equation 3.

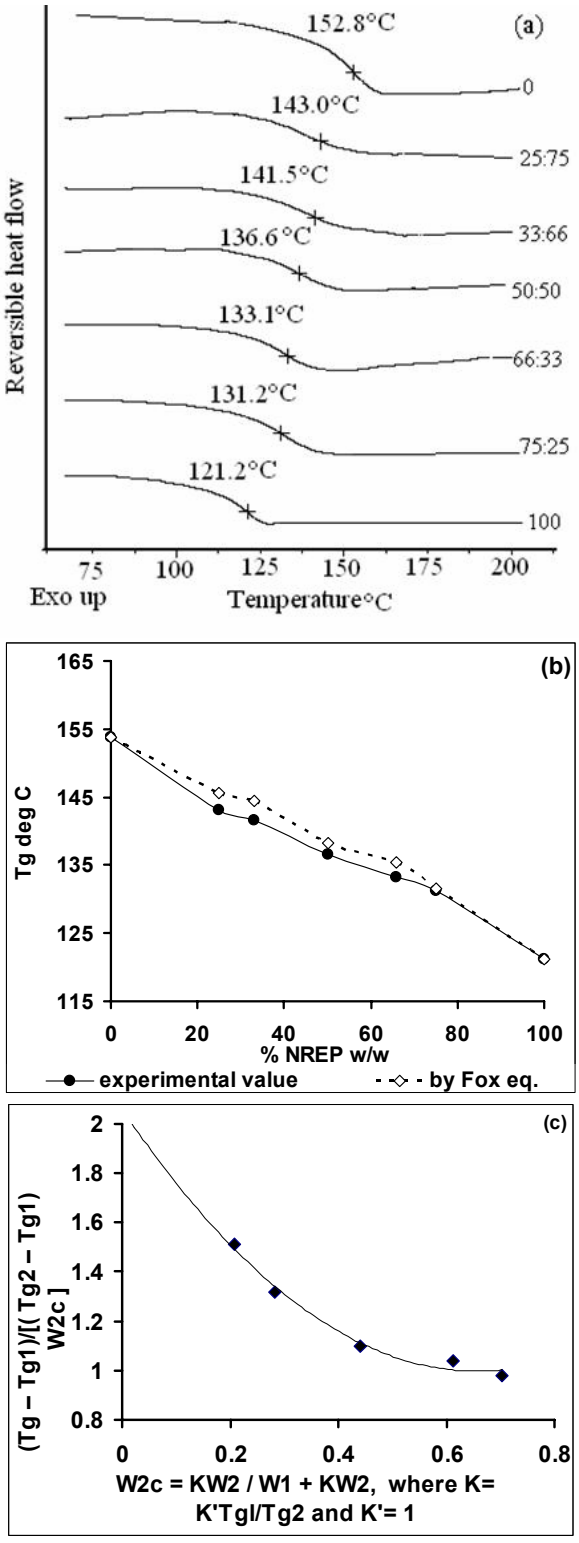

Fig.6.13. Thermal analysis of NREP-CAP blends. (a)Thermograms for NREP-CAP blends. (b) T_g *vs* Composition plot. (c)T_g composition data as per equation 3.

6.5.2. Drug release from micro particles

From the DSC and FTIR studies it was evident that interactions of NREP with enteric and pH independent polymers reported herein were of a limited magnitude so that the blends were miscible but did not result in complexation. An advantage of using NREP as the cationic polymer in combination with enteric polymers is that a hydrophobic coherent film can be formed. The hydrophobic nature of the film coating is particularly useful in case of CA. CA tends to gel in presence of moisture and loses its bioavailability. The FTIR studies of NREP blends with all polymers showed presence of free pyridine groups. These blends are expected to show pH dependent behavior at acidic pH as the free pyridine is available for protonation under acidic conditions. Hence these blends are ideal for the gastric delivery of CA which is absorbed primarily in upper gastric region.

Another advantage of using these hydrophobic blends is that the coated micro particles can be used in the pediatric formulations such as granules for reconstitution. These coatings would provide sustained release and also taste masking.

The dissolution of CA from NREP based micro particles is shown in **Fig. 6.14**. NREP releases about 80 % CA in 30 min and 90 % in 60 min. The release of CA from NREP based micro particles occurs by dissolution of the polymer resulting from protonation of pyridine nitrogen. Both the formulations (F1 and F2 see compositions in **Table 6.4**) show a very rapid release at pH 1.2. It has been reported in the past that once the solvent has diffused into the glassy polymer reaching a critical concentration, the polymer chain disentanglement dominates and the polymer begins to dissolve [79]. Various models for dissolution of polymer have been proposed in the past [80].The dissolution of glassy polymer involves three steps. In the first step solvent molecules diffuse into the polymer matrix. This is followed by the relaxation of polymer chains initiated by the penetration of the solvent molecules and formation of a swollen gel. In the final step polymer chains diffuse out from the gel into the solvent reservoir. This is shown in **Fig. 6.15** adapted from Peckan et al [80]. In the present investigation CA is dispersed in the matrix of NREP polymer and the dissolution of the polymer causes the release of CA into surrounding buffer medium.

The sorption of the solvent in glassy polymer can follow Fickian, anomalous or Case II transport mechanism. In most cases as the sharp penetration front of solvent progresses it separates the glassy core from the swollen rubbery phase. The magnitude of polymer relaxation is dependent on relative rate of solvent penetration resulting in either Fickian or non Fickian behavior [81]. In the present investigation the content of NREP was high in all the polymer blend formulations (F3-F19) as seen from **Table 6.4**. So it is expected that all of CA would be released immediately due to dissolution of NREP. However the blending of NREP with EC, EL and CAP has resulted in sustained release of CA. The release is sustained in blends due to the polymer-polymer interactions. The release rate decreases as K_1 increases. The interactions of NREP with these polymers result in slow progress of the buffer in the glassy core causing the delay in release. FTIR analysis shows the presence of free pyridine groups of NREP even after blending. The ionization of this free pyridine results in rapid penetration of the acidic buffer resulting in swelling and then dissolution of the polymer. Desorption of the dissolved polymer is seen as pores in the SEM images (**Fig. 6.16-6.24**). The drug release is also governed by the polymer relaxation. We observed that as the extent of interaction between NREP blends increased, the rate of buffer penetration slowed in comparison to the rate of polymer relaxation. This is reflected in the release attaining Fickian pattern for NREP-HPMCP and NREP-CAP blends where the extent of interaction is highest as seen from the highest K_1 value obtained for this blend (**Table 6.3**). The release profiles from polymer blends are discussed in more detail in following sections. **Table 6.4** shows the formulations based on NREP and its blends. The release exponents are summarized in **Table 6.5**. In the present system the CA release has to be attained in gastric region before the transit in small intestine and hence a rapid release followed by slow release for 3-4 hrs is preferred. It may be noted that the burst release is favored in targeted and pulsatile drug delivery systems [82].

Table 6.4 CA formulations based on NREP and its blends with polymers

Formulation	CA (mg)	NREP (mg)	Other polymers	Total Polymer content
F1	600	1200	------	1200 mg
F2	600	600	------	600 mg
F3	600	300	Zein 600 mg	900 mg
F4	600	300	Zein 150 mg and EC 25 mg	475 mg
F5	600	300	EC 45 mg	345 mg
F6	600	300	EC 60 mg	360 mg
F7	600	300	EC 100 mg	400 mg
F8	600	200	ES 100 mg	300 mg
F9	600	200	EL 100 mg	300 mg
F10	600	300	HPMCP 50 mg	350 mg
F11	600	200	HPMCP 200 mg	400 mg
F12	600	200	HPMCP 300 mg	500 mg
F13	600	300	HPMCP 25 mg and EC 15 mg	340 mg
F14	600	300	HPMCP 25 mg and ES 15 mg	340 mg
F15	600	230	CAP 70 mg	300 mg
F16	600	270	CAP 50 mg	320 mg
F17	600	300	CAP 25 mg	325 mg
F18	600	300	CAP 20 mg and EL 20 mg	340 mg
F19	600	300	CAP 25mg and EC 15 mg	340 mg

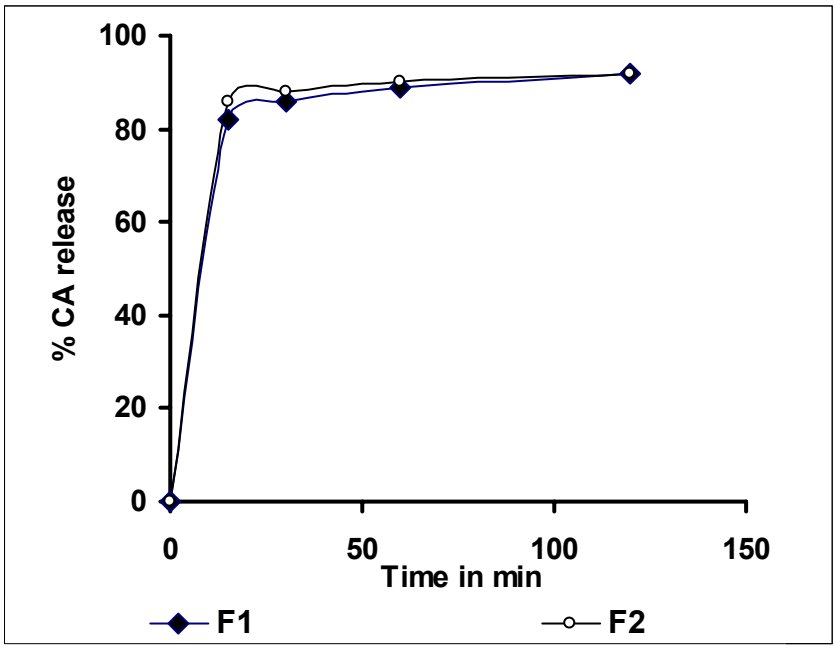

Fig. 6.14 CA release from NREP microparticles

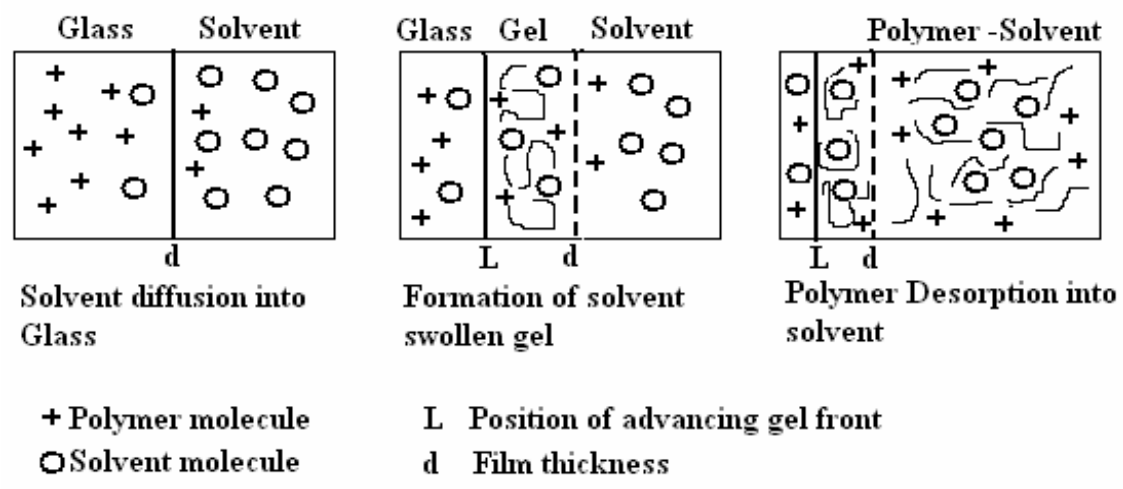

Fig. 6.15 Schematic of polymer dissolution

6.5.2.1. NREP-Zein based CA micro particles

The DSC analysis had shown that NREP and Zein were immiscible at all compositions and FTIR spectrum showed that NREP-Zein did not interact. So it is expected that formulations based on NREP-Zein would exhibit rapid initial release due to dissolution of NREP at acidic pH. Assuming this, higher concentration of Zein was used in formulation, F3, for making micro particles to sustain CA release at gastric pH. The evaluation of the extent of interaction between polymers by Schneider equation provides a measure to decide the blend composition for formulations. For polymers, which exhibit better interactions, lower amount of polymer in blends can lead to the same release profile. **Fig. 6.16** shows release of CA from NREP-Zein based micro particles. The NREP-Zein blends released 45 %, 54 %, 60 %, 65 % and 80 % of CA in 30, 60, 120,180 and 240 min respectively. The release of CA from F3 for 4 hrs was found to be desirable; however the total amount of polymer required for attaining the desired release pattern was very high (900mg).

In an attempt to achieve similar release profiles with lower polymer loading, formulation F4 based on NREP, Zein and EC blends was designed. From the FTIR and thermal analysis it was found that EC was miscible with NREP. The extent of interaction between NREP-EC was quantified in Schneider equation and the interaction was low but was better than that exhibited by Zein, which was immiscible. So EC was introduced along with Zein in blends with NREP assuming it would be useful to sustain the CA release. The total polymer content in F4 was lowered to 475 mg from 900 mg as seen for F3. The lowering of Zein content in F4 resulted in slight increase of CA in basic pH than in F3 as seen in **Fig. 6.16**. Also it may be noted that the interaction between NREP-EC is better than NREP-Zein and so the initial release of formulation F3 and F4 is comparable in spite of reduction in total polymer content. The SEM of the micro particles of F4 (**Fig. 6.16 b**) shows the numerous voids created due to the dissolution of NREP. The release data on treatment with equation 4 put forth by Ritger and Peppas [31] showed that value of k was higher, indicative of burst release and this further validates the assumptions drawn from the DSC and FTIR studies for miscibility of NREP with Zein. The higher release was expected due to immiscibility of NREP and

Zein due to dissolution of NREP at acidic pH. The release of CA was sustained up to 4 hr in formulation F3 and F4 when compared to the release from micro particles based on NREP as seen in formulation F1 and F2.

Table 6.5 Kinetic parameters based on Equation (4)

Formulation	Kinetic parameter (*k*)	Release exponent (*n*)	Correlation coefficient
F3	51.2	0.20	0.98
F4	58.8	0.26	0.97
F5	66.0	0.24	0.98
F6	66.0	0.23	0.91
F7	60.2	0.18	0.93
F8	55.0	0.20	0.96
F9	55.9	0.21	0.86
F10	60.0	0.22	0.97
F11	46.7	0.42	0.99
F12	35.1	0.46	0.99
F13	-----	-----	------
F14	----	-----	----
F15	34.6	0.43	0.98
F16	39.0	0.44	0.97
F17	----	-----	-------
F18	53.7	0.17	0.97
F19	47.8	0.40	0.93

(----- the release was fast so parameters could not be calculated)

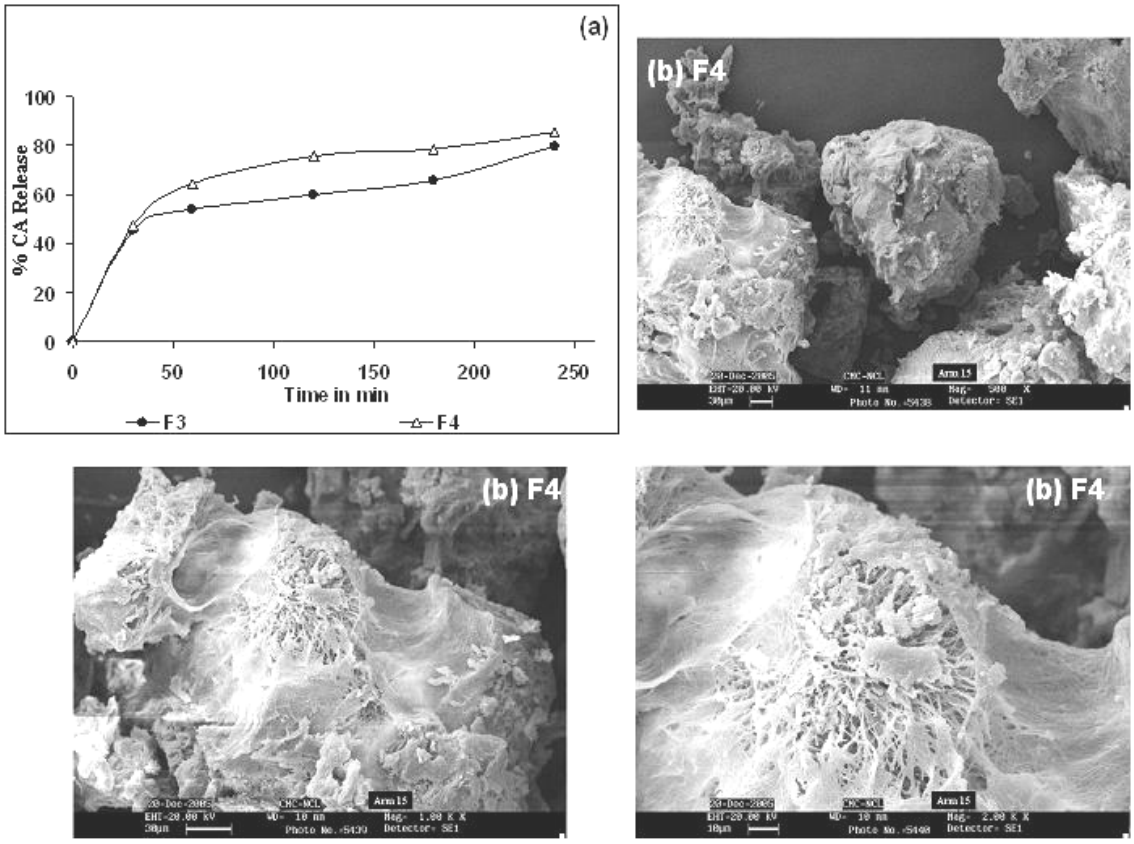

Fig.6.17 (a) CA release from NREP-Zein blends, 11(b)

SEM for microparticles (F4)

6.5.2.2. NREP-EC based CA micro particles

The DSC and FT-IR analyses show that NREP-EC blends are miscible but exhibit weak interactions. Since the interaction is weak, it can be overcome by the interaction between the acidic buffer and NREP, hence a burst release followed by slow release thereafter is expected. The release for F5 and F6 based on NREP-EC is shown in **Fig. 6.17 (a)**. The rapid release from these micro particles initially is from the pores generated by dissolution of NREP as seen in the SEM images of the micro particles (**Fig. 6.17b**). The higher value of kinetic parameter for F5 and F6 (k= 66, each) further substantiates this. After the initial rapid release of CA, it is slowed thereafter due to the effect of NREP-EC miscibility and the interactions between the two. With slight increase in concentration of EC in F6, the release was slowed after 2 hrs (**Fig. 6.17a**). The weak interaction of NREP with EC makes it difficult to control initial rapid release. This is because the extent of interaction is weak and the pyridine from NREP will protonate and cause initial rapid release. To verify this, dissolution of CA from another formulation (F7) with higher content of EC (100 mg) was investigated. The initial release from F7 was comparable to F5 and F6 but retardation in CA release after 1 hr was observed. Any further increase in EC quantity to lower the initial release would not be useful, also this would result in further retardation of release after 1 hr than that seen in F7 and this was not desirable. Such formulations were not attempted. Instead polymers showing increased interaction than EC with NREP were investigated.

6.5.2.3. NREP-ES based micro particles

The values of fitting parameters K_1 and K_2 for the system NREP-ES are higher than those for NREP-EC exhibiting better miscibility with NREP than EC. The FTIR spectrum of NREP-ES showed a shift for the pyridine group from 1597 to 1601 cm^{-1} indicating participation of pyridine nitrogen in hydrogen bonding with ES. Such behavior was not seen in FTIR spectrum of NREP-EC. It was expected that the initial release from NREP-ES blend would be lower than that observed for NREP-EC system and this has been confirmed. However the value of fitting parameter K_1 derived from

Schneider equation is not very high for NREP-ES blends hence the initial burst release would be observed even on altering the blend compositions at acidic pH. Since the hydrogen bonding between NREP-ES is weak and does not result in generation of pyridinium units, it would be overcome by acidic buffer responsible for this release pattern.

Release of CA from formulations based on NREP-ES micro particles (F8) is shown in **Fig. 6.18 (a)**. The higher interaction exhibited by NREP-ES than NREP-EC enabled us to retard CA release from F8 than that seen for F5 and F6. It may be noted that the total polymer loading in F8 is 300 mg as compared to 345 mg and 360 mg in F5 and F6 respectively. Also in comparison to the formulations based on Zein (F3 and F4) the NREP-ES based formulation at lower content of polymer was able to retard the CA release. This is attributed to the enhanced interaction between NREP-ES than in NREP-EC/ Zein.

The initial burst effect is seen for F8 and this is because of lower K1 values. The FTIR spectrum of NREP-ES shows that the pyridine nitrogen is not converted to pyridinium units and this free nitrogen ionizes at acidic pH. The data treatment by Peppas and Ritger equation showed higher value of *k* for F8 (55.0) and the SEM images (**Fig. 6.18 (b)**) for micro particles after dissolution further substantiate this. The release is slowed thereafter reaching 74 % at the end of 4 hr for ES based formulation due to the interaction of ES with NREP. Further formulations with increase in ES would result in retarding the dissolution of CA and were not attempted. Also a lowering of ES would result in further increase in initial release, which was not desirable. Since K_1 is not very high for NREP-ES blends the initial burst release at acidic pH cannot be suppressed by altering the blend compositions and similar observations were seen in case of NREP-EC. Hence such formulations were not attempted either.

There is marked difference in the morphology of the NREP-ES based micro particles as compared to those from NREP-Zein and NREP-EC. The NREP-ES blend is less porous as compared to the NREP-Zein and NREP-EC as seen from **Fig. 6.16-6.17**.

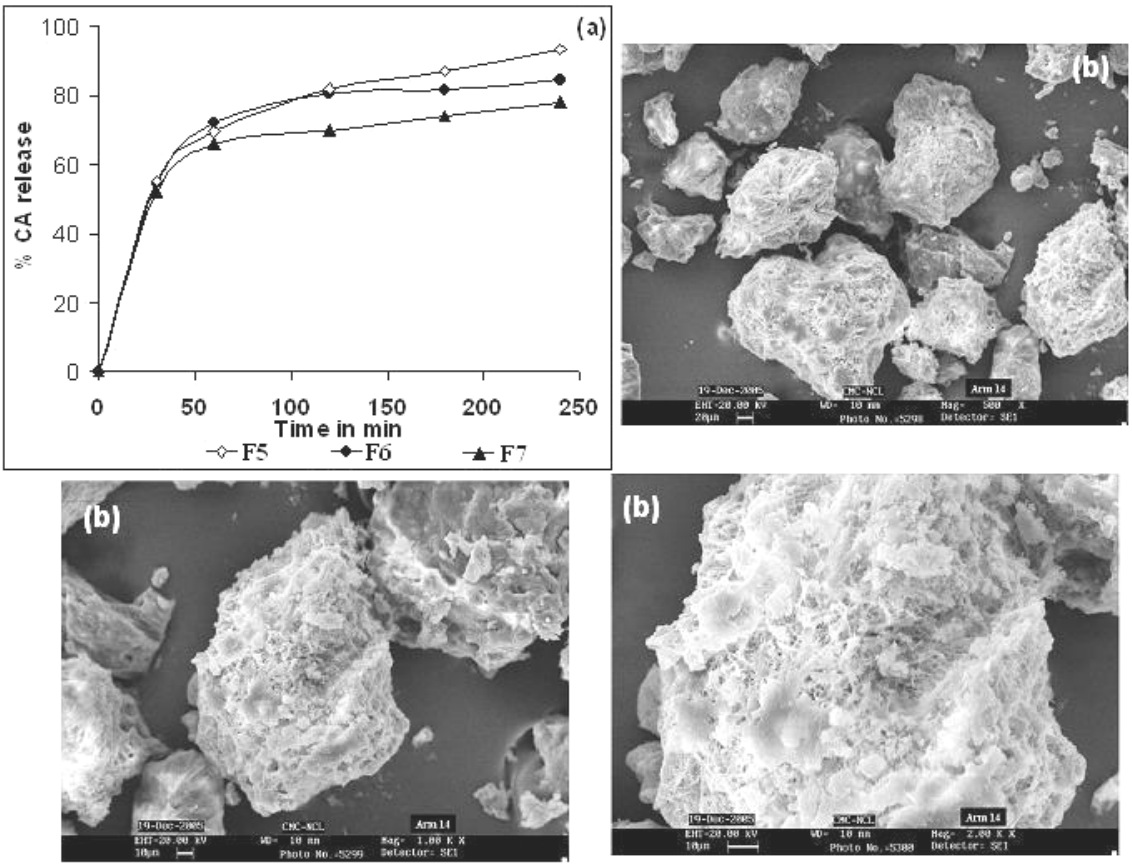

Fig.6.17 (a) CA release from NREP-EC blends, 12(b) SEM for microparticle F6 formulation

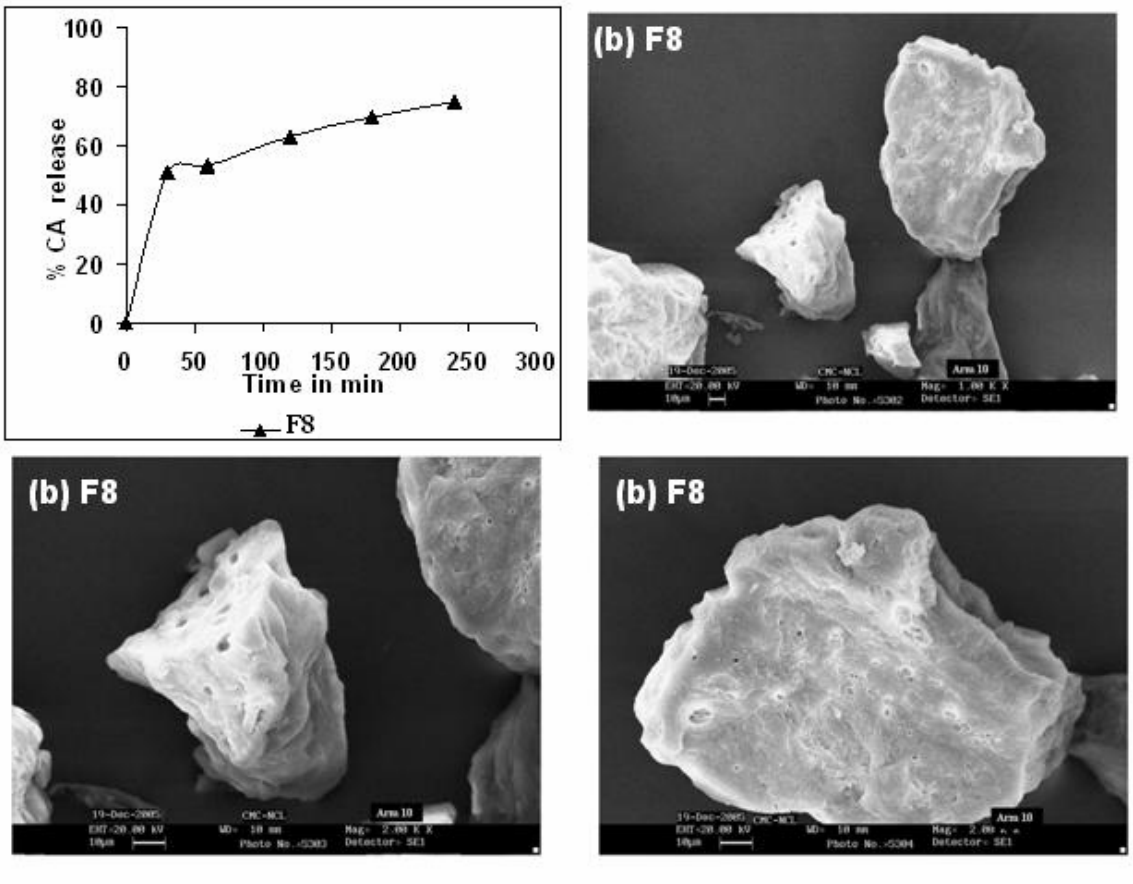

Fig. 6.18 (a) CA release from NREP-ES blends, 13 (b) SEM for microparticles (F8)

6.5.2.4. NREP-EL based micro particles

Release of CA from formulations based on NREP-EL micro particles (F9) is shown in **Fig. 6.19 (a)**. The higher interaction exhibited by NREP-EL than NREP-EC enabled us to retard CA release from F9 than that seen for formulations F2 to F7. It may be noted that the total polymer loading in F9 is 300 mg as compared to higher loading in F2 to F7. The F9 formulation showed rapid initial release of CA in 30 mins. which was retarded thereafter. From the NREP-EL FTIR spectrum it is seen that pyridine nitrogen participates in hydrogen bonding (shift from 1597 to 1601 cm^{-1}). However it is not converted to pyridinium units, so once this bonding is overcome by the acidic buffer protonation of pyridine nitrogen will contribute to burst release. The extent of burst is lower in NREP-EL than that seen in NREP-EC as hydrogen bonding with pyridine is not seen in NREP-EC. The data treatment by equation 4 showed higher value of *k* for F9 (55.9). The SEM images (**Fig. 6.19(b)**) for micro particles after dissolution further substantiate this. The release is slowed thereafter reaching 80 % at end of 4 hr for EL based formulation due to the interaction of EL with NREP. Further formulations with increase in EL, would result in retarding the dissolution of CA and were not attempted. Also a lowering of EL would result in further increase in initial release, which was not desired. Since K_1 is not very high for NREP-EL blends, the initial burst release at acidic pH can not be suppressed by altering the blend compositions and similar observations were seen in case of NREP-EC. Hence such formulations were not attempted either.

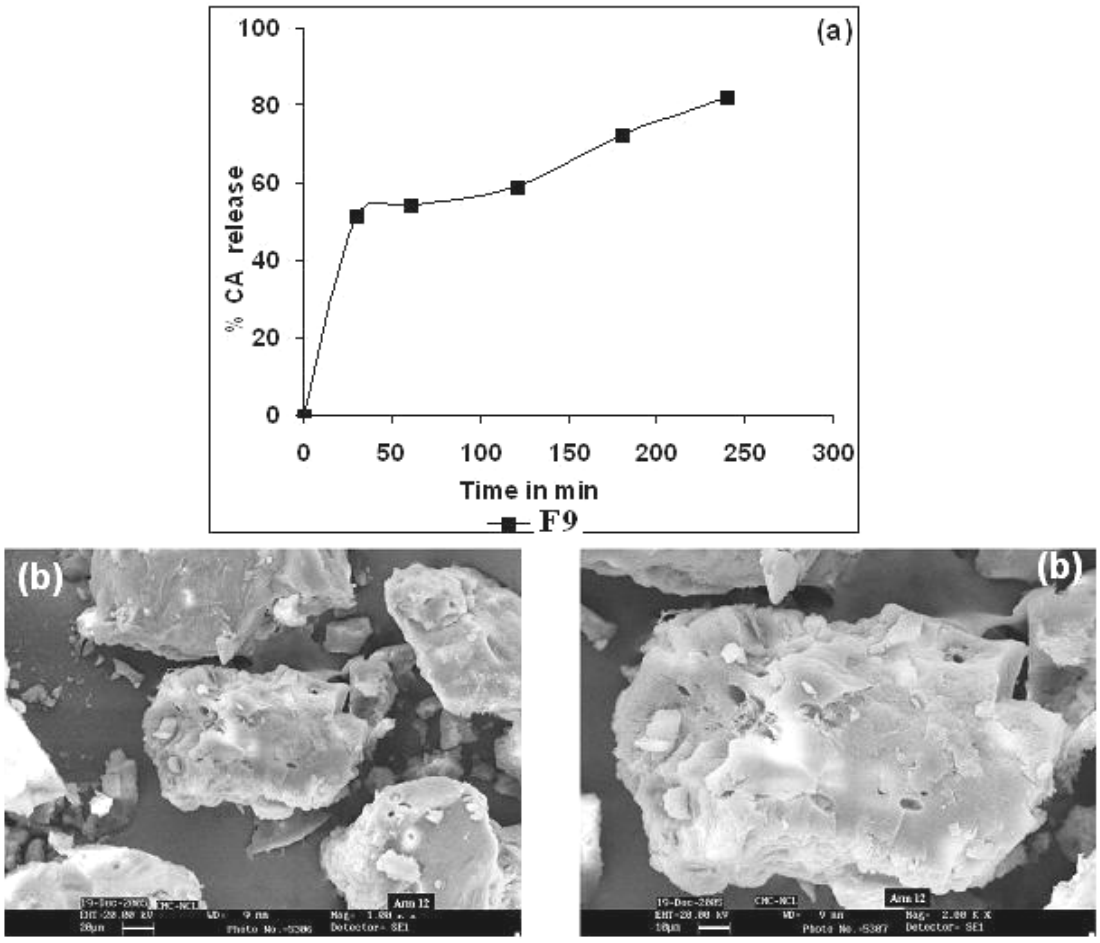

Fig. 6.19 (a) CA release from NREP-EL blends, 11 (b) SEM for microparticles (F9)

6.5.2.5. NREP-HPMCP based CA micro particles

HPMCP exhibited the strongest interaction with NREP than the other three polymers as seen from the K_1 and K_2 values obtained from the Schneider plots for NREP-HPMCP blends. The FTIR analysis revealed that pyridine nitrogen is partially converted to pyridinium units by HPMCP (slight appearance of new band at 1637 cm^{-1}). This indicates that all of pyridine nitrogen is not free and therefore protonation of pyridine by acidic buffer would be affected suppressing the initial rapid release. Hence incorporation of smaller quantities of HPMCP would retard the drug release. Formulation F10 containing 50 mg of HPMCP and 300 mg of NREP was considered for sustaining CA release.

The release from F10 is shown in **Fig. 6.20 (a)**. At this composition the CA release is 53 %, 65 %, 76% and 87 % after 30, 60, 120 and 240 min respectively. Due to stronger interaction between NREP- HPMCP even small amount of HPMCP (50 mg) blended with large amounts of NREP (300 mg) was effective in retarding the release up to 4 hr. As compared to the earlier formulations the release from F10 is retarded and this can be attributed to the higher extent of interaction between NREP-HPMCP than the other blends investigated. The release data treatment by the equation 4 showed the value of kinetic parameter k= 60 indicating the initial burst release. As seen from the FTIR spectrum part of pyridine present in NREP-HPMCP blend is free and is available for protonation under acidic conditions and is responsible for this initial burst release. The SEM of micro particle is shown in **Fig. 6.20 (b)**. The surface morphology of NREP-HPMCP micro particles is very different from that observed in earlier formulations (F4, F5, F8 and-F9). It shows less porosity than that seen for earlier formulations.

To validate the earlier assumption that extent of interaction affects the release pattern from the polymer blends, two formulations F11 and F12 with higher HPMCP content were made. As the content of HPMCP in the blend increased, the amount of free pyridine in NREP-HPMCP is lowered. So the dissolution of NREP in acidic buffer would be retarded resulting in suppressed initial release. From the T_g *vs* composition plots it was seen that at 50:50 % w/w NREP-HPMCP the experimental T_g values were

close to weight average T_gs. Assuming good miscibility of the polymers at this blend ratio, the above polymer compositions were considered. The CA release from these micro particles is shown in **Fig. 6.21**. The F11 formulation containing 200 mg HPMCP showed faster release than F12 containing 300 mg HPMCP. Both formulations F11 and F12 showed retarded release as compared to F10. The release data of formulation F11 and F12 on treatment with Peppas equation showed that release from these formulations was diffusion controlled as evidenced by n = 0.42 and 0.46 respectively (k = 46 and 35.1 respectively). Release from these formulations is largely affected by the miscibility and interactions within these polymers. Since the extent of interaction between NREP-HPMCP is highest as seen in higher values of parameter K_1 and K_2 as shown in **Table 6.3** the diffusion-controlled release is expected. Due to better miscibility of NREP-HPMCP at above-mentioned compositions a burst release is not observed as seen in formulations based on Zein, EC, ES and EL. The SEM images (**Fig. 6.21(b)**) show that some part of NREP has dissolved creating craters (the particle does not show void / empty space) but the drug is largely release from the matrix.

To validate if low extent of interaction results in rapid release from blends, a third component exhibiting lower interaction with NREP was introduced. Two formulations F13 and F14 with EC and ES respectively were formulated. The release from these was compared to validate if extent of interaction would alter release pattern. The release of CA from F13 when compared with F10, F11 and F12 was faster as seen from the **Fig. 6.21**. The formulation F13 released 76 % in 30 min and 97% after 4hr. The higher release from F13 can be explained from the lower extent of interaction between NREP-EC as observed from the K1 values calculated by Schneider equation. From **Table 6.3** it can be seen that K_1 for NREP-EC is lower than NREP-HPMCP. This accounts for higher CA release from F13. The extent of interaction between polymers plays an important role in tailoring the drug release. The SEM for formulation F13 (**Fig. 6.21**) shows voids generated as a result of dissolution of CA and NREP. This is also reflected in the 76 % CA released in 30 min.

The release of CA from F14 was slightly retarded as compared to the release from F13 as seen from **Fig. 6.20(a)**. It was observed that the K_1 value for ES was greater than that obtained for EC and hence slight retardation was observed. The extent

of interaction contributes to the observed release pattern. The SEM for F14 shows formation of pores contributing to the initial burst release (**Fig. 6.21**). The SEM for F14 shows that it has a closed porous structure and an open pore structure is seen in case of F13 formulation (**Fig. 6.21**).

When polymers constituting the blends exhibit weak interaction, the release pattern shows a significant burst followed by sustained release. When the interactions are strong, the burst is suppressed and the release is also sustained. The extent of initial burst release and the period of sustained release can be manipulated by the judicious choice of polymer constituents as well as the polymer compositions. The parameters of the Schneider equation thus provide a guideline for the choice of the blend constituents. Reverse enteric polymers are commonly used when the drug is to be released immediately at gastric pH. Sustained release can be achieved by blending NREP with enteric and pH independent polymers. A wide range of polymeric excipients are miscible with NREP and exhibit different interactions quantified in terms of the fitting parameters K_1 and K_2 in Schneider equation.

For sustained release of CA at gastric pH NREP blends provide the pH responsive release desired. Incorporation of HPMCP, which has relatively higher extent of interaction helps to sustain the release over extended time periods at lowest possible loading. Ethylcellulose and Eudragit S, which exhibit weak interaction with NREP when blended along with HPMCP, enhance initial release of CA without altering the release at later stage. Since the absorption window of CA is limited to the upper gastric region this release pattern is most preferred.

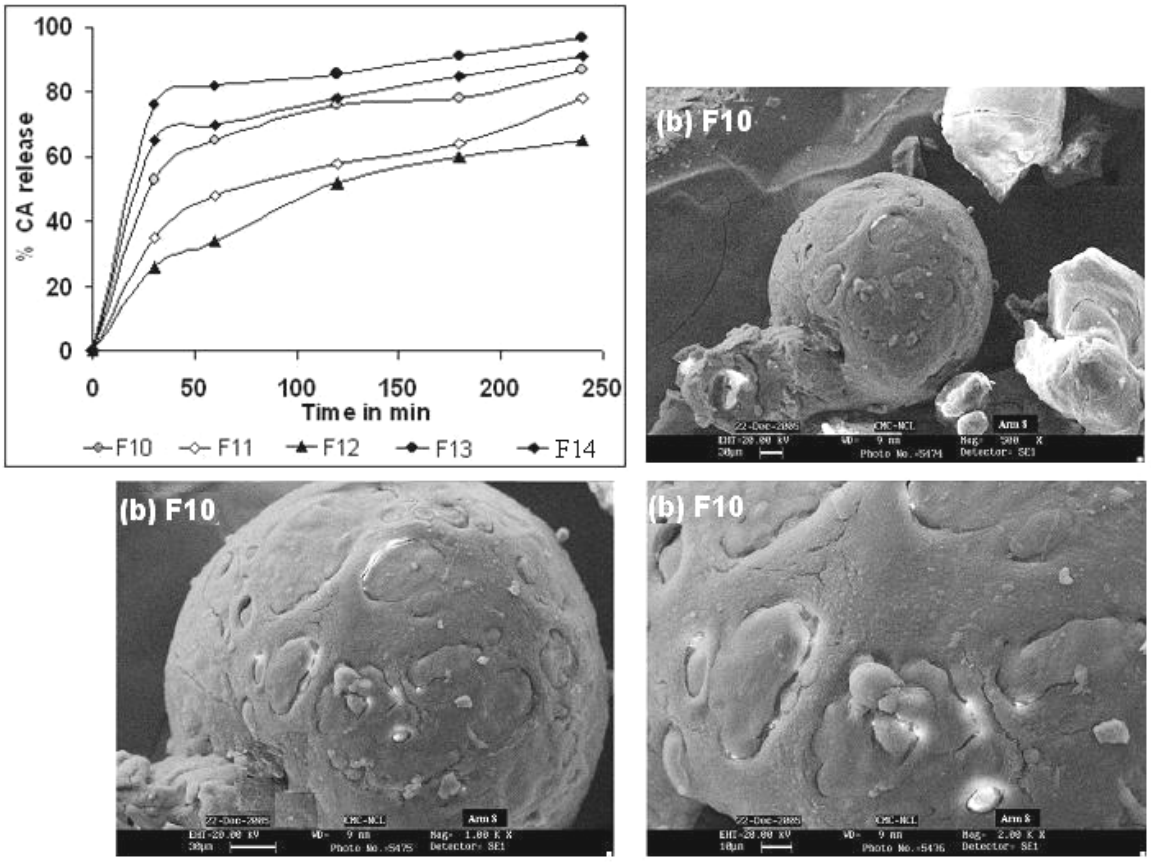

Fig. 6.20 (a) CA release from NREP-HPMCP blends, 14 (b)

SEM for micro particles (F10)

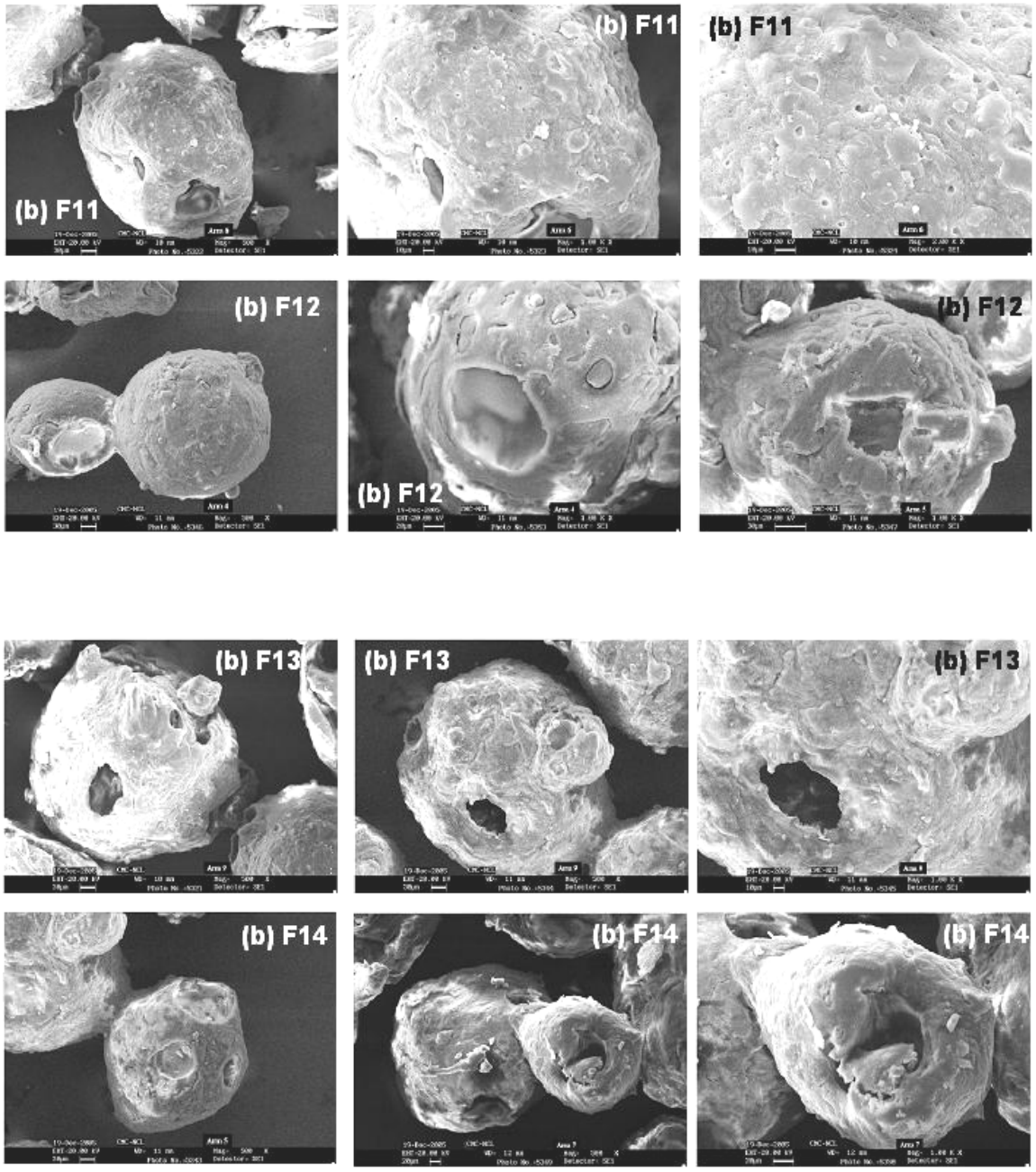

Fig. 6.21 SEM for microparticles (F11-14)

6.5.2.6. NREP-CAP based CA micro particles

CAP exhibited strongest interaction with NREP amongst all polymers investigated herein. This is evident from the K_1 and K_2 values obtained. Incorporation of smaller quantities of CAP would therefore retard the drug release effectively. The NREP-CAP blends had shown partial conversion of pyridine to pyridinium units as seen from FTIR spectrum. The availability of free nitrogen in NREP-CAP blends is lower and hence the release would be retarded, as pyridine nitrogen protonation in acid buffer would be affected. Hence CA micro particles based on the NREP-CAP were made incorporating lower amount of CAP (F15) as seen from **Table 6.4**. The release of CA from NREP-CAP blends is shown in **Fig. 6.22(a)**. This blend composition is very close to the composition, which exhibited values comparable to the weight average T_gs calculated by Fox equation. So it was expected that at this concentration the drug release should be retarded substantially. From the **Fig. 6.22(a)** it can be seen that the release of CA has indeed been retarded as a result of the strong interaction between CAP with NREP. At the end of 3 hrs in gastric pH, 57 % CA was released and further 8 % was released at the end of 4 hrs. As compared to earlier compositions the total polymer content in F15 is lowest 300 mg and yet it has retarded the CA release. Any further increase in CAP would result in further retardation. The SEM image of micro particles (**Fig. 6.22(b)**) at this composition does not reveal pores as observed in earlier compositions suggesting that the drug release is diffusion controlled without the desorption of polymer. The value of diffusional exponent; n = 0.43 and k = 34 from Peppas and Ritger equation confirmed this. From these results it is clear that release from micro particles is diffusion controlled. These results substantiate our predictions drawn from the extent of interaction from Schneider equation. Since CA has limited absorption window the above release profile would be too slow. Another formulation F16 with lower amount of CAP was formulated (**Table 6.4**). The NREP-CAP blend at this composition did not show initial burst though the release was faster than F15. The release data on treatment with equation 4 showed the value of diffusional exponent; n = 0.44 and k = 39 indicating a diffusion controlled release. F15 released 74 % of CA at the end of 4 hr. To enhance the release further, CAP was lowered and NREP content

was increased as seen in **Table 6.4** for F17. At this polymer blend composition the effect of NREP is dominant and CA is released almost immediately (83 %) in 60 min with burst release. The SEM image (**Fig. 6.23(b))** of the micro particles after dissolution shows formation of large pores due to rapid dissolution of NREP at gastric pH 1.2.

To optimize the release, further addition of a third component, which exhibited lower interaction with NREP, was considered. As seen from **Table 6.3** all polymers exhibited lower values of K_1 than NREP-CAP indicating lower interactions with NREP hence we chose EL as enteric and EC as pH independent polymer for incorporation in NREP-CAP blends to increase the release rate.

CA micro particles from polymer blends containing NREP, EL and CAP (F18) were formulated. The release for this formulation is shown in **Fig. 6.22(a)** and it was faster than that for F15 and F16. The release profile of F18 when treated according to Peppas and Ritger equation showed higher value of k= 53.7 indicating burst release. This rapid initial release is expected as EL has weak interaction with NREP than CAP. However the release was slowed after 2 hr reaching 75 % at end of 4 hr. This is because both CAP and EL exhibit interactions with NREP causing slow ionization of the polymers thereafter. The SEM images for micro particles are shown in **Fig. 6.24**.

To overcome this, another formulation of CA (F19) containing EC, which exhibits lower interaction with NREP than EL and CAP, was used. The release for F19 was faster than that for F18 as expected with 81 % release after 4 hr. The release profile of F11 when analyzed according to Peppas and Ritger equation showed that the diffusional exponent approached 0.43 (n=0.40) and k=47.8. The slight increase in CAP content from 20 mg in F18 to 25 mg in F19 has resulted in diffusion-controlled release due to strong interaction between CAP-NREP. However the higher value of k = 47.8, suggests initial burst release which may be due to weak interaction of EC with NREP.

When polymers constituting the blends exhibit weak interactions, the release pattern shows a significant burst followed by sustained release. When the interactions are strong, the burst is suppressed and the release is also sustained. The extent of initial burst release and the period of sustained release can be manipulated by the judicious choice of polymer constituents as well as the polymer compositions. The parameters of the Schneider equation thus provide a guide line for the choice of the blends

constituents. Reverse enteric polymers are commonly used when the drug is to be released immediately at gastric pH. Sustained release can be achieved by blending NREP with enteric and pH independent polymers. A wide range of polymeric excipients are miscible with NREP and exhibit different interactions quantified in terms of the fitting parameters K_1 and K_2 in Schneider equation.

For sustained release of CA at gastric pH NREP blends provide the pH responsive release desired. Incorporation of CAP which has relatively higher extent of interaction helps to sustain the release over extended time periods at lowest possible loading. Ethylcellulose and Eudragit L, which exhibits a weak interaction with NREP when blended along with CAP enhances the initial release of CA without altering the release at later stage. Since the absorption window of CA is limited to the upper gastric region this release pattern is most preferred.

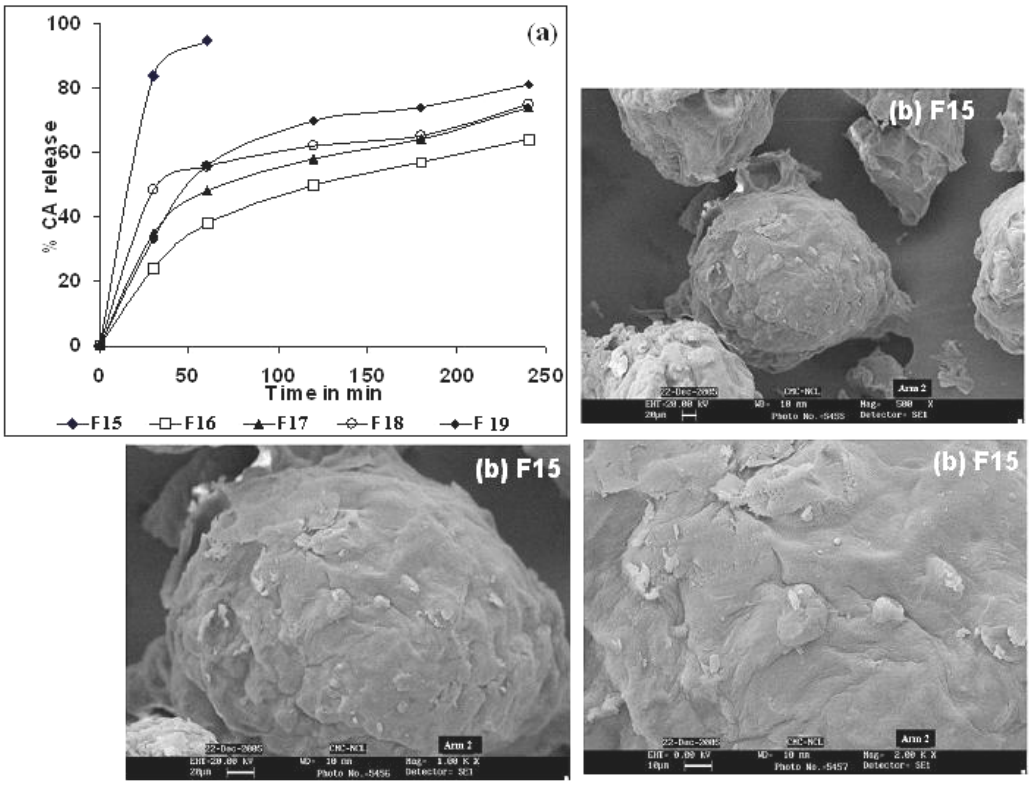

Fig. 6.22 (a) CA release from NREP-CAP, 12 (b) SEM for micro particles (F15)

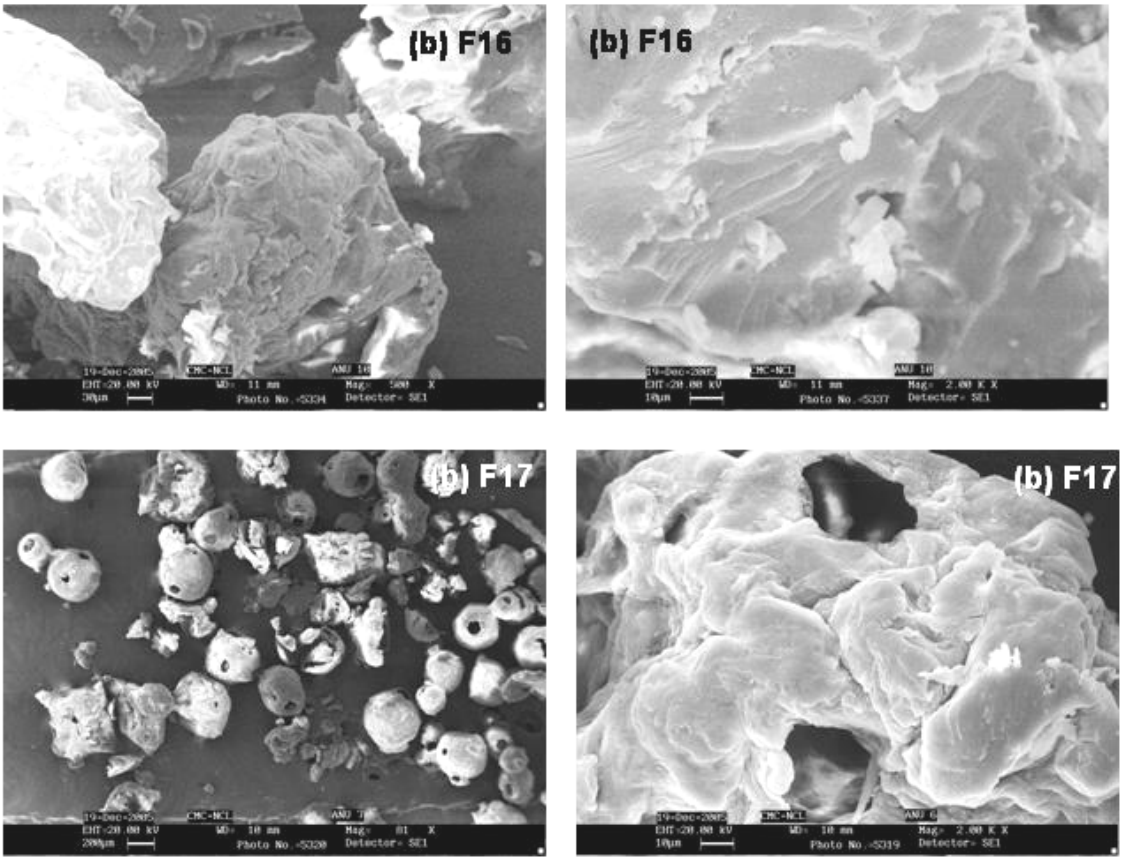

Fig. 6.23 (b) SEM for micro particles (F16-F17)

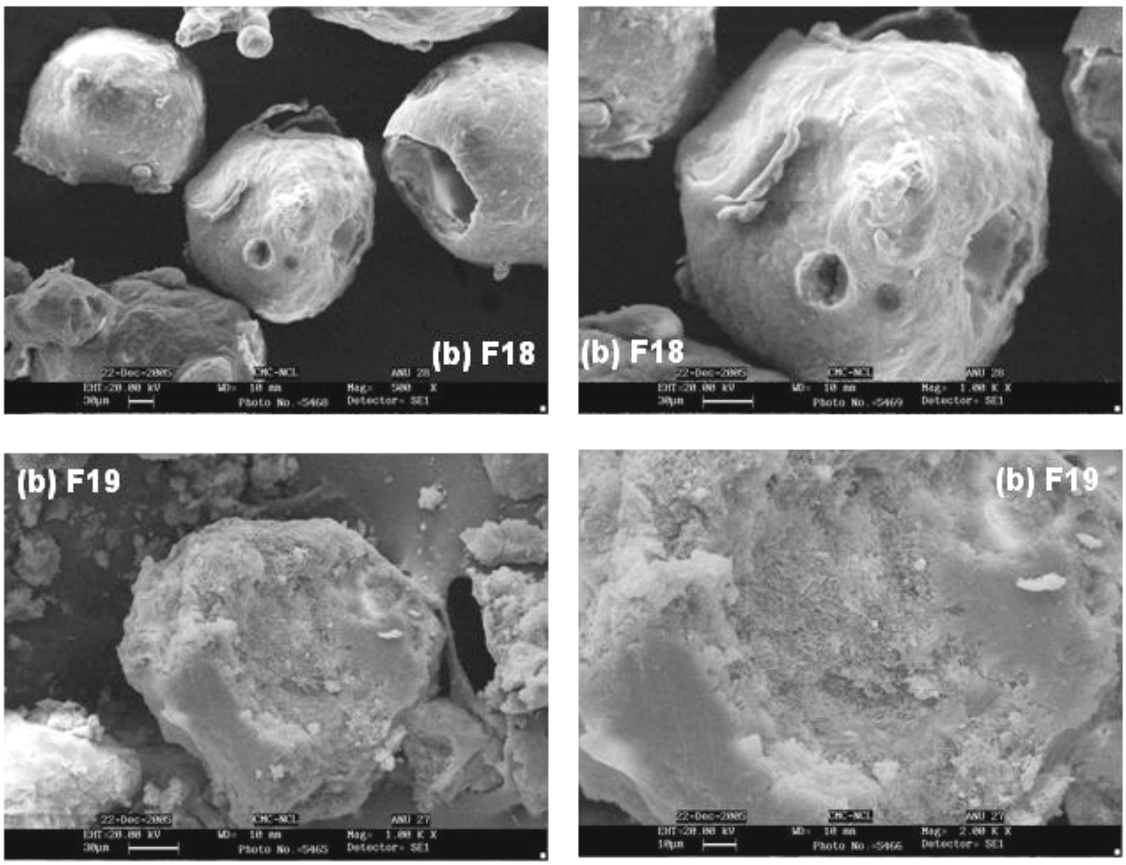

Fig. 6.24 (b) SEM for micro particles (F18 and F19)

6.4. CONCLUSION

The release rates of the drugs from the excipient blends can be systematically varied only if the blends are miscible. NREP was found to be miscible with EC, ES, EL, HPMCP and CAP at all compositions as evident from the appearance of single T_g in blends. This is governed by the degree of interactions between the blend constituents. The data treated by Schneider equation showed that the order of interaction of these polymers with NREP was CAP > HPMCP > EL > ES > EC. The nature of interaction between polymers affected the release. Release from blends containing CAP, which exhibits the strongest interaction is diffusion controlled even at low CAP content. Also blends of NREP-HPMCP exhibit diffusion-controlled release but the content of HPMCP required to attain the same is more than that required for CAP and this is due to lower interaction between NREP-HPMCP than NREP-CAP. Blends containing EC, which exhibit weak interaction showed fast release of CA due to dissolution of NREP. The understanding of interactions between the constituents of polymer blends from FTIR studies and quantification of the degree of interaction achieved by thermal analysis and evaluation of the parameters by Schneider equation has been exploited to tailor the release of Cefuroxime axetil in the gastric region. By judicious choice of polymers, which exhibit strong and weak interactions with NREP, different release patterns can be obtained. The blends reported here can be further tailored to attain the sustained release in intestinal region. The miscibility of reverse enteric and enteric polymers without complexation provides a new set of blends, which can be optimized to attain variety of release patterns from film coatings.

6.5. REFERENCES

1) R.C. Rowe Materials used in the film coating of oral dosage forms. In: A.T. Florence (Ed), Materials used in Pharmaceutical Formulation. Blackwell; Oxford, 1984. p. 2-34.
2) J.B. Dressman, G.M. Derbin, G. Ismailos, C. Jarvis, A. Ozturk, B.O. Palsson, T.A. Wheatley J. Controlled Rel 1995, 36, 251-260.
3) N.K. Ebube, AB. Jones, Int. J. Pharm. 2004, 272, 19–27.
4) M.A. Frohoff-Hulsmann, A. Schmitz, B.C. Lippold, Int. J. Pharm. 1999, 177, 69–82.
5) F. Lecomte, J. Siepmann, M.Walther, R.J. MacRae, R. Bodmeier, J. Controlled Rel. 2003, 89, 457–471.
6) J. Liu, S Lin, L Li, E. Liu, Int. J. Pharm. 2005, 298,117–125.
7) N. Nyamweya, SW Hoag. Pharm. Res. 2000, 17, 625-631.
8) L.A. Kanis, FC Viel, JS Crespo, JR Bertolino, A.T.N Pires, V. Soldi, Polymer 2000, 41, 3303–3309.
9) M. Mayo-Pedrosa, C. Alvarez-Lorenzo, A. Concheiro J. Therm. Anal. Cal. 2004, 77, 681–693.
10) J.S. Ahn, HK Choi, CS Cho. Biomaterials 2001, 22, 923-928.
11) C.G.L. Khoo, S Frantzich, A Rosinski, M Sjostrom, J. Hoogstraate Eur. J. Pharm. Biopharm. 2003, 55, 47–56.
12) J. Yin, K Luo, X Chen, VV. Khutoryanskiy Carbohydrate Polymers 2006, 63, 238–244.
13) H. Kim, R. Fassihi J. Pharm. Sci. 1997, 86, 323-328.
14) W. Gunder, BH Lippold, BC. Lippold, Eur. J. Pharm. Sci. 1995, 3, 203-214.
15) T. Yamada, H. Onishi, Y. Machida J. Controlled Rel. 2001, 75, 271–282.
16) S.M. Samani, H. Montaseri, A. Kazemi, Eur. J. Pharm. Biopharm. 2003, 55, 351–355.
17) C. Sanchez-Lafuente, MT Faucci, M Fernandez-Arevalo, J lvarez-Fuentes, AM Rabasco, P. Mura, Int. J. Pharm. 2002, 234, 213–221.
18) S.P. Lyu, R Sparer, C Hobot, K. Dang, J. Controlled Rel. 2005, 102, 679–687.

19) F. Siepmann, J. Siepmann, M. Walther, R.J. MacRae, R. Bodmeier, J. Controlled Rel. 2005, 105, 226– 239.
20) A. Dashevsky, K Kolter, R Bodmeier, Eur. J. Pharm. Biopharm. 2004, 58, 45–49.
21) M.Z.I .Khan, Z Prebeg, N. Kurjakovic, J. Controlled Rel. 1999, 58, 215–222.
22) M.G. Kulkarni, A.R. Menjoge, US 20050137372, 23 June, 2005
23) M.G. Kulkarni, A.R. Menjoge, US 20050136114, 23 June, 2005
24) MLL Lorenzo-Lamosa, M. Cuna, JL Vila-Jato, D Torres, M. J. Alonso, J. Microencap. 1997, 14, 607-616.
25) H.A. Schneider Glass Transition (Theoretical Aspects), The Polymeric Materials Encyclopedia. CRC Press, Inc, 1996.
26) H.A. Schneider, Polymer, 1989, 30, 771-779.
27) H A. Schneider, J. Res. Natl. Inst. Stand. Technol. 1997, 102, 229-248.
28) A.R. Menjoge, MG. Kulkarni U.S. Patent Application US 2005281874, 22 Dec, 2005.
29) O. Olabishi, L.M. Robeson, M.T. Shaw, Polymer-polymer miscibility, Academic Press, INC (London) Ltd. 1979
30) M.J. Brekner, HA Schneider, HJ Cantow, Makromol. Chem. 1988, 189, 2085 - 2097.
31) P.L. Ritger, NA Peppas, J. Controlled Rel. 1987, 5, 23-36.
32) D. S. Roy, B D Rohera, Eur. J. Pharm. Sci. 2002, 16, 193–199
33) J. Arora., G. Jain, H. Sen, US Patent, US 5,948,440, 7 September 1999.
34) Ceftin Prescription Information, Physicians' Desk Reference 2003 pp 1918-1922
35) H. Sen, RS Kshirsagar, AR Menjoge, US Patent, US 6932981, 23 Aug 2005.
36) A. Finn, M. Straughn Meyer, J. Chubb, Biopharm. Drug Disposit. 1987, 8, 519-526.
37) C. J. Campbell, L. J. Chantrell, R. Eastmond, Biochem. Pharmacol. 1987, 36, 2317–2324.
38) N. Ruiz-Balaguer, A. Nacher, V.G. Casabo, M. Merino, Antimicrob. Agents. Chemother. 1997, 41, 445–448.

39) M.V. Risbud, A.A. Hardikar, S.V.Bhat, R.R. Bhonde, J. Control. Rel. 2000, 68, 23–30.

40) N.J. Joseph, S. Lakshmi, A. Jayakrishnan J. Control. Rel., 2002, 79, 71–79.

41) Y. Satoa, Y. Kawashimab, H. Takeuchib, H. Yamamotob, Y. Fujibayashi J. Control Rel. 2004, 98, 75– 85.

42) R. Wiwattanapatapeea, A. Pengnoob, M. Kanjanamaneesathianc, W. Matchavanicha, L Nilratanad, A. Jantharangsrie, J. Control. Rel., 2004, 95, 455–462.

43) S.K. Jain, A.M. Awasthi , N.K. Jain, G.P. Agrawal, J. Control. Rel. 2005, 107, 300– 309.

44) P.L. Bardonnet, V. Faivre, W.J. Pugh, J.C. Piffaretti, F. Falson, J. Control. Rel., 2006, 111, 1 – 18.

45) N. Talwar, H. Sen, J.N. Staniforth, US Patent, US 6261601, 17 July 2001.

46) N. Talwar, H. Sen, J.N. Staniforth, US Patent, US 6,960,356, 1 Nov 2005.

47) T. Tokumura, Y. Machida, J. Control. Rel., 2006, 110, 581 – 586.

48) D.S. Deutsch, J. Anwar, US Patent, US 4,897,270, 30 January 1990.

49) W. H. Jo, C. A. Cruz, D. R. Paul, J. Polym. Sci.: Part B: Polym. Phys. 1989, 27, 1057-1076.

50) M. Jiang, M. Li, M. Xiang, H. Zhou, Adv. Polym. Sci. 1999, 146, 121-196.

51) L.A. Utracki, Polymer alloys and blends, thermodynamics and rheology. Hanser Publishers, Oxford University Press, New York, 1990.

52) R.I. Moustafine, T.V. Kabanovaa, V.A. Kemenovab, G. Van den Mooterc J. Control. Rel. 2005, 103,191-198.

53) R.I. Moustafine, T.V. Kabanovaa, V.A. Kemenovab, G. Van den Mooterc Int. J. Pharm. 2005, 294, 113-120.

54) L.C. Cesteros, E. Meaurio, I. Katime, Macromolecules, 1993, 26, 2323-2330.

55) A. Torikai, S. Hiraga, K. Fueki, Poly. Deg. Stab. 1992, 37, 73-76.

56) V. Rao, P.V. Ashokan, M.H. Shridhar, Mater. Sci. Engg. A. 2000, 281, 213–220.

57) L.C. Cesteros, J.L. Velada, L. Katime Polymer, 1995, 36, 3183-3189.

58) J. Ruokolainen, G Brinke, O. Ikkala, Macromolecules, 1996, 29, 3409-3415.

59) O. Ikkala, J. Ruokolainen, M. Torkkeli, J. Tanner, R. Serimaa, G. Brinke, Colloids Surf A: Physicochem. Eng. Aspects 1999, 147, 241–248.

60) I. Iliopoulos, R. Audebert, Eur. Polym. J., 1988, 24, 171-175.

61) Y. Pan, F. Xue, Eur. Polym. J., 2001, 37, 247-249.

62) R.V. Yarapathi, S.M. Reddy, S. Tammishetti, Reac. Func. Polym. 2005, 64, 157–161.

63) S.H. Goh, S.Y. Lee, X. Zhou, K. L. Tan, Macromolecules 1998, 31, 4260-4264.

64) H. Kosonen, S. Valkama, J. Hartikainen, H. Eerika1inen, M. Torkkeli, K. Jokela, R. Serimaa, F. Sundholm, G. Brinke, O. Ikkala, Macromolecules 2002, 35, 10149-10154.

65) K.G. Duodu, H. Tang, A. Grant, N. Wellner, P.S. Belton, J.R.N. Taylor, J. Cereal Sci. 2001, 33, 261–269.

66) A. Katime, C.C. Iturbe. Hydrogen-bonded blends, The Polymeric Materials Encyclopedia. CRC Press, Inc. 1996.

67) J.K. Chen, S.W. Kuo, H.C. Kao, F.C. Chang, Polymer 2005, 46, 2354–2364.

68) D.E. Bugay, W.P. Findlay Pharmaceutical excipients: Characterization by IR, Raman, and NMR spectroscopy. Marcel Dekker, 1999.

69) V. Suthar, A. Pratap, H. Raval, Bull. Mater. Sci. 2000, 23, 215–219.

70) J.Y. Lee, P.C. Painter, M.M. Coleman. Macromolecules 1988, 21, 954-960.

71) F. Cilurzo, P. Minghetti, F. Selmin, A. Casiraghi, L. Montanari. J. Control. Rel. 2003, 88, 43–53.

72) A. H Kibbe, Handbook of Pharmaceutical Excipients, 3rd Edition, American Pharmaceutical Association 2000.

73) S.Y. Lin, C.M. Liao, G.H. Hsiue, R. C. Liang, Thermochim. Acta 1995, 245,153-166.

74) L.C. Cesteros, J.R. Isasi, I. Katime, Macromolecules 1993, 26, 7256-7262.

75) M.J. Krupers, F.J. Van Der Gaag, J. Feijent, Eur. P & N J. 1996, 32, 785-790.

76) M.V. Meftahi, J.M.J. Frechet, Polymer 1988, 29, 477 - 482.

77) J. Macoshi, S. Nakamura, K. Murakami, J. App. Polym. Sci. 1992, 45, 2043-2048.

78) H.A. Schneider, Polym. Bulletin 1998, 40, 321-328.

79) B. Narasimhan, N.A. Peppas, Macromolecules 1996, 29, 3283-3291.

80) O. Pekcan, S. Ugur, Y. Yllmaz, Polymer 1997, 38, 2183-2189.

81) P. Lee, C.J. Kim, J. Membrane Sci., 65, 1992, 77-92

82) X. Huang, C.S. Brazel, J. Control Rel., 2001, 73, 121–136.

83) S.Y. Lin, H. L. Yu, J. Polym. Sci: Part A: Polym. Chem. 1999, 37, 2061–2067

84) S.K. Jain, A.M. Awasthi, N.K. Jain, G.P. Agrawal, J. Control. Rel. 2005, 107, 300– 309.

85) N. Pearnchob, R. Bodmeier, Eur. J. Pharm. Biopharm. 2003, 56, 363–369.

86) M.I. Beck, I. Tomka, E. Waysek, Int. J. Pharm. , 1996, 141,137-150.

87) G. Sertsou, J. Butler, A. Scott, J. Hempenstall, T. Rades, Int. J. Pharm. 2002, 245, 99-108.

88) E.P. Segundo, A. Ganem-Quintanar, V. Alonso-Perez, D. Quintanar-Guerrero, Int. J. Pharm. 2005, 294, 217–232.

89) A. J.M. Valente, H.D. Burrows, A.Y. Polishchuk, M.G. Miguel, V. M. M. Lobo. Eur. Polym. J. 2004, 40,109–117.

90) V. Rao, P.V. Ashokan, M.H. Shridhar, Polymer 1999, 40, 7167–7171.

91) V. Rao, P.V. Ashokan, J.V. Amar, J. App. Polym. Sci. 2002, 86, 1702–1708.

92) R. Shukla, M. Cheryan, Ind. Crops Products 2001,13, 171–192.

93) P.B. Donnell, C. Wu, J. Wang, L. Wang, B. Oshlack, M. Chasin, R. Bodmeier, J.W. McGinity, Eur. J. Pharm. Biopharm. 1997, 43, 83-89.

CHAPTER 7

Miscibility of NREP & Enteric Polymers Mechanistic Investigations

7.1. INTRODUCTION

Polymer blends in general are immiscible, since entropy of mixing is small and does not compensate for unfavorable endothermic heat of mixing [1]. Miscibility is achieved by incorporating functional groups in either or both components of blends. The interactions between functional groups, which could be electrostatic, dipole-dipole resonance, proton transfer and hydrogen bonding, result in exothermic mixing leading to miscibility [2]. Strong interactions could be achieved by incorporating proton accepting pyridyl and dimethylamino groups and proton donating carboxyl and hydroxyl groups in the polymers constituting the blends. Thus poly (4-vinyl pyridine) is immiscible with polystyrene, but is miscible with poly (4-hydroxy styrene). Poly (4-hydroxy styrene is immiscible with poly (styrene-co-4-vinyl pyridine) when the latter contains 20 % 4-VP, but is miscible when the pyridine monomer content is increased to 50 % [3].

It is believed that 2-(N, N- dimethylamino ethyl methacrylate has greater ability to hydrogen bond than 4-vinyl pyridine units with carboxylic acids [4]. Moustafine et al [5, 6] reported that the reverse enteric polymer Eudragit® E formed an inter-polymer complex with enteric polymer Eudragit® L and sodium alginate. The blends of Eudragit E result in complex formation with polyacids and these cannot be used for film coating applications.

Introduction of hydrogen bonds in polymers which originally lack proton acceptor / donor groups enhances miscibility of otherwise immiscible blends. Indeed, Jiang et al. [2] showed that a blend comprising a proton acceptor polymer, which is immiscible with another polymer, could be made miscible by incorporating in the latter, functional groups, which can hydrogen bond with the proton acceptor polymer. Further strengthening of hydrogen bonds leads to formation of inter-polymer complexes. "Macromolecular complexes" are intermolecular associate of two different polymers bound together by secondary binding forces. These are usually divided into four classes, known as polyelectrolyte, hydrogen-bonding, stereo and charge-transfer complexes. The complexation of polymer components with controllable hydrogen bonding in

solution is largely dependent on the structural parameters of the polymer. This can be schematically represented as shown in Scheme 7.1:

Use of polymer-polymer complexes like polyvinylacetate phthalate-PVP, carboxyvinyl polymer-HPC, PVP-polyacrylic acid (PAA) for drug delivery, has been reported [7]. The polyelectrolyte complex of PAA and poly dimethylamino ethyl methacrylate has been evaluated for colon specific drug delivery [8]. Synthetic polyelectrolytes were evaluated for drug and gene delivery and protein separations [9].

Once the polyelectrolyte complexes are formed, they are insoluble in aqueous and non-aqueous solvents. The drug loading in these complexes is achieved by imbibing these gels in the drug solution, followed by washing to remove the drug on the surface. The process is tedious, time consuming and not easy to reproduce. Hence these systems have not been practiced extensively in the industry.

In our earlier chapter we have seen that the cationic polymer NREP synthesized by us did not result in complexation with the polyacids like Eudragit L, Eudragit S, Cellulose acetate phthalate and Hydroxypropyl methylcellulose phthalate. Instead miscible blends were obtained and these were found useful to sustain the release of Cefuroxime axetil in the gastric pH.

In this chapter we have undertaken the detailed mechanistic investigation of the nature of interactions between Eudragit E and the polyacids like Eudragit L, Eudragit S, Cellulose acetate phthalate and Hydroxypropyl methylcellulose phthalate. We investigated the effect of the polymer structure, charge density and basicity of functional monomer on interactions with different polymers like Zein, Ethylcellulose and polyacids like Eudragit L, Eudragit S, Cellulose acetate phthalate and Hydroxypropyl methylcellulose phthalate. These investigations provided useful insights for obtaining controlled hydrogen bonding in NREP without resulting in polyelectrolyte complex formation. Miscible blends, which can be used for film coating applications were obtained.

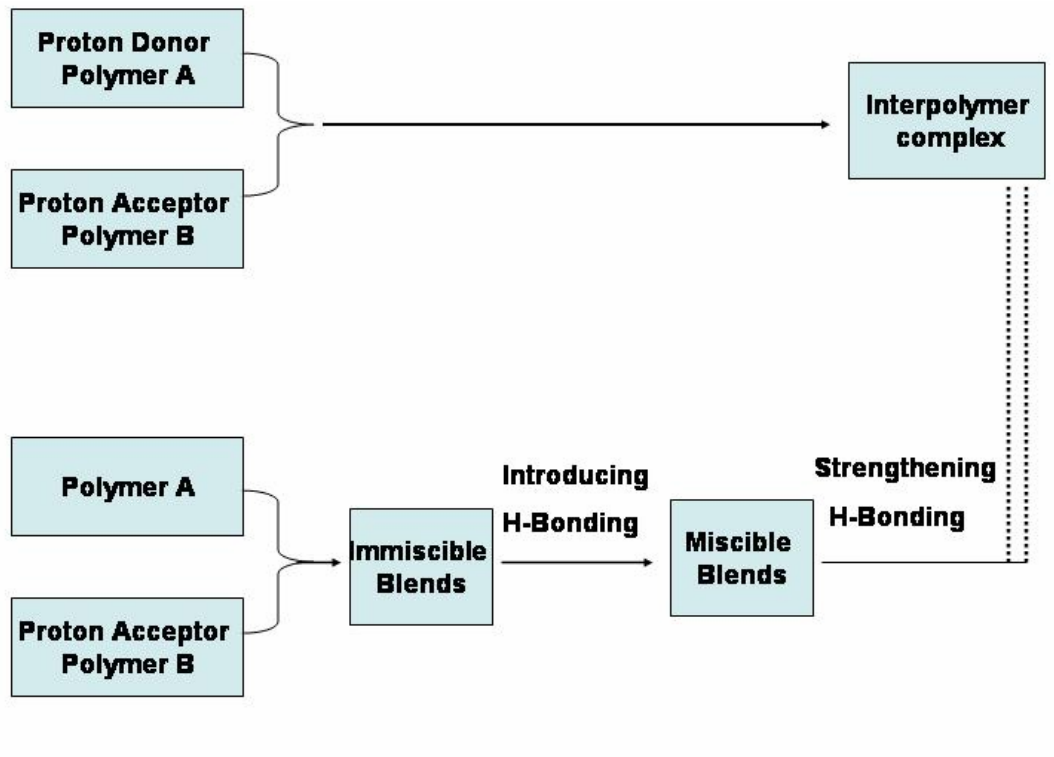

Scheme 1. Schematic representation of the relationships between hydrogen bonding and miscibility /complexation in systems containing inherent interacting sites and controllable hydrogen bonding

7.2. MATERIALS AND METHODS

7.2.1. Materials

The film forming polymers: Eudragit® EPO (EE), Eudragit® L 100 (EL), Eudragit® S 100 (ES) (Degussa / Rohm Pharma), Hydroxypropyl methylcellulose phthalate (HPMCP) (Eastman), Cellulose acetate phthalate (CAP) (Eastman) and Ethylcellulose (EC) were gift from Lupin Laboratories Ltd, India and Zein was purchased from Sigma-Aldrich. The solvents methanol (MeOH) and chloroform ($CHCl_3$) were purchased from Qualigens. Dimethylformamide was purchased from Merck.

Methyl methacrylate (MMA), 2-hydroxy ethyl methacrylate (HEMA) dimethylaminoethyl methacrylate (DMAEMA) and 4-vinyl pyridine were purchased from Sigma-Aldrich.

7.2.2. Polymerization

MMA-*co*-HEMA-*co*-DMAEMA

Terpolymer of MMA-HEMA-DMAEMA (60-25-15 % w/w respectively) was synthesized by free radical polymerization. In a 100 ml round bottom flask methyl methacrylate, 2-hydroxy ethyl methacrylate and dimethylamino ethylmethacrylate were added to 40 ml of dimethyl formamide. Solution polymerization of the monomer mixture was carried out using 1 % azobisisobutyronitrile as initiator at 65°C for 18 h. The polymer solution was concentrated on a rota-evaporator. The polymer was purified by dissolving in dichloromethane-methanol mixture (1:1), and precipitating in diethyl ether. The solid polymer was collected by filtration and dried under vacuum for 48 hrs at room temperature.

MMA-*co*-VP

The copolymer of MMA-VP (70-30 % w/w respectively) was synthesized by free radical polymerization method as described above.

7.2.3. Preparation of polymer blends

The polymer blends of EE with EL, ES, CAP, HPMCP and Zein were prepared by adding solutions of these polymers in mixture of methanol and chloroform. The polymer blends were prepared in the ratio (25 / 75), (33 / 66), (50 / 50), (66 / 33) and (75 / 25) w/w of EE with EL, ES, HPMCP, CAP, EC and Zein. These blends were used for further physicochemical characterization.

The polymers EL, ES, CAP, HPMCP and Zein were blended with copolymer MMA-VP and terpolymer MMA-HEMA-DMAEMA respectively, as described above.

7.2.4. Physicochemical characterization of polymer blends

7.2.4.1. FTIR spectroscopy

The interactions between NREP-EL, ES, CAP, HPMCP and Zein were examined by analyzing the samples by FTIR using Perkin Elmer model Spectrum One in diffused reflectance mode. 2-3 mg of samples were thoroughly mixed and triturated with potassium bromide (100 mg) and placed in the sample holder. The samples were scanned from 4000 to 450 cm^{-1}. The measuring conditions were resolution, 4.0; zero fitting, 2.0; sample scan, 16; acquisition, single sided. The peak assignments were made for the neat polymer samples of EE, EL, ES, CAP, HPMCP and Zein. These were compared with the peaks obtained for the polymer blends.

7.2.4.2. DSC analysis

The polymers EE, EL, ES, CAP, HPMCP and Zein and blends of EE-with the polymers listed, were subjected to thermal analysis using TA Instruments DSC Q100 V9.0 built 275, using MDSC heat-only method, with nitrogen as purge gas at a flow rate of 50 ml/min. The modulation amplitude was $\pm$ 0.53°C every 40 s. Indium was used to calibrate the enthalpy and temperature values. The experiments were conducted in hermetically sealed aluminium pans. The weight of each sample was in the range 1-2 mg and the heating rate was 5°C/ min from 10 to 200°C.

7.3. RESULTS AND DISCUSSION

7.3.1. FTIR spectroscopy

Infrared spectroscopy is extensively used in the analysis of polymer blends [10]. While polymer blends are rendered miscible by various types of associations, hydrogen bonding is the most common [2]. The hydrogen bonding in polymer blends affects absorption bands in the region 3500-3600 cm^{-1}. The other regions largely affected by polymer miscibility include the C=O stretching (1734 cm^{-1}), $-CH_2$ symmetric stretching (2886 cm^{-1}) and the finger print region (1300 - 650 cm^{-1}) [11]. In case of polyelectrolyte complexes resulting from interactions between polyacids and polybases, a new absorption band in the region 1500 - 1600 cm^{-1} corresponding to carboxylate salt is seen [5,6]. In the present investigation this technique has been used to substantiate the findings of the thermal analysis reported in next section.

7.3.1.1. FTIR spectra of EE

The peak assignment for EE is as follows IR (KBr, cm^{-1}) **Fig. 7.1**:

2949 – 2874 (Methyl C-H asym / sym stretch); 2821- 2770 (methylamino, N-CH_3, C-H stretch); 1728 (C=O, ester); 1454 (Methyl C-H asym / sym bend); 1273 -1240

(C-O stretch); 1148 (Aliphatic amine C-N stretch; C-O stretch, ester). The peaks assigned are comparable to those assigned by Lin et al. and Juppo et al [12, 13].

EE is a terpolymer comprising MMA, BuMA and DMAEMA and contains both proton accepting and donating groups. The carbonyl groups from MMA, BuMA and DMAEMA act as proton acceptors and are capable of interacting with the proton donating groups. The nitrogen from dimethylamino group of DMAEMA is a strong base and acts as proton acceptor and is capable of forming hydrogen bonds. The participation of carbonyl and nitrogen of dimethylamino ethyl methacrylate in hydrogen bonding has been reported in the past [15].

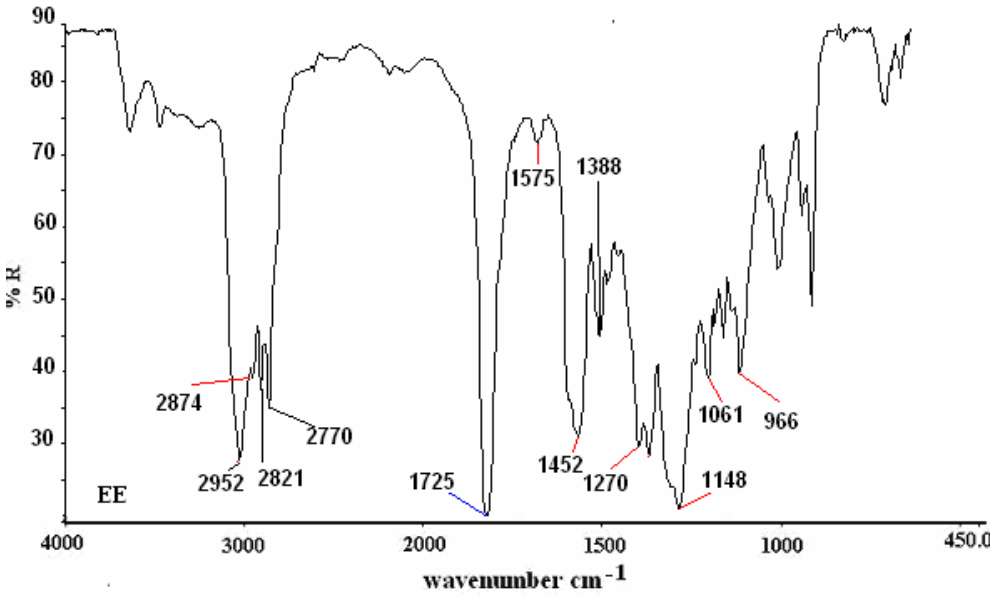

Fig. 7.1. FTIR spectrum of EE.

Carbonyl stretching region (1650-1740 cm^{-1}) in EE

The band corresponding to carbonyl from MMA, BuMA and DMAEMA in EE is seen at 1725 cm^{-1}. This band does not show appearance of prominent shoulder at lower wave number. The carbonyl band is typical proton acceptor in hydrogen bonding and it splits into two contributions, one corresponding to nonbonded carbonyl groups in

the blend (~1730 cm^{-1}), and one at lower wave numbers (~1703 cm^{-1}) corresponding to hydrogen bonded carbonyl. Similar changes in carbonyl band of poly(MMA) have been reported in case of blends with poly(4-vinylphenol) [15]. Since such feature is not observed in EE it can be assumed that self-associations (intra molecular) involving the carbonyl groups are not profound in EE.

Methyl and methylamino (sym/asym) stretch

The basic dimethylamino group in EE exhibits bands corresponding to symmetric / asymmetric methyl and methylamino stretch in the region 2949-2874 cm^{-1} and 2821- 2770 cm^{-1} respectively. These bands are important and exhibit significant changes due to alteration in the dimethylamino structure of EE [5, 6,12].

Potential interactions with EE

Since EE is a strong polybase with average pKa of basic monomer DMAEMA 8.4 [16], it acts as a strong proton acceptor. The carbonyl and methylamino groups in EE can form hydrogen bonds with acid hydroxyls from polyacids. If the interaction between polyacids and polybases involves proton transfer, it could lead to salt formation [17]. The changes in spectra of polymers containing DMAEMA forming a polysalt on blending with polyacids are reflected in loss or reduction in intensity of bands corresponding to dimethylamino groups and appearance of new bands in the region 1550-1560 cm^{-1} [5,6].

In the present chapter we investigate the carbonyl stretching, methyl and methylamino symmetric / asymmetric stretching bands in neat EE for changes arising as a result of blending with different polymers, also appearance of new bands as a result of polysalt formation was examined.

7.3.1.2. FTIR spectra of EE blends

7.3.1.2.a EE-Zein blends

ZEIN: IR (KBr, cm^{-1}); 1657 (amide I, C=O stretching vibrations); 1542 (amide II, N-H bending viration) see **Fig. 7.2**. These assignments are similar to those disclosed by Duodu et al. [18]. The broad band of amide I corresponds to two populations of carbonyl groups; those which are free and the rest involved in intramolecular associations with NH groups similar features for amide bands in poly (ether amide) were reported in past [15]. If these intramolecular associations are overcome, then this polymer can form miscible blends.

Polyamides act as proton acceptors and are capable of hydrogen bonding with proton donor groups like carboxylic, hydroxyl and phenolic groups [15,19]. The amide II bands shift to lower wave numbers on hydrogen bonding [15]. The amide I mode is complex mode having main contributions from the carbonyl groups and a shift to higher wave number on hydrogen bonding of the carbonyl groups in amide I mode is reported [19].

Zein contains amide groups so it will act as proton acceptor like EE. Also Zein exhibits self-associations. Hence favorable interactions between EE and Zein contributing to miscibility are not possible. Blending of solutions of EE and Zein resulted in immediate phase separation at all compositions. The FTIR spectrum of EE-Zein is additive in nature exhibiting no shift in frequencies for bands corresponding to amide I and II, carbonyl and dimethylamino groups. The bands for amide I and carbonyl of EE appear in close proximity and the intensity of the carbonyl band of EE shows a change.

From the spectrum it appears that these polymers do not exhibit interaction and hence these should exhibit phase separation with appearance of two T_gs.

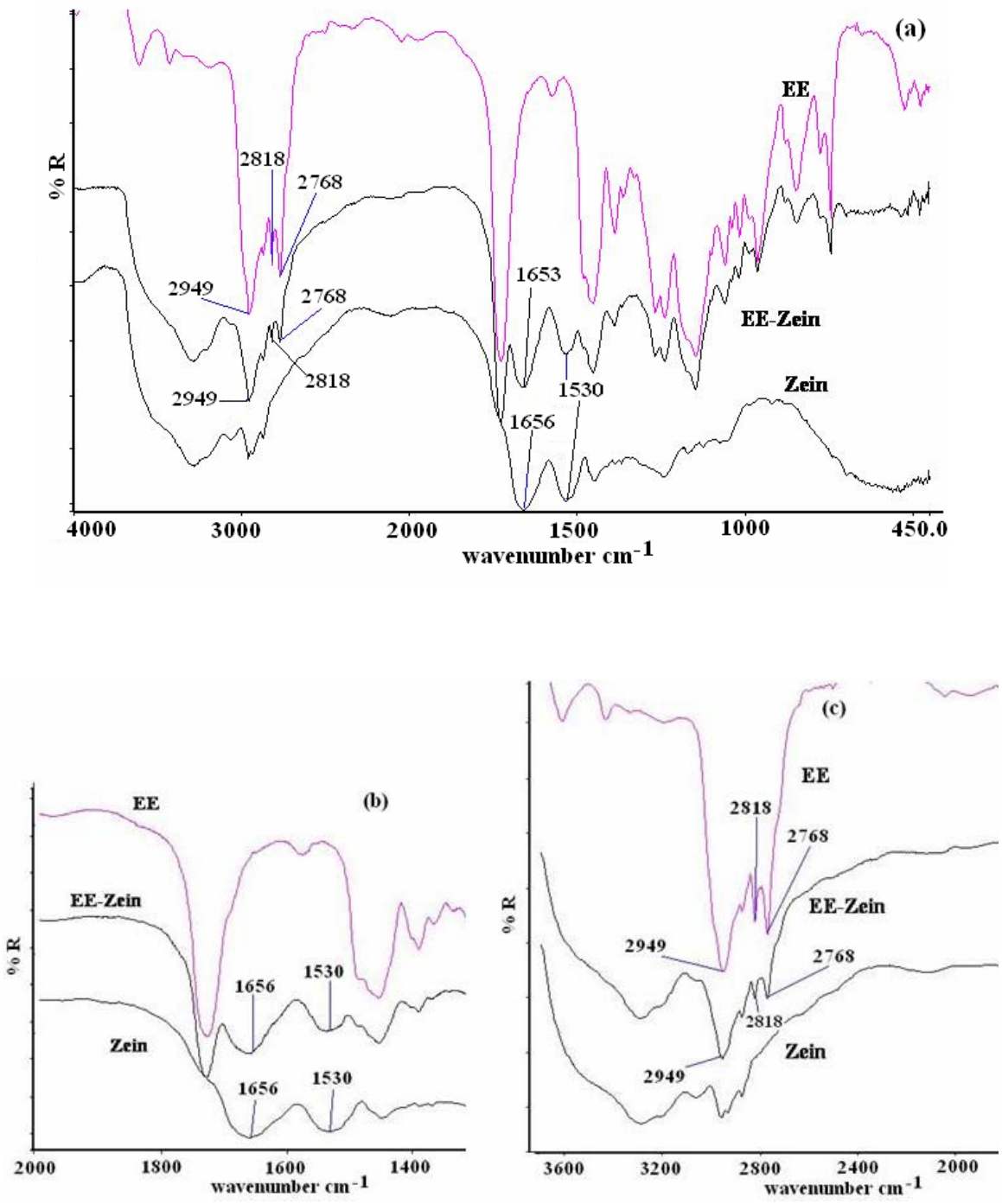

Fig. 7.2. FTIR spectra of EE-Zein blends: (a) overlay of EE-Zein blends. (b) and (c) Scale expanded spectra.

7.3.1.2.b EE-EC blends

EC: IR (KBr, cm^{-1}); 3487 (broad band for OH groups); 2976, 2878 (methyl C-H asym / sym stretch); 1448, 1486 (methylene C-H bend); 1375 (C-H bending), 1131, 1064 (cyclic ether C-O stretch in C-O-C). These assignments are similar to those described in by Bugay and Findlay, Suthar et al. [20, 21]. The spectrum of EE-EC blend is shown **Fig. 7.3** and the scale expanded spectrum is seen in **Fig. 7.3 (a) & (b)**.

The presence of cellulosic hydroxyls in EC enables it to participate in hydrogen bonding. The band corresponding to free hydroxyl group in EC is seen at 3485 cm^{-1} see **Fig. 7.3** It does not show a shoulder at lower frequency corresponding to hydrogen bonded hydroxyls. EE can form miscible blends with EC via hydrogen bonding involving hydroxyl-carbonyl and hydroxyl-nitrogen groups from EC and EE respectively. The films of EE-EC blends are translucent and indicate partial miscibility between polymers.

Hydroxyl stretching region

EC showed a band corresponding to the free hydroxyl at 3483 cm^{-1}. In EE-EC blend the band appears at same wave number with fall in intensity and slight appearance of shoulder at lower wave number (~3200 cm^{-1}) suggesting participation of hydroxyls from EC in intermolecular associations. Lee at al. (1988) [23] reported that hydrogen bonds arising in many blends differ in strength. Strong bands appear at 2800, 2500 and 1800 cm^{-1}, moderate to intermediate strength bands at 3100-2800 cm^{-1} and weak structure less broad band at 3300 cm^{-1}. Since the hydrogen bonded hydroxyl in EE-EC blend is just emerging at 3200 cm^{-1} it is evident that the association between these polymers is weak.

Carbonyl stretching region

The carbonyl frequency in EE (1725 cm^{-1}) does not show prominent shoulder at lower wave number whereas in EE-EC blend the carbonyl band shows a split in two regions with one corresponding to free carbonyl groups in EE (maximum at 1727 $cm^{-1)}$ and the other appearing as shoulder at lower frequency (1602 cm^{-1}). This shoulder is

more profound in the blend than in neat EE. This indicates the participation of carbonyl groups of MMA / BuMA / DMAEMA from EE in hydrogen bonding with hydroxyl groups from EC.

Methyl and methylamino (sym/asym) stretch

The EE-EC blend spectrum shows bands corresponding to dimethylamino groups at 2770 and 2820 $cm^{-1.}$ A fall in intensity of these bands as compared to neat EE is observed as seen from the scale-expanded spectrum. This suggests partial involvement of the dimethylamino groups of EE in hydrogen bonding with hydroxyls from EE. The FTIR spectrum of EE-EC shows that the polymers do not interact strongly and so the EE-EC blends can be expected to be partially miscible.

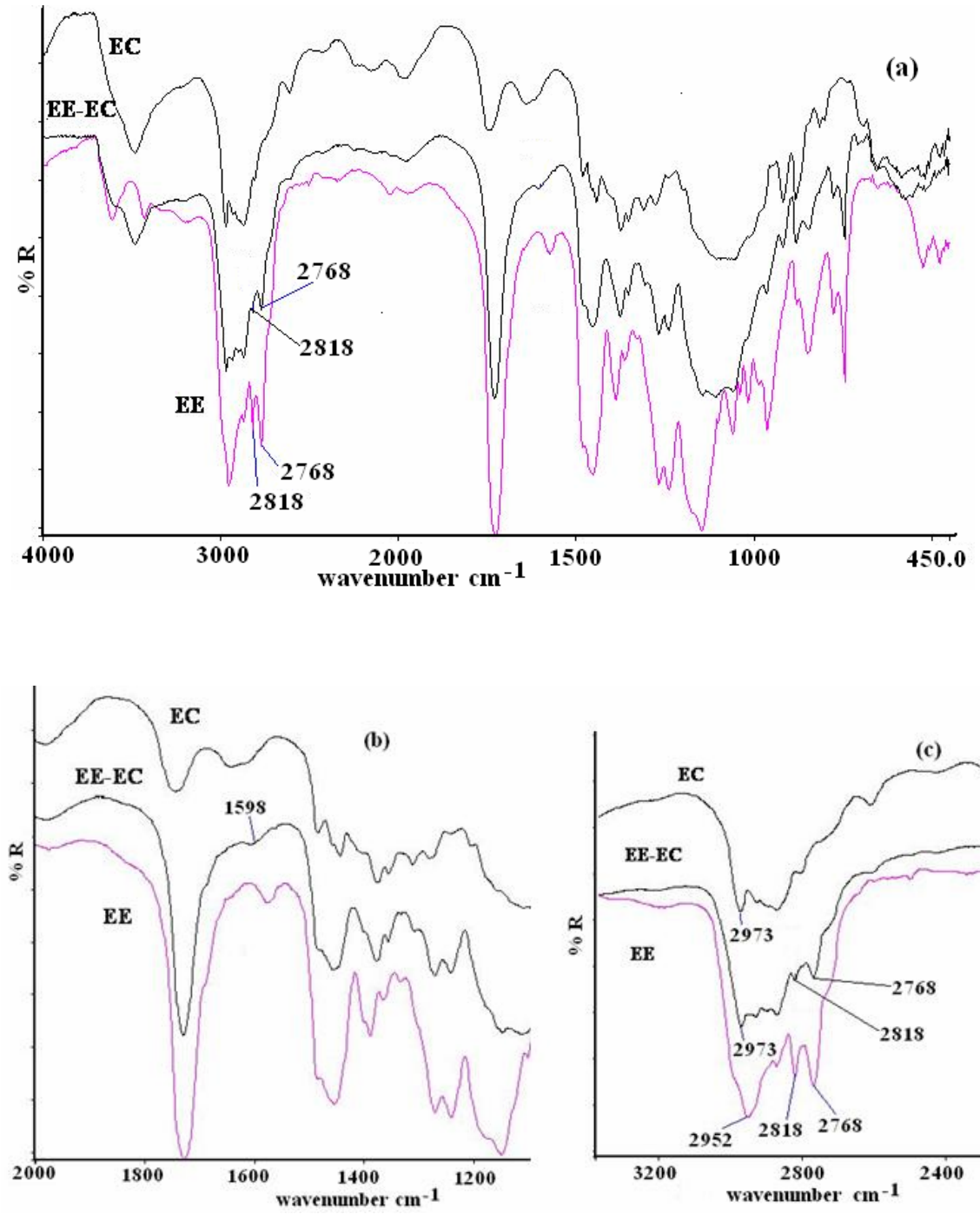

Fig. 7.3. FTIR spectra of EE-EC blends: (a) Overlay of EE-EC blends. (b) and (c) Scale expanded spectra.

7.3.1.2.c EE-EL and ES blends

The peak assignment for EL and ES are as follows IR (KBr, cm^{-1}) see **Fig. 7.4 and 7.5**:

EL: 2500-3500 (OH groups); 2950-2997 (Methyl C-H asym / sym stretch); 2836 (Methoxy (CH_3-O-), C-H stretch); 1723 (esterified carboxylic acid, C=O); 1388, 1449, 1484 (Methyl C-H vibrations, asym / sym stretch), 1162, 1269 (ester vibrations).

ES: 2500-3500 (OH groups); 2950-2997 (Methyl C-H asym / sym stretch); 2839 (Methoxy (CH_3-O-), C-H stretch); 1728 (esterified carboxylic acid, C=O); 1388, 1449, 1484 (methyl C-H vibrations, asym / sym stretch); 1150, 1193, 1270 (ester vibrations). These values are similar to those assigned by Cilurzo et al. [23].

Both EL and ES are polyacids and contain acid hydroxyl groups. EL is expected to show stronger interactions with polybase than ES as it has higher content of methacrylic acid than ES [24]. The spectra of EL and ES in the hydroxyl-stretching region show presence of free hydroxyl groups in region 3500-3550 cm^{-1} and a shoulder at lower frequency (3200 cm^{-1}), which is an indication of hydrogen bonded hydroxyls. The spectra of EL and ES in the carbonyl stretching region show a maximum at 1727 cm^{-1} corresponding to C=O and a shoulder at lower frequency (1635 cm^{-1}). The presence of a shoulder indicates self-association in these polymers arising from the hydrogen bonding between the acid hydroxyls (COOH) and the carbonyl from the acrylic groups. Existence of association between C=O and acid hydroxyls in Eudragit® L is reported in the past [25]. The salt formation of EL and ES results in two new bands at 1560 cm^{-1} and between 1400-1300 cm^{-1}[5, 6, 23]. The blends of these polymers with EE were examined for the carboxylate salt formation.

The spectra for EE-EL and EE-ES blends are shown in **Figs. 7.4 and 7.5**. Blending of EE with EL and ES is expected to show changes in the hydroxyl, carbonyl, methyl and methylamino-stretching region. Polyelectrolyte complexes were obtained on blending aqueous buffer solutions of EE and EL with appearance of a new band corresponding to the carboxylate salt [5]. Similar results are expected on blending non-aqueous solutions of EE with EL and ES respectively. Polymer complexes are formed when the molar masses of the interacting polymers are not less than the critical value [2]. The technical specifications of EE, EL and ES show that the dimethylamino ethyl

methacrylate content is 50 % and the methacrylic acid content in EL and ES is 50 and 33% respectively. The concentrations of the functional groups are high enough in these polymers to contribute to strong interactions leading to complex formation. These complexes are insoluble in most organic solvents like methanol, isopropanol, acetone, DCM, $CHCl_3$ etc their mixtures and also in aqueous media of pH 1.2 and 5.8 but swell in these media.

Solvents affect the polymer blend miscibility leading to complex formation [2]. Complexation results when the solvent -polymer interaction is overcome by interactions between proton donating and proton accepting polymer. Methanol is a protic solvent and exhibits interactions with proton accepting polymers. In the present investigation EE-EL and EE-ES formed complex from solutions of polymer in MeOH–$CHCl_3$ (1:2 v/v), indicating stronger interaction between polymer-polymer than polymer-solvent.

Miscibility of these polymers was investigated in aprotic solvent, DMF. Since DMF is aprotic solvent, it is expected that it will interact with proton donating polyacids thereby affecting the interaction of EL and ES with EE. Contrary to this, it was observed that EE formed complexes with EL at all compositions after about 30 min. EE showed complexation with EL irrespective of any solvent.

Hydroxyl stretching region

The band corresponding to free hydroxyl groups in EE-EL blend is seen at 3591 cm^{-1} showing a shift of + 74 cm^{-1} as compared to neat EL indicating participation hydroxyls in hydrogen bonding. This band shows a broad structureless shoulder at 3210 cm^{-1} indicative of hydrogen-bonded hydroxyls. The hydroxyls from the carboxylic acid of EL can form hydrogen bonds with the dimethyl amino groups of DMAEMA or the carbonyl from MMA, BuMA and DMAEMA of EE respectively.

In EE-ES blends the band corresponding to free hydroxyl groups is seen at 3609 cm^{-1} showing a shift of +61 cm^{-1} as compared to neat ES indicating participation hydroxyls in hydrogen bonding. This shift is lower (+61) as compared to that seen in EE-EL (+74) blends suggesting lower interaction between EE-ES than the later. The band 3609 cm^{-1} in EE-ES shows a broad structureless shoulder at 3224 cm^{-1} indicative

of hydrogen-bonded hydroxyls. Since EL and ES differ only in content of methacrylic acid [24] the nature of interactions between EE and ES is similar to that seen in EE-EL.

Carbonyl stretching region

The carbonyl band in EE-EL (1725 cm^{-1}) does not show a split nature like that seen in EL with maxima at 1725 cm^{-1} and a shoulder at 1638 $cm^{-1.}$ So this band in EE-EL appears narrower than that seen in EL. This is because self-association between the carboxylic carbonyls and hydroxyls within EL and ES is overcome and the carboxylic hydroxyl now participates in interpolymer association with EE. This causes liberation of carboxylic carbonyl from self association and this is reflected in the spectrum which shows maximum at 1725 cm^{-1} and appearance of a new band 1562 cm^{-1} as seen in scale expanded spectrum **Fig. 7.4 (b)**. The new band at 1562 cm^{-1} is for the carboxylate salt formed due to the charge transfer between EE and EL. Similar results were reported by Moustafine et al [5,6] for complexation of EE with methacrylic acid and sodium alginate.

The carbonyl stretching region of EE-ES shows similar feature like that seen for EE-EL (see **Fig.7.5 (b)**) with appearance of new band corresponding to carboxylate salt at 1559 cm^{-1}.

Methyl and methylamino (sym/asym) stretch

The scale expanded spectra of EE-EL and EE-ES blends in the region 3200-2500 show disappearance of the bands corresponding to methyl (sym/asym) and methylamino (sym/asym) stretch at 2949 – 2874 cm^{-1} and 2821- 2770 cm^{-1} respectively (**Fig. 7.4 (c) and 7.5 (d)**). This change is associated with proton transfer to the methylamino group in EE accompanied by carboxylate salt formation. Changes in the methylamino region with loss in bands corresponding to these groups have been reported in the past [5, 6, 26].

The intermolecular associations between EE-EL and EE-ES are strong and charge transfer resuls in polyelectrolyte salt formation. Hydrogen bonding between these polymers results from participation of acid hydroxyls of EL and ES with carbonyl, and methylamino groups of monomer DMAEMA of EE. From the FTIR results it is

expected that EE-EL a EE-ES should exhibit single composition dependent T_g values with large positive deviations from Fox equation.

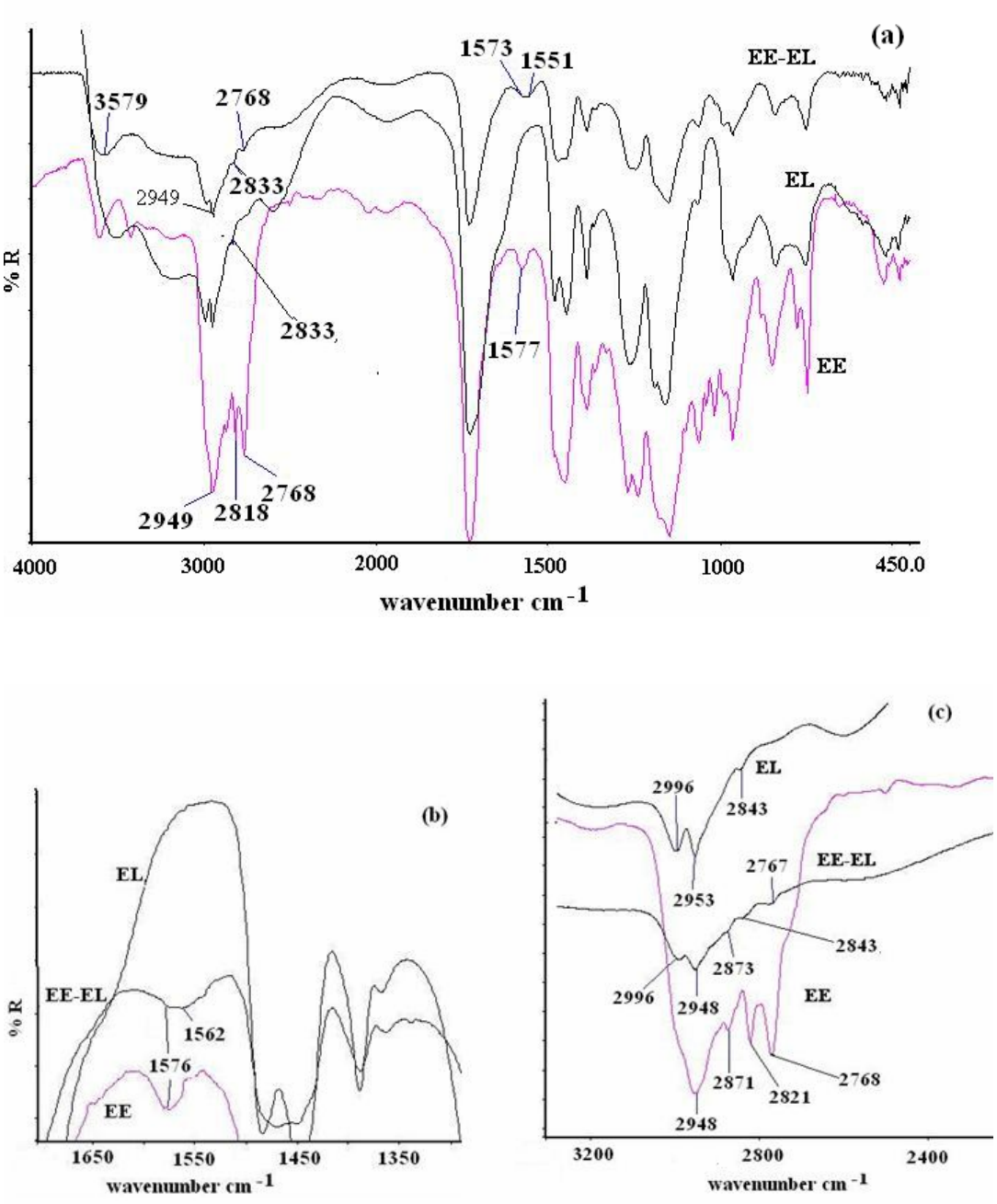

Fig.7.4. FTIR spectra of EE-EL blends: (a) Overlay of EE-EL blends.

(b) and (c) Scale expanded spectra.

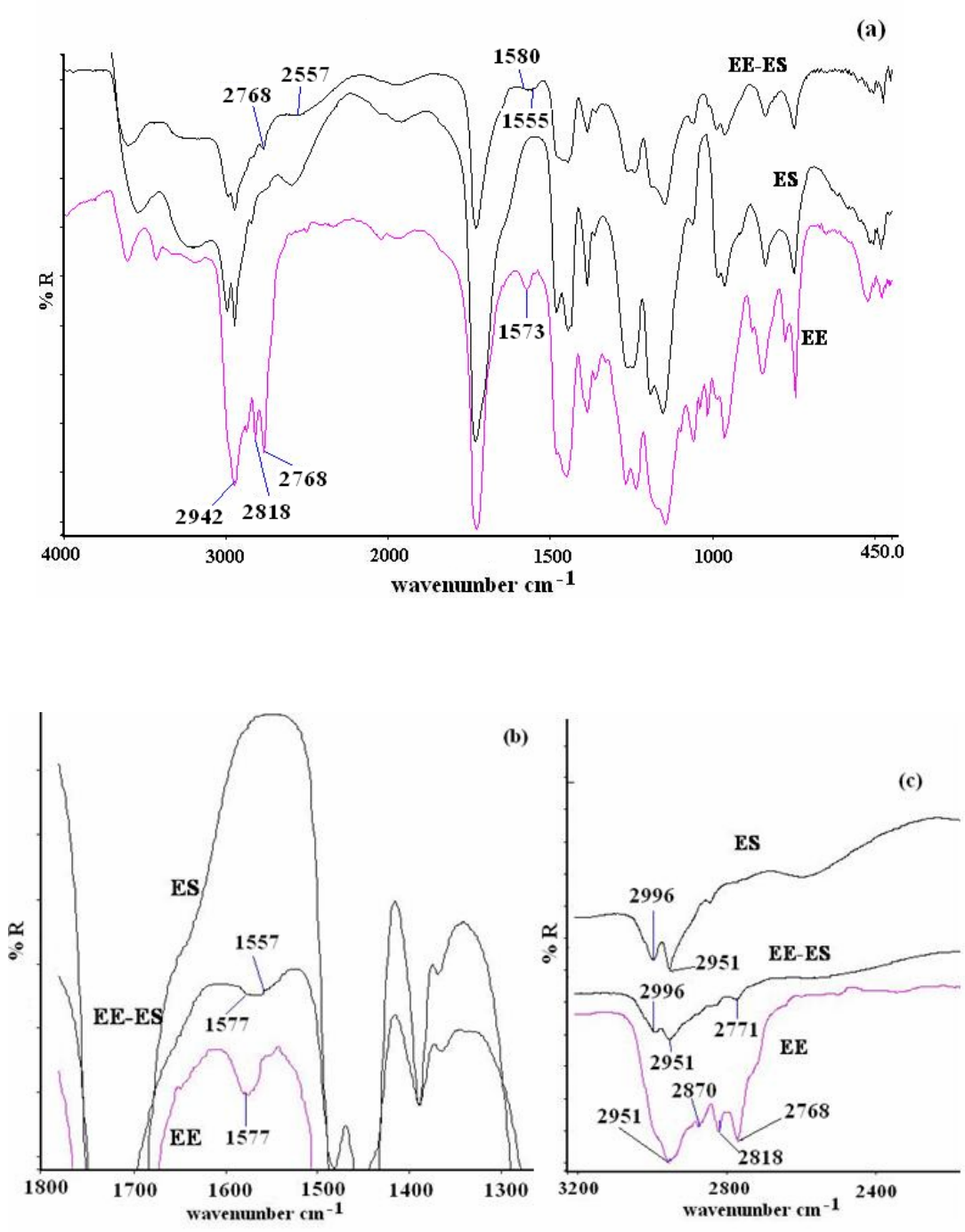

Fig. 7.5. FTIR spectra of EE-ES blends: (a) Overlay of EE-ES blends. (b) and (c) Scale expanded spectra.

7.3.1.2.d EE-CAP and EE-HPMCP blends

The peak assignments for CAP and HPMCP are as follows IR (KBr, cm^{-1}) see **Fig. 7.6 and 7.7**;

CAP: 3570-3200 (OH group); 2980, 2883 (methyl C-H asym / sym stretch); 1750, 1725, 1701 (C=O ester, carboxylic acid); 1599 (C=C conjugated vinyl, aromatic ring); 1492 (methylene C-H bend); 1284 (ester bond C-O-C), 1140- 1071 (cyclic ether C-O stretch in C-O-C); 746 (monosubstituted aromatic ring).

HPMCP: 3460 (O-H groups); 2989, 2884 (methyl C-H asym / sym stretch); 2938 (methylene C-H asym / sym stretch); 2828 (methoxy O-CH_3), 1725 (C=O, ester); 1599 (C=C conjugated vinyl, aromatic ring); 1448, 1486 (methylene C-H bend); 1285 (ester bond C-O-C); 1128,1067 (cyclic ether C-O stretch in C-O-C); 949 (aromatic C-H in plane bend), 746 (monosubstituted aromatic ring). These assignments are similar to those described by Bugay and Findlay 1999 [20].

Both CAP and HPMCP contain cellulosic hydroxyls in addition to acid hydroxyls. The carboxylic groups in CAP and HPMCP are attached to the aromatic ring and are therefore more amenable to dissociation due to stabilization effects of the ring. Propyl and methyl groups in HPMCP contribute to steric hindrance, limiting its interaction with EE. We believe that CAP with only acetate groups attached to cellulose structure, would exhibit stronger interactions than HPMCP with NREP. These presumptions are validated by the values of parameters of Schneider equation discussed in the next section

The FTIR spectra for EE-CAP and EE-HPMCP blends are shown in **Fig. 7.6 & 7.7.** FTIR spectrum of CAP and HPMCP shows bands for free hydroxyl groups at 3483 and 3473 cm^{-1} respectively. The carbonyl band appears at 1725 cm^{-1} for both CAP and HPMCP and shows a shoulder at lower frequency. This is an indication of self-association in these polymers arising out of hydrogen-bonded carbonyl with acid hydroxyls or cellulosic hydroxyls. Similar feature was observed in carbonyl stretching region of ES and EL.

Both CAP and HPMCP contain cellulosic hydroxyls in addition to acid hydroxyls. The carboxylic groups in CAP and HPMCP are attached to the aromatic ring

and are therefore more amenable to dissociation due to stabilization effects of the ring. Propyl and methyl groups in HPMCP contribute to steric hindrance, limiting its interaction with EE. We believe that CAP with only acetate groups attached to cellulose structure, would exhibit stronger interactions than HPMCP with EE. These presumptions are validated by the values of parameters of Schneider equation discussed in the next section.

Blending of EE with HPMCP and CAP results in complex formation almost immediately and this is a manifestation of strong interaction between these polymers. The FTIR spectra of EE-HPMCP and EE-CAP complexes are shown in **Fig. 7.6 & 7.7** respectively. Both the spectra show overall band broadening and fall in intensity as a result of strong interaction. FTIR spectra of CAP and HPMCP show bands for free hydroxyl groups at 3483 and 3473 cm^{-1} respectively. The carbonyl band appears at 1725 cm^{-1} for both CAP and HPMCP and shows a shoulder at lower frequency (~1635 cm^{-1}). This is an indication of self-association in these polymers arising out of hydrogen-bonded carbonyl with acid hydroxyls or cellulosic hydroxyls. Similar feature was observed in carbonyl stretching region of ES and EL.

Hydroxyl stretching region

In EE-HPMCP and EE-CAP spectra significant band broadening is seen in the hydroxyl stretching region, 2500-3000 cm^{-1}. The frequency for free hydroxyl group of HPMCP shifts from 3473 to 3477 cm^{-1} and a shoulder (broad structureless band) at lower wave number (~ 3200 cm^{-1}) appears. Similarly, the EE-CAP blends show band corresponding to free hydroxyl at 3550 cm^{-1}, which when compared to that in neat CAP shows a shift of + 67 cm^{-1} from that at 3483 cm^{-1}. The band for free hydroxyl in EE-CAP shows a prominent shoulder at 3331 cm^{-1} corresponding to hydrogen-bonded hydroxyl. This feature is more prominent in EE-CAP than EE-HPMCP indicating stronger interaction between the former. These changes are indicative of contribution of hydroxyls from HPMCP and CAP in hydrogen bonding with carbonyl or methylamino groups in EE.

Carbonyl stretching region

The carbonyl band in EE-HPMCP and EE-CAP (1729 cm^{-1}) does not show a split nature like that seen in either neat HPMCP or CAP, with maxima at 1725 cm^{-1} and a shoulder at 1638 cm^{-1}. The carbonyl band in EE-HPCMP and EE-CAP appears narrower than that seen in neat HPMCP and CAP. The self-association between the carboxylic carbonyls and hydroxyls (either acid hydroxyls or cellulosic) as seen in neat HPMCP and CAP is overcome on blending these with EE due to the participation of carboxylic hydroxyl in interpolymer association with EE. This causes liberation of carboxylic carbonyl in self-associated structure and this is reflected in the spectrum which shows maximaum at 1729 cm^{-1} with a shift of + 4 cm^{-1} than that seen in neat EE, HPMCP and CAP. A new band appears in EE-HPMCP and EE-CAP blends at 1559 and 1560 cm^{-1} respectively as seen in scale expanded spectra **Fig. 7.6(b) and 7.7(b)** This corresponds to the carboxylate salt formed due to the charge transfer between EE and HPMCP / CAP.

Methyl and methylamino (sym/asym) stretch

The scale expanded spectra of EE-HPMCP and EE-CAP blends in the region 3200-2500 show disappearance of the bands corresponding to methyl (sym/asym) and methylamino (sym/asym) stretch at 2949 – 2874 cm^{-1} and 2821- 2770 cm^{-1} respectively (**Fig. 7.6(c) and 7.7(c)**). This change is associated with proton transfer from acid hydroxyl of HPMCP and CAP to the methylamino group in EE resulting in carboxylate salt formation.

The intermolecular associations between EE-HPMCP and EE-CAP are strong with charge transfer resulting in polyelectrolyte salt formation. From the FTIR results it is expected that both EE-HPMCP and EE-CAP should exhibit single composition dependent T_g values with large positive deviations from Fox equation. The extent of interaction between these polymers is quantified by fitting the blend T_g data to Schneider equation [1, 27].

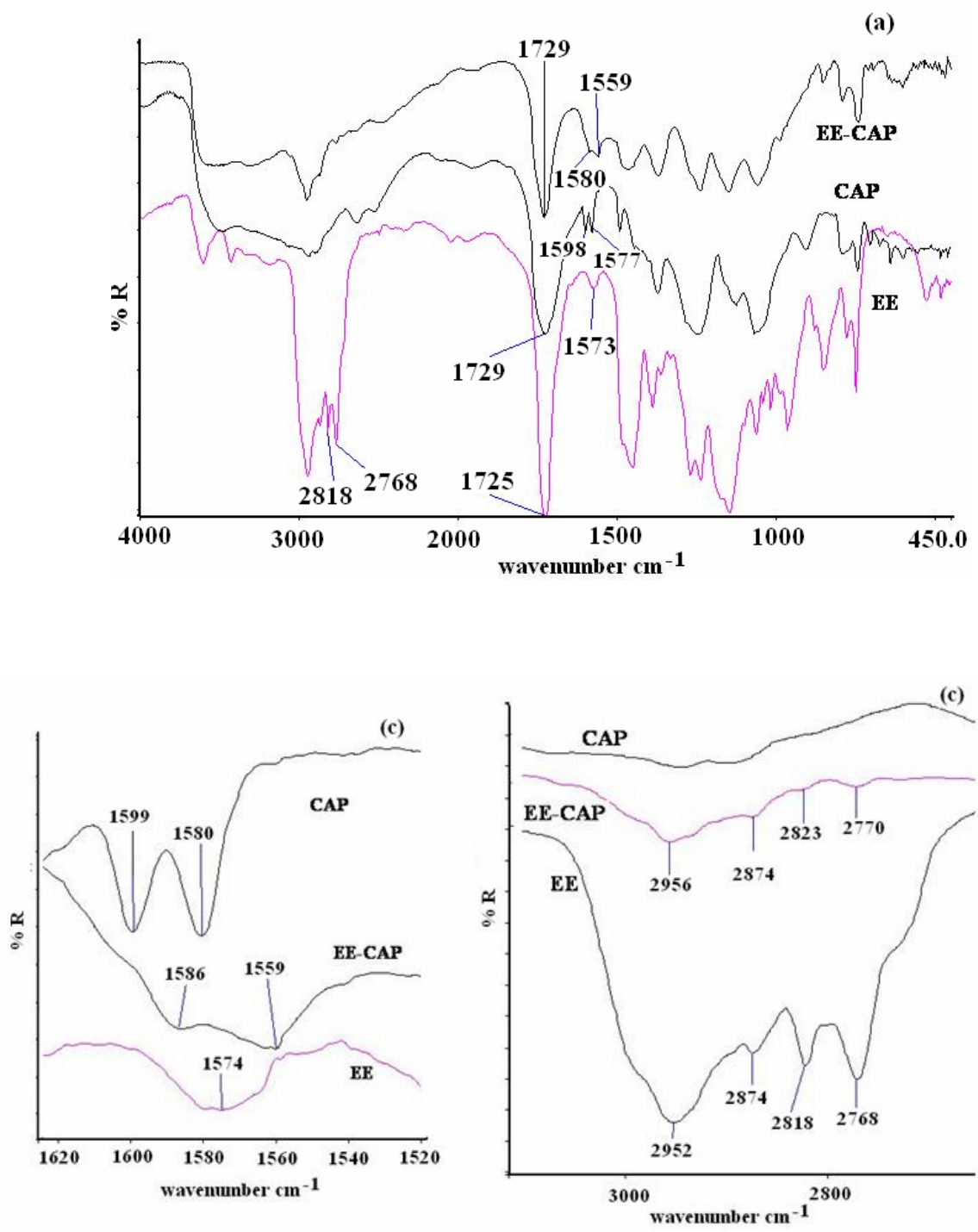

Fig. 7.6. FTIR spectra of EE-CAP blends: (a) Overlay of EE-CAP blends. (b) and (c) Scale expanded spectra.

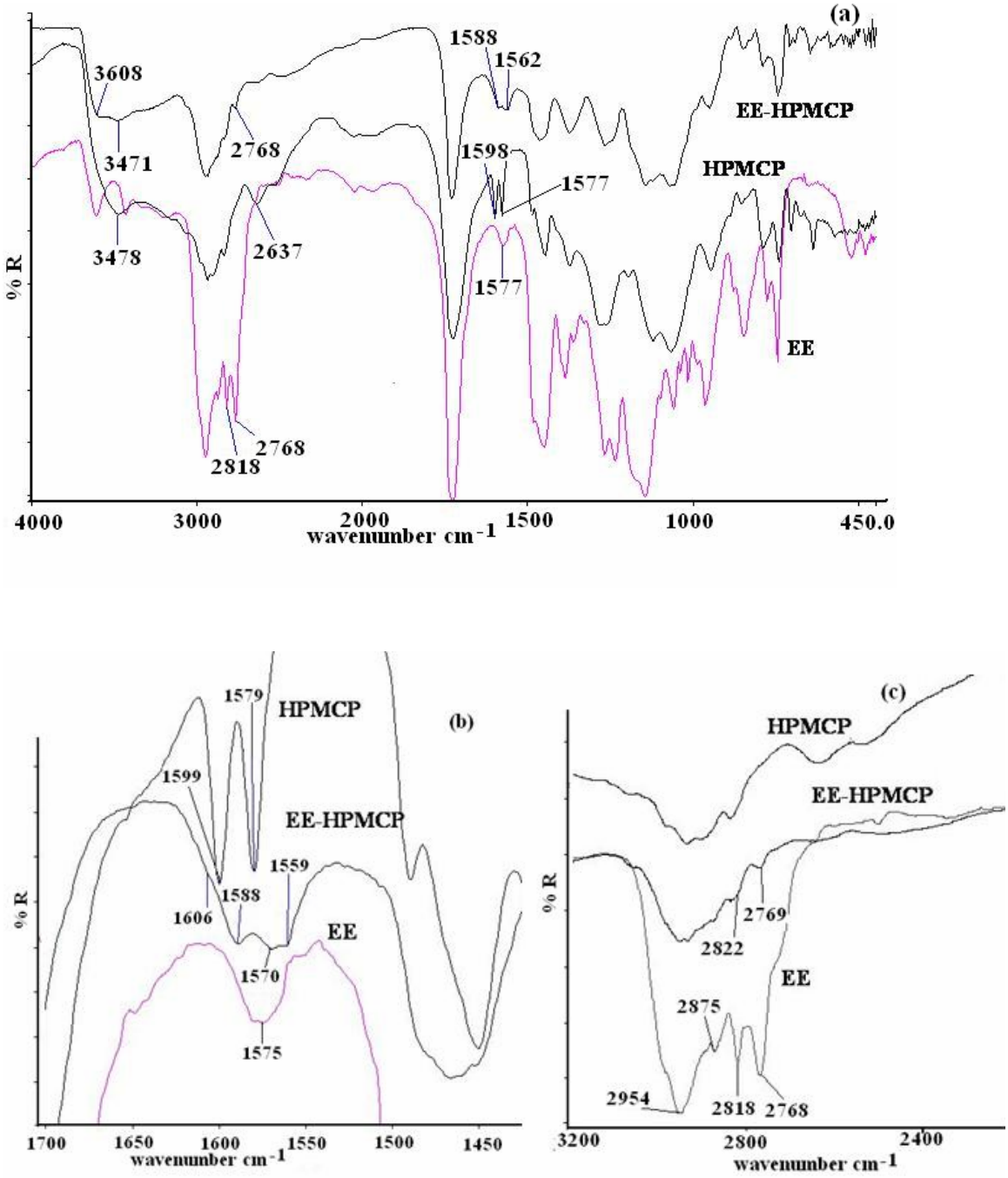

Fig.7.7. FTIR spectra of EE-HPMCP blends: (a) Overlay of EE-PMCP blends.

(b) and (c) Scale expanded spectra.

7.3.2. Thermal analysis

The T_g of individual polymers determined by MDSC is shown in **Table 7.1** and is in good agreement with the values reported in literature.

Fox equation, which assumes volume additivity of mixing, provides the simplest framework to correlate T_gs of blends. The extent of interactions was determined by using the third power equation derived by Schneider. The detailed discussion on this is covered in Chapter 6 section (**6.3.1.).** The equations are as follows:

$$\frac{1}{T_g} = \frac{X_1}{T_{g1}} + \frac{X_2}{T_{g_2}} \qquad \textit{Eq 1}$$

$$\frac{(T_g - T_{g1})}{(T_{g2} - T_{g1})} = (1+K_1)\phi - (K_1+K_2)\,\phi^2 + K_2\phi^3 \qquad \textit{Eq 2}$$

$$\frac{(T_g - T_{g1})}{(T_{g2} - T_{g1})} = (1+K_1)W_{2c} - (K_1+K_2)W_{2c}^2 + K_2 W_{2c}^3 \qquad \textit{Eq 3}$$

Table 7.1: Glass transition temperatures of neat polymers

Polymer	T_g observed (° C)	T_g reported (° C)	Reference No.
EE	55.3	44.5, 46	[12, 34]
EL	164	157,160, 162	[23, 25, 26]
ES	172.8	163, 171, 179	[23, 26, 35]
EC	135.8	133.4, 125	[36-38]
HPMCP	137	~150	[39]
CAP	153.75	140, 160-170	[40-43]
Zein	164.4	156,164,165	[28, 44,45]

7.3.2.1. EE-Zein blends

The EE-Zein blends exhibited complete phase separation at all compositions and this was reflected in thermal analysis with appearance of two T_gs for all compositions (**Fig. 7.8**). The **Figs. 7.8(a)** and **7.8(b)** show the DSC thermograms and T_g *vs*. composition plots for EE-Zein blends. Each T_g corresponds to the phase rich in that polymer. The EE rich phase shows T_g at 45-48 °C and the Zein rich phase shows T_g at 169-173 °C. The T_g of neat Zein has shifted from 164 °C to higher value (169 to 173 °C) in blends while opposite results were observed for the EE rich phase where the T_g shifted to a lower value from 55.4 °C to 45 to 48 °C. The shift in T_g of amorphous Zein films from 165°C to higher value (~170 °C) due to conformational change from random coil to α and β form leading to partial crystallization is reported in the past (46). Presence of moisture cleaves the intra and / or intermolecular bonding in Zein contributing to these effects. The fall in T_g of EE could be due to the presence of Zein molecules in between the polymer chains. Since both Zein and EE are proton-accepting polymers they do not interact, which results in immiscibility.

Mayo-Pedrosa et al. [19] reported increase in T_g of poly(NIPA) in its immiscible blends with poly(vinyl pyrrolidone) due to limited amount of phase mixing. Normally partially miscible blends exhibits shift in T_gs towards each other. In case of EE-Zein a reverse behavior was observed. The possible reasons could be either the crystallization of amorphous Zein or its limited phase mixing with EE. To investigate this, the polymer fractions in each phase were determined. The weight fraction of each phase was calculated by equation 4 to 7.

Phase composition in polymer blends to obtain apparent weight fractions of polymers has been reported in past (47, 48). The fraction of polymer in each phase can be determined from Fox equation (Eq.1). The Eq. 1 can be rearranged to

$$w'_1 = (T_{g1b}-T_{g2}) / (T_{g1}-T_{g2}) \text{ and} \qquad \textit{Eq 4}$$

$$w''_1 = (T_{g2b}-T_{g2}) / (T_{g1}-T_{g2}) \qquad \textit{Eq 5}$$

where, w'_1 and w''_1 are the apparent weight fractions of EE in the first T_g transition phase and second T_g phase respectively. T_{g1b} and T_{g2b} is the observed T_g of the first and second T_g phase in blends respectively and T_{g1} and T_{g2} are the T_g's for neat polymers 1 and 2.

The overall weight fraction of each phase in blends of EE with Zein was investigated using the following equations:

$$W_{1T} = w'_1 W' + w''_1 W'' \text{ and} \qquad \textit{Eq 6}$$

$$W_{2T} = w'_2 W' + w''_2 W'' \qquad \textit{Eq 7}$$

Where W' is the overall weight fraction of phase rich in polymer component with higher T_g and W'' is the overall weight fraction of phase rich in polymer component with lower T_g. W_{1T} and W_{2T} are the overall weight fractions of EE and the other polymer used in blends, and w'_1 and w''_1 are obtained from the equations 4 and 5 respectively. The values w'_2 and w''_2 were obtained from $w'_2 = 1 - w'_1$ and $w''_2 = 1 - w''_1$. The weight fraction of each phase was calculated by equations 4 to 7. The T_{g1} phase shows complete absence of Zein and T_{g2} phase shows absence of EE (See **Table 7.2**). The T_{g1} phase shows complete absence of Zein and T_{g2} phase shows absence of EE (See **Table 7.2**). This confirms that the increase in T_g of Zein is due to its crystallization as has been reported in the past [28] and the EE-Zein blends show complete phase separation at all compositions.

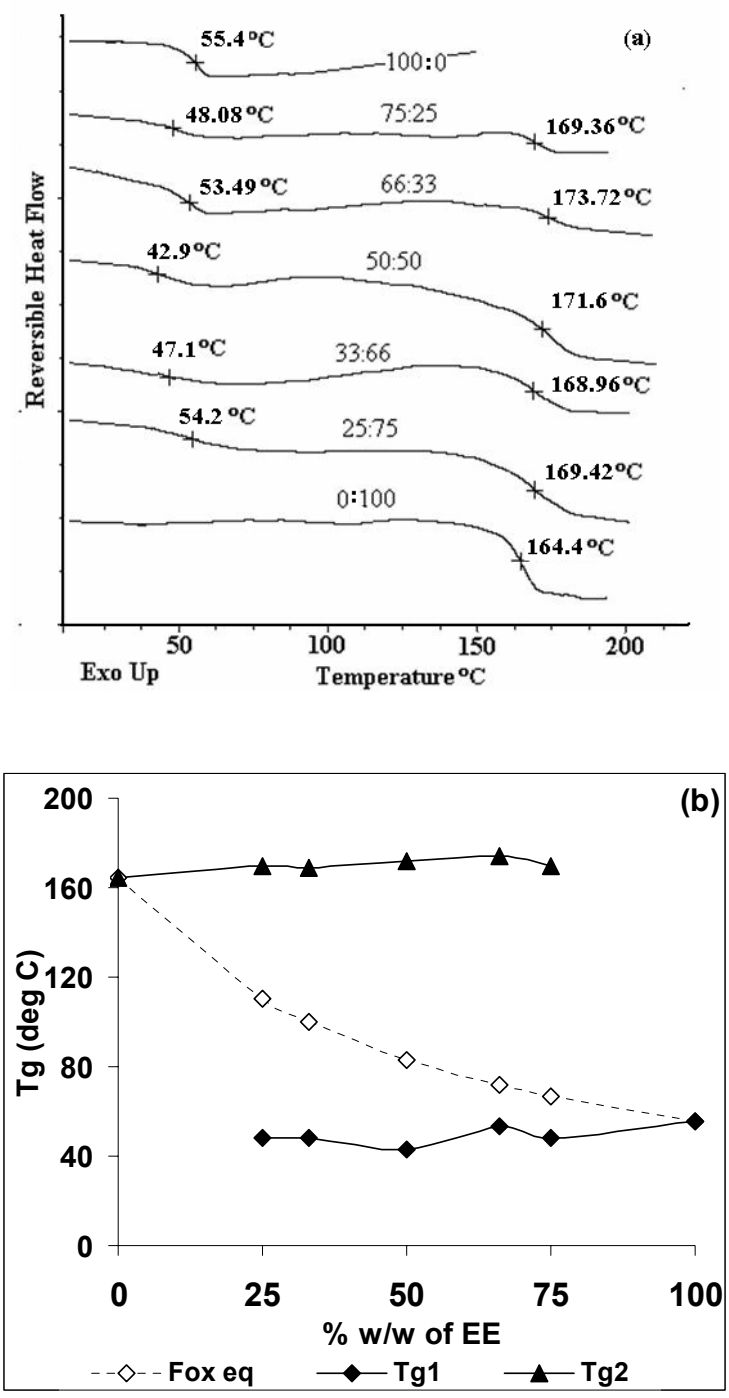

Fig.7.8. Thermal analysis EE-Zein blends, (a) DSC Thermograms (b)T_g *vs.* composition plot

7.3.2.2. EE-EC blends

EE-EC blends showed formation of clear transparent films at all compositions and one would deduce these polymers to be miscible exhibiting a single-phase behavior. However these polymers are partially miscible as reflected by the thermal analysis with appearance of two T_gs with each phase being rich in a component. The thermograms for EE-EC blends are shown in **Fig. 7.9(a)** and the T_g *vs.* composition plot is shown in **Fig. 7.9 (b)**. The EE rich phase shows T_g at 51-61 °C and the EC rich phase shows T_g at 120-130 °C. The T_gs of EE and EC shift towards each other in blends indicating partial miscibility between the two.

The partially miscible EE-EC blends have a T_g phase rich in one component, which coexists with some fraction from the other component. The weight fraction of EE in each phase was determined by using the equations 4 and 5. The overall weight fraction of each phase in blends of EE with EC was studied using the equations 6 and 7.

The treatment of the blend T_g with equations 4 to 7 showed that T_{g1} phase was rich in EE component and its fraction in T_{g2} phase was negligible (See **Table 7.2**). The presence of small amounts of associated EC with EE increases T_g of EE from 55.3 to 61.5 °C. The overall weight fraction of each polymer was found to increase with increase in its concentration. The weak association between EE and EC was evident from the nature of interactions investigated by FTIR and the partial miscibility observed by thermal analysis further substantiates this.

The thermal and FTIR analysis of EE-EC blends provides insight for the release pattern that can be observed on blending these polymers. Under acidic buffer conditions the EE-EC blend compositions described here would show an initial burst with slight retard in release thereafter. This is predicted from the partial miscibility observed as investigated from thermal analysis and further the FTIR studies showed partial involvement of methylamino groups of EE in hydrogen bonding with EC.

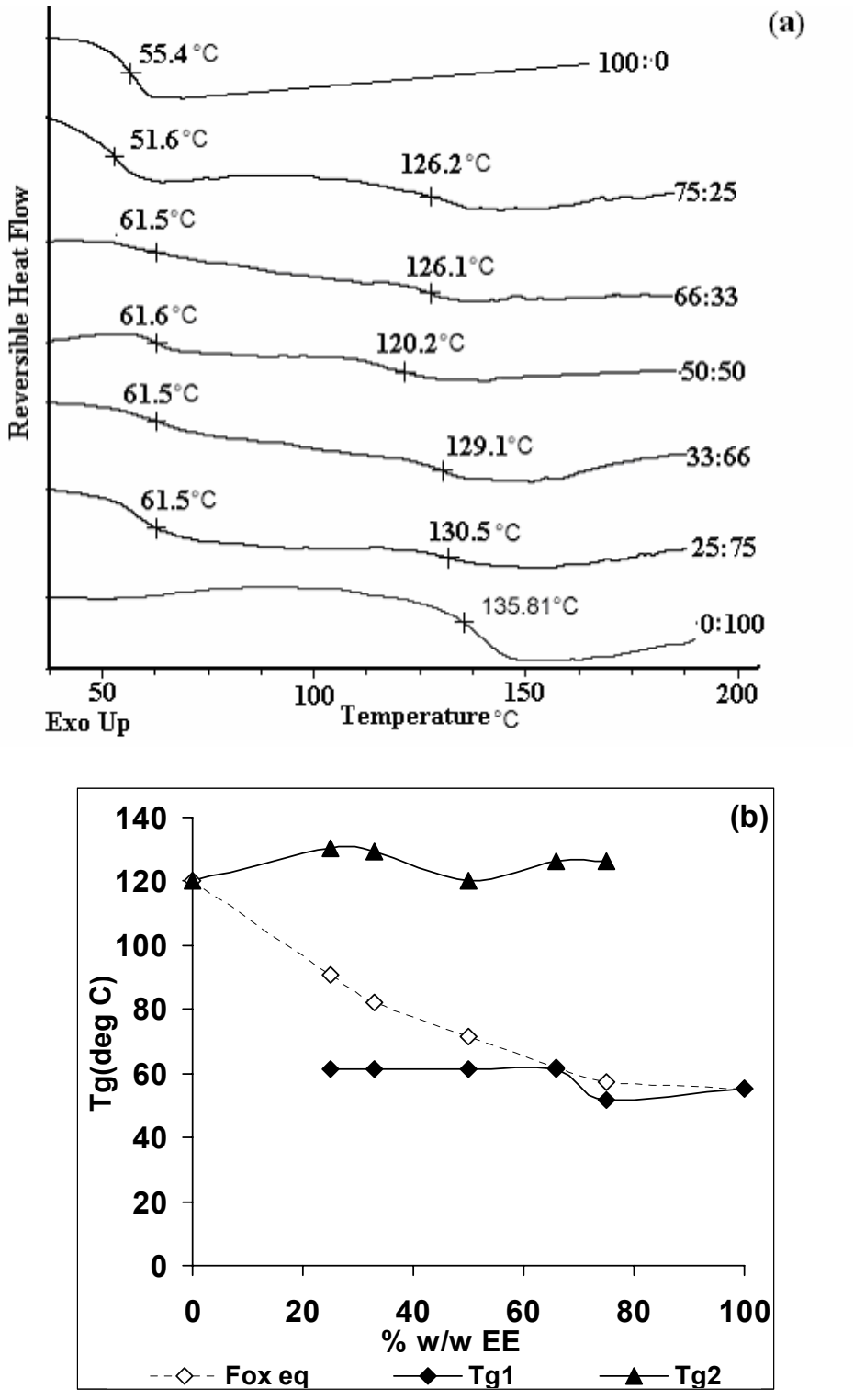

Fig.7.9. Thermal analysis for EE-EC blends, (a) DSC Thermograms (b)T_g *vs.* composition plot

Table 7.2: Weight fraction of EE in EE-EC and EE-Zein blends

EE-EC blend	Wt fraction of EE in T_{g1} phase	Wt fraction of EE in T_{g2} Phase	Total wt fraction of EE phase	Total wt fraction of EC phase
25:75	.92	.08	.21	.78
33:66	.92	.08	.29	.71
50:50	.92	.08	.42	.57
66:33	.92	.08	.67	.32
75:25	1.04	------	.69	.30
EE-Zein blend	**Wt fraction of EE in T_{g1} phase**	**Wt fraction of EE in T_{g2} Phase**	**Total wt fraction of EE phase**	**Total wt fraction of Zein phase**
25:75	1.0	----	.2	.8
33:66	1.0	----	.26	.73
50:50	1.0	-----	.40	.59
66:33	1.0	----	.61	.38
75:25	1.0	---	.80	.19

Table 7.3: Parameters of the Schneider equation

Blend	$K=T_{g1}/T_{g2}$	K_1	K_2	K_1-K_2
EE-ES	0.32	2.11	6.58	-4.47
EE-EL	0.33	5.13	24.35	-19.22
EE-HPMCP	0.40	2.76	7.45	-4.69
EE-CAP	0.36	5.10	22.15	-17.05

7.3.2.3. EE-EL and EE-ES blends

EE formed complex with EL and ES at all compositions immediately in MeOH–$CHCl_3$ (1:2 v/v). The precipitate was separated from the solvent and dried for 3 days under vacuum at room temperature. These samples were then analyzed for T_g. Specific interactions between polymers arise from the complementary dissimilarity in their structures. When these interactions are of acid-base nature, they result in charge transfer with polyelectrolyte salt formation. The T_g *vs* composition curves for such systems result in large positive deviations from additivity with the curve exhibiting either convex or sigmoidal behavior [2, 27].

The **Fig. 7.10 (a)** shows DSC thermograms for EE-EL and **Fig. 7.10(b)** shows T_g *vs* composition plots. In the present investigation, the experimentally obtained T_g values for EE-EL blends show large positive deviations from the weight average values of T_gs calculated by Fox equation, as expected. The T_g values of the EE-EL polyelectrolyte complex are in the range of 102-130°C. and are higher than weight average T_g values by 20-30°C. Strong intermolecular hydrogen bonding restricts the motion of polymer segments and therefore increase in T_g is observed.

The data treatment by Schneider equation (**Fig. 7.10 (c)**) for EE-EL blends resulted in K_1 and K_2 values of 5.13 and 24.35 respectively (**Table 7.3**). The value $K_1 > 0$ is expected since polyelectrolyte complexes exhibiting positive deviations for T_gs are observed from volume additivity. The higher values of K_1 indicate that interaction energy of the hetero contacts has exceeded that of average homo molecular contact [27]. From the FTIR spectrum for EE-EL blend, it was concluded that the hetero contact between the acid hydroxyl of EL and tertiary nitrogen of methylamino group was established with charge transfer. The charge density influences formations of hetero contacts and in case of EE and EL, both have high charge densities favoring the interactions. The value of K_1 (5.13) > 0 in EE-EL is due large contributions of energetic effects due to hetero contact formations. The stronger interactions arise from local chain orientations between the blend components to contribute to favorable hetero contacts, which results in a closer packing of the polymer blend giving higher T_g values than predicted from additivity [29]. The local interchain orientation to establish hetero

contact contributes consequently to conformational redistributions. The large K_1 values are therefore associated with large K_2 values as local chains orient to establish hetero contact which is reflected in $K_2 > 0$. Similar observations were reported by Schneider [27]. The parameter K_2 is difference of effects of redistributions predominantly in environment of component 1 and component 2 respectively. $K_2 > 0$ reflects more conformational changes occurring in EE than in EL. This is expected as EL exhibits better self-associations than EE as seen in FTIR analysis imparting some rigidity to the polymer chains. The K_2 (24.35) > 0 indicates more conformational change in EE environment than in EL and as a result of charge transfer the stiffening of the donor chain takes place contributing to higher T_g values. Hence T_g of the polyelectrolyte is greater than T_g for neat EE. Schneider, [27] reported that for absolute values of $[K_2] > [K_1]$, the sign of difference of fitting parameters (K_1-K_2) is always opposite to K_1 and corresponding T_g *vs* composition curves are S shaped. Our findings are similar to this as seen from the sigmoidal curves obtained for EE-EL blends and the corresponding values of fitting parameters as shown in **Table 7.3**.

At blend compositions 25:75, 33:66 and 50:50 w/w of EE-EL single composition dependent T_g is observed. However with increase in EE content at 66:33 and 75:25 % w/w in EE-EL blend, results in appearance of two T_gs. Both these compositions exhibit a weak transition at 58 and 55°C along with the major transition corresponding to the polyelectrolyte complex at 102 and 111.6°C respectively. This indicates that the phase rich in EE is not miscible with the polyelectrolyte complex. At higher concentrations of EE all the carboxylic hydroxyls of EL have been consumed in interaction with methylamino groups in EE forming with further free fraction of EE.

Both EL and ES are structurally similar and differ only in content of methacrylic acid. ES has 33 % and EL has 50 % of methacrylic acid [50]. The two polymers are therefore expected to show similar interactions with EE and this was evident from the FTIR analysis. However the extent of interaction would be different owing to different charge densities on ES and EL. The **Fig. 7.11 (a)** shows DSC thermograms for EE-ES blends and **Fig. 7.11(b)** shows T_g *vs* composition plots. As seen in case of EE-EL, the EE-ES blends show positive deviations from the weight average values of T_gs calculated by Fox equation. The T_g values of the EE-ES polyelectrolyte complex are

lower than that seen in EE-EL blends due to lower extent of interaction between the two.

The K_1 and K_2 values obtained for EE-ES blends are 2.11 and 6.58, respectively (see **Fig. 7.11(c)** and **Table 7.3**). The nature of hetero contact between EE-ES is similar to that in the case of EE-EL as seen from the FTIR analysis. The lower content of methacrylic acid in ES reduces the extent of interaction between EE-ES as compared to EE-EL and this is reflected in lower values of fitting parameters K_1 and K_2 for EE-ES blends than that seen in EE-EL (**Table 7.3**). The value $K_1 > 0$ for EE-ES blends is expected since polyelectrolyte complex with positive deviations for T_gs are observed from volume additivity. The values of $K_1>0$ indicates that interaction energy of the hetero contacts has exceeded that of average homo molecular contact [27]. Consequently the local interchain orientation to establish hetero contact contributes to conformational redistributions so that for EE-ES blends $K_2 > 0$. This reflects more conformational changes occurring in EE than in ES. This is expected as ES exhibits better self-association than EE as seen in FTIR analysis, imparting some rigidity to the polymer chains. The K_2 (6.58) > 0 indicates more conformational change in EE environment than in ES and as a result of charge transfer the stiffening of the donor chain takes place contributing to higher T_g values. Hence T_g of the polyelectrolyte complex is greater than T_g for neat EE. The T_g vs composition plots (**Fig. 7.11 (b)**) of EE-ES are convex, characteristic of hydrogen-bonded blends.

At blend compositions 25:75, 33:66, 50:50 and 66:33 w/w of EE-ES single composition dependent T_g is observed. For EE-ES blends with higher content of ES (66 and 75% w/w respectively) the T_g is comparable to the weight average value obtained from Fox equation. However increase in EE content at 75:25 % w/w in EE-ES blend, results in appearance of two T_gs. A weak transition around 58 °C along with the major transition corresponding to the polyelectrolyte complex at 82°C is seen. This indicates that the phase rich in EE is not miscible with the polyelectrolyte complex. This observation is similar to that observed in case of EE-EL blends. At higher concentrations of EE all the carboxylic hydroxyls of ES have been consumed in interaction with methylamino groups in EE forming polyelectrolyte complex and further presence of free fraction of EE.

The weight fractions involved in forming the EE-EL and EE-ES complex in systems showing excess of EE were determined using equation 4 and 5. The weight fraction of EE in EE-EL blends at 66 %w/w of EE is 97 % in EE rich and 57.1% in complex. The EE-EL blend at 75 % w/w of EE has 100 % of EE in EE rich phase and 48.3 % of EE in complex. The EE-ES blend at 75 % w/w of EE has 97.7 % of EE in EE rich phase and 77.4 % of EE in complex phase.

Once the polyelectrolyte complexes are formed they are insoluble in most of the aqueous and non-aqueous solvents. Hence the removal of the excess of free polymer not involved in complexation but entrapped within the complex is difficult and requires repeated washing. The swelling behavior of the free polymer entrapped would be different from that of the complex and hence controlling drug release from such complexes co-existing with free polymer would be difficult.

The determination of weight fractions required for achieving complexation at various compositions in EE-EL and EE-ES blends described in present investigation provide an insight for achieving polyelectrolyte complexes without having a free / excess polymer phase.

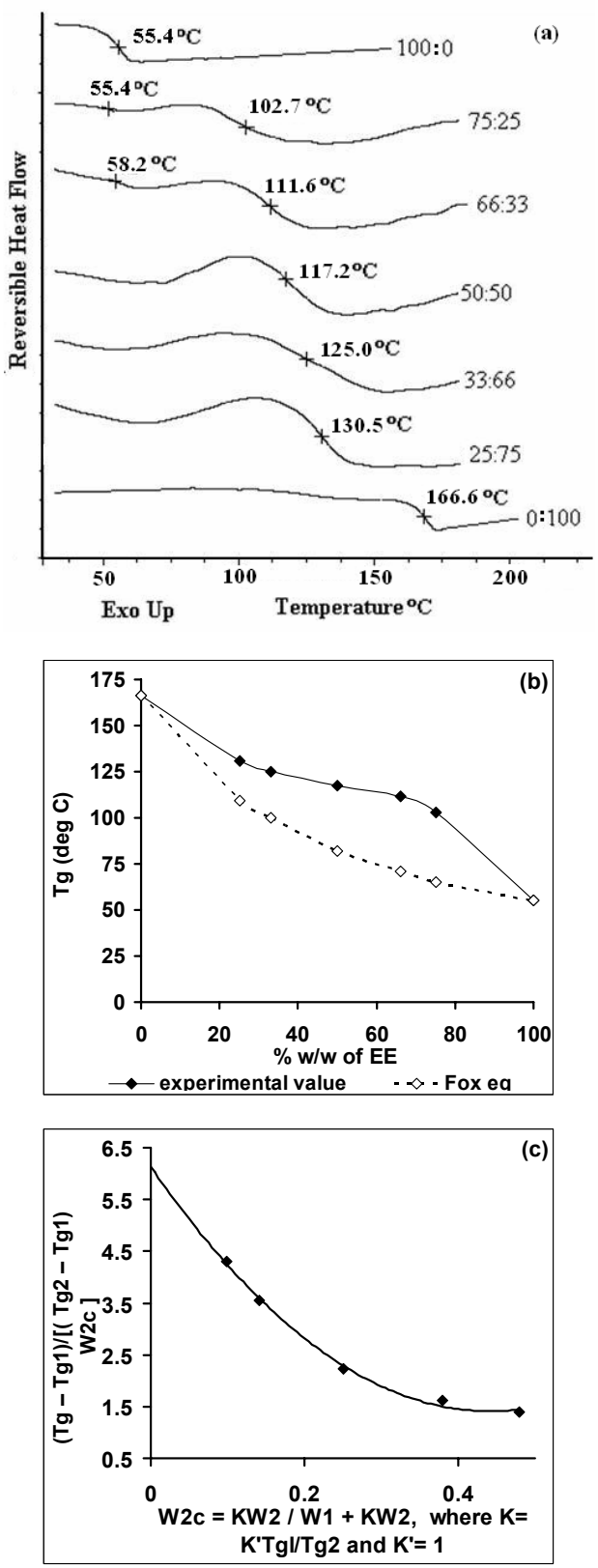

Fig.7.10. Thermal analysis of EE-EL blends, (a) DSC Thermograms (b)T_g *vs.* composition plot (c) Plots for Schneider equation

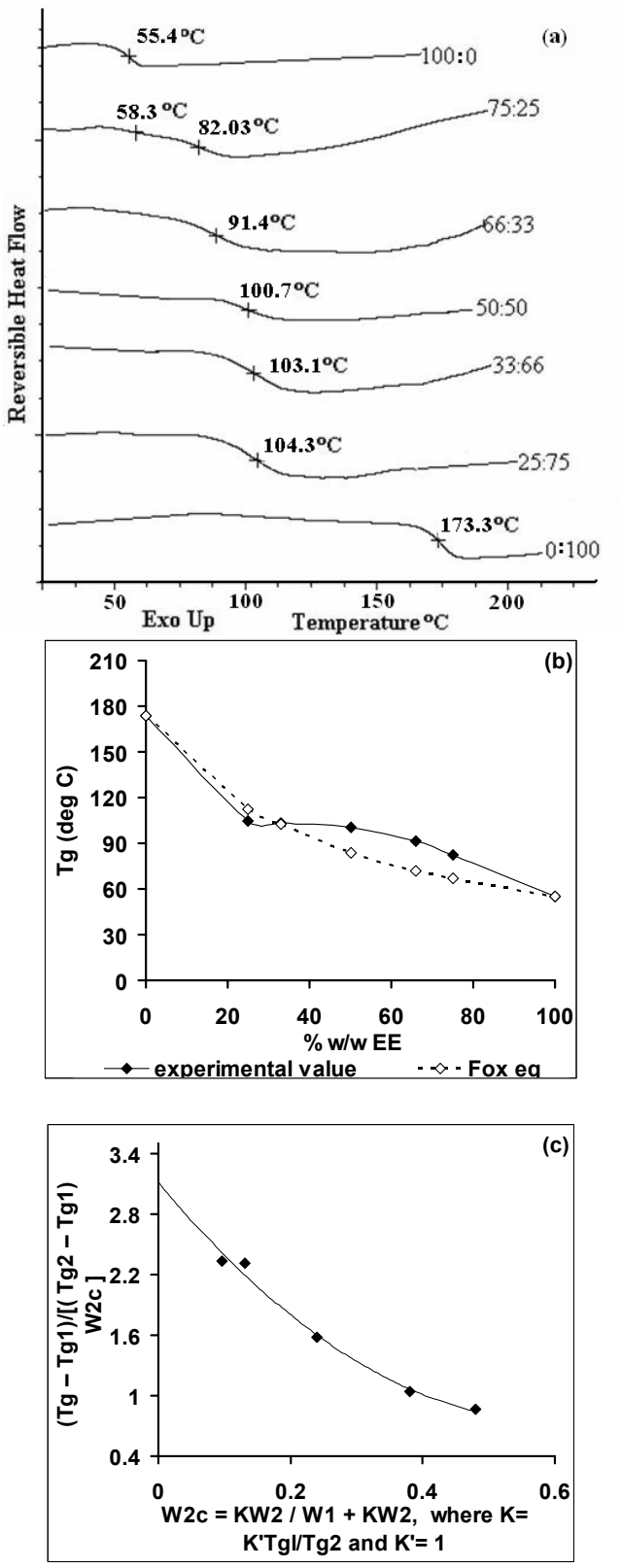

Fig.7.11. Thermal analysis EE-ES blends, (a) DSC Thermograms (b)T_g *vs.* composition plot, (c) Plots for Schneider equation

7.3.2.3. EE-CAP and EE-HPMCP blends

EE formed polyelectrolyte complex with HPMCP and CAP almost instantaneously at all compositions exhibiting a very strong interaction between these polymers. This was expected since the HPMCP and CAP have higher content of hydroxyls than in EL and ES. **Figs. 7.12(a) and 7.13(a)** show the DSC thermograms for EE-CAP and EE-HPMCP blends respectively and the plot of T_g *vs*. composition for these systems is shown in **Figs. 7.12 (b) and 7.13 (b)**. The T_g *vs* composition curves for both these systems exhibit large positive deviations (+ 20~30°C) from additivity and are sigmoidal in nature, characteristic for hydrogen-bonded blends. Strong intermolecular hydrogen bonding restricts the motion of polymer segments leading to increase in T_g.

The data treatment by Schneider equation (**Fig. 7.12(c)**) for EE-CAP blends gave values of fitting parameters K_1 and K_2 of 5.1 and 22.15 respectively (**Table 7.3**). Both EL and CAP exhibit strong interaction with EE and the values of fitting parameters K_1 and K_2 are comparable as seen in **Table 7.3**. The value $K_1 > 0$ is expected since polyelectrolyte complex with positive deviations for T_gs are observed from volume additivity. The higher values of K_1 indicate that interaction energy of the hetero contacts has exceeded that of average homo molecular contact [27]. From the FTIR spectrum for EE-CAP blend it was concluded that the hetero contacts between the acid and cellulosic hydroxyl of CAP and tertiary nitrogen of methylamino group were established with charge transfer. Both EE and CAP have high charge densities favoring the interactions for hetero contact formations which is reflected in value of K_1 (5.1) > 0 due to large contributions of energetic effects. The favorable hetero contacts contribute stronger interactions arising from local chain orientations between the blend components to contribute, which results in a closer packing of the polymer blend giving higher T_g values than estimated from additivity rule. [29]. As a result of charge transfer the stiffening of the donor chain takes place contributing to higher T_g values. Hence T_g of the EE-CAP polyelectrolyte complex is greater than T_g for neat EE. The local interchain orientation to establish hetero contact contributes consequently to conformational redistributions which is reflected in $K_2 = 22.15$. The parameter K_2 is difference of effects of redistributions predominantly in environment of component 1

and component 2 respectively. $K_2 > 0$ reflects more conformational changes occurring in EE than in CAP and this is expected as CAP has a bulky cellulosic structure and exhibits better self-association than EE imparting some rigidity to the polymer chains.

At blend compositions 50:50, 66:33 and 75:25 w/w, single composition dependent T_g is observed for EE-CAP blends. The blends showing single T_g indicate complete involvement of polymers in complex formation. However with increase in CAP content at 33:66 % w/w EE-CAP blend, results in appearance of two T_gs one major transition corresponding to the T_g of complex (115.6 °C) and the second for the free fraction of the CAP (178.5 °C). The shift in T_g of CAP at this blend composition in EE-CAP blends as compared to T_g of neat CAP suggests that it is associated with the polyelectrolyte complex or EE via hydrogen bonding. At higher concentrations of CAP 25:75 % w/w in EE-CAP blend a T_g at 126.5 °C corresponding to polyelectrolyte complex is seen and crystallization of excess CAP is seen at 178 °C.

HPMCP differs from CAP due to the presence of the propyl and methyl side groups on the cellulosic structure. However, both these polymers contain phthalic acid and cellulosic hydroxyls, which form hydrogen bonds with EE (as seen from FTIR analysis). Hence the two polymers were expected to show similar interactions with EE. However the extent of interaction was found to be different as revealed from the T_g data treatment by Schneider equation. As seen in case of EE-CAP, the EE-HPMCP blends show large positive deviations from the weight average values of T_gs calculated by Fox equation (**Fig. 7.13(b)**). The T_g values of the EE-HPMCP polyelectrolyte complex are lower than that seen in EE-CAP blends due to lower extent of interaction between the former.

The values for fitting parameters K_1 and K_2 obtained for EE-HPMCP blends are 2.76 and 7.45, respectively (see **Fig. 7.13(c)** and **Table 7.3**). The nature of hetero contact between EE-HPMCP is similar to that in case of EE-CAP as seen from the FTIR analysis. The presence of propyl and methyl groups in HPMCP contribute for the steric hindrance and this is reflected in lower values of fitting parameters K_1 and K_2 for EE-HPMCP blends than that seen in EE-CAP (**Table 7.3**). Amongst the K_1 values for the three systems, the values is highest in EE-EL which might be due to the similar structural symmetry in polydonor and polyacceptor resulting in increased mobility of

the interacting groups by spacer length between the acceptor group and polymeric backbone. The charge density, favorable structural / steric symmetry influences formations of hetero contacts by 'zipp' like arrangement at the interacting sites [29, 30]. The structurally symmetric polydonor and polyacceptor show better hetero contact formation due to the increased mobility of the interacting groups by spacer length between the acceptor group and polymeric backbone [29, 30].

The value $K_1 > 0$ for EE-HPMCP blends is expected since polyelectrolyte complex with positive deviations for T_gs are observed from volume additivity. $K_2 > 0$ reflects more conformational changes occurring in EE than in HPMCP. This is expected as HPMCP has bulky cellulosic structure as compared to EE. The K_2 value (22.15) in EE-CAP blend is greater than the K_2 values (7.45) in EE-HPMCP, which is due to presence of side propyl and methyl groups contributing to steric effects. Also HPMCP exhibits better self-association than EE as seen in FTIR analysis imparting additional rigidity to the polymer chains. The K_2 (7.45) > 0 indicates more conformational change in EE environment than in HPMCP and as a result of charge transfer the stiffening of the donor chain takes place contributing to higher T_g values. Hence T_g of the polyelectrolyte is greater than T_g for neat EE.

In case of EE-HPMCP and EE-CAP at weight fractions 25:75% w/w, 33:66 % w/w and 33:66 % w/w respectively, appearance of two T_gs was observed and the weight fractions in each phase were determined using equation 4 and 5. At 33:66% w/w EE-HPMCP blend, the EE concentration was found to be 37 % and 21 % at T_{g1} and T_{g2} respectively. The concentration of EE in the EE-HPMCP blend at 25:75% w/w was found to be 33 % and 9 % at T_{g1} and T_{g2} phase respectively. The presence of 9 % of EE in T_{g2} phase explains the shift in T_g of HPMCP from 137.41° C to 130° C at 25:75 % w/w EE-HPMCP blend. The amount of EE forming complex with HPMCP and CAP at 33 (EE) : 66 % w/w was found to be comparable, with 38 % of EE in T_{g1} phase and 26 % in Tg_2 phase. Such phase separation in close proximity is not well resolved by conventional DSC techniques. The most common observation in such cases is a single phase behavior with increased transition width. It is the advantage of the modulated temperature DSC where the overlapping thermal events are well resolved. Similar observations were put forth by Song et al. [31].

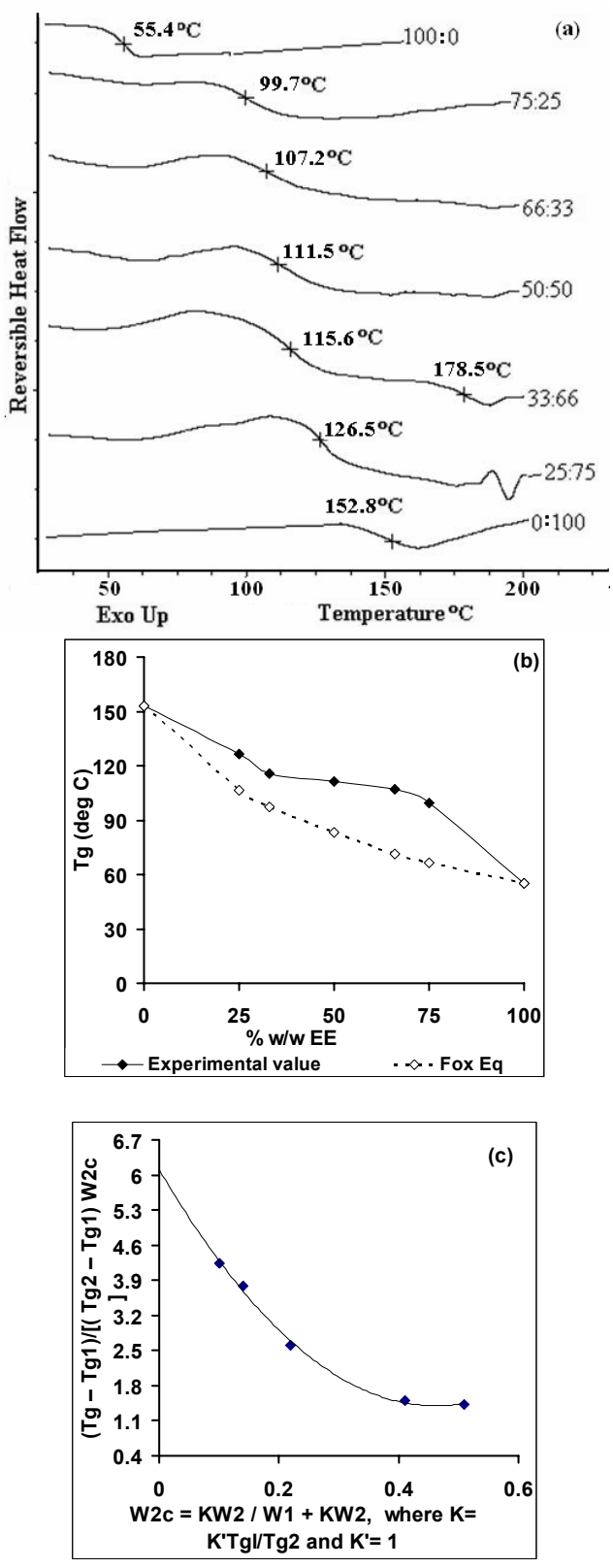

Fig.7.12 Thermal analysis of EE-CAP blends, (a) DSC Thermograms (b)T_g *vs.* composition plot (c) plots for Schneider equation

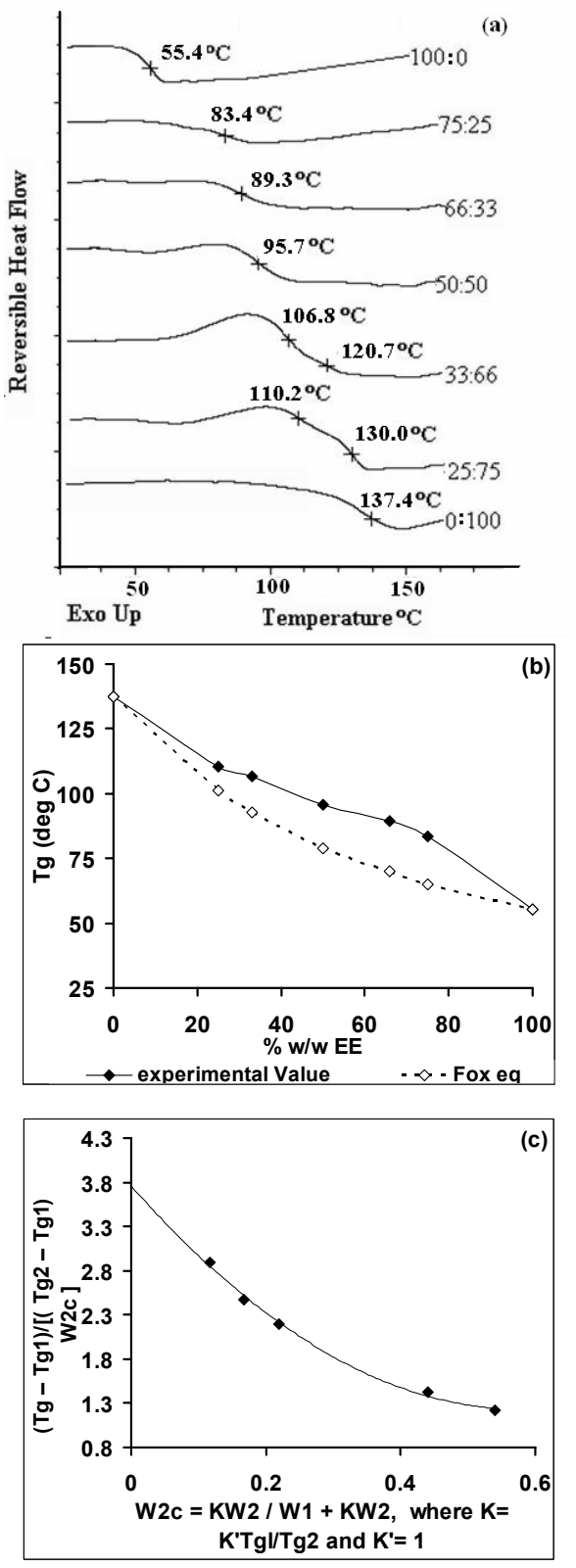

Fig.7.13. Thermal analysis of EE- HPMCP blends, (a) DSC Thermograms (b)T_g *vs*. composition plot (c) Plots for Schneider equation

7.3.3. Effect of monomer basicity on polymer-polymer interactions

In this chapter we have seen that strong interaction between EE and polyacids leads to complex formation. However NREP did not form complex with any of these polyacids. To investigate the possible reasons for this, following approaches were considered 1) Effect of structural defect, content of basic monomer, and solvent 2) The basicity of functional monomer 4-VP *vs.* DMAEMA.

1) Effect of structural defect, content of basic monomer and solvent

Complex formation is inhibited either due to presence of structural defects or low concentration of interacting sites [2, 3, 17, 22, 32]. NREP has low 4VP content and presence of nonionic HEMA, which can be considered as structural defect contributing to its miscibility but inhibiting complexation.

In order to replicate a situation similar to that of NREP we synthesized a terpolymer with composition MMA-HEMA-DMAEMA (60-25-15 % w/w respectively). The blends of this polymer were prepared with EL and HPMCP in MeOH-$CHCl_3$ (20:80 v/v). We observed that at all compositions these blends resulted in complex formation with immediate precipitation.

The solvents affect polymer miscibility and protic solvents like methanol and ethanol have`` favored complexation of p(DMAEMA) with p(vinyl phenol), whereas complexation did not result in aprotic solvents like DMF. Methanol shows favorable interactions with proton accepting polymer and DMF exhibits more interactions with proton donating polymer [14]. To investigate the effect of solvent the blends of this terpolymer with EL and HPMCP were attempted in DMF. The blend solution turned turbid followed by precipitation after 30 min at all compositions. The behavior was thus similar to that exhibited by EE upon blending with EL and HPMCP. The interaction of terpolymer with EL and HPMCP is stronger than its interaction with solvent.

From these observations it can be concluded that introduction of the nonionic structural defect HEMA did not reduce the intermolecular interactions between MMA-HEMA-DMAEMA (60-25-15 % w/w respectively) with EL and HPMCP. These

observations are opposite to that seen in case of NREP, which shows miscibility at all compositions without complexation. The possible reason could be the lower basicity of 4VP than DMAEMA or lower content of 4VP.

To investigate effect of structural defects due to HEMA and also the content of 4VP in NREP affecting its interactions with acid hydroxyls of EL and HPMCP, we synthesized a copolymer MMA-VP (70:30 % w/w). The content of 4VP was double in MMA-VP copolymer (30%) than NREP (15%). Blends of this polymer were prepared with EL and HPMCP in MeOH-$CHCl_3$ (20:80 v/v). At all compositions the blends did not result in turbidity and did not show precipitation even after 1 hr. Films from these solutions were cast. In absence of HEMA it was expected that the copolymer of MMA-VP with VP content higher than NREP should exhibit stronger interactions with EL and HPMCP resulting in complex formation. However this was not observed. The results suggest that in the present systems investigated the more basic nature of DMAEMA as compared to 4VP is the likely reason for its stronger interactions with acid hydroxyls, which lead to complexation.

2) The basicity of functional monomer in 4 VP vs. DMAEMA

The pKa of 4-VP is 5.4 and that of DMAEMA is 8.4. The difference in the interaction of DMAEMA and 4-VP based polymers in present investigations towards the polyacids studied is more profound because of the differences in the basicity of these monomers. Bouslah et al.[4,33] have reported polymer blends based on poly[styrene-*co*-(cinnamic acid)] / poly[(ethyl methacrylate) –*co* -(2-dimethylamino ethylmethacrylate)] blends and p(ethyl methacrylate-*co*-4-vinylpyridine) / p(styrene-*co*-cinnamic acid). Comparison of these systems revealed that [*N,N*-dimethylamino] ethyl methacrylate units had greater ability to hydrogen bond with carboxylic acid groups of the p(styrene-*co*-cinnamic acid) than 4-vinylpyridine units. Our findings are similar to those reported by Bouslah et al. [4].

2) Effect of structural / steric symmetry and spacer length between functional group and polymer main chain on polyelectrolyte complex formation

From the DSC and FTIR study it was inferred that all polymers containing acid hydroxyls formed strong interaction with EE leading to polyelectrolyte complex formation. Charge transfer interactions resulting from hetero contact formation between poly acceptor and polydonor are enhanced with increased spacer length between electron acceptor group and polymer main chain backbone [27, 29, 30]. The probability of charge transfer is influenced by favorable structural / steric symmetry factors which contribute to formation of hetero contacts. The polyacceptor / polydonor with structural symmetry show better interaction due to increased mobility in interacting groups because of the presence of spacer length in acceptor group and polymeric back bone [27, 29, 30]. The presence of spacer ethyl chain in DMAEMA from polymeric backbone provides it with better mobility to form hetero contact with polyacids resulting in complexation. When the structures of polymers EE, EL, CAP and HPMCP are considered both EE and EL have similar polymer backbone and also the similar spacer groups separating the functional groups from the polymer main chain. This provides better flexibility for these polymers to undergo conformational redistributions to form hetero contacts. This is reflected in the largest K_1 and K_2 values obtained for EE-EL systems than EE-ES, EE-CAP and EE-HPMCP blends. The values of K_1 and K_2 are less in EE-ES due to lower charge density of ES. However in spite of higher charge density in case of both CAP and HPMCP it shows lower interaction with EE and this is due to the dissimilarity in the structures of EE and these polymers. Both CAP and HPMCP do not have long spacer groups separating the functional groups from polymer backbone, the presence of the cellulosic ring imparts rather rigid structure to these polymers impeding the chain mobility and this is reflected in lower K_1 and K_2 for these polymers than that seen for EE-EL as seen from **Table 7.3** .

When the values of fitting parameters K_1 and K_2 for EE blends are compared against those obtained for NREP blends, the former are much higher. The spacer length between electron acceptor group and polymer main chain backbone as seen in EE provides it the leverage for better hetero contact formation with polyacids than for

NREP. The presence of aromatic ring in NREP directly attached to the polymer main chain backbone makes this polymer more bulky / rigid with restricted segmental motion than EE hence NREP forms miscible blends without complexation as seen in EE. In the present systems the probability of charge transfer is influenced by favorable structural symmetry factors and spacer length between electron acceptor group and polymer main chain backbone in polyacceptor / polydonor.

7.4. CONCLUSIONS

Polymer blends are widely used in drug delivery in various different forms like film coating, matrix formulations and polyelectrolyte complexes. The polymer-polymer interaction determines the phase behavior in blends contributing to immiscibility, partial miscibility, miscibility and complexation. The thermal analysis showed that blends of EE-Zein and EE-EC are immiscible and partially miscible at all compositions respectively due to weak interactions exhibited by these polymers. In contrast, the blends of NREP-EC were miscible and this can be attributed to presence of hydroxyl groups from HEMA in NREP. EE formed polyelectrolyte complexes at all compositions with EL, ES, CAP and HPMCP unlike blends of NREP, which were miscible at all compositions. The values of fitting parameters K_1 and K_2 were higher for EE blends with polyacids than those seen in blends of NREP. The higher extent of interactions exhibited by EE than NREP is attributed to higher charge density, higher pKa values of DMAEMA than 4-VP and absence of nonionic structural defect like HEMA in the polymer EE. The structural symmetry between EL, ES and EE helps in enhanced interactions leading to complexation. The presence of spacer ethyl chain in DMAEMA from polymeric backbone confers better mobility to form hetero contact with polyacids resulting in complexation. These investigations were very useful for understanding the underlying reasons for not observing the complexation in case of NREP. The lower charge density, lower pKa value of 4-VP, strong self associations in NREP, presence of nonionic structural defect HEMA and absence of spacer chain between 4-VP and polymeric back bone, all contribute to its miscibility without complexation. The novelty of this work is, it provided miscible blends of NREP with enteric polymers capable of

film coating. This new set of polymer blends helped us manipulate CA release profiles for extended period at gastric pH.

7.5. REFERENCES

1) H.A. Schneider Glass Transition (Theoretical Aspects), The Polymeric Materials Encyclopedia. CRC Press, Inc, 1996.
2) M. Jiang, M. Li, M. Xiang, H. Zhou, Adv Polym Sci 1999, 146, 121-196.
3) M.V. Meftahi, J.M.J. Frechet, Polymer 1988, 29, 477 - 482.
4) N. Bouslah, N. Haddadine, D. Bendiabdallah, F. Amrani, Polymer Bulletin 1999, 42, 701–708.
5) R.I. Moustafine, T.V. Kabanovaa, V.A. Kemenovab, G. Van den Mooterc, J. Controlled Rel. 2005, 103,191-198.
6) R.I. Moustafine, T.V. Kabanovaa, V.A. Kemenovab, G. Van den Mooterc, Int. J. Pharm. 2005, 294, 113-120.
7) V. Kumar, T. Yang, Y. Yang, Int. J. Pharm. 1999, 188, 221–232.
8) A.El-Hag A. Said, Biomaterials, 2005, 26, 2733–2739.
9) B. C. Anderson, S. K. Mallapragada, Biomaterials 2002, 23, 4345–4352.
10) W. H. Jo, C. A. Cruz, D. R. Paul, J. Polym Sci: Part B: Polym. Phys. 1989, 27, 1057-1076.
11) L.A. Utracki, Polymer alloys and blends, thermodynamics and rheology. Hanser Publishers, Oxford University Press, New York, 1990.
12) S.Y. Lin, H. L. Yu, J Polym Sci: Part A: Polym. Chem. 1999, 37, 2061–2067.
13) A.M. Juppo, C. Boissier, C. Khoo. Int. J. Pharm. 2003, 250, 385-/401.
14) X.-D. Huang, S. H. Goh, S. Y. Lee, Z. D. Zhao, M. W. Wong and C. H. A. Huan, Macromolecules, 1999, 32, 4327-4331.
15) Katime A, Iturbe CC. Hydrogen-bonded blends, The Polymeric Materials Encyclopedia. CRC Press, Inc 1996.
16) S. R. Van Tomme, M. J. V. Steenbergen, S. C. D. Smedt, C. F. V. Nostrum and W. E. Hennink, Biomaterials, 2005, 26, 2129–2135.
17) I. Iliopoulos and R. Audebert. Eur. Polym. J., 1988, 24, 171-175.
18) K. G. Duodu, H. Tang, A. Grant, N. Wellner, P. S. Belton , J. R. N. Taylor J. Cereal Science. 2001, 33, 261–269.

19) M. Mayo-Pedrosa, C. Alvarez-Lorenzo, A. Concheiro, J. Therm. Anal. Cal. 2004, 77, 681–693.

20) D.E. Bugay and W.P. Findlay, Pharmaceutical excipients: Characterization by IR, Raman, and NMR spectroscopy. Marcel Dekker, 1999.

21) V. Suthar, A. Pratap and H. Raval. Bull. Mater. Sci. 2000, 23, 215–219.

22) J.Y. Lee, P.C. Painter and M.M. Coleman, Macromolecules, 1988, 21, 954-960.

23) F. Cilurzo, P. Minghetti, F. Selmin, A. Casiraghi and L. Montanari, J. Controlled Rel. 2003, 88, 43–53.

24) A. H Kibbe, Handbook of Pharmaceutical Excipients, 3rd Edition, American Pharmaceutical Association 2000.

25) S.Y. Lin, C.M. Liao, G.H. Hsiue and R.C. Liang. Thermochim Acta 1995, 245, 153-166.

26) S.Y. Lin, H.L. Yu and M.J. Li., Polymer, 1999, 40, 3589–3593.

27) H A. Schneider, J. Res. Natl. Inst. Stand. Technol. 1997, 102, 229-248.

28) J. Macoshi, S. Nakamura and K. Murakami. J. App. Polym. Sci. 1992, 45, 2043-2048.

29) HA. Schneider. Polymer, 1989, 30, 771-779.

30) H.A. Schneider. Polym Bulletin, 1998, 40, 321-328.

31) M. Song, A. Hammiche, H. M. Pollock and D. J. Houston. Polvmer, 1996, 31, 5661-5665.

32) M.J. Krupers, F.J. Van Der Gaag, J. Feijent, Eur P&N J 1996, 32, 785-790.

33) N. Bouslah, R. Hammachin, F. Amrani, Macromol. Chem. Phys. 1999,200, 678–682.

34) N. Bouslah, R. Hammachin, F. Amrani, Macromol. Chem. Phys. 1999,200, 678–682.

35) H. Eerikainen and E. I. Kauppinen. Int. J. Pharm. 2003, 263, 69–83.

36) S.K. Jain, A.M. Awasthi, N.K. Jain and G. P. Agrawal., J. Controlled Rel. 2005,107, 300– 309.

37) Rowe RC. *Materials used in the film coating of oral dosage forms*. In: A.T. Florence (Ed), Materials used in Pharmaceutical Formulation. Blackwell; Oxford, 1984. p. 2-34.

38) N. Pearnchob and R. Bodmeier. Eur. J. Pharm. Biopharm. 2003, 56, 363–369.

39) M.I. Beck, I. Tomka and E. Waysek. Int. J. Pharm. 1996, 141,137-150.

40) G. Sertsou, J. Butler, A. Scott, J. Hempenstall and T. Rades. Int. J. Pharm. 2002, 245, 99-108.

41) E.P. Segundo, A. Ganem-Quintanar, V. Alonso-Perez and D. Quintanar-Guerrero Int. J. Pharm. 2005, 294, 217–232.

42) A.J.M. Valente, H.D. Burrows, A.Y. Polishchuk, M.G. Miguel and V.M.M. Lobo. Eur. Polym. J. 2004, 40,109–117.

43) V. Rao, P.V. Ashokan and M.H. Shridhar. Polymer, 1999, 40, 7167–7171.

44) V. Rao, P.V. Ashokan and J.V. Amar. J. App. Polym. Sci., 2002, 86, 1702–1708.

45) R. Shukla and M. Cheryan. Ind. Crops Products. 2001, 13, 171–192.

46) P.B. Donnell, C. Wu, J. Wang, L. Wang, B. Oshlack, M. Chasin, R. Bodmeier, and J.W. McGinity. Eur. J. Pharm. Biopharm. 1997, 43, 83-89.

CHAPTER 8

Blends of NREP with Fatty Acids: Enhancing Drug Release at Gastric pH

8.1. INTRODUCTION

Commonly used lipid vehicles in formulations of drugs are medium chain triglycerides, long chain triglycerides, waxes and derived lipids (fatty acids). Fatty acids are used for the controlled delivery and taste masking of therapeutic agents, although the mechanisms involved in the release process are poorly understood [1]. Fatty acids are long chain carboxylic acids and the saturated fatty acids; palmitic and strearic acid are frequently used in formulations. Stearic acid and its corresponding salts have been used in pharmaceutical technology for many years, particularly as the magnesium salt in tablet and capsule formulations. A more recent development has been the use of stearic acid as monoliths or in micro / nano encapsulated formulations whereby the fatty acid is used to confer controlled drug release properties [1].

Lipids are associated with properties like water repellency, non-toxicity and freedom from objectionable odor and color and they impart a smooth texture to the compositions. These properties make the lipids good candidates for taste masking applications. However fatty acids do not exhibit good film forming properties. Integral coatings with lipids alone need larger amount of lipids since the medicament has to be dispersed completely in the lipid matrix. The techniques like melt granulation and spray congealing also need large amount of the molten lipids, since the drug has to be dispersed within the lipid matrix. A novel hydrophobic matrix coating which delays the hydration of the core, containing 61 – 95 % by weight of fatty acid is described in US Patent 4,797,288 [2]. These dry drug particles were designed either for chewing or swallowing and the coating provides taste masking. Lipids are hydrophobic in nature and so the release of the medicament is greatly impaired when lipids are used in higher amounts. Also the use of lipids alone tends to delay the release of the drug.

The release of drugs from lipid vehicle results from dispersion of the drug in the intestine due to the formation of lipid degradation products, which aid in enhanced solubilization and dispersion of the drug in the intestine. The pancreatic lipase causes the digestion of the lipid formulation and the drug is transferred from the formulation into the intestinal environment, where it is incorporated into mixed micelles, containing bile salts, phospholipids and lipolytic products [3].

To enhance the release of drugs from lipid based formulations use of polymers in combination with the lipids has been investigated. US Patent 5,972,373 [4] describes taste masked pharmaceutical compositions with good bioavailability using the coating compositions consisting of polyvinylacetal diethylaminoacetate, Eudragit E and glyceryl monostearate. A taste masked formulation of rebamipide containing fatty acid glycerol esters easily water-soluble substances is described in Patent Application JP 2001288117 [5] Water soluble or swelling substances are used to enhance release of the drug from lipid matrix. GB Patent 2081092 [6] describes the use of waxy materials and high molecular weight water swellable material where the later is added to improve dissolution and subsequently the absorption of the drug. The use of water swelling materials along with lipids in taste masking compositions is not preferred, especially so in case of liquid oral formulations.

To overcome the above limitations the use of hydrophobic polymers like ethyl cellulose or enteric polymers in combination with lipids for taste masking which prevent the leaching of the drug in the surrounding aqueous media in liquid orals has been opted. A substantially tasteless pharmaceutical composition containing a matrix wax core and a hydrophobic polymer is described in patent EP 0670716 [7]. Taste masked composition of Clarithromycin containing glycerol fatty acid ester / stearyl alcohol and a polymer selected from hydroxypropyl methylcellulose phthalate, hydroxypropyl methylcellulose acetate succinate, carboxymethyl ethyl cellulose, methacrylic acid copolymer L, methacrylic acid copolymer LD and methacrylic acid copolymers are described in Patent Application WO 01/91761 [8]. However such formulations employing hydrophobic / enteric polymers with lipids tend to retard or delay the drug release respectively.

To enhance the release / dissolution of drugs from the lipids based formulations the use of gastric soluble polymer Eudragit E in combination with the lipids has been tried in the past. These formulations provide an immediate release of the drug and also the taste masking effect. Eudragit E is soluble up to pH 5 and shows a swelling up to pH 5.5 [9] and is known to interact with certain drugs like Cefuroxime axetil [10]. A commercial product based on stearic acid, coated Cefuroxime axetil marketed as a pediatric oral suspension, is available [1]. Robson et al. 1999 [11] demonstrated that

Cefuroxime axetil is released in alkaline environment due to formation of water-soluble sodium salt. Since Cefuroxime axetil is hydrolyzed in intestine it cannot be absorbed. As a result, its bioavailability is adversely affected [12-14]. Hence a lipid formulation capable of taste masking and releasing the drug in stomach is warranted.

In the present chapter we have investigated the blends of NREP with different fatty acids for taste masking Cefuroxime axetil and Ciprofloxacin HCl. We have accomplished taste masking without significantly altering the release and availability of the drug at gastric pH. The drug release from "Ceftum" was compared to that from the formulations developed using NREP and Cefuroxime axetil. All the formulations investigated released Ciprofloxacin HCl and Cefuroxime axetil rapidly at pH 1.2. Also the preparation of these taste masked compositions by emulsification solvent evaporation, hot melt granulation and spray-drying methods is described.

8.1.1. Materials

Ciprofloxacin HCL and Cefuroxime axetil were gift samples from Lupin Laboratories Ltd. Stearic Acid, palmitic acid, cetylalcohol, Glyceryl monostearate, Hydrogenated Castor oil were also gifted by Lupin Laboratories Ltd. Hydrochloric acid was purchased from Merck. Chloroform was purchased from Thomas Baker. Polyvinyl alcohol was purchased from S.D. Fine Chemicals Ltd.

8.2. IMMEDIATE RELEASE TASTE MASKED CIPROFLOXACIN HCL FORMULATIONS USING NREP-FATTY ACIDS BLENDS

8.2.1. Methods

8.2.1.1. Melt granulation method

Taste masked particles were obtained by melt granulation method. Lipid was placed in a jacketed vessel attached to a circulating water bath. Temperature of circulating water was set such that lipid is maintained at 3-5°C above melting point.

NREP was dispersed in molten lipid under stirring followed by addition of Ciprofloxacin Hydrochloride. Temperature of circulating water was gradually lowered to cool the molten lipid. The solid mass thus obtained was sized by passing thorough 40-mesh sieve. The compositions containing lipid-NREP blends are shown in **Table 8.1**.

8.2.1.2. Slab casting

Taste masked compositions are made by casting slabs of lipid- polymer containing the drug. The lipid- polymer solution in organic solvent is cast in a tray containing the drug in a solution form or in a dispersed form. Solvent is allowed to evaporate and particles are obtained by sizing the mass through 40-mesh sieve.

Compositions containing various lipid-NREP blends are shown in **Table 8.2**. Ciprofloxacin hydrochloride was added to lipid-polymer solution in 7 ml chloroform. The solution was poured in a tray to cast the slab. Solvent was allowed to evaporate at 25°C for 2-3 hrs. Residual solvent was removed by placing the composition in vacuum at 25°C for 24 hrs. Taste masked particles were prepared by sizing the mass obtained.

8.2.1.3. Determination of drug content

The drug content was determined at 276 nm using Shimadzu UV160 IPC UV Visible spectrophotometer. Ciprofloxacin HCL content was determined by dissolving 50 mg of sample in 2 ml of methanol and sonicating for 5 min. Then the volume was made to 250 ml using 0.01 N HCl. The solution was filtered and diluted further for the analysis. Each sample was analyzed in triplicate. The drug content is shown in **Table 8.3.**

Table 8.1, Formulations by melt granulation

Formulation	Lipid		NREP	Ciprofloxacin HCl
F1	Stearic acid	1.75 g	0.10 g	0.583 g
F2	Palmitic Acid Stearic Acid	0.87 g 0.87 g	0.10 g	0.583 g

Table 8.2, Formulations by slab casting

Formulation	Lipid		NREP	Ciprofloxacin HCl
F3	Stearic acid	0.84 g	0.10 g	0.583 g
F4	Palmitic acid	0.84 g	0.10 g	0.583 g
F5	Cetyl Alcohol	0.84 g	0.10 g	0.583 g
F6	Palmitic Acid Stearic Acid	0.42 g 0.42 g	0.10 g	0.583 g
F7	Stearic acid Cetyl Alcohol	0.42 g 0.42 g	0.10 g	0.583 g

Table 8.3 Ciprofloxacin HCl: content and efficiency of loading

Formulation	Lipid: NREP ratio	Loading Efficiency (%)	Cipro loading (%)
F1	17.5	98	55
F2	17.4	95.6	23
F3	8.4	97	36
F4	8.4	96	37
F5	8.4	96	37
F6	8.4	97	36
F7	8.4	98	38

8.2.1.4. In-vitro dissolution test

Ciprofloxacin hydrochloride release from the taste masked particles was determined in 900 ml of 0.1 N hydrochloric acid buffer, at 37 ± 0.5°C, using USP type II apparatus rotated at 100 rpm. The samples were withdrawn at 15, 30, 45, and 60, min. The amount withdrawn each time was replaced with fresh media to maintain the sink conditions.

8.3.3. Results and discussions

8.3.3.1. Dissolution studies

The Ciprofloxacin HCl loading efficiency of all formulations was good as seen in **Table 8.3**. Though the fatty acids are not soluble in the aqueous media at acidic pH all the formulations showed rapid release of Ciprofloxacin HCl. The rapid release is due to the dissolution of NREP. This is desired due to better absorption of ciprofloxacin from gastric region [15,16]. The release of Ciprofloxacin HCL is shown in **Table 8.4**. The release from Formulations F1 and F2 was slower than that from F3-F7 due to higher content of fatty acid. The formulations F4 and F5 showed faster release than formulation F3 containing stearic acid. Since NREP is insoluble at neutral and near neutral pH so it's blending with the hydrophobic fatty acids provides the desired taste masking.

Table 8.4, Ciprofloxacin HCl release at acidic pH 1.2

S.No	Composition		% Drug released (min)			
			30	60	120	180
F1	Stearic acid	1.75 g	69.8	77.5	84.5	87.0
	NREP	0.10 g				
	Ciprofloxacin HCL	0.58 g				
F2	Palmitic acid	0.87 g	70.5	75.4	80.0	84.0
	Stearic Acid	0.87 g				
	NREP	0.10 g				
	Ciprofloxacin HCL	0.58 g				
F3	Stearic acid	0.84 g	83.8	87.7	88.0	93.3
	NREP	0.10 g				
	Ciprofloxacin HCL	0.58 g				
F4	Palmitic acid	0.84 g	91.5	95.0	96.2	98.0
	NREP	0.10 g				
	Ciprofloxacin HCL	0.58 g				
F5	Cetyl Alcohol	0.84 g	91.1	92.4	94.2	95.0
	NREP	0.10 g				
	Ciprofloxacin HCL	0.58 g				
F6	Palmitic acid	0.42 g	88.8	90.8	92.0	93.0
	Stearic Acid	0.42 g				
	NREP	0.10 g				
	Ciprofloxacin HCL	0.58 g				
F7	Cetyl Alcohol	0.42 g	82.5	90.0	94.3	97.3
	Stearic Acid	0.42 g				
	NREP	0.10 g				
	Ciprofloxacin HCL	0.58 g				

8.3. IMMEDIATE RELEASE TASTE MASKED CEFUROXIME AXETIL FORMULATIONS USING NREP-FATTY ACIDS BLENDS

8.2.1. Methods

8.2.1.1. Microencapsulation by emusification solvent evaporation

Compositions containing various lipid-NREP blends are shown in **Table 8.5**. The lipid-NREP blend was prepared by dissolving it in 7 ml of chloroform. Cefuroxime axetil was added to this solution under stirring. This solution was added dropwise to distilled water bath under mechanical stirring. 0.1 % by weight polyvinyl alcohol was added to the distilled water, to facilitate the dispersion of the oil phase containing the drug. A constant mechanical stirring rate of 500 rpm at room temperature was maintained for a 3-4 hours. The solvent was allowed to evaporate and the micro particles so obtained were separated by filtration, and freeze dried for 7 hrs.

8.2.1.2. Microencapsulation by spray drying

The taste-masked microparticles of Cefuroxime axetil were obtained by spray drying. The lipid and NREP blend was prepared by dissolving it in chloroform. To this solution Cefuroxime axetil was added under stirring. This solution was spray dried. The conditions for spray drying are summarized below.

The drying gas used was air. The gas inlet temperature to the spray was 75° C. The gas outlet temperature was 45°C. The feed pump RPM was set between 25-30 / min. The aspiration was set between 50-60. The atomization air pressure was set between 1.8- 2 kg/cm^2. Compositions obtained by spray drying are shown in **Table 8.6**.

8.2.1.3. Melt granulation method

The lipid was placed in the jacketed vessel attached to circulating water bath. The temperature of the circulating water was set such that the lipid was maintained at 3-5°C above the melting point of the lipid. NREP was dispersed in the molten lipid under stirring followed by addition of Cefuroxime axetil. The temperature of the circulating water was gradually lowered to cool the molten lipid. The solid mass thus obtained was sized by passing thorough 40-mesh sieve. The compositions containing the various lipid-NREP blends are shown in the **Table 8.7**.

8.2.1.4. Determination of drug content

The drug content was determined at 278 nm using Shimadzu UV160 IPC UV Visible spectrophotometer. Cefuroxime axetil content was determined by dissolving 50 mg of sample in 2 ml of methanol and sonicated for 5 min. Then the volume was made to 50 ml using 0.07 N HCl. The solution was filtered and diluted further for the analysis. Each sample was analyzed in triplicate. The drug content of the various compositions is shown in **Table 8.8**.

8.2.1.5. In-vitro dissolution test

The drug release from the NREP- fatty acid blends was evaluated by placing the samples containing Cefuroxime equivalent to 125 mg in a basket containing 900 ml of 0.07 N HCl. The dissolution was carried out in Electrolab USP type II apparatus at 75 rpm at 37 $\pm$ 0.5°C. The samples were collected after 30, 60, 90, 120, 180 and 240 min. to follow drug release. The amount of drug released was estimated at 278 nm using the Shimadzu UV Spectrophotometer. The dissolution tests were done in triplicate. The release from the microspheres was compared with that from “Ceftum”, a commercial wax coated preparation from Glaxo Ltd in 0.07 N HCl as dissolution media.

The dissolution of the Ceftum sample containing Cefuroxime axetil was done on sample weight 4.18 g equivalent to one dose of 125 mg (41.8 g/ 50 ml with 5 ml equivalent to 125 mg of Cefuroxime). The sample was wetted in dissolution media removed from 900 ml of media prior to dissolution and then placed in dissolution vessel again. The glass beaker used for wetting the sample was rinsed with dissolution media removed in excess prior to dissolution and again placed in the dissolution vessel. The rest of the procedure was the same as described for NREP-fatty acid blends.

Table 8.5, Formulations obtained by emusification solvent evaporation

Formulation	Lipid	NREP	Cefuroxime axetil
F1	Stearic acid 0.45 g	0.15 g	0.30 g
F2	Palmitic acid 0.50 g	0.30 g	0.60 g
F3	Cetyl Alcohol 0.40 g	0.20 g	0.60 g

Table 8.6, Formulations obtained by spray drying

Formulation	Lipid	NREP	Cefuroxime axetil
F4	Stearic acid 3.0 g	1.0 g	3.0 g
F5	Stearic acid 1.5 g Palmitic acid 1.5 g	1.0 g	3.0 g
F6	Stearic acid 2.0 g Glyceryl monostearate 1.0 g	1.0 g	3.0 g
F7	Stearic acid 2.0 g Hydrogenated Castor oil 1.0 g	1.0 g	3.0 g

Table 8.7, Formulations obtained by melt granulation

Formulation	Lipid		NREP	Cefuroxime axetil
F8	Stearic acid	3.6 g	0.15 g	0.90 g
F9	Cetyl Alcohol	2.3 g	0.15 g	0.90 g
F10	Palmitic Acid Stearic Acid	1.2 g 1.2 g	0.20 g	0.45 g
F11	Lauric Acid	2.4 g	0.20 g	0.45 g
F12	Palmitic Acid	2.4 g	0.20 g	0.45 g

Table 8.8, Cefuroxime axetil: content and efficiency of loading

Formulation	Lipid: NREP ratio	Loading Efficiency (%)	Cef loading (%)
F1	3.0	90	30
F2	1.66	93	40
F3	2.0	94	47
F4	3.0	95	41
F5	3.0	98	42
F6	3.0	96	41.5
F7	3.0	98	42
F8	24.0	97	19
F9	15.3	97	26
F10	12.0	95	14
F11	12.0	95	14.3
F12	12.0	98	14.4

8.3.3. Results and discussion

"Ceftum" showed Cefuroxime axetil release of 40 %, 50 %, 65 % and 69 % in 0.07 N HCl at the end of 30, 60, 120 and 180 min respectively. "Ceftum" contains stearic acid coated microspheres of Cefuroxime axetil. Since the fatty acids are known to react with the alkaline media forming water-soluble salts, the slow release under acidic conditions is expected. Taking in to account the absorption window of Cefuroxime axetil limited to upper gastric region, we developed compositions based on blends on fatty acids and NREP. All the compositions investigated showed rapid release under acidic pH. The release of all the compositions investigated was faster than that seen for "Ceftum". The blending of NREP with fatty acids provided the desired hydrophobic character to the compositions to mask the bitter taste. The presence of NREP aided in rapid release at gastric pH. The release from the micro particles prepared by emulsification solvent evaporation, spray drying and melt granulation is shown in **Tables 8.9, 8.10 and 8.11** respectively.

Table 8.9, Cefuroxime axetil release at acidic pH 1.2

Formulation	Composition		% Cef. released in 30 min
F1	Stearic acid	0.45 g	98.0
	NREP	0.15 g	
	Cefuroxime axetil	0.30 g	
F2	Palmitic acid	0.50 g	99.6
	NREP	0.30 g	
	Cefuroxime axetil	0.60 g	
F3	Cetyl Alcohol	0.40 g	96.8
	NREP	0.20 g	
	Cefuroxime axetil	0.60 g	

Table 8.10, Cefuroxime axetil release at acidic pH 1.2

Formulations	Composition		% Cef. released (min)			
			30	60	120	180
F4	Stearic acid NREP Cefuroxime axetil	3.0 g 1.0 g 3.0 g	70.7	81.0	92.6	93.2
F5	Palmitic acid Stearic acid NREP Cefuroxime axetil	1.5 g 1.5 g 1.0 g 3.0 g	87.4	95.1	98.4	--
F6	Stearic acid Glyceryl monostearate NREP Cefuroxime axetil	2.0 g 1.0 g 1.0 g 3.0 g	96.5	97.5	98.0	--
F7	Stearic acid Hydrogenated Castor oil NREP Cefuroxime axetil	2.0 g 1.0 g 1.0 g 3.0 g	73.3	81.2	91.4	97.0

Table 8.11, Cefuroxime axetil release at acidic pH 1.2

Formulations	Composition		% Drug released				
			Time in min				
			30	60	120	180	240
F8	Stearic acid NREP Cefuroxime axetil	3.60 g 0.15 g 0.90 g	55.4	61.0	65.0	71.0	73.0
F9	Cetyl Alcohol NREP Cefuroxime axetil	2.30 g 0.15 g 0.90 g	54.7	64.6	70.0	78.0	81.5
F10	Palmitic Acid Stearic Acid NREP Cefuroxime axetil	1.20 g 1.20 g 0.20 g 0.45 g	53.6	58.7	62.0	68.0	72.0
F11	Lauric Acid NREP Cefuroxime axetil	2.40 g 0.20 g 0.45 g	62.4	64.5	70.0	77.1	82.2
F12	Palmitic Acid NREP Cefuroxime axetil	2.40 g 0.20 g 0.45 g	55.3	62.0	65.0	73.3	78.0

8.4. CONCLUSIONS

Fatty acids have been investigated for taste masking applications. Fatty acids like stearic acid release the drug on formation of soluble sodium salt in intestinal region. This restricts their applications for drugs absorbed from gastric region. Cefuroxime axetil and Ciprofloxacin using NREP-fatty acid blends were investigated for drug release at gastric pH. The formulations were made by emulsification solvent evaporation technique, spray drying and holt melt granulations. The blends of NREP with fatty acids provide gastric release of drugs. These formulations are highly hydrophobic and hence are very effective for taste masking. The advantage of using these formulations is that gastric release for both Cefuroxime axetil and Ciprofloxacin HCL is attained due to dissolution of NREP.

8.5. REFERENCES

1) S. Qi, D. Deutsch, D. Q.M. Craig, J. Pharm. Sci., 2006, 95, 1022-1028.
2) C. Sharma; J.J. Shaw; R. K. Yang, US Patent 4,797, 288, 10 January 1989.
3) M. Grove, G. P. Pedersen, J.L. Nielsen, A. Mu Llertz, J. Pharm. Sci., 2005, 94, 1830–1838.
4) T. Yajima, K. Ishii, S. Itai, M. Nemoto, K. Suetake, N. Tsukui; US Patent 5,972,373 , 26October 1999.
5) Y. Tomohira, Y. Inoue, T. Nakamura, Y. Kimura, Patent Application JP 2001288117, 2001
6) Yamanouchi Pharma Co Ltd, GB Patent 2081092, 17 February 1982.
7) R.C. Cuca, R. S. Harland, T. C. Riley, Y. Lagoviyer; R S. Levinson, EP 0670716, 13 September 1995.
8) K. Abe, K. Kawahara, T. Yajima, PCT Application WO 0191761, 2001
9) Eudragit E specification and Technical literature 2004
10) M. L. Lorenzo-Lamosa, M. Cuna, J. L. Vila-Jato, D. Torres, M. J. Alonso, J. Microencap. 1997, 14, 607-616.
11) H. J. Robson, D.Q. M. Craig, D. Deutsch, Int. J. Pharm. 1999,190, 183-192.
12) A. Finn, A. Straughn, M. Meyer, J. Chubb, Biopharm. Drug Disposit. 1987, 8, 519-526.
13) C. J. Campbell, L. J. Chantrell, R. Eastmond, Biochem. Pharmacol. 1987, 36, 2317–2324
14) N. Ruiz-Balaguer, A. Nacher, V.G. Casabo, M. Merino, Antimicrob. Agents. Chemother. 1997, 41, 445–448.
15) N. Talwar, H. Sen, J.N. Staniforth, US Patent, US 6261601, 17 July 2001.
16) N. Talwar, H. Sen, J.N. Staniforth, US Patent, US 6,960,356, 1 Nov 2005.

CHAPTER 9

Enhancement of Bioavailability by Polymorphism Inhibition

9.1. INTRODUCTION

Often a chemical substance exists in different ordered states [1]. This is referred to as polymorphism. The polymorphic form, in which the drug is present, is often influenced by the processing techniques. The various crystallographic forms also include pseudo polymorphic forms. It is well known that differences due to polymorphism and pseudo polymorphism observed in drugs are critical because physical and chemical properties of different crystalline form influence their bioavailability.

Drugs and excipients can crystallize in more than one crystallographic form (polymorph, crystalline modifications). Although polymorphs of a substance share the same chemical formula, difference in crystalline structure can affect the physiochemical parameters of the substance such as, solubility, dissolution rate, density which in turn can affect their important pharmaceutical properties such as bioavailability, stability of drug as well as formulation technology of dosage form [2-6] As the awareness of these effects has increased formulators are charged with the responsibility to formulate a product which is physically and chemically stable [7]. Most drugs exhibit structural polymorphism, and it is preferable to develop the most thermodynamically stable polymorph of the drug. The physically more stable polymorphic form has lowest energy state, highest melting point and least aqueous solubility [5]. The other forms are the metastable forms, which have higher energy, low melting point and greater solubility.

There are occasional situations in which the development of a metastable crystalline or amorphous form is justified because a medical benefit is achieved [7]. These are special situations which require a faster dissolution rate or higher drug concentration in order to achieve rapid absorption and efficacy. Since the metastable forms have greater solubility and hence greater bioavailability, they are preferred in the formulations [8]. Drugs present in the amorphous forms have higher energy and greater aqueous solubility. This assures reproducible bioavailability of the product over its shelf life under a variety of real-world storage conditions. Thus the order of dissolution of the different solid forms of drug is amorphous > metastable > crystalline.

When the process of *in vivo* drug release is slower than the process of absorption, absorption is said to be dissolution rate-limited [9]. Since dissolution precedes absorption in the overall process, any change in the drug release or dissolution process will subsequently influence drug absorption. In general, drugs, which are slightly soluble in water and are highly crystalline, exhibit low bioavailability since they have low solubility and low dissolution rate in the gastrointestinal tract. It is well known that converting a crystalline compound into its amorphous state will substantially increase the aqueous solubility of the compound, thereby increasing its bioavailability.

The intrinsic solubility of a substance depends on its solid phase. The lattice energies of physical forms (amorphous, polymorphs or solvates) are responsible for the difference in solubility and dissolution rates. The difference in solubility between amorphous and crystalline material can be up to several hundred times [10]. Crystalline solids, due to their highly organized, lattice-like structures typically require a significant amount of energy for dissolution. The energy required for a drug molecule to escape from a crystal, for example, is greater than is required for the same drug molecule to escape from a non-crystalline, amorphous form. Because of the effect of solid state forms on solubility and dissolution rate, the use of amorphous, different polymorphs or solvates would be expected to influence the bioavailability. As a method for obtaining amorphous substances rapidly cooling from melt, precipitation from suitable solvent systems, grinding or forming a solid dispersion is considered [11-14].

Technologies have been developed to suppress the crystallization of the amorphous drugs. Simple strategies for the improvement of drug formulation like increasing the solubility of drugs and thus increasing the fraction of the dose absorbed. The techniques utilized commonly are simple barrier methods including coating and encapsulation. Some of them include use of the chemical carriers to increase gastrointestinal absorption for the oral delivery of molecules difficult to formulate.

Amorphous Nicardipine and Cefditoren pivoxil obtained by grinding and pulverization are disclosed in US Patent 4,673,564 and Patent Application WO 02/087588 respectively [15,16]. Sustained release composition of amorphous Nicardipine was obtained by friction-pulverizing crystalline Nicardipine in the presence of hydroxypropylmethyl cellulose. The pulverization of crystalline Nicardipine to a fine

powder was carried out in a ball mill or a vibrating ball mill for a period of at least 10 to 16 hours.

The use of polymers for obtaining and retaining the drug in amorphous form is reported in the past. The crystalline antifungal drug Itraconazole was converted into the amorphous form, by dissolving it in the molten solution of glyceryl monostearate, followed by the addition of hydroxy propyl methyl cellulose as stabilizer. This was formulated as granules with gradual cooling below 5ºC and / or rapidly cooling the granules as described in US Patent 6,497,905 [17]**.** Amorphous paroxetine was obtained by mixing paroxetine free base with water and polyvinylpyrrolidone having an average molecular weight of about 10,000 to about 450,000 followed by drying. Poly vinyl pyrrolidone is preferred since it does not control or delay the release of paroxetine from a solid tablet formulation [18]. An osmotic delivery system for Carbamazepine having an outer wall of cellulose acetate and a core of hydroxy propyl methyl cellulose as protective colloid vinyl pyrrolidone and vinyl acetate having a molecular weight of 60,000-15,000 is described in US Patent 4,857,336 [19]. The outer coat is permeable to water but the core is impermeable to it and inhibits the crystal growth of Carbamazepine hydrate. A controlled release formulation of amorphous Carvedilol obtained by preparing solid dispersion of crystalline form is disclosed in Patent Application WO 03/024426 [20]. The polymers polyethylene glycol and polyethylene oxide having a molecular weight of about 20,000 are used for stabilization of Carvedilol. This further increases the shelf life of drug.

Drugs like Carbamazepine are better absorbed in anhydrous and amorphous form and the conversion to the crystalline, dihydrate form leads to lower solubility and also lower bioavailability [6, 21]. Further the drug molecules like Celecoxib have low aqueous solubility and so the amorphous form is preferred for rapid release formulation. Yet the drug shows a tendency to crystallize in presence of the gastric medium. Such drugs require a protective polymer coating, which acts as a moisture barrier and prevents the polymorphic transformation of the drug. Cefuroxime axetil tends to gel in presence of the aqueous media [22]. Also if the tablets are not protected from moisture during storage; they result in poor dissolution and lower bioavailability. CA can exist in

three polymorphic forms [23]. Crystalline CA shows melting point at 175-180°C and substantially amorphous high melting form exhibits melting point at 135-137°C and a low melting amorphous form having melting point in the range 70- 80°C [23, 24]. CA is more bioavailable orally from the amorphous form than from the crystalline form [25, 26].

There have been numerous ways to obtain Cefuroxime axetil in an amorphous form to improve its bioavailability. A co-precipitate of Cefuroxime axetil and a water-soluble excipient, povidone, is described by Sherman in Patent Application WO 99/08683 [27]. Despite the use of a water-soluble excipient, the dissolution of Cefuroxime axetil from the co-precipitate is not facilitated significantly and accordingly, the bioavailability of Cefuroxime axetil contained in the co-precipitate is relatively low. A solid dispersion of amorphous Cefuroxime axetil containing silicon dioxide, microcrystalline cellulose, cross-linked povidone, cross-linked sodium carboxymethylcellulose is described in US Patent 6,107,290 [28]. A composition containing silicon dioxide as a micro environmental pH adjuster and as an anti gelling agent for Cefuroxime axetil is described in Patent Application WO 99/44614 [29]. The silicon dioxide avoids the gelling of drug in the tablet core due to the absorption of moisture from air and also due to the penetration of gastric fluid for improving the bioavailability. Methods disclosed in these patents may be useful for solid oral dosage forms but may not be applicable for liquid oral preparation where the bitter taste may not be masked.

In the present chapter we have shown that amorphous drugs undergo polymorphic transformations during the processing stages. These drugs were stabilized using high molecular weight NREP polymers. The co-precipitates obtained by dispersing Cefuroxime axetil and Celecoxib were retained in amorphous form in the presence of high molecular weight NREP. However in presence of low molecular weight polymers, the drugs were converted to crystalline form. The use of high molecular weight NREP at lower loadings was found to inhibit crystallization. The physical state of samples was determined by X ray diffraction analysis. The in-vitro dissolution studies showed that the dissolution of drugs was faster from the

formulations containing high molecular weight NREP. This is due to the rapid dissolution of the amorphous form over the crystalline forms.

9.2. MATERIALS AND METHODS

9.2.1. Materials

Methyl methacrylate (MMA), 2-hydroxy ethyl methacrylate (HEMA) and 4-vinylpyridine (4-VP), were purchased from Sigma-Aldrich. Azobisisobutyronitrile was obtained from local suppliers. All other chemicals were analytical grade. Tetrahydrofuran for chromatography was purchased from Merck. Deuterated chloroform ($CDCl_3$) was purchased from Sigma Aldrich.

9.2.2. Synthesis of the NREP

The trace impurity of EGDMA was removed from HEMA before polymerization to yield soluble polymer. Freshly distilled monomers MMA and 4-VP were used for polymerization. In a 250 ml round bottom flask MMA, HEMA and 4-VP were added to 80 ml of dimethyl formamide. Solution polymerization of the monomer mixture was carried out using azobisisobutyronitrile as initiator at 65°C for 18 h. The polymer solutions were concentrated on a rota-vapor. The polymers were dissolved in (1:1) dichloromethane-methanol mixture and precipitated in water to remove unreacted monomers. Polymers were dried at 27°C under vacuum for 72 h.

The higher molecular weight polymers used for inhibition of the crystallization of the polymorphic drug at lower polymeric loading were synthesized using the monomer composition optimized earlier, by varying the amount of initiator and the solvent. Two approaches were used for attaining high molecular weight 1) The initiator concentration with respect to the monomer content was reduced 2) the amount of the inert solvent with respect to the monomer content was reduced. The polymer composition, molecular weight and intrinsic viscosity of the polymer are summarized in **Table 9.1**.

Table 9.1: **NREP composition, molecular weight and intrinsic viscosity**

No.	Monomer	Wt %	Initiator [a]	Solvent [a]	Molecular Weight M_w	Intrinsic viscosity g / dl
P1	MMA HEMA VP	60 25 15	0.09	72.66	53,677	0.1365
P2	MMA HEMA VP	60 25 15	0.09	61.46	79,743	0.3684
P3	MMA HEMA VP	60 25 15	0.09	34.72	2,25,497	0.6945
P4	MMA HEMA VP	60 25 15	0.09	68.03	63,189	0.3080
P5	MMA HEMA VP	60 25 15	0.045	68.03	1,25,280	0.4882
P6	MMA HEMA VP	60 25 15	0.0225	68.03	1,94,344	0.5703
P7	MMA HEMA VP	60 25 15	0.0225	51.53	2,72,177	0.9011
P8	MMA HEMA VP	60 25 15	0.045	34.72	3,38,021	1.2135

a : % weight by monomer

9.2.3. Polymer characterization

9.2.3.1. Molecular weight determination by GPC

Weight average molecular weight of the polymer was determined by GPC (Waters 590 programmable HPLC pump, Waters 410 differential refractometer) using polystyrene standard (Polysciences Inc. USA) as reference. The polymer sample 3 mg was dissolved in 1 ml of tetrahydrofuran and eluted through Styragel columns at a flow rate of 1ml / min at 25 °C.

9.2.3.2. Intrinsic viscosity determination

The intrinsic viscosity for polymer solutions in dimethyl formamide was determined by using the Ubbelohde Viscometer for dilution sequences, (Schott Gerate, GmbH.) at 30°C in the range 0.1 to 1 % w/w. 1 g of polymer was dissolved in 100 ml of pure solvent for 2 days at room temperature. The polymer solution was filtered and volumes were made by addition of neat solvent. The solutions were placed in the water bath at 30°C and were allowed to equilibrate at this temperature before beginning the experiment.

9.2.3.3. Fabrication of polymer films

The polymer films were cast using the solvent evaporation technique. The polymer films were cast by spreading the polymer solution (12 % w/v) in chloroform on a surface of mercury supported horizontally by glass (casting area 28.26 cm $^{2)}$. The solvent was allowed to evaporate at room temperature for 48 h. After solvent evaporation the films were cautiously pulled off from the surface. The films were allowed to dry at room temperature under vacuum for 24 h.

9.2.3.4. Water uptake by polymer film

The water uptake of the polymer was determined by thermo gravimetric analysis (TGA) using Perkin Elmer thermal analysis TGA 7 unit. The sample was heated from 30 to 200 °C at a heating rate 10°C /min. The water uptake was expressed as percent weight loss.

9.2.3.5. XRD analysis

The physical state of drug was determined by X ray diffraction analysis. Rigaku D max 2500 X ray diffractometer with copper target (Cu $K\alpha_1$ radiation) and 18 KW rotating anode type generator was used. The samples were scanned from 5 to 60° 2θ at a speed of 3° 2θ / min at ambient temperature. The X ray powder diffraction patterns for CA, polymers EE, NREP, physical mixtures and CA-EE and CA-NREP blends were measured.

9.3. CEFUROXIME AXETIL- NREP CO-PRECIPITATES

9.3.1. Co-precipitation in nonsolvent

The solid dispersions were obtained by co-precipitating Cefuroxime axetil and NREP in the nonsolvent. Cefuroxime axetil and NREP were dissolved in acetone containing 0.5–10 % water. The resulting mixture was added to petroleum ether maintained at 5 ° C. The co-precipitate so obtained was dried under vacuum for 24 hrs at room temperature and sized to obtain ASTM mesh 40/60 particles. Both high and low molecular weight NREP was used along with Cefuroxime axetil. The formulations are shown in **Table 9.2**.

9.3.2. Co-precipitation by solvent evaporation

The solid dispersions were obtained by tray drying Cefuroxime axetil and NREP solution. Cefuroxime axetil and NREP were dissolved in acetone containing 0.5-10 % water and casting the solution on the tray and drying under vacuum at room temperature and sizing to obtain ASTM mesh 40/60 particles. Both high and low molecular weight polymers were used. The formulations are shown in **Table 9.3**.

9.3.3. Determination of drug content

The drug content was determined at 278 nm using Shimadzu UV160 IPC UV Visible spectrophotometer. 50 mg of sample was dissolved in 2 ml of methanol and sonicated for 5 min. The volume was made to 50 ml using 0.07 N HCl. The solution was filtered and diluted further for analysis. Each sample was analyzed in triplicate.

Table 9.2 CA solid dispersion prepared by coprecipitation in non solvent

Formulation	NREP Mw	NREP-CA ratio	CA content
F1	63,189	1 : 2	3.0 g
F2	63,189	2.9 : 1	1.35 g
F3	3,38,021	1 : 2	3.0 g
F4	3,38,021	2.9 : 1	1.35 g

Table 9.3 CA solid dispersion prepared by coprecipitation by solvent evaporation

Formulation	NREP Mw	NREP-CA ratio	CA content
F5	63,189	1 : 2	3.0 g
F6	63,189	2.9 : 1	1.35 g
F7	3,38,021	1 : 2	3.0 g
F8	3,38,021	2.9 : 1	1.35 g

Table 9.4 CA: content and efficiency of loading

Formulation	Loading Efficiency (%)	CA loading (%)
F1	90	60
F2	92	23
F3	93	62
F4	92	23
F5	98	65
F6	96	24
F7	97	64
F8	100	25

9.3.4. In-vitro dissolution test

The drug release from the microspheres was evaluated by placing the microspheres containing Cefuroxime equivalent to 125 mg in a basket containing 900 ml of 0.07 N HCl. The dissolution was carried out in Electrolab USP type II apparatus at 75 rpm at 37 $\pm$ 0.5°C. The samples were collected after 30, 60, 90, 120, 180 and 240 min. to follow drug release. The amount of drug released was estimated using the Shimadzu UV Spectrophotometer at 278 nm. The dissolution tests were done in triplicate.

9.4. CELECOXIB - NREP CO-PRECIPITATES

9.4.1. Co-precipitation in nonsolvent

The solid dispersions were obtained by co-precipitating Celecoxib and NREP in the nonsolvent. Celecoxib and NREP were dissolved in acetone containing 0.5–10 % water. The resulting mixture was added to petroleum ether maintained at 5 ° C. The co-precipitate so obtained was dried under vacuum for 24 hrs at room temperature and sized to obtain ASTM mesh 40/60 particles. Both high and low molecular weight polymers were used along with Celecoxib. The formulations are shown in **Table 9.1**.

9.4.2. Determination of drug content

The drug content was determined at 251 nm using Shimadzu UV160 IPC UV Visible spectrophotometer. Celecoxib content was determined by dissolving 20 mg of sample in 2 ml methanol and sonicated for 5 min. To this was added 5 ml of 0.1 N HCL and stirred for 10 min on spnix vortex. The volume was made to 50 ml using 0.1 N NaOH solution. The solution was filtered and diluted further for the analysis. Each sample was analyzed in triplicate.

9.4.3. In-vitro dissolution test

The drug release from the samples was evaluated by placing the sample containing Celecoxib equivalent to 100 mg in 100 ml of 0.1 N HCl for 30 min and then the release was studied by addition of 900 ml of 0.1N NaOH, at 37 $\pm$ 0.5°C, using USP type II apparatus at 100 rpm. The samples were withdrawn at 15, 30, 45, 60, 90, 120,180 and 240 min from 0.1N NaOH solution. The amount withdrawn each time was replaced with fresh media to maintain the sink conditions. The dissolution results are given in respective tables for each example. The dissolution tests were done in triplicate.

Table 9.5 Celecoxib solid dispersion prepared by coprecipitation by solvent evaporation

Formulation	NREP Mw	NREP-Celecoxib ratio	Celecoxib content
F9	63,189	0.75	1.0 g
F10	63,189	3.0	0.6 g
F11	2,72,177	0.75	1.0 g
F12	2,72,177	3.0	0.6 g

Table 9.6 Celecoxib: content and efficiency of loading

Formulation	Loading efficiency (%)	Celecoxib loading (%)
F9	96	55
F10	96	24
F11	94	54
F12	92	23

9.5. RESULTS AND DISCUSSION

Theoretical considerations:

Correlation between dissolution, bioavailability and polymorphism

Drugs with very low solubility are difficult to formulate. It is generally recognized that low solubility and/or dissolution rate in the gastro-intestinal tract, compromise oral bioavailability [30, 31]. Often, poor drug dissolution/solubility rather than limited permeation through the epithelia of the gastrointestinal tract are responsible for low oral bioavailability [32].A strong correlation between the *in-vitro* dissolution time determined for dosage form and in-vivo drug release is established. In view of this relationship it is clear that dissolution time determined for a composition is one of the fundamental characteristic for consideration when designing the dosage form. To enhance dissolution many drugs are converted to amorphous forms. While the preparation of amorphous systems may be desirable, there are a number of difficulties associated with their use. Amorphous materials are thermodynamically unstable and will tend to revert to the crystalline form on storage (devitrification); such behaviour has been well documented for a number of drugs [30].

One of the methods to enhance drug dissolution is by formation of solid dispersions. This is obtained by co-precipitation technique where the drug and carrier are dissolved in a solvent, and this solution is then added to an antisolvent. The drug and polymer then precipitate out simultaneously in the antisolvent. However, as the precipitation process occurs in a solvent and antisolvent mixture, plasticization and resulting high molecular mobility contribute to molecular rearrangement causing crystallization [33]. Crystallization may have deleterious effects on dissolution performance of the resultant solid dispersion [34]. High molecular mobility may exist for a longer time in co-precipitation than in processes such as co-evaporation [35, 36], in which solvents are removed by drying [34].

The recrystallisation of the drugs occurs by slow solid-state transition at the surface of the drug particle. This causes the reduction in apparent solubility of the

substance [37]. The amorphous materials are in metastable or disordered state. These drugs at favourable conditions like evaluated temperature and /or humidity convert to ordered form or crystalline state. Amorphous materials have a glass transition temperature above which the molecular mobility increases significantly and hence, crystallization is more likely to occur [30]. The absorbed moisture acts as a plasticizer causing increased molecular mobility resulting in recrystallisation or deactivation [33]. The solubility of the amorphous materials is greater than the crystalline materials. The reduction in the apparent solubility after storage of amorphous powder at high relative humidity indirectly indicates that a very slow recrystallisation process is occurring. [33,38]. Similar behavior has been reported for pharmaceutical excipients, emphasizing the effect of temperature on crystallisation rate under different relative humidity conditions by Dalton and Hancock [39].

In the subsequent discussion retention of the two drugs Cefuroxime axetil and Celecoxib in metastable form by the polymers synthesized by us is disclosed. Both the drugs require enhanced dissolution for rapid absorption. The pH sensitive polymers of the present invention have exhibited taste masking and crystallization inhibition at lower loadings for these drugs. The pH sensitive polymers having high molecular weight and higher solution viscosity in the present invention retain the amorphous drugs in the same form and further inhibit the conversion of the drug in the crystalline form in the presence of the solvents. The polymers are hydrophobic and do not show water uptake even on exposure to 7 days. Further the polymer does not need any adjuvant like a channelising agent or a water-soluble or water swellable excipient to aid in the release of the drug in the stomach.

9.5.1. Polymer characterization

The polymers synthesized were characterized for increase in molecular weight and intrinsic viscosity. The molecular weight was found to increase with the reduction in solvent amount as seen in composition P1, P2 and P3. The molecular weight was found to increase as the amount of initiator was reduced as seen in compositions P4, P5 and P6. Further the lowering of initiator and also the solvent simultaneously resulted in

polymers with higher molecular weights than the earlier compositions. The highest molecular weight was obtained for composition P9. The intrinsic viscosity is a function of molecular weight of polymer. This correlation was seen in all the compositions investigated as shown in **Table 9.1**. The intrinsic viscosity increased with increase in molecular weight. The polymer composition P9 and P 4 were used for investigations for determining the effect on crystallization inhibition.

9.5.2. Water uptake by polymers

The amount of moisture taken up by polymers was measured by themogravimetric analysis. The molecular weight of the polymer has an influence on the water sorption. As the molecular weight increases the dissolution is retarded. In the polymers investigated the ionization of functional monomer 4-VP is zero at pH 4 and hence both the polymers with 63,189 and 3,38,021 molecular weight showed negligible water uptake of upto 2 % on exposure to water for 7 days. The TGA data is shown in **Fig. 9.1**.

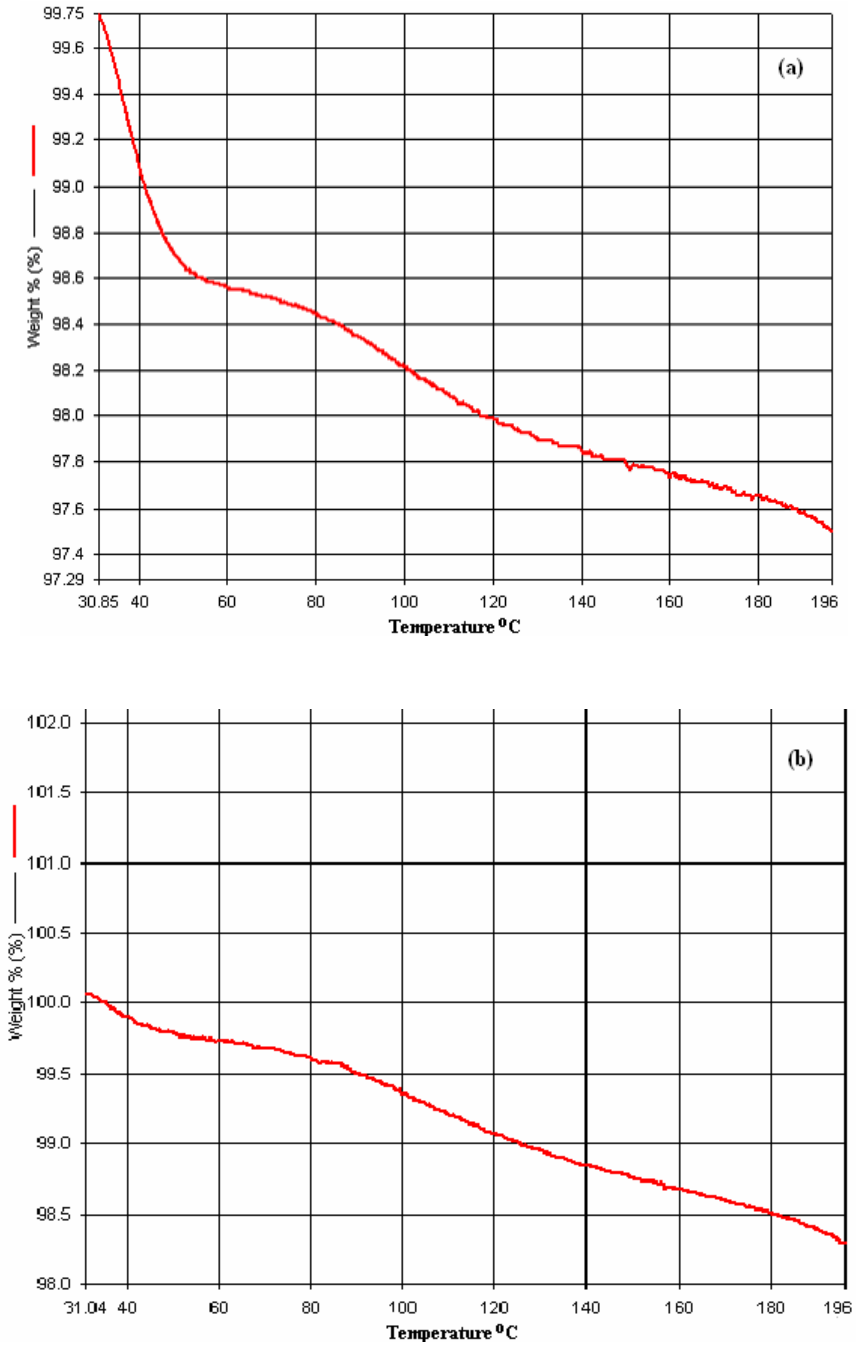

Fig. 9.1 TGA analysis for (a) low (63,189) and (b) high (3,38,021) molecular weight polymer

9.5.3. Solid Dispersion of Cefuroxime axetil

The formation of solid dispersion results in enhanced dissolution rate and this is due to one of the following mechanisms; eutectic formation, increased surface area of the drug due to precipitation in the carrier, solid solution formation, improved wettability due to intimate contact with a hydrophilic carrier, precipitation as a metastable crystalline form or a decrease in crystallinity. Both properties of the carrier-drug combination and the method of manufacture influence the type of solid dispersion. [34].

Contrary to this, the solid dispersion prepared by precipitation in nonsolvent and those prepared by solvent evaporation using lower amounts of polymer showed crystallization of Cefuroxime axetil. The compositions F1 and F5 showed lower dissolution of Cefuroxime axetil than compositions F2 and F6 containing the same polymer (Mw= 63,189) in higher loading. The effect of solvent causing the plasticization of the drug-carrier system resulting in increased mobility has been described in past. This caused the conversion of amorphous Cefuroxime axetil to crystalline form. The conversion of amorphous Cefuroxime axetil to crystalline form was detected by XRD analysis. The dissolution of Cefuroxime axetil was retarded as a result of this. Only 55-60 % of Cefuroxime axetil was released after 4 hrs. The slow dissolution of drugs on crystallization is reported in the past.

The compositions F3 and F7 were formulated using lower content of high molecular weight polymer (Mw= 3,38,021). At lower polymer loading these compositions showed rapid dissolution of Cefuroxime axetil. The XRD analysis for these compositions showed the drug in amorphous form. The increased molecular weight of the polymer restricts the segmental motion of the polymer chains and retains the smaller drug molecules entrapped in the same form without its conversion to crystalline form. At higher polymer loading with higher molecular weight the Cefuroxime axetil release was fast as expected. The dissolution of Cefuroxime axetil from compositions F1 to F 8 is shown in **Fig. 9.2 and 9.3**. The X ray diffractograms for the compositions are shown in **Fig. 9.4 and 9.5**.

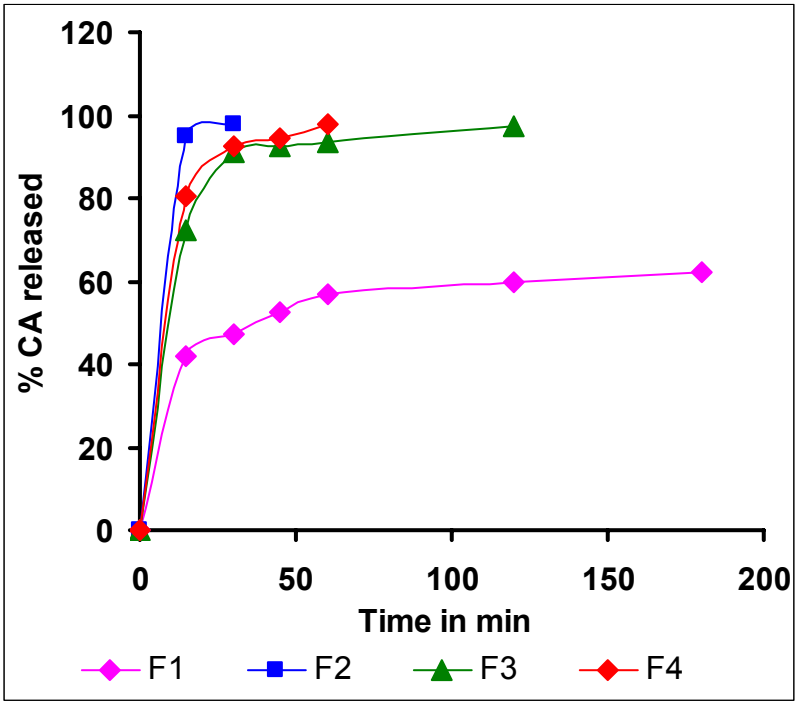

Fig 9.2 Dissolution of Cefuroxime axetil from solid dispersions prepared by precipitation in nonsolvent

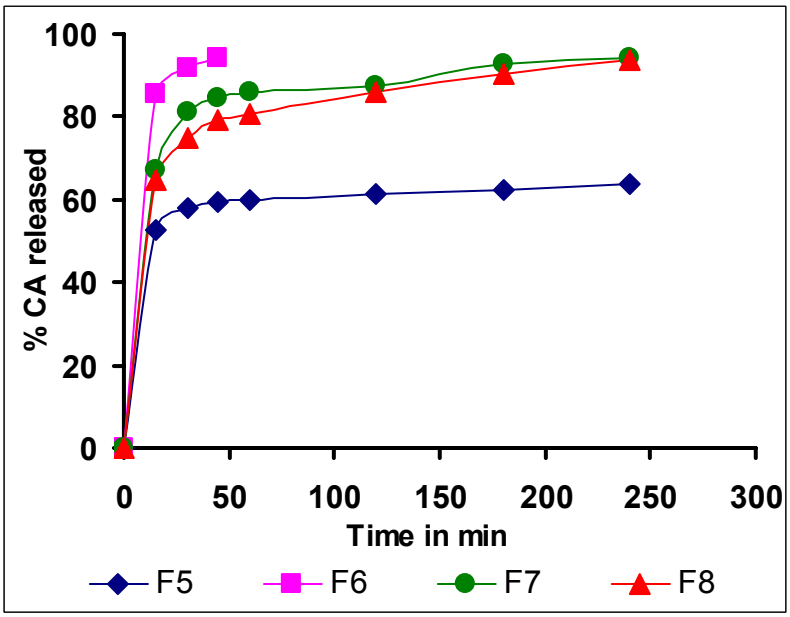

Fig. 9.3 Dissolution of Cefuroxime axetil from solid dispersions prepared by solvent evaporation

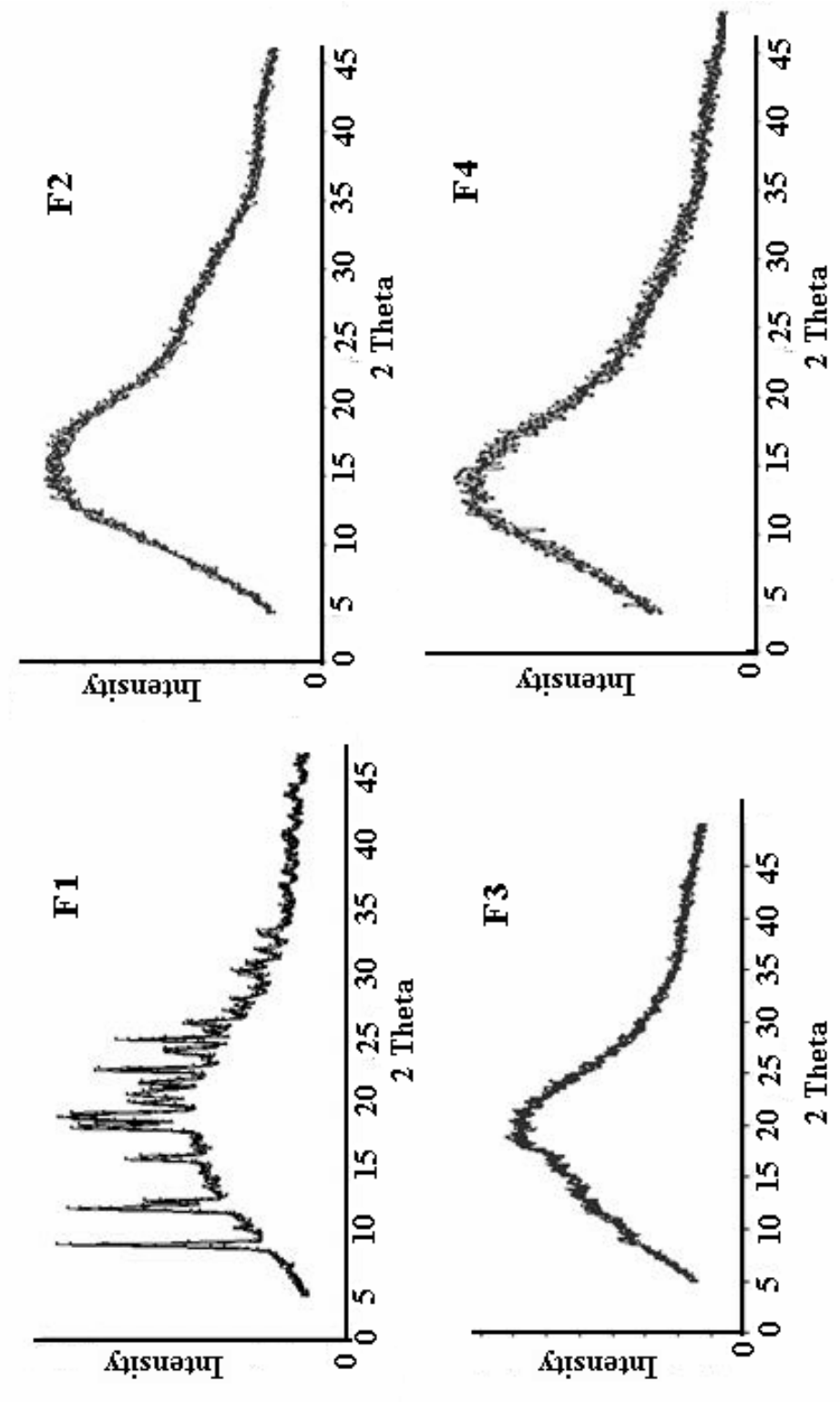

Fig. 9.4 XRD analysis of solid dispersions prepared by precipitation in nonsolvent

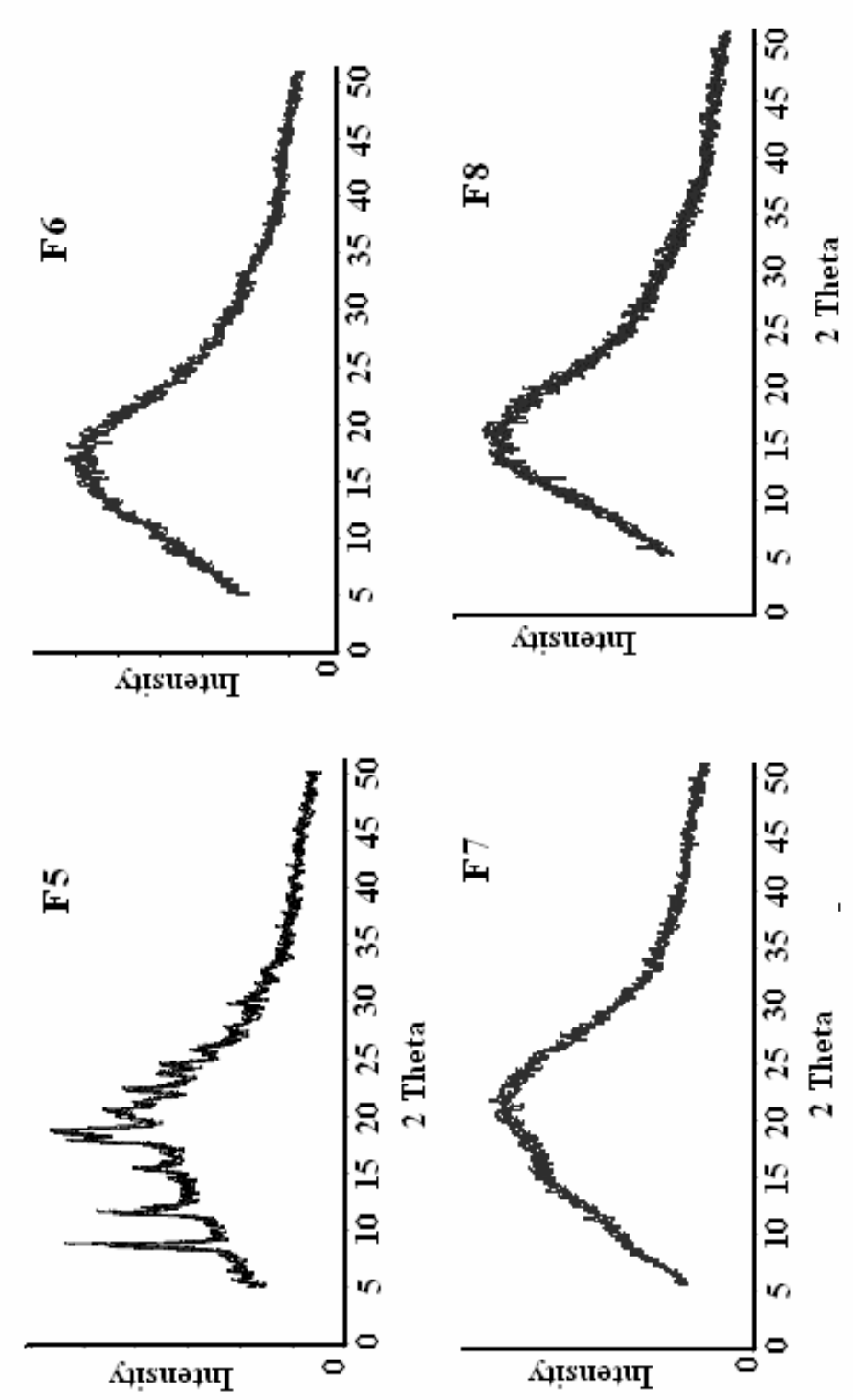

Fig. 9.5 XRD analysis of solid dispersions prepared by solvent evaporation

9. 5. 4. Solid dispersion of Celecoxib

The Celecoxib solid dispersions prepared using lower molecular weight polymer at lower content lead to crystallization of Celecoxib. This was reflected in lower dissolution of Celecoxib from the composition F9 as shown in **Fig. 9.6**. The XRD analysis for this composition showed the conversion of amorphous Celecoxib to crystalline form (**Fig. 9.7**). The composition F10 with higher loading of polymer (Mw = 63,189) showed rapid dissolution of Celecoxib. The composition F11 with equivalent amount of polymer (Mw= 3, 38,021) as that of composition F9 showed rapid dissolution of Celecoxib and it was retained in amorphous form as seen from the XRD analysis (**Fig. 9.7**). The composition F12 with higher high molecular weight polymer showed rapid dissolution of Celecoxib and retained it in amorphous form. The higher molecular weight polymer was able to retain Celecoxib in amorphous form at low and high polymeric loading.

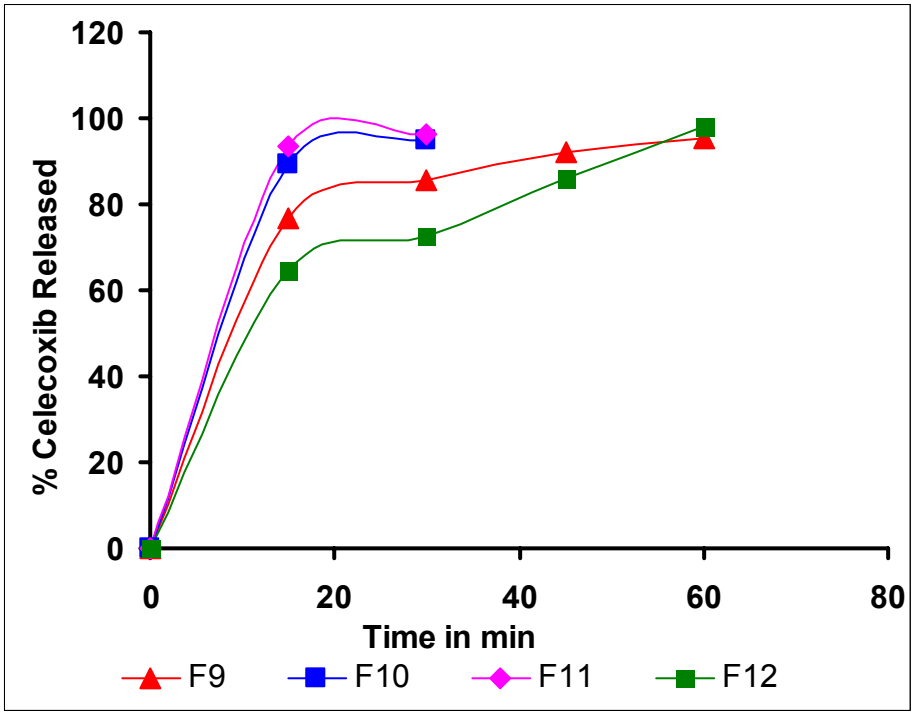

Fig. 9.6. Celecoxib release from the solid dispersions

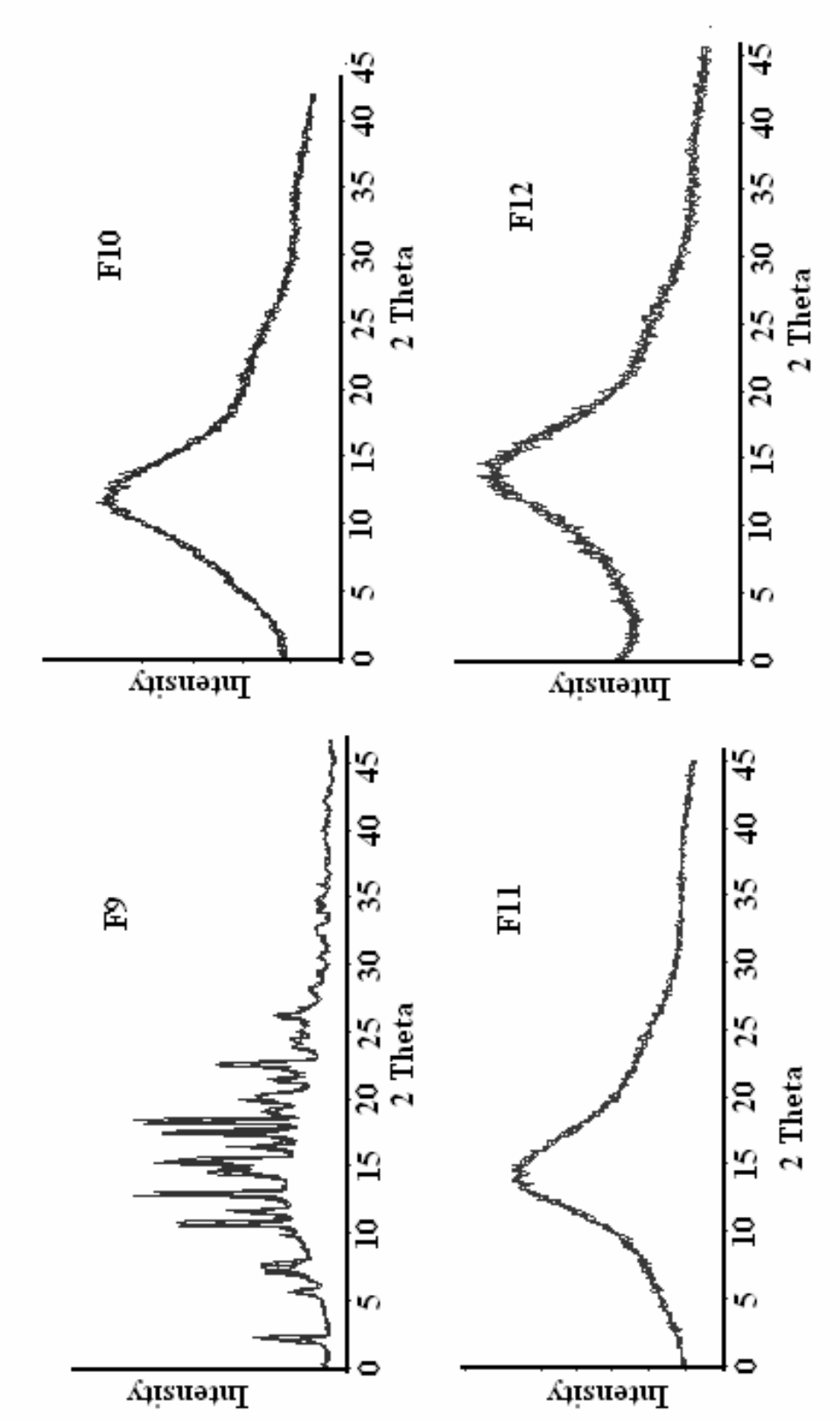

Fig. 9.7 XRD analysis of Celecoxib solid dispersions

9. 6. CONCLUSIONS

This chapter describes the polymer (NREP) attributes which inhibit conversion of amorphous Cefuroxime axetil to crystalline form. There are special situations *eg*. Cefuroxime axetil and Celecoxib which require a faster dissolution rate in order to achieve rapid absorption and efficacy. The metastable forms of these drugs have greater solubility and hence greater bioavailability so they are preferred in the formulations. Co-precipitation of drugs is often used to enhance the dissolution of drugs. The co-precipitates of Cefuroxime axetil and Celecoxib with low molecular weight NREP (M_w = 63,189) caused crystallization of the drugs. This was confirmed by XRD analysis. The residual solvent used for co-precipitate preparation causes the plasticization of the polymer. This results in increased segmental motion causing the crystallization of the drug. The crystallization of Cefuroxime axetil and Celecoxib resulted in low dissolution of these drugs. Hence polymer compositions of high molecular weight were synthesized by 1) lowering the initiator to monomer ratio 2) lowering the solvent to monomer ratio and 3) simultaneous lowering of initiator and solvent to monomer ratio. The polymers were characterized by GPC for molecular weight. The intrinsic viscosity of polymers was found to increase with increase in molecular weight. The highest molecular weight polymer was obtained by synthesis using the third condition stated above. The correlation between increase in molecular weight and decrease in chain ends is well established. With increase in molecular weight the number of chain ends is reduced and this restricts the segmental motion of polymers which is reflected in increased T_g for high molecular weight polymers. The co-precipitates obtained by using high molecular weight NREP (M_w = 3,38,021) polymer was found to retain Cefuroxime axetil and Celecoxib in amorphous form. This ensured the rapid dissolution of these drugs thereby enhancing bioavailability. The high molecular weight NREP has restricted segmental motion than low molecular weight NREP and retains these drugs molecules in the same form avoiding the recrystalisation. Often drugs tend to change to stable form from metastable form on absorption of moisture. Hence hydrophobic polymers are used for such drugs. There is a concern using hydrophobic polymers as they tend to retard the release. Cefuroxime axetil has a tendency to gel in presence of moisture adversely

affecting its bioavailability. Amorphous Celecoxib formulations on exposure to moisture result in poor dissolution of drug. The advantage of using high molecular weight NREP is it retains the drug in amorphous form, its hydrophobic nature inhibits moisture permeation and yet ensures rapid gastric release.

9.7. REFERENCES

1) P. Di Martino, M. Scoppa , E. Joiris , G. F. Palmieri, C. Andres, Y. Pourcelot , S. Martelli, Int. J. Pharm. 2001, 213, 209–221.
2) J.K. Haleblain, W. Mc Crone, J. Pharm. Sci., 1969, 58, 911- 929.
3) S. Byrn, R. Pfeiffer, M. Ganey, C. Hoiberg, G. Poochikian, Pharm. Res., 1995, 12, 945 - 954.
4) G.G.Z. Zhanga, D. Lawa, E.A. Schmittb, Y. Qiub, Adv. Drug Deliv. Rev. 2004, 56, 371 – 390.
5) D. A. Snider, W. Addicks, W.Owens, Adv. Drug Deliv. Rev., 2004, 56, 391– 395.
6) R. Nair, S. Gonen, S. W. Hoag, Int. J. Pharm., 2002, 240,11–22.
7) D. Singhal, W. Curatolo, Adv. Drug Deliv. Rev., 2004, 56, 335–347.
8) D. Murphy, F. Rodrıguez-Cintron, B. Langevin, R.C. Kelly, N. Rodrıguez-Hornedo, Int. J. Pharm., 2002, 246, 121-134.
9) S.B. Jaiswal, D.M. Bramhankar, "Biopharmaceutics and Pharmacokinetics a Treatise", 1st Ed., Vallabh Prakashan, Delhi, India, 1995
10) L.F. Huang, W.Q. Tong, Advan. Drug Del. Rev., 2004, 56, 321– 334.
11) Y. Yoshihashi, H. Kitano, E. Yonemochi, K. Terada, Int. J. Pharm., 2000, 204, 1-6.
12) D.Q.M. Craig, P.G. Royall, V.L. Kett, M.L. Hopton, Int. J. Pharm. 1999,179, 179–207.
13) G. Sertsou, J. Butler, A. Scott, J. Hempenstall, T. Rades, Int. J. Pharm., 2002, 245, 99-108.
14) M. Saito, T. Ugajin, Y. Nozawa, Y. Sadzuka, A. Miyagishima, T. Sonobe, Int. J. Pharm. 2002, 249, 71-79.
15) H. Kawata, M. Aruga, T. Ohmura, T. Sonobe, S. Yoneya, C. Sone, US Patent 4,673,564, 16 June 1987.
16) O. Masato, WO 02/087588, 7 November 2002.
17) R. S. Vladyka, D. F. Erkoboni, P. R. Stergios, US Patent 6,497,905, 24 Dec 2002.
18) W. A. Hein, S.C. Chang, H.H.D. Kao, US Patent 6,168,805, 2 January 2001.
19) S. Khanna, T. Riittimann, US Patent 4,857,336, 15 August 1989.

20) G. Fischer, D. Bar-Shalom, L. Slot, A.M. Lademann, C. Jensen, WO 03/024426, 27 March 2003.
21) E.O. Machiste, P. Giunchedi, m. Setti, U. Conte, Int. J. Pharm., 1995, 126, 65-72.
22) D.S. Deutsch, J. Anwar, US Patent, US 4,897,270, 30 January 1990.
23) J.S. Woo, H.C. Chang, US Patent US 6107 290, 22 August 2000.
24) H. Jo, J.H. Yu, J. H. Yun, S. J. Hwang, J.S. Woo, Preparation of amorphous form of cefuroxime axetil using supercritical fluid processing. Controlled Release Society 29 th Annual Meeting Proceedings, 2002, Abstract 057.
25) H.A. Crisp, J.C. Clayton, US Patent 4,820,833, 11 April 1989.
26) B. Tejchman, M. Jarominska, M. Horodecka, I. Oszczapowicz, Acta Polon. Pharm.-Drug Research. 1995, 52, 477-482.
27) B.C. Sherman, Patent Application WO 99/08683, 25 Feb 1999.
28) J. S. Woo, H. C. Chang, US Patent 6,107,290, 22 August 2000.
29) C.J. Keun; K.H. Young; L. S. Hee; P.K J. Hwa; P.J. Woo Patent Application WO 99/44614 (EP 1066040), 19 February 2003.
30) M. D. Ticehurst, P. A. Basford , C. I. Dallman , T.M. Lukas, P.V. Marshall , G.Nichols, D. Smith, Int. J. Pharm. 2000, 193, 247–259.
31) X.Wang, A. Michoel, G.V. Mooter, Int. J. Pharm. 2004, 272, 181–187.
32) S. Verheyen, N. Blaton, R. Kinget, G. V. Mooter Int. J. Pharm. 2002, 249, 45-/58
33) C. Ahlneck, G. Zografi, Int. J. Pharm. 1990, 62, 87-/95.
34) G. Sertsou , J. Butler, A. Scott , J. Hempenstall, T. Rades Int. J. Pharm. 2002, 245, 99-/108.
35) T. Matsumoto, G. Zografi, Pharm. Res. 1999, 16, 1722-/1728.
36) M. Nagarsenker, S. Garad, Int. J. Pharm. 2000, 160, 251-/255.
37) M. Mosharraf, T. Sebhatu, C. Nystrom, Int. J. Pharm. 1999, 177, 29–51.
38) T. Sebhatu, M. Angberg, C. Ahlneck, Int. J. Pharm. 1994, 104, 135–144.
39) C.R. Dalton, B.C. Hancock, Int. J. Pharm. 1997, 156, 143–151.
40) M.J. Brekner, H. A. Schneider, H.J. Cantow, Makromol. Chem.1988,189, 2085-2097.
41) Y. Miwa, K. Yamamoto, M. Sakaguchi, M. Sakai, S. Makita, S. Shimada, Macromolecules 2005**,** 38, 832-838.

CHAPTER 10

Conclusions & Suggestions for Further Work

10.1. CONCLUSIONS

The present work was focused on 1) enhancing bioavailability of drugs by ensuring the delivery (release / dissolution) of drugs at their site of absorption or target site thereby enhancing their absorption 2) enhancing palatability of drugs with immediate release in stomach 3) avoiding inactivation of drug arising from drug-polymer interaction 4) providing sustained gastric release of drugs 5) inhibiting conversion of drug from metastable / amorphous form to stable crystalline form in presence of moisture, enhancing dissolution and bioavailability. The synthesis of reverse enteric polymer (NREP) was undertaken. This polymer was used for formulation development of different drugs *viz* Cefuroxime axetil, Ciprofloxacin HCl, Clarithromycin and Celecoxib.

Cefuroxime axetil and Ciprofloxacin HCL are better absorbed from upper gastric region. The existing reverse enteric polymer Eudragit E completely inactivates Cefuroxime axetil. Further Eudragit E is soluble upto pH 5 and permeable above it and hence cannot be used in the taste masking formulation of highly water-soluble drug Ciprofloxacin HCl. Clarithromycin is used in treatment of *H. pylori* infections in pediatric patients and needs to be released in gastric region for local action. Clarithromycin is extremely bitter and needs coating to enhance patient compliance. However polymer coatings which bring about slow release of Clarithromycin at acidic pH, result in degradation of drug. As a result the drug is not available for the treatment. Clarithromycin has extremely short half-life of 1.47 hrs; in acidic pH hence rapid release is desired. In case of amorphous Celecoxib, the slow permeation of aqueous media in dosage converts the drug to stable form leading to poor dissolution. The present work is interdisciplinary in nature integrating the polymer (NREP) development with biopharmaceutical consideration of the drugs enabling site-specific delivery of drugs ensuring their bioavailability.

The important conclusions arrived at from the work discussed in earlier Chapters are summarized below.

1. The polymer architecture affects the physicochemical properties like pH dependent behavior, glass transition temperature, interactions with drug and other excipients. The polymer, Eudragit E caused inactivation of Cefuroxime axetil due to high charge

density and presence of strong basic co-monomer DMAMEA. Further the co-monomer composition also affected the permeability of Eudragit E at pH > 5 (*page no.35-36, 92, 153,158*). To overcome these limitations a series of reverse enteric co-polymers and ter-polymers containing hydrophobic, basic and hydrophilic monomers were synthesized.

2. The ter-polymer compositions containing monomers methyl methacrylate (MMA), 2-hydroxy ethyl methacrylate (HEMA) and 4-vinyl pyridine (4-VP) contributed to rapid solubility at pH < 4 and hydrophobicity at pH > 4 (*page no. 82-86, 90-93*).

3. As a result of self-associations within NREP, the basic pyridine group is not available for interaction with acidic drugs. This prevents inactivation of the drug and retains it in biologically active form (*page no.87-88, 162*).

4. The self-associations in NREP resulted in T_g (121.2^{0}C), greater than that anticipated from weight average value (103 ^{0}C). This enhanced ability to withstand formulation processes involving heat like coating and heat sealing without becoming tacky (*page no. 94-95*) whereas the T_g of Eudragit E is 45 ^{0}C (*page no. 136)*.

5. The intramolecular associations impart rigid behavior to NREP preventing strong binding with cell membranes thereby reducing cell damage. NREP meets *in-vitro* and *in-vivo* biological reactivity test as per USP 26 NF XXI, 2003 (*page no. 95, 98-99*).

6. The reverse enteric nature of NREP resulted in rapid dissolution of CA at gastric pH but suppressed the release at salivary pH. Since the absorption window of CA is limited to upper gastric region, rapid release at site of absorption ensures bioavailability (*page no. 111-113*).

7. CA encapsulated in NREP was more effective in masking bitter taste than the commercially marketed product “Ceftum” (*page no.* 114).
8. The encapsulation of Ciprofloxacin HCl and Clarithromycin using NREP showed rapid release of these drugs under gastric conditions. Dissolution is rate-limiting step

in absorption of drugs administered orally. Thus encapsulation of these drugs by NREP provided site specific release along with taste masking ability (*page no. 120, 122*).

9. Physicochemical interactions between Cefuroxime axetil (CA) and Eudragit E (EE) as well as CA and NREP were evaluated. CA was completely inactivated by EE (*page no. 153-155*).

10. A detailed investigation of interactions between CA-EE by FTIR and NMR showed the conversion of CA to Cefuroxime (acid form) due to interaction with EE. The HPLC showed generation of high level of impurities. The major impurities were Cefuroxime, Δ- 2 isomer and sulphoxides (*page no.146, 153, 154*). The T_g of Eudragit E was enhanced in the presence of CA. This was due to formation of Cefuroxime resulting due to charge transfer in CA-EE blends causing the rigidization of the donor chain (EE) (*page no. 137-138*).

11. The investigations of interactions between NREP-CA by XRD analysis showed that CA is retained in the amorphous form in presence of NREP. The DSC analysis showed that the endotherm of CA is retained and that the NREP is plasticized by CA (*page no. 137*). This was further confirmed by IR and NMR analyses which show absence of interactions (*page no.142-143 and 148-149*).

12. The HPLC analysis for CA-NREP showed that the extent of impurities is low, the resolution between diastereomers is unaltered and the conversion of CA to Cefuroxime and Δ- 2 isomer, is very low and within acceptable limits. The fraction of diastereomer B in CA is within the pharmacopoeial limits. Aging studies up to six months showed that CA is compatible with NREP (*page no.158*). Thus NREP was found suitable for providing rapid release of CA without causing inactivation, thus ensuring bioavailability (*page no.155-156*).

13. The HPLC analysis of CA and its interaction with basic monomer 4-vinyl pyridine and dimethylamino ethyl methacrylate showed that CA was immediately inactivated

in presence of DMAEMA. However CA was stable in presence of 4-VP. The absence of interaction between CA and NREP has been attributed to the low content of vinyl pyridine in the polymer as well as its weakly basic character. This explains why CA is retained in biologically active form in NREP (*page no.* 157-159).

14. Blends of reverse enteric polymer Eudragit E with enteric polymers resulted in polyelectrolyte complexes insoluble in various solvents and hence cannot be used for film coating. The polymer; NREP, developed by us forms miscible blends with enteric and pH independent polymer (*page no.167, 253, 259*).

15. The FTIR analysis showed that blends of NREP with Ethylcellulose, Eudragit L, Eudragit S, hydroxypropyl methylcellulose phthalate and cellulose acetate phthalate were rendered miscible by hydrogen bonding (*page no.183- 197*).

16. The thermal analysis (DSC) showed that all blends of NREP with other polymers were miscible, exhibiting negative deviations in T_g from volume additivity calculated by Fox equation. The extent of interaction between NREP and polymers was quantified by thermal analysis in terms of fitting parameters K_1 and K_2 of the Schneider equation. Based on these values, the extent of interactions between NREP and these polymers have been ranked in the order CAP > HPMCP > EL > ES > EC. Zein was immiscible with NREP (*page no. 199, 198-210*).

17. The extent of polymer-polymer interactions governed CA release for extended period at gastric pH. The data treatment by Peppas equation showed burst release with high value of kinetic parameter *k* for blends exhibiting weak interaction. As the extent of interaction increased, the CA release from microspheres becomes diffusion controlled with the value of diffusional exponent $n = 0.43$. These blends provided site specific sustained release of CA (*page no. 220, 229, 230*).

18. The blending of Eudragit E with polyacids Eudragit L, S, CAP and HPMCP resulted in polyelectrolyte complexation, as a result of charge transfer (*page no. 255 and 260*).

The investigations of various blends provided useful insights for controlled hydrogen bonding in NREP as to avoid complex formation, thus enabling film formation.

19. The analysis of the DSC data in frame work of Schneider equation showed that the values of fitting parameters K_1 and K_2 were higher for Eudragit E blends with polyacids than those seen in blends of NREP (*page no. 270-280, 284*). The higher charge density, higher pKa value of DMAEMA than 4-VP and absence of nonionic structural defect like HEMA in the polymer Eudragit E contribute to these (*page no. 284-286*). The presence of spacer ethyl chain in DMAEMA from polymeric backbone confers better mobility to form hetero contact with polyacids. Based on the values of parameters K_1 and K_2 the interactions between EE and these polymers have been ranked in the order EL > CAP > HPMCP > ES > EC (*page no. 269*).

20. The lower charge density, lower pKa value of 4-VP, strong self associations in NREP, presence of nonionic structural defect HEMA and absence of spacer chain between 4-VP and polymeric back bone, all contribute to its miscibility without complexation (*page no. 281-283*).

21. The blends of NREP with fatty acids provide immediate gastric release of Cefuroxime axetil and Ciprofloxacin HCl resulting from rapid dissolution of NREP. These formulations were highly hydrophobic and hence very effective for taste masking (*page no. 294,300, 303*).

22. The co-precipitates of Cefuroxime axetil and Celecoxib with low molecular weight NREP (M_w = 63,189) caused crystallization of the drugs as evidenced from the XRD analysis (*page no. 322,323,325*). The co-precipitates containing high molecular weight NREP (M_w = 3,38,021) retained Cefuroxime axetil and Celecoxib in amorphous form (*page no. 322,323,325*). This ensured the rapid dissolution of these drugs thereby enhancing bioavailability. The advantage of using high molecular weight NREP is it retains the drug in amorphous form, its hydrophobic nature inhibits moisture permeation and yet ensures rapid gastric release (*page no.321,322,324*).

10.2. SUGGESTIONS FOR FURTHER WORK

The work described in the present investigation is aimed at development of a new cationic polymer, capable of delivering the drugs at gastric pH either immediately or in a sustained manner without interaction and thus ensuring bioavailability. The development of this polymer is advancement over the existing polymer Eudragit E and has several advantages over it. These have been elaborately described in Chapter 3, 5, 6 and 7. With the progress of work several facets for application of the polymer have emerged. However all of these could not be taken to completion within the stipulated timeframe. Suggestions for future work which could be undertaken to exploit the ideas further are summarized below;

1. NREP interacts with polyacids forming miscible blends**.** Certain drugs like Erythromycin, Ephedrine and Propranolol HCl exhibit interactions with polyacids like Eudragit L and S. The effect of blending polybase NREP with these polyacids in overcoming the interaction of polyacid with basic drugs could be investigated. Since the miscibility of the polymers is already established, the blends can be expected to inhibit binding of basic drugs to anionic polymers.

2. The blends of NREP with EC, HPMCP, CAP, Eudragit L and S can be optimized for tailoring sustained release along the gastrointestinal tract or in the intestinal region.

3. Normally seal coat with polymers such as shellac and ethyl cellulose is used to protect many of the moisture sensitive drugs. Apart from this, special packaging materials are used to restrict the moisture permeation. These retard the drug release. NREP is hydrophobic in nature and our investigations by thermogravimetric analysis showed very little moisture uptake by polymer. The use of NREP as a barrier coating material to protect the moisture sensitive drug could be evaluated.

4. The blends of fatty acids and NREP were used for tailoring the drug release. The mechanistic investigations for these blends can be undertaken to elucidate the nature of interactions between the blend constituents.

5. Polyelectrolyte complexes of Eudragit E were obtained with polyacids. The influence of blend compositions on the drug release pattern from these polyelectrolyte complexes can be investigated.

6. The utility of NREP coating in development of other dosage forms like rapidly disintegrating, chewable and conventional tablets can be evaluated.

7. The *in-vivo* drug release from NREP and its blends can be evaluated to establish the *in-vitro in-vivo* correlation.

List of Publications

Patents

Granted

- Himadri Sen, Rajesh Kshirsagar, Anupa R. Menjoge
  US 6,932,981 B2 Rapidly Disintegrating Sustained Release Cefuroxime Axetil Composition

Published Applications

- Mohan G. Kulkarni, Anupa R. Menjoge
  US 20050137372, pH sensitive polymer and process for preparation thereof

- Mohan G. Kulkarni, Anupa R. Menjoge
  US 20050136114, Taste masked pharmaceutical compositions comprising bitter drug and pH sensitive polymer,

- Mohan G. Kulkarni, Anupa R. Menjoge
  US20050136115, Taste masked pharmaceutical composition comprising pH sensitive polymer

- Anupa R. Menjoge, Mohan G. Kulkarni
  US20050281874, Coating compositions for bitterness inhibition

- Anupa R. Menjoge, Mohan G. Kulkarni
  US20060141053, Pharmaceutical composition for improving palatabilit*y* of drugs and process for preparation thereof

Communications

- A.R. Menjoge, M.G. Kulkarni,
  Miscible blends of Reverse Enteric Polymer with Enteric and pH independent polymers: Mechanistic Investigations for Tailoring Drug Release,
  Communicated to Biomacromolecules 2006

- A.R. Menjoge, M.G. Kulkarni,
  Development of Cationic Polymer Compatible with Cefuroxime axetil: Enhancement of Palatability with Immediate Gastric Release
  Communicated to Biomacromolecules 2006

- A.R. Menjoge, M.G. Kulkarni,
  Mechanistic Investigations of Phase Behavior in Eudragit® E Blends
  Communicated to International Journal of Pharmaceutics 2006

- A.R. Menjoge, S. V. Patel, M. G. Kulkarni
  Polymer blends of new reverse enteric polymers for extended gastric and intestinal release

Manuscript in preparation

- A.R. Menjoge, M.G.Kulkarni
  Influence of polymer molecular weight on molecular motions: crystallization inhibition
  Manuscript in preparation

Posters

- Anupa R. Menjoge, Mohan. G. Kulkarni,
  Novel Reverse Enteric polymers; Evaluation for Taste masking Technologies, 32nd Annual Meet and Exposition of Controlled Release Society, Miami, Florida, 06/2005

- Mohan. G. Kulkarni, Anupa R. Menjoge**,**
  New Polymeric Excipient for Oral Drug Delivery AAPS Annual Meeting and Exposition, Nashville Tennessee, Nov 2005.

- Anupa R. Menjoge, Mohan. G. Kulkarni,
  Stimuli sensitive polymers for Drug Delivery, Macro2004, International Conference On Polymers for Advanced Technologies, Thiruananthapuram, India, 15-17 Dec 2004.

- Anupa R. Menjoge, Mohan. G. Kulkarni,
  Stimuli sensitive polymers for Drug Delivery, Symposium of Polymer Science 2003, organized by Society of Polymer Science Local Chapter, Pune, 07/2004.

Hardiness and ability to grasp the content, help

survive the crucibles, emerge stronger,

and committed, finding opportunities,

where others despair

Warren Benis

Ms. ANUPA RAMESH MENJOGE

B-1/12, Anubandh Society Pune-India ☎+91-9890034127
✉ a.menjoge@ncl.res.in +91-02024335307

EDUCATION

Ph.D Pharmaceutical Sciences since 02/2002
Thesis: "Enhancing Bioavailability of Drugs" (**submitted 08/2006**)
Advisor: Dr.M.G. Kulkarni, H.O.D.,
Polymer Science & Engineering Division,
National Chemical Laboratory, CSIR, India.

Master of Pharmacy (Pharmaceutics) 12/1998
Department of Pharmaceutical Sciences,
Nagpur University, India
Overall: 76.1/100; Rank: 1

Bachelor of Pharmacy 08/1996
Nagpur College of Pharmacy,
Nagpur University, India
Overall: 66.0 /100;

Post Graduate Diploma in Intellectual Property Rights & Patent Law 03/2004
Symbiosis Law College,
Symbiosis Deemed University, Pune, India
Overall: 65.2 /100; Rank: 1

AWARDS AND ACCOMPLISHMENTS

- Qualified Graduate Aptitude Test (GATE-1997) with **93.47 percentile** an All-India Examination conducted by the Indian Institutes of Technology **(IITs)**.
- **1st Position** at Master of Pharmacy (Nominated For Salehbhai Vali Gold Medal**),** 1998.
- **1st Position** at P.G. Diploma in Intellectual Property Rights & Patent Law, 2004.
- **Best Poster** (**1st Prize**) at Symposium of Polymer Science 2004, organized by Society of Polymer Science Local Chapter, Pune, India.
- **2nd Prize** for Best Business Plan Competition organized by Human Resource Development group CSIR India and (IIM) Indian Institute Management Bangalore, 2005.

- **Awarded Travel grant** by CSIR India ($ 1,200 USD) to attend and present research paper at 32nd Annual Meet and Symposium, Controlled Release Society, Miami, Florida, June 2005.

HONORS AND FELLOWSHIPS

- **Awarded Research Associate Fellowship by CSIR, India (**Human Resource Development group Council of Scientific and Industrial Research India). **2006-2007**

- Paper entered nomination for "Innovative aspects of Oral Drug Delivery Graduate/Post-Doc award **CRS 2005** at the 32nd Annual Meet and Exposition Controlled Release Society 2005.

- **Awarded Senior Research Fellowship for PhD. by CSIR, India (**Human Resource Development group Council of Scientific and Industrial Research India). **2002-2006**

- Received **MHRD Scholarship for Postgraduate study (M.PHARM**) from Ministry of Human Resources Development (MHRD), Government of India. **1997-1998**

PATENTS

Granted

- **US 6,932,981 B2,** Rapidly Disintegrating Sustained Release Cefuroxime Axetil Composition, Himadri Sen, Rajesh Kshirsagar, Anupa R. Menjoge.

Published Applications

- **US 20050137372**, pH sensitive polymer and process for preparation thereof
  Mohan G. Kulkarni, Anupa R. Menjoge

- **US 20050136114**, Taste masked pharmaceutical compositions comprising bitter drug and pH sensitive polymer
  Mohan G. Kulkarni, Anupa R. Menjoge

- **US20050136115**, Taste masked pharmaceutical composition comprising pH sensitive polymer
  Mohan G. Kulkarni, Anupa R. Menjoge

- **US20050281874**, Coating compositions for bitterness inhibition
  Anupa R. Menjoge, Mohan G. Kulkarni.

- **US20060141053**, Pharmaceutical composition for improving palatability drugs and process for preparation thereof
  Anupa R. Menjoge, Mohan G. Kulkarni.

COMMUNICATIONS

- A.R. Menjoge, M.G. Kulkarni,
  Miscible blends of Reverse Enteric Polymer with Enteric and pH independent polymers: Mechanistic Investigations for Tailoring Drug Release,
  Communicated to *Biomacromolecules* 2006

- A.R. Menjoge, M.G. Kulkarni,
  Development of Cationic Polymer Compatible with Cefuroxime axetil: Enhancement of Palatability with Immediate Gastric Release
  Communicated to *Biomacromolecules* 2006

- A.R. Menjoge, M.G. Kulkarni,
  Mechanistic Investigations of Phase Behavior in Eudragit® E Blends
  Communicated to *International Journal of Pharmaceutics* 2006

- A.R. Menjoge, S. V. Patel, M. G. Kulkarni
  Polymer blends of new reverse enteric polymers for extended gastric and intestinal release
  Manuscript in preparation

- A.R. Menjoge, M.G.Kulkarni
  Influence of polymer molecular weight on molecular motions: crystallization inhibition
  Manuscript in preparation

POSTERS

- Anupa R. Menjoge, Mohan. G. Kulkarni, Novel Reverse Enteric polymers; Evaluation for Taste masking Technologies, 32nd Annual Meet and Exposition of Controlled Release Society, Miami, Florida, 06/2005

- Mohan. G. Kulkarni, Anupa R. Menjoge**, "**New Polymeric Excipient for Oral Drug Delivery" AAPS Annual Meeting and Exposition, Nashville TN, Nov 2005.

- Anupa R. Menjoge, Mohan. G. Kulkarni, "Stimuli sensitive polymers for Drug Delivery" Macro2004, International Conference on Polymers for Advanced Technologies, Thiruananthapuram, India, 15-17 Dec 2004.

- Anupa R. Menjoge, Mohan. G. Kulkarni, "Stimuli sensitive polymers for Drug Delivery" Symposium of Polymer Science 2003, organized by Society of Polymer Science Local Chapter, Pune, 07/2004.

EXPERIENCES

Research Scientist (Formulation Development) 01/2000-02/2002

Lupin Research Park, Lupin Ltd.
Pune India

- Formulation & Development of novel non-infringing oral drug delivery systems
- Developed rapidly disintegrating: matrix, delayed release, immediate release tablets and particulate coating
- Co-ordination of stability studies and bioavailability studies. Develop Study Protocols Stability testing of pharmaceutical compositions as per the ICH and SUPAC guidelines.
- Data analysis and interpretation, Deliverables creation – reports and presentations.
  Output: US Patent 6,932,981 B2

Lecturer in Pharmaceutics 06/1999-12/1999

Institute of Pharmacy
Wardha India

- Impart Lectures in Physical Pharmacy, Pharmaceutics-dosage form technology
- Worked as undergraduate research advisor

RESEARCH EXPERIENCE (PhD Thesis)

- Research work is primarily focused on designing and evaluation of polymers for novel drug delivery systems (non-infringing conventional and modified Oral dosage forms and Taste masking of bitter drugs.)

- Tailor polymer compositions with desired stimuli responsive behavior
  Polymer composition optimization / synthesis
  Polymerization Techniques: solution / bulk polymerization
  Physicochemical characterization of polymers: glass transition temperature by MDSC, molecular weight determination by GPC, FTIR, NMR, equilibrium swelling studies.

  Biocompatibility Evaluation: *in-vitro, in-vivo* biological reactivity tests as per USP.

- Drug-polymer interactions / compatibility: evaluation by DSC, FTIR, HPLC, NMR.

- Polymer-Polymer Miscibility: Theoretical aspects of glass transition behavior, Miscibility determination by applying Fox, Couchman, Kwei and Schneider equation.

Determination of extent of interactions using parameters K_1 and K_2, from Schneider equation
Detailed investigations for nature of interactions by FTIR

- Microencapsulation of drugs: By Spray drying, Fluid bed coating (Wurster), and emulsification solvent evaporation techniques. Characterization: SEM, ESEM and In-vitro drug release

TECHNICAL SKILLS

- **Area of Expertise**
  Biomaterials for drug delivery, stimuli sensitive polymers, Synthesis and characterization

  Formulation development of Rapidly Disintegrating Tablets, Conventional Tablets, Sustained, Matrix and delayed Release Tablets
  Particulate coating and Microencapsulation: by fluid bed coater, spray drying technique and emulsification solvent evaporation technique.

  Taste masking of bitter drugs
  Polymer Blends: Miscibility determination by thermal and FTIR analysis
  Drug-Polymer Compatibility / interactions

- **Patent Drafting**
  Experienced in drafting PCT and US patent specifications

- **Experimental Techniques**
  Acquainted with basic polymerization techniques like solution, bulk polymerization etc. Hands on experience in handling equipments and analysis using FTIR, UV-Visible spectroscopy, DSC, MDSC, TGA, GPC, HPLC and XRD.
  Acquainted with analysis by NMR spectroscopy, SEM and ESEM

- **Pharmaceutical Equipment Handling**
  Hands on experience in operating Lab scale equipments like Tableting machines, Roller compacter, Planetary mixture, Fluid bed coater, Spray dryer, Fluid bed granulator / drier, Perforated tablet coating pans, Colloid mills, Multipurpose equipment from Erweka, Dissolution apparatus USP type I, II and III etc.

- **Data Mining Tools**
  Well Acquainted with online patent databases like Scifinder, STN, Delphion and CACD (chemical abstracts), USPTO, esp@cenet.
  Well acquainted with online journal database like Sciencedirect, Wileyinterscience, Springer online, ACS journals, Taylor and Francis and other online database searches.

- **Computer Proficiency**
  Skilled in the MS Office Well acquainted with software's like Chem Draw, ACD spec view

STRENGHTS

- A broad, interdisciplinary scientific background in Pharmacy and Biopolymers
- A quantitative and analytical approach to synthesis of Biopolymers and characterization
- Broad dosage form experience
- Awareness of patent law and patent drafting skills
- Experience in effective writing and oral presentation skills
- Experience in handling analytical and pharma related equipments and data interpretation

WORKSHOPS

- **Technology Entrepreneurship**

  Conducted by: Human Resource Development Group CSIR, India, and (IIM) Indian Institute Management Bangalore (2005)
  Venue: NCL Pune India

- **Intellectual Property Rights and Patent Law**
  Conducted by: Nalsar, University of Law, Hyderabad, India
  Venue: NCL Pune, India

REFERENCES

Dr. M.G. Kulkarni	Head, Polymer Science & Engineering Division, National Chemical Laboratories, Pune, India Email: mgk@che.ncl.res.in Phone : + 91-020- 25890765 Mobile : 9422309762
Dr. B. D. Kulkarni	Deputy Director and Head Chemical Engineering & Process Development Division, National Chemical Laboratories, Pune, India Email; bdk@ems.ncl.res.in , Phone: +91-020- 25893041
Dr. J. Suryakumar	Associate Director Formulations, Lupin Research Park, Lupin Ltd. 464, Village Nande, Pune, India Phone + 91-020-25126161